UCLouvain
Institute of Mechanics,
Materials and Civil Engineering

Exploring options for a fossil-free European energy system

The role of renewable fuels

Doctoral dissertation presented by
Paolo THIRAN
in partial fulfilment of the requirements for
the degree of Doctor in Engineering Sciences

September 2024

Thesis committee

Pr. Hervé JEANMART (UCLouvain, Supervisor)
Pr. Francesco CONTINO (UCLouvain, Supervisor)
Pr. Sandra SOARES FRAZAO (UCLouvain, President)
Pr. Emmanuel DE JAEGER (UCLouvain, Secretary)
Pr. Sylvain QUOILIN (ULiège)
Pr. Valentin BERTSCH (Ruhr-Universität Bochum)

«*Exister est un fait, vivre est un art. Tout le chemin de la vie, c'est de passer de l'ignorance à la connaissance, de la peur à l'amour.*»

Frédéric Lenoir.
Petit traité de vie intérieure (2010)

«*L'extinction des espèces ne résultera que de la mort douloureuse d'un nombre incalculable d'individus. Ce ne sont pas alors des statistiques qui diminueront, mais des vivants qui expireront. La souffrance peut-elle ne pas être prise en compte ? Derrière la vie, il y a les vivants. Tout est là. Ce ne sont pas des idées qui vont devoir - par nos choix - tenter de survivre à l'effondrement : ce sont des personnes.*»

Aurélien Barrau.
Le plus grand défi de l'histoire de l'humanité (2019)

«*Si nous voulons pouvoir dire quelque chose du monde futur, dessiner les contours théoriques d'une société à venir qui ne soit pas hyper-industrielle, il nous faut reconnaître l'existence d'échelles et de limites naturelles. L'équilibre de la vie se déploie dans plusieurs dimensions ; fragile et complexe, il ne transgresse pas certaines bornes. Il y a certains seuils à ne pas franchir. Il nous faut reconnaître que l'esclavage humain n'a pas été aboli par la machine, mais en a reçu figure nouvelle. Car, passé un certain seuil, l'outil, de serviteur, devient despote. (...) J'appelle société conviviale une société où l'outil moderne est au service de la personne intégrée à la collectivité, et non au service d'un corps de spécialistes. Conviviale est la société où l'homme contrôle l'outil.*»

Ivan Illich.
La Convivialité (1973)

Acknowledgments

Doing a thesis is like climbing a mountain in the fog. And this summit, I sweated hard to reach. I almost turned back several times. If I've managed to reach it, it's largely thanks to the people around me.

First of all, my direct professional circle, the Sustainable Energy Research Group. I'd like to thank every member of this group for making it a dynamic, open-minded team that thinks about the world. In particular, the group of researchers with whom I began my thesis during COVID... We stuck together to survive this difficult start: Martin, Aurélia, Xavier and Arnaud. I'd also like to thank the person who convinced me to start research, who passed on his model to me and who played a real mentoring role when I started my thesis: Gauthier. Then there are the researchers who came afterwards, who kept the research group thriving and with whom I became friends: Sébastien, Antoine, Pierre, Zakarie, Nicolas and Arthur. Nor do I want to forget my office mates, with whom I loved discussing and rebuilding the world (sometimes a little too much): Martin, Pablo, Angelos, Sébastien, Arnaud and Baptiste. In my creative process, I often need to explain my ideas and confront them with the opinions of others. I'd like to thank these people for their listening, their availability, their patience and their insights: Martin, Aurélia, Xavier, Gauthier and Antoine. I came to disturb you many times in your work to discuss and your door was always open. Thank you so much! Without you, my thesis wouldn't have been the same.

I'd also like to express my warmest thanks to my two promoters, Hervé and Francesco, who have always been open and willing to listen, and have never stopped believing in me. I think they're even more convinced of what I'm doing than I am. They welcomed me in my moments of doubt. They challenged me to go further in my work and trusted me to take the right path. They even trusted me to slow-travel to conferences, whether it was by train-bus-boat to Cyprus or by bike back from Copenhagen. I could never have finished this thesis without their support.

I would like to thank the members of my supervisory panel and jury. They agreed to follow my work and challenge it to improve it. I thank them all.

In my professional circle, I would like to thank the wider circles to which I belong. First of all, the BEST (Belgian Energy System Transition) project, of which my thesis is a part and which financed it with the support of the Transition Fund of the FPS Economy. In particular, I'd like to thank Véronique for managing the project and all the researchers who made it such a rewarding experience. Secondly, I'd like to thank my research unit, the TFL. In particular, a great thank you to our secretary, Isabelle, who is always there to help us out when we're struggling with administrative matters at UCLouvain. Finally, thanks to UCLouvain for the research environment and facilities. In particular, the computational resources have been provided by the Consortium des Équipements de Calcul Intensif (CÉCI), funded by the Fonds de la Recherche Scientifique de Belgique (F.R.S.-FNRS) under Grant No. 2.5020.11 and by the Walloon Region.

My thesis would not have been the same without the various collaborations I was lucky enough to benefit from. The main one, which has been a real exchange and trained me for the future, is with Matija Pavičević. Thank you Matija for this fruitful collaboration. Others followed, and I'd like to thank the various researchers with whom I had the pleasure of collaborating on various projects: Jonathan Dumas, Antoine Dubois, Sylvain Quoilin, Umair Tareen, Pablo Jimenez Zabalaga, Julien Jacquemin, Pierre Jacques and Sébastien Meyer.

Finally, I can't talk about my professional environment without mentioning Ingés en Transition. This project carried me a lot during my thesis years and helped me to give meaning to what I do and to share my interrogations with others. It's a great project that we've set up, and a great space for exchange and reflection. I hope this Horde will grow and lead to engineers more in alignment with the socio-environmental challenges of our time.

After the professional sphere, there's my personal environment. And here again I consider myself lucky and supported. First of all, there's my family: my first fans and lifelong supporters. The foundation of my life! Thank you Mum and Dad for always listening to me when I talk about what I'm passionate for, and thank you for comforting me in difficult times. Then there are all my roommates, past and present, who have sometimes seen me toil, sometimes wander, and have accepted and supported me like that. Thanks to SoumSoum, Noukiks, Odile, Cam, Shwifty, Maki, Frimousse, Djudju, Tanuk, le Q, Marie, Chap, le Feu, Clem and Lama. And all those other friends who believed in me and agreed not to forget me even when I was a "ghost" at the end of my thesis. The list is too long to mention them all. Finally, there's Sarù. Thank you, you've been there, with the fair and simple presence of the person who accompanies me and listens to me in my thesis adventures. I don't think you realize what an essential support you've been for me.

Remerciement

Faire une thèse c'est comme gravir un sommet dans le brouillard. Et ce sommet, j'ai bien sué pour l'atteindre. J'ai failli faire demi-tour plusieurs fois. Si j'ai réussi à l'atteindre, c'est en grande partie grâce à mon entourage.

Tout d'abord mon entourage professionnel direct, le Sustainable Energy Research Group. J'aimerais remercier chaque membre de ce groupe d'en faire une équipe dynamique, ouverte et qui se pose des questions sur le monde. En particulier, le groupe de chercheureuses avec qui j'ai commencé ma thèse durant la COVID... On s'est bien serré les coudes pour survivre à ce démarrage difficile : Martin, Aurélia, Xavier et Arnaud. J'aimerais aussi remercier celui qui m'a convaincu de faire de la recherche, qui m'a légué son modèle et qui a joué un réel rôle de mentor pour mes débuts de thèse : Gauthier. Ensuite, je pense aux chercheurs qui sont arrivés par après, qui ont continué de faire vivre le groupe de recherche et avec qui je me suis lié d'amitié : Sébastien, Antoine, Pierre, Zakarie, Nicolas et Arthur. Je ne veux pas non plus oublier mes compagnons de bureau avec qui j'ai adoré discuter et refaire le monde (parfois un peu trop) : Martin, Pablo, Angelos, Sébastien, Arnaud et Baptiste. Dans mon processus de création, j'ai souvent besoin d'expliquer mes idées et de les confronter à l'avis d'autres. J'aimerais remercier ces personnes pour leur écoute, leur disponibilité, leur patience et leurs reflets : Martin, Aurélia, Xavier, Gauthier et Antoine. Je suis venu vous déranger de nombreuses fois dans votre travail pour discuter et votre porte était toujours ouverte. Merci ! Sans vous ma thèse n'aurait pas été pareil.

J'aimerais également remercier du fond du cœur mes deux promoteurs, Hervé et Francesco, qui ont toujours été ouverts et à l'écoute et n'ont jamais cessé de croire en moi. Je pense qu'ils sont plus convaincus de ce que je fais que moi-même. Ils ont su m'accueillir dans mes moments de doutes. Ils m'ont challengé pour approfondir mon travail et m'ont fait confiance pour la voie à suivre. Ils m'ont même fait confiance pour mes voyages en slow travel pour aller en conférence que ce soit le train-bus-bateau jusqu'à Chypre ou le vélo pour revenir de Copenhague. Je n'aurais jamais pu finir cette thèse sans leur soutien.

Je remercie les membres de mon panel de supervision et de mon jury. Ils ont accepté de

suivre mon travail et de le challenger pour l'améliorer. Merci à eux.

Dans mon entourage professionnel, je voudrais remercier les plus larges cercles dont je fais partie. Tout d'abord, le BEST (Belgian Energy System Transition) project dont ma thèse fait partie et qui l'a financé avec le soutien du Fond Transition du SPF Economie. J'aimerais remercier en particulier Véronique pour la gestion du projet et toustes les chercheureuses qui en ont fait un projet enrichissant. Ensuite, j'aimerais remercier mon pôle de recherche, le TFL. En particulier, un grand merci à notre secrétaire, Isabelle, qui est toujours là pour nous aider quand on galère avec l'administratif à l'UCLouvain. Finalement, merci à l'UCLouvain pour le cadre de recherche et les équipements. En particulier, les moyens de calcul ont été fournis par le Consortium des Équipements de Calcul Intensif (CÉCI), financé par le Fonds de la Recherche Scientifique de Belgique (F.R.S.-FNRS) sous la convention n° 2.5020.11 et par la Région Wallonne.

Ma thèse n'aurait pas été la même sans les différentes collaborations dont j'ai eu la chance de bénéficier. La principale, qui aura été un réel échange et qui m'a formé pour la suite, est avec Matija Pavičević. Merci à toi Matija pour cette fructueuse collaboration. Ensuite s'en sont suivie d'autres et j'aimerais remercier les différents chercheurs avec qui j'ai eu le plaisir de collaborer sur divers projets : Jonathan Dumas, Antoine Dubois, Sylvain Quoilin, Umair Tareen, Pablo Jimenez Zabalaga, Julien Jacquemin, Pierre Jacques et Sébastien Meyer.

Pour finir, je ne peux pas parler de mon entourage professionnel sans parler d'Ingés en Transition. Ce projet m'a beaucoup porté pendant mes années de thèse et m'a aidé à donner du sens à ce que je fais et à partager mes questionnements avec d'autres. C'est un beau projet que nous avons mis sur pied et un bel espace d'échange et de réflexion. J'espère que cette Horde grandira et mènera à des ingénieurs plus alignés avec les défis socio-environnementaux de notre temps.

Après la sphère professionnelle, il y a mon entourage personnel. Et là encore je m'estime chanceux et soutenu. Tout d'abord, il y a ma famille : mes premiers fans et soutiens de toujours. Le socle quoi ! Merci Maman et Papa pour votre écoute quand je raconte ce qui me passionne et merci pour votre réconfort dans les moments difficiles. Ensuite, il y a toustes mes colocs présent·e·s et passé·e·s qui m'ont vu tantôt trimer, tantôt errer et m'ont accepté et soutenu comme ça. Merci à SoumSoum, Noukiks, Odile, Cam, Shwifty, Maki, Frimousse, Djudju, Tanuk, le Q, Marie, Chap, le Feu, Clem et Lama. Puis toustes ces autres copaines qui ont cru en moi et ont accepté de ne pas m'oublier même quand j'étais un « fantôme » sur la fin de ma thèse. La liste est trop longue pour toustes les citer. Finalement, il y a Sarù. Merci, tu as été là, avec la présence juste et simple de celle qui m'accompagne et m'écoute dans mes péripéties de thèse. Je pense que tu ne te rends pas compte du soutien essentiel que tu as été pour moi.

Abstract

With climate change, human societies must phase out fossil fuels. However, fossil fuels are versatile energy sources. They are present everywhere in our energy systems and daily lives. Studying fossil-free alternative energy systems is a complex task as it must integrate all energy-consuming sectors and consider their synergies. Focusing on Europe, this thesis addresses the following research question:

How can Europe build a fossil-free energy system by 2050?

For many uses, electricity can substitute fossil fuels. In a system where renewable sources produce electricity, the gain is twofold. Not only is the system based on low-carbon energies, but the electrification of uses also implies greater efficiency. However, some energy uses cannot be supplied by electricity and still require fuels. Due to their versatility, renewable fuels derived from biomass or electricity are crucial for achieving the total phase-out of fossil fuels in Europe. However, production costs and efficiency challenges exist compared to alternatives like direct electrification. They are scarce and strategic resources. An integrated approach at a large spatial scale is needed to study their strategic production and use. Therefore, this thesis addresses the underexplored integration of renewable fuels in the European energy system and answers the following research question:

What is the strategic role of renewable fuels in a fossil-free European energy system?

This thesis develops the EnergyScope Multi-Cells optimization model to answer those two research questions. This multi-regional model is built with a whole-energy system approach, considering all energy sectors and carriers. It is suitable to study a high penetration of renewable energy sources in the system. Its structure enables a direct comparison of renewable fuels with competing alternatives.

With this model, this thesis analyzes a first scenario (Reference) of a fossil-free and nuclear-free European energy system. It highlights the essential role of renewable fuels in fossil-free energy systems. They supply 43% of the final energy. Their production consumes 52% of the gross available energy (6449 TWh). These fuels are essential for defossilizing specific

sectors such as aviation, shipping, freight, non-energy demand, industrial heat, and busses. Additionally, they contribute to addressing the spatio-temporal disparity of renewable energy sources through seasonal storage and energy exchange between countries.
To challenge this Reference scenario, we propose a hybrid method combining scenario analysis and near-optimal space exploration. We apply this method to generate twelve alternative system designs. These alternatives include investing in nuclear energy or in energy sufficiency. These system designs are analyzed to underline the differences with the results of the first scenario and the common outcomes. This analysis highlights key trade-offs and must-haves for a European fossil-free energy system. In particular, it underlines the need for a high deployment of photovoltaic (PV) and wind turbines, reaching at least an energy production that is 6 times and 4 times the current production in Europe, respectively. Electricity production increases drastically in all system designs, up to 3.4 times the current production. This increased electricity production is linked with a high electrification of energy services, 49 to 62% of the final energy consumption, and a substantial production of electrofuels, using from 20 to 50% of the electricity production. Furthermore, the strategic role of renewable fuels appears in all system designs. They supply 30 to 45% of the final energy consumption. Their role in addressing the spatio-temporal disparity is essential. They transport 69 to 84% of the energy exchanged between countries and represent 39 to 54% of the storage capacity installed.
Based on those results, phasing out fossil fuels in Europe is feasible but requires high deployment of renewable energies such as wind and PV. A fossil-free energy system will rely heavily on renewable fuels.

Keywords
Energy system optimization model; EnergyScope; whole-energy systems; European energy system; fossil-free energy systems; near-optimal space exploration; scenario analysis; renewable fuels.

Résumé

En raison du changement climatique, les sociétés humaines doivent sortir de la dépendance à l'égard des combustibles fossiles. Cependant, les combustibles fossiles sont des sources d'énergie polyvalentes. Elles sont présentes partout dans nos systèmes énergétiques et dans nos vies quotidiennes. L'étude des systèmes énergétiques alternatifs sans combustibles fossiles est une tâche complexe puisqu'elle doit intégrer tous les secteurs consommateurs d'énergie et prendre en compte leurs synergies. En se concentrant sur l'Europe, cette thèse aborde la question de recherche suivante :

Comment l'Europe peut-elle se doter d'un système énergétique sans combustibles fossiles d'ici 2050 ?

Pour de nombreuses utilisations, l'électricité peut remplacer les combustibles fossiles. Dans un système où des sources renouvelables produisent de l'électricité, le gain est double. Non seulement le système est basé sur des énergies à bas carbone, mais l'électrification des usages induit une plus grande efficacité. Néanmoins, certaines utilisations d'énergie ne peuvent pas être alimentées par l'électricité et nécessitent encore des combustibles. En raison de leur polyvalence, les combustibles renouvelables dérivés de la biomasse ou de l'électricité sont essentiels pour parvenir à l'élimination totale des combustibles fossiles en Europe. Cependant, des problèmes de coûts de production et d'efficacité existent par rapport à des alternatives comme l'électrification directe. Ces combustibles renouvelables sont des ressources rares et stratégiques. Une approche intégrée à grande échelle spatiale est nécessaire pour étudier leur production et leur utilisation stratégiques. Par conséquent, cette thèse traite du sujet sous-exploré de l'intégration des combustibles renouvelables dans le système énergétique Européen et répond à la question de recherche suivante :

Quel est le rôle stratégique des combustibles renouvelables dans un système énergétique européen sans combustibles fossiles ?

Cette thèse développe le modèle d'optimisation EnergyScope Multi-Cells pour répondre à ces deux questions de recherche. Ce modèle multirégional est construit avec une approche toutes-énergies du système énergétique, en tenant compte de tous les secteurs et vecteurs énergétiques. Il est adapté à l'étude d'une forte pénétration des sources d'énergie renouvelables dans le système. Sa structure permet une comparaison directe des combustibles renouvelables avec les alternatives concurrentes.

Avec ce modèle, cette thèse analyse un premier scénario (Référence) d'un système énergétique européen sans fossile et sans nucléaire. Elle met en évidence le rôle essentiel des combustibles renouvelables dans les systèmes énergétiques sans combustibles fossiles. Ils fournissent 43% de l'énergie finale. Leur production consomme 52% de l'énergie brute disponible (6449 TWh). Ces carburants sont essentiels pour défossiliser des secteurs spécifiques tels que l'aviation, le transport maritime, le fret, la demande non-énergétique, la chaleur industrielle et les autobus. En outre, ils contribuent à remédier à la disparité spatio-temporelle des sources d'énergie renouvelables, grâce au stockage saisonnier et à l'échange d'énergie entre pays.

Pour challenger ce scénario de Référence, nous proposons une méthode hybride combinant l'analyse de scénarios et l'exploration de l'espace quasi-optimal . Nous appliquons cette méthode pour générer douze systèmes alternatifs. Ces alternatives considèrent entre-autres la possibilité d'investir dans le nucléaire ou dans la sobriété énergétique. Ces solutions sont analysées pour souligner les différences et les convergences avec les résultats du premier scénario. Cette analyse met en évidence les compromis clés et les éléments indispensables à un système énergétique européen sans combustibles fossiles. Elle souligne en particulier la nécessité d'un déploiement important de panneaux photovoltaïques et d'éoliennes, pour atteindre au minimum une production d'énergie respectivement 6 fois et 4 fois supérieure à la production actuelle en Europe. La production d'électricité augmente considérablement dans toutes les configurations du système, jusqu'à 3,4 fois la production actuelle. Cette augmentation de la production d'électricité est liée à une forte électrification des services énergétiques, 49 à 62% de la consommation finale d'énergie, et à une production substantielle d'électrocarburants, utilisant de 20 à 50% de la production d'électricité. En outre, le rôle stratégique des combustibles renouvelables apparaît dans toutes les configurations du système. Ils représentent 30 à 45% de la consommation finale d'énergie. Leur rôle dans la gestion des disparités spatio-temporelles est essentiel. Ils transportent 69 à 84% de l'énergie échangée entre les pays et représentent 39 à 54% de la capacité de stockage installée.

Sur la base de ces résultats, l'élimination progressive des combustibles fossiles en Europe est réalisable mais nécessite un déploiement massif d'énergies renouvelables telles que l'éolien et le photovoltaïque. De plus, un système énergétique sans énergie fossile dépendra fortement des combustibles renouvelables.

Mots-clefs
Modèle d'optimisation des systèmes énergétiques ; EnergyScope ; systèmes toutes-énergies ; système énergétique européen ; systèmes énergétiques sans énergies fossiles ; exploration de l'espace quasi-optimal ; analyse de scénarios ; carburants renouvelables.

Contents

List of Figures

List of Tables

Acronyms and abbreviations

CE	Correlation error
DCE	Duration curve error
DE	Design error
TSE	Time series error
aDE	Apparent design error
BEV	Battery electric vehicle
CCGT	Combined cycle gas turbine
CHP	Cogeneration of heat and power
CO_2	Carbon dioxyde
COP	Coefficient of performance
CSP	Concentrated solar power
DHN	District heating network
DNI	Direct normal irradiance
EGS	Enhanced geothermal system
EHB	European Hydrogen Backbone
ENTSOE	European Network of Transmission System Operators for Electricity
ENTSOG	European Network of Transmission System Operators for Gas
ERAA	European resource adequacy assessment
ESOM	Energy system optimisation model
EU	European Union
EUD	End-use demand
EV	Electric vehicle
FEC	Final energy consumption
FT	Fischer-Tropsch
GHG	Greenhouse gas
GHI	Global horizontal irradiance
GIS	Geographic information system

GWP	Global warming potential
HP	Heat pump
HRE4	Heat Roadmap Europe
HVAC	High voltage alternating current
HVC	High value chemical
HVDC	High voltage direct current
IAM	Integrated assessment model
IEA	International Energy Agency
JRC	Joint Research Center
LCA	Life cycle assessment
LHV	Lower heating value
LP	Linear programming
MERRA-2	Modern-Era Retrospective analysis for Research and Applications, version 2
MGA	Modelling to generate alternatives
NED	Non-energy demand
NHTS	National Household Travel Survey
OPSD	Open power system data
PHEV	Plug-in hybrid electric vehicle
PHS	Pumped hydro storage
PT	Parabolic trough
PV	Photovoltaic
RE	Renewable energy
REP	Renewable energy potential
RES	Renewable energy sources
SC	Space cooling
SH	Space heating
SOC	State of charge
ST	Solar tower
TD	Typical day
TYNDP	Ten-Year Network Development Plan
UTC	Coordinated universal time
V2G	Vehicle-to-grid

List of publications

Chapter 2 is built on a peer-reviewed journal publication:

> Thiran, P., Jeanmart, H., & Contino, F., (2023). "*Validation of a Method to Select a Priori the Number of Typical Days for Energy System Optimisation Models.*" In Energies 2023, (Vol. 16, Page 2772 16, 2772). URL: https://doi.org/10.3390/EN16062772

This paper is the extension of a peer-reviewed conference publication:

> Thiran, P., Contino, F., & Jeanmart, H. (2022). "*Validation of Methods to Select a Priori the Number of Typical Days for Energy System Optimisation Models*". In proceeding of SDEWES 2022 conference.

The implementation of shipping and aviation demands in the model, described in Chapter 1, is adapted from a peer-reviewed conference proceeding :

> Jacquemin, J., Thiran, P., Quoilin, S. (2024). "*Decarbonizing Western Europe: Extension of the Model 'EnergyScope Multi-Cells' for the Analysis of Renewable Fuel Potential*". In proceedings of Latin America SDEWES 2024 conference.

Chapter 3, 4 and 5 are currently being adapted for publication in a peer-reviewed journal:

> Thiran, P., Jeanmart, H., & Contino, F., (2024). "*The role of renewable fuels in a fossil-free European whole-energy system*". (To be submitted).

Other publications are not presented in the thesis.
In a peer-reviewed conference publication, we published an analysis of the application of EnergyScope Multi-Cells to the Italian energy system divided into three regions:

> Thiran, P., Hernandez, A., Limpens, G., Prina, M. G., Jeanmart, H., & Contino, F. (2021). "*Flexibility options in a multi-regional whole-energy system: the role of energy carriers in the Italian energy transition.*" In proceedings of ECOS 2021 conference.

In parallel with the development of the European model, we tested several extensions on the regional model, EnergyScope. We studied the alternative indicators for the energy transition: the energy return on investment. We analyzed the impact of the energy transition in Belgium on that indicator in a peer-reviewed journal publication:

> Dumas, J., Dubois, A., Thiran, P., Jacques, P., Contino, F., Cornélusse, B., & Limpens, G. (2022). “*The energy return on investment of whole energy systems: application to Belgium*”. In Biophysical Economics and Sustainability, (Vol. 7(4)). URL: https://doi.org/10.1007/s41247-022-00106-0

We adapted near-optimal space exploration techniques to this multi-objective problem. We explored minimal levels of endogenous and exogenous energy sources for a net-zero Belgian energy system in a peer-reviewed journal publication:

> Antoine Dubois, Jonathan Dumas, Paolo Thiran, Gauthier Limpens, & Damien Ernst, (2023). “*Multi-objective near-optimal necessary conditions for multi-sectoral planning*”. In Applied Energy (Vol. 350). URL: https://doi.org/10.1016/j.apenergy.2023.121789

To improve the technical resolution of the regional model, we coupled it with a dispatch model of the electricity network that integrates more operation constraints. We published a paper in a peer-reviewed conference proceedings:

> Pavicevic, M., Thiran, P., Limpens, G., Contino, F., Jeanmart, H., & Quoilin, S. (2022). “*Bi-directional soft-linking between a whole energy system model and a power systems model*”. In proceedings of IEEE PES/IAS PowerAfrica conference, (1–5). URL: https://doi.org/10.1109/PowerAfrica53997.2022.9905392

We applied the EnergyScope to non-European countries: Uganda and Bolivia. We published these studies in peer-reviewed conference proceedings:

> Limpens, G., Thiran, P., Lara, E., Pavicevic, M., & Quoilin, S. (2022). “*Competitiveness of economic growth based on renewable energy: the case of Uganda to 2035.* In proceedings of IEEE PES/IAS PowerAfrica conference, (1–5). URL: https://doi.org/10.1109/PowerAfrica53997.2022.9905398

> Jimenez Zabalaga, P., Balderrama, S., Pavicevic, M., Cardozo, E., Thiran, P., Limpens, G., & Jeanmart, H. (2023). “*Towards Low-Carbon Energy Systems: The Case of Bolivia Until 2035*” In proceeding of ECOS 2023 conference (p.2006-2018). URL: https://doi.org/10.52202/069564-0182

We participated in developing and studying sufficiency scenarios at a European scale. We studied the impact of sufficiency measures in Europe with the PyPSA-Eur model in peer-reviewed conference proceedings:

> Tareen, M. U., Meyer, S., Thiran, P., Hernandez, A., Quoilin, S. (2023). "*Modeling the impact of energy sufficiency measures in European integrated energy systems using PyPSA-Eur*". In proceedings of ECEMP 2023 conference. URL: https://hdl.handle.net/2268/307557.

> Tareen, M. U., Meyer, S., Thiran, P., Hernandez, A., Quoilin, S. (2023). "*Modeling the impact of energy sufficiency measures on European integrated energy systems*". In proceedings of ECOS 2024 conference. URL: https://hdl.handle.net/2268/321049.

We participated in the publication of the method and results of the CLEVER project in a peer-reviewed journal:

> Wiese, F., Taillard, N., Balembois, E., Best, B., Bourgeois, S., Campos, J., Cordroch, L., Djelali, M., Gabert, A., Jacob, A., Johnson, E., Meyer, S., Munkácsy, B., Pagliano, L., Quoilin, S., Roscetti, A., Thema, J., Thiran, P., Toledano, A., Vogel, B., Zell-Ziegler, C., Marignac, Y. (2024). "*The key role of sufficiency for low demand-based carbon neutrality and energy security across Europe*". (Accepted) In Nature Communications.

Introduction

Overview

- Climate change and urgency to phase out fossil fuels.
- Importance of whole-energy system approach.
- Role of renewable fuels to reach fossil-free energy systems.
- Contributions and novelty.
- Thesis structure overview.

Modern societies rely heavily on energy. Energy provides us with many services and is inherent to our way of life whether we see it or not, from our transportation modes to the products we consume and the appliances we use. However, nowadays, most of this energy comes from fossil fuels. In Europe, more than 80% of the gross available energy supply comes from oil, fossil gas and coal [1–3]. These energy sources are the main ones responsible for greenhouse gas emissions and, therefore, for anthropogenic climate breakdown [4]. To mitigate climate change, it is of utmost importance to phase out their use as soon as possible [5]. This work tries to answer this question for Europe:

How can Europe build a fossil-free energy system by 2050?

However, our modern energy systems have always relied on fossil fuels and exploring options based on other energies, such as renewables, is a highly uncertain and complex problem [6–8]. Researchers have developed models to represent what an energy system with lower greenhouse gas emissions can look like [9–11]. Two main categories of models study climate mitigation pathways: integrated assessment models (IAMs) and energy system optimisation models (ESOMs).

Integrated assessment models have traditionally been used to explore climate mitigation pathways [12–21]. They are designed to represent complex physical and social systems, focusing on the interactions between the economy, society and the environment [22–24]. Their broad scope covers all energy-consuming sectors and their interactions with other systems. However, these models suffer from low spatio-temporal and technological details, essential when representing renewable-based energy systems [6, 25–27]. Therefore, these models underestimate the deployment of variable renewable energy sources [28–30] and the role of sector coupling and energy exchanges in their integration [31]. Hence, these models tend to overestimate the need for backup power plants and carbon capture and storage [32–36].

On the contrary, energy system optimisation models are bottom-up techno-economic models representing an energy system's spatio-temporal and technical characteristics in much more detail [37–39]. However, this more detailed representation comes at the cost of less cross-sectoral integration. Historically, this field has focused on the electricity sector [10, 39–42]. However, electricity represents nowadays only 21% of the energy consumed in Europe [1]. Although electrification will increase the electricity production, not all sectors can be electrified [43–48]. Therefore, a trend in recent years has been to integrate more sectors into the models [39, 40, 49, 50]. For instance, Brown et al. [51] have upgraded their PyPSA-Eur model by integrating space heating and private mobility demands. Later on, Neumann et al. [52] upgraded the same model by integrating all energy-consuming sectors (e.g. industry, freight, aviation, shipping). Other models have been upgraded similarly to integrate more sectors [53–55]. However, in all these models, the energy demand is included as the final energy consumption, making a priori assumptions about end-use technologies. By doing this, they miss possible synergies of sector coupling with efficiency and flexibility [42, 56, 57]. Two well-known models define the energy demand through end-use: TEMOA [58] and TIMES [59, 60]. However, they feature other weaknesses which make them unsuitable for our work. TEMOA was first developed as an electricity-only model [58] and further expanded to other demands such as space heating, hot water and passenger mobility [61, 62]. But, it never fully covered all the energy sectors. TIMES considers all energy sectors but it is not open-source which has been identified as an essential quality by the energy system modelling community. As summarized by Pfenninger et al. [63], open data and software are essential to better engage with decision-makers and continue to deliver robust policy advice in a transparent and reproducible way. Furthermore, both TEMOA and TIMES have a low temporal resolution and miss some challenges of the integration of variable renewable energy sources. Additionally, in existing energy system optimization models, the integration of multi-energy carriers is often only partially done [40]. For instance, the most recent study with PyPSA [52] only includes electricity and hydrogen exchanges between different regions. However, nowadays, energy fluxes through methane and petroleum products are much larger than electricity exchanges. Furthermore, several studies suggest that if a global hydrogen market arises, it will rely on other gaseous and liquid carriers, such as methane or ammonia, to be transported over long distances [48, 64, 65]. Overall, it is uncertain which types of energy carriers will transport the bulk energy in future energy systems. Thus, the models should consider all types of energy carriers for energy exchanges.

This is why Contino et al. [66] propose whole-energy system modelling as the advisor of the energy transition. The idea is to represent the entire energy system with all energy-consuming sectors and all energy carriers. This approach also has the particularity of defining the energy demand in terms of end-use demand. It quantifies the demand as close as possible to the service provided by the energy rather than as final energy in the form of fuel or electricity. This energy demand quantification approach allows the model to use all synergies from the energy sources to the end-uses to integrate high shares of renewable energies at the lowest cost.

Another motivation for using a whole-energy system approach is the potential role of renewable fuels in net-zero energy systems. Indeed, several studies have shown that electrification of end-uses such as space heating and passenger mobility is a crucial enabler towards a net-zero energy system [41, 51, 56, 67]. However, not all sectors can be electrified. For instance, sectors such as aviation, very-high-temperature heat, shipping and non-energy demand have no promising alternatives for direct electrification and need fuels [44–46, 68–70]. Many studies underline the potential of green hydrogen and its derivative to supply those needs [43, 47, 48, 71, 72]. However, these energy carriers need consequent infrastructures and are subject to energy losses to produce them. It makes them a strategic resource as they are costly to produce. Another source of fuel for these applications is biomass [73]. It is often overlooked in energy system models [46, 52, 53, 74]. However, it is currently the largest renewable energy source in the world (67% in 2018) [75]. Although its current use is mainly for heating, this might change with the defossilization of the system and because of the versatility of biomass [73]. Indeed, biomass feedstocks can be used as such (e.g. in boilers producing heat) or upgraded to more advanced fuels such as methane or methanol for specific applications. Therefore, Rixhon et al. [76] propose the concept of synthetic fuels as the grouping of both electro- and biofuels. In this work, we will talk about renewable fuels, a particular category of synthetic fuels produced from renewable energy sources. In this category, we also include the direct use of biomass for final use. With fossil fuels phase-out, renewable fuels become essential for many uses, from aviation to energy exchanges. However, they are strategic resources as they are costly to produce, with losses through the energy conversion chain and competing interests with other uses. Therefore, there is a need to model the different conversion paths and uses for renewable fuels in an integrated model representing competing interests for those fuels and competing solutions for the different energy demands. It brings forward the following research question:

What is the role of renewable fuels in a fossil-free European energy system?

This thesis fills this gap in the integrated modelling of a fossil-free whole-energy system for Europe by developing the EnergyScope Multi-Cells model. This model extends the open-source regional whole-energy system optimisation model, EnergyScope [41]. The original model represents one region with its energy resources, conversion system and demands. We extend it by making it multi-regional: it represents multiple interconnected regions with, each one its own energy resources, conversion system and demands. We apply this novel model to a fossil-free and nuclear-free European energy system and analyse the role of renewable fuels in this system. Additionally, this model is open-source and documented. Indeed, transparency is one of the key challenges of energy system planning [63, 77]. All the information about data availability, code availability, and documentation are in the Appendix A.

One key challenge with growing model size and complexity is the computational burden [78]. This challenge is exacerbated by the need for several model evaluations to represent the impact of uncertainties or propose different solutions to reach carbon neutrality. Many techniques exist to reduce the complexity of those models while keeping their accuracy [79]. One of those techniques has seen a growing interest in recent years for its efficiency: temporal aggregation using typical days [80]. The general idea is to use the fact that many days during the year have similar spatio-temporal patterns regarding energy demand and renewable energy production. Therefore, we can represent the entire year with only a subset of days called typical days. However, the impact of this technique on energy system design was never quantified, and no simple method exists to select the number of typical days. We fill this gap by developing a metric to evaluate the error in the energy system design due to the use of typical days. With this metric, we validate the use of typical days for multi-regional whole-energy system models. We compare this design error with a priori evaluations of the error on time series. From this comparison, we develop a simple method to select the number of typical days for an ESOMs. Applying this to our European model of 34 countries, we choose 16 typical days and reach the following performances: one model evaluation takes around 20 hours and uses 208GB of memory. With a working model, we apply it to a fossil-free and nuclear-free European energy system to answer the two research questions stated above.

When planning for the long-term future, more than one scenario is required. A complete uncertainty quantification is not feasible due to the computational burden and the lack of characterisation of the numerous uncertain parameters of our model. For instance, Rixhon et al. [8], for a regional model of Belgium, needed 1595 model evaluations to analyse the impact of the uncertainty on input data on the system's total cost. For a carbon-neutral Belgian energy system in 2050, they obtained a standard deviation of 15% on the total system cost. However, their analysis does not provide insights into the design of the energy system. Furthermore, our European model has more input parameters and uncertainties than their Belgian model. Characterising the uncertainty of input parameters is a complex and demanding task [7]. Both the uncertainty characterisation and propagation become heavier and heavier as the model size and complexity rise [7, 81]. Therefore, we opt for an alternative approach: studying different scenarios. Those scenarios follow a storyline and regroup different uncertainties. Furthermore, scenario analysis can integrate compromises with other socio-economic-environmental dimensions not modelled in the energy system optimisation model [82].

A third approach to face the uncertainty of future energy systems is through modelling to generate alternatives (MGA) based on the exploration of the near-optimal space [58]. This approach comes from the following conclusion: it is impossible to fully address structural and parametric uncertainty in large planning models. Furthermore, energy system design problems have a flat optimum. Many solutions are nearly as good as the optimal one in terms of cost and can lead to very different designs. Therefore, many interesting solutions may lie in the near-optimal region. For instance, Pickering et al. [53] have explored 441 technically feasible designs for a carbon-neutral European system. These solutions are cost-effective options, with less than a 10% cost increase compared to the optimum. Pickering et al. compared them by looking at seven key indicators, such as storage capacity, biofuel utilisation and heat electrification. They showed that a diversity of options is feasible to reach carbon neutrality. For instance, they present system designs with 0.03 TW of storage discharge capacity in Europe and others with 11 TW. Furthermore, as shown by Finke et al. [83], an energy system design obtained through the exploration of the near-optimal space in one direction can be equivalent to a cost minimisation with modified cost terms and vice versa. In other words, exploring the near-optimal space addresses from another perspective than global sensitivity analysis the parametric uncertainty from input data.

Similarly to many other studies[84–95], Pickering et al. use a method that guarantees they can explore all the parts of the near-optimal space as thoroughly as possible. However, this approach requires many model evaluations, i.e. 441 in this case. Dubois et al. [85] propose another approach for exploring the near-optimal space. They explore it in a chosen direction up to the intersection with the near-optimal space boundary. This method focuses on finding the boundary of the near-optimal space for some variables of interest, thus encircling the possible designs. For instance, they explore the minimal new capacity of onshore wind, offshore wind and utility PV to reach a carbon-neutral European electricity system for different cost increases compared to the optimal cost [85]. In another study, they applied the same method to minimise the imports of renewable fuels in a carbon-neutral Belgian energy system [86]. This near-optimal space exploration method provides very different options with few model evaluations.

However, all these studies explore the near-optimal space while keeping the same scenario with the same assumptions. The solution space, the optimal design and the near-optimal space depend on the chosen assumptions. These studies might miss some interesting designs. To overcome this limitation, we develop a hybrid method that combines scenario analysis and near-optimal space exploration. Considering different scenarios opens different design spaces, which leads to new optimal designs and near-optimal spaces.

We apply the hybrid method to three scenarios and three near-optimal directions. The three different scenarios for a fossil-free European energy system are: (i) the Reference scenario with a high-demand projection and no nuclear energy; (ii) the Sufficiency scenario with a low demand and no nuclear energy; (iii) the Nuclear scenario with a high-demand and nuclear energy. For each of these scenarios, we explore three directions with the approach of Dubois et al.: (i) minimising the onshore renewables (i.e. utility PV, onshore wind and concentrated solar power (CSP)); (ii) minimising the use of biomass; (iii) minimising the expansion of the cross-border electricity network. These scenarios and exploration directions are a way to integrate other socio-politico-environmental concerns of the transition that are not modelled in our techno-economic model. For instance, the Sufficiency scenario raises the question of societal organisations to reduce our consumption of energy services. The Nuclear scenario represents the impact of a political decision to invest massively in nuclear power plants. We choose the three exploration directions because they are essential in the results of the Reference scenario in the optimal case but lead to adverse environmental and socio-political impacts (e.g. land use, social acceptance).

Finally, this thesis explores 12 different options for a fossil-free European energy system. It highlights the key characteristics of a fossil-free system that appear regardless of the design —the must-haves— and shows where there is space for a choice and the counterparts of the different choices —the trade-offs.

Contributions and outline of the thesis

To answer the above research questions, this thesis explores the different options for a fossil-free European energy system. It is composed of three methodological chapters and two result chapters. The three methodological chapters bring the following contributions:

- **EnergyScope Multi-Cells.** This energy system optimization model has several features that make it unique and a good candidate for answering the challenges identified by energy system modelling reviews [6, 10, 41, 66, 96]: (i) a good spatio-temporal resolution, with its multi-regional formulation and an hourly resolution over the year; (ii) a whole-energy system approach, including the coverage all the energy sectors, with a technology-rich portfolio, the quantification of all energy demands as end-use demands, and the modelling of all energy carriers both in local energy systems and for energy exchanges; (iii) open-source and documented. I developed it by extending the regional whole-energy system model, EnergyScope, to a multi-regional model with a whole-energy approach to energy exchanges.
- **A fossil-free European whole-energy system model.** This thesis proposes the implementation of a fossil-free European whole-energy system model with EnergyScope Multi-Cells. It provides a brand-new and complete database for this whole-energy system modelling with two alternative scenarios quantifying the investment in nuclear energy and a low demand for each European country.
- **A method to select a priori the number of typical days for an energy system optimisation model.** This thesis shows the link between the time series error due to typical days clustering and the design error on the energy system. Thereby, it validates the use of time series error as an a priori metric to select the number of typical days.
- **A hybrid method to explore a diversity of options.** This work develops a hybrid method combining scenario analysis and near-optimal space exploration. This method provides alternative system designs that are as good as the optimal one in terms of cost and can feature other advantages.

The chapters are structured as follows:

- **Chapter 1: European whole-energy system model.** This chapter presents the energy system optimization model and its implementation for a fossil-free and nuclear-free European energy system (the Reference scenario). The model's description is divided into two parts: the optimization model and the European application. Indeed, the EnergyScope Multi-Cells model is suitable for any multi-regional whole-energy system and has already been applied to other case studies. In this thesis, we apply it to Europe.
- **Chapter 2: Representing spatio-temporal variability through typical days.** This chapter presents the validation of the typical days' method for a multi-regional whole-energy system optimization model. It develops a metric to evaluate the design error due to this technique. By comparing it with a priori quantification of the time series error due to typical days, this chapter proposes a method to select the number of typical days for any energy system optimization model.
- **Chapter 3: The role of renewable fuels in a fossil-free European energy system.** With a working and efficient model from the two previous chapters, this chapter analyzes the Reference scenario results. It provides key insights into the design of a fossil-free and nuclear-free European energy system. In particular, it underlines the critical role of renewable fuels in defossilizing hard-to-abate sectors and for energy storage and exchanges.
- **Chapter 4: Hybrid method to explore a diversity of options.** This chapter presents the hybrid method combining scenario analysis and near-optimal space exploration and its application to Europe. It details the assumptions of the two alternative scenarios: Sufficiency and Nuclear. It motivates and describes the three near-optimal space exploration directions.
- **Chapter 5: Diversity of options of a fossil-free European energy system.** This chapter analyzes the twelve system designs obtained with the hybrid method. It presents the different responses of the different scenarios to each near-optimal direction exploration. It highlights the main trade-offs and must-haves for a fossil-free system.

Finally, the conclusion summarizes five main outcomes of the thesis and proposes five perspectives for future works.

In each chapter, we use the following convention:

> At the end of the chapter's introduction, a paragraph providing the structure of the chapter is outlined with a grey vertical bar.

1 European whole-energy system model

All models are wrong, but some are useful.
George P. Box

Chapter overview

- A generic multi-regional whole-energy system optimisation model: EnergyScope Multi-Cells.
- Modelling a fossil-free European energy system in 2050.

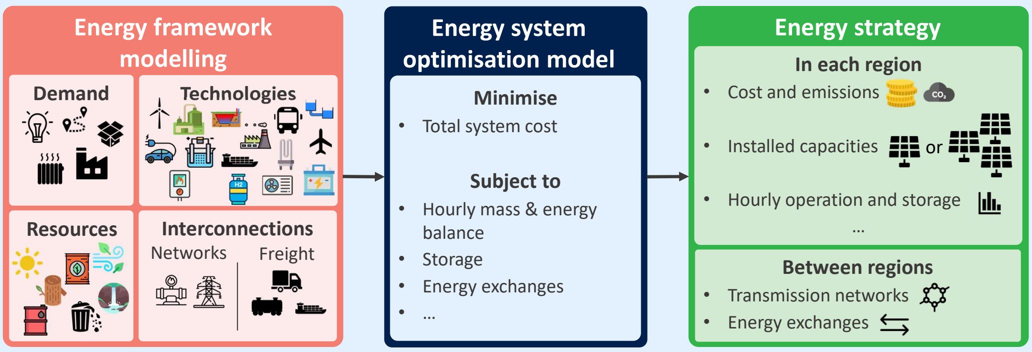

Figure 1.1: Overview of the energy system modelling framework.

This chapter presents the modelling approach used to study :

How can Europe build a fossil-free energy system by 2050?

We develop a multi-regional whole-energy system model, EnergyScope Multi-Cells, applied to Europe in 2050. It is a linear programming model optimising the annualised total cost of the system under several constraints: power balance for each energy carrier, exchanges between cells, storage level, availability of resources, etc. This model is built as an extension of the open-source model EnergyScope TD [41].

EnergyScope TD is a generation expansion planning model. Compared to other models of this category, it has two main specificities. Firstly, it is a whole-energy system model [66]. This means that it considers all the different energy sectors and their specific energy demand. This has the advantage of putting forward synergies between sectors and competition for the same resources. Secondly, it defines the energy demand as end-use demand (EUD) and not as final energy consumption (FEC). This has the advantage of being closer to real energy services and everyday life. Furthermore, this allows for underlining synergies between end-use technologies and other technologies in the energy system. For instance, Limpens et al. [56] showed with EnergyScope TD applied to Belgium the synergy between PV production and decentralised heat pumps (HPs) with a thermal storage. This kind of synergy could not be considered with models based on a FEC approach. For these reasons, we based our work on extending this model towards a multi-regional model. The validity of both the original model [8, 42, 56, 73, 97–101] and the extension [102–104] was verified in previous studies.

Figure 1.2 illustrates with a conceptual example the extension of EnergyScope TD to EnergyScope Multi-Cells. This extension adds the possibility of representing different regions, also called cells. Each cell is considered as one node with its own energy demand, resources and energy conversion system. At each node, the energy balance for each energy carrier is ensured for all time steps, and each cell can exchange different energy carriers with other cells. As the model is developed into a whole-energy system perspective, electricity is not the only carrier considered for energy exchanges between regions. The model is designed to consider also other types of energy carriers such as gaseous and liquid fuels. Some are transported through networks (e.g. electricity, methane or hydrogen), and others are transported through freight (e.g. ammonia, methanol or woody biomass). Both the quantity exchanged and the interconnector sizes, or the freight needed to transport these resources, are optimised by the model.

> The modelling is done in two steps; see Figure 1.1. Firstly, Section 1.1 presents the energy system optimization model. This model is kept it as generic as possible such that it can be used with any multi-regional whole-energy system. For instance, it has already been used to model Italy divided into three main regions [102] and to model Western Europe into six macro-regions [104, 105]. Secondly, Section 1.2 presents the modelling of a European fossil-free energy system in 2050.

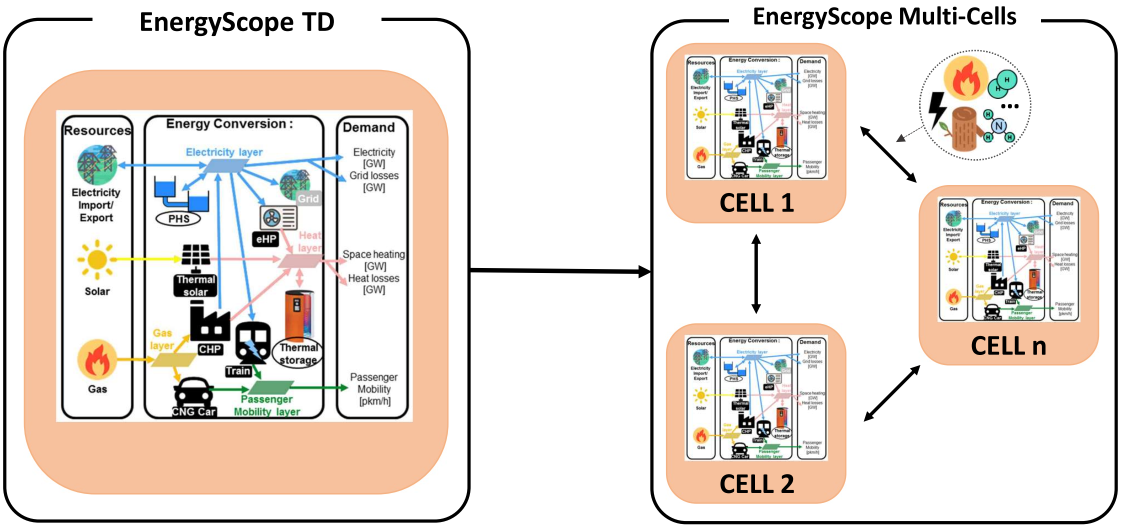

Figure 1.2: Conceptual example of an energy system modelled with EnergyScope TD and extension to EnergyScope Multi-Cells. Adapted from [99]. Abbreviations: combined heat and power (CHP), compressed natural gas (CNG), electrical heat pump (eHP), gigawatt (GW), pumped hydro storage (PHS), passenger-kilometre (pkm).

Contributions

To keep a self-sustaining description of the model, the entire model is described in this chapter. As many parts of the previous works [99, 106] are taken as such or barely modified, my contributions to developing the European model are detailed here.

Regarding the optimisation model, most equations, variables, and parameters remained unchanged, but a region dimension was added to them. For instance, the quantity of PV panels installed is defined for each region. This is not the case for all parameters and variables. Some are considered constant across regions (e.g. efficiency of technologies). Other parts of the model were extended or modified either to develop the multi-regional version or to improve its representation of a whole-energy system:

- Separating the mathematical formulation for resources from the one for technologies. It is justified by the fact that in a multi-regional model, some resources can also be exchanged between different regions considered in the model. It adds the distinction between a resource produced locally or imported from the exterior of the overall system, giving different costs (Eq (1.6)), life-cycle emissions (Eq. (1.9)) and availabilities (Eqs. (1.14) and (1.15)).
- Adding equations to allow the exchanges between regions Eqs. (1.24) - (1.27). Adapting

the layer balance to include these exchanges into the balance of each region, Eq. (1.17).

- Modelling two main types of interconnections according to their mean of exchange: network (Eqs. (1.29)-(1.35)) or freight (Eqs. (1.36)-(1.37)). For network exchanges, the possibility of retrofitting the methane transmission network to a hydrogen transmission network is also modelled.
- Adding new demands to the model, aviation and shipping, to go further into the whole-energy system approach, and because they might become important consumers of renewable fuels. These demands and the technologies to provide them were adapted from a master thesis I co-supervised [107]. This master thesis was adapted into a peer-reviewed conference paper [108].
- Adapting the detailed formulation of the non-energy demand (NED) done by Rixhon et al. [101] for Belgium to a multi-regional model.
- Adding $CO_{2,net}$ accountability, Eq. (1.10). In previous versions of the model, the emissions of resources are accounted for over its entire life. It includes direct and indirect emissions. Although this is a relevant accountability, it does not align with the international accountability that only considers net emissions. We add this accountability in parallel with the existing one to make it easier to compare with other studies.
- Adapting the equation of hourly capacity factor to account explicitly for the curtailment, Eq. (1.12). A new variable to compute the curtailment is added. It simplifies the postprocessing compared to previous versions but does not change the results. In the previous version, the curtailment had to be computed as the difference between the actual and potential production of renewable assets. Now, it is described by a variable and directly output from the model.
- Improving the modelling of vehicle-to-grid (in collaboration with Gauthier Limpens). Adapting the storage availability equation for *EVs_BATT* to better account for the fact that riding cars cannot be plugged in. Adding an equation to force a certain minimal state of charge (SOC) at any hour of the day.
- Modelling CSP technologies with the possibility of sizing collector field, storage and power block. Considering the land use competition between utility PV and CSP. This modelling was adapted from Dommisse and Tychon. [109] and improved.
- Adding space and process cooling demands and technologies, adapted from [42, 109].

For the implementation of the European energy system model, Dommisse and Tychon [109] produced a database for EnergyScope for each European Union (EU) country for 2035.

In this work, we improved the database and adapted it for 2050. All the elements that are not cited here are taken directly from Dommisse and Tychon.

- Redefining potentials for wind, solar and biomass for each European country based on ENSPRESO database [110].
- Refining the modelling of biomass by dividing it into five different feedstocks with different costs and availability. Updating the entire conversion chain for these five feedstocks. This extension is adapted from
- Computing actual and potential capacity for hydropower for each European country by combining the JRC Hydro Power Plants database [111], the e-highway database per country [112] and the JRC study for new pumped hydro storage (PHS) potentials [113].
- Computing and projecting the EUDs for each European country in 2035 and 2050.
- Computing and projecting the aviation and shipping demands and adding of technologies to supply those, adapted from [107].
- Computing the NED for 2019 in each European country and projecting it to 2035 and 2050. This data extraction method is adapted from Rixhon et al. [101].
- Recomputing and checking time series consistency across the different countries.
- Collecting data for non-EU countries: United Kingdom, Norway, Switzerland, Albania, Bosnia and Herzegovina, Montenegro, North Macedonia, Serbia and Kosovo.
- Updating the cost data for the main renewable energy sources (wind and PV) and differentiating utility-scale PV from rooftop PV. Those data come from the Danish Energy Agency's Technology Catalogue [114].
- Adding emission factors for net emissions computation.
- Adding all the data and modelling for exchanges: actual network capacities, network expansion capacity, network losses, costs, typical distances between countries, retrofitting possibility of methane network to hydrogen network.

In addition to these contributions, I developed a Python framework for EnergyScope TD and EnergyScope Multi-Cells that automates the data preprocessing, the model run, and some of the data postprocessing. This integrated pipeline eases the use of the model.

The model is open-source and documented. The latest version is stored on the GitHub repository [115]. The full documentation describing both the optimization model and the representation of the European energy system is kept up to date on a ReadTheDocs [116]. The model version and the model evaluation analyzed in Chapters 3 and 5, with the results, graphs and analysis scripts are stored on Zenodo [117].

1.1 Multi-regional whole-energy system optimisation model

This section presents the mathematical formulation of the energy system optimization model. It is a linear programming (LP) problem [118] and is composed of the following elements:

- In italic capital letters, the *SETS* are collections of distinct items (as in the mathematical definition), e.g. the *TECHNOLOGIES* set regroups all the available technologies (PV, combined cycle gas turbine (CCGT), electrolyser, battery, methanol truck, etc.).
- In italic lowercase letters, the *parameters* are known values (inputs) of the model, such as the cost of technologies, the efficiency of technologies, the energy demand or the availability of resources.
- In bold with the first letter in uppercase, the **Variables** are unknown values of the model, such as the installed capacity of PV. These values are determined (optimised) by the solver.
- The **Constraints** are inequality or equality relations between parameters and variables. They can be indexed over the *SETS*. For instance, each element of the *SET TECHNOLOGIES* can be installed with a capacity (**variable F**) that is bounded by minimum and maximum (*parameters* f_{min} and f_{max}).
- The **Objective function** which is minimised (or maximised) while respecting all the constraints.

The model optimises the design of the energy system to meet the energy demand at each hour and minimise the total annual cost of the overall system. In each region, the model determines each technology's installed capacity and operation at each hour. Between regions, the model determines the interconnection installed and the energy exchanged in each period.

In the following, we present the complete formulation of the model in two parts. First, all the terms used are summarised in a figure and tables: Table 1.1 and 1.2 for *SETS*, Tables 1.3 to1.5 for *parameters*, and Tables 1.6 and 1.7 for **Variables**. Second, the equations representing the constraints and the objective function are formulated in Figure 1.3 and Eqs. (1.1)-(1.68) and described in the following paragraphs.

The model uses an approach based on TDs. The method is explained in more detail and validated in Chapter 2. Basically, it allows for reducing the computational burden while capturing spatio-temporal variability at different timescales, from hourly to seasonal. It reaches that by: (i) solving most temporal dependant variables on each hour of a set of representative days called TDs; (ii) solving equations related to storage on a recomposed synthetic time series to capture longer-term variability.

1.1.1 Sets, parameters and variables

Tables 1.1 and 1.2 list and describe the *SETS* with their relative indices used in the equations. Tables 1.3 to 1.5 list and describe the model *parameters*. Tables 1.6 and 1.7 list and describe the independent and dependent **Variables**, respectively.

Table 1.1: List of sets and subsets related to the spatial and temporal part of the optimisation problem with their index. The set name is as close as possible to the name in the code. The index is the short name on which we index the equations in this document. It is used in capital letters when it points to the entire set and in lowercase letters when it points to each set instance.

Set name	Index	Description
Regions		
REGIONS	*REG*	Regions
RWITHOUTDAM	-	Subset of regions without hydro dams
Periods		
PERIODS	*T*	Time periods, hours of the year[a]
HOURS	*H*	Hours of the day
TYPICAL_DAYS	*TD*	Typical days

[a] As the model uses typical days, a mapping is necessary to go from hourly data on typical days to hourly data over the entire year. In the equations, this mapping is noted as $t(h, td) \in T$. More information about this mapping is explained in the Chapter 2.

Table 1.2: List of sets and subsets related to demands, resources and technologies with their index. The set name is as close as possible to the name in the code. The index is the short name on which we index the equations in this document. It is used in capital letters when it points to the entire set and in lowercase letters when it points to each set instance.

Set	Index	Description
Demands		
SECTORS	*S*	Sectors of the energy system
END_USES_INPUT	*EUI*	EUD inputs to the model
END_USES_TYPES	*EUT*	EUD types in the model
END_USES_CATEGORIES	*EUC*	EUD categories
EUT_OF_EUC(euc)	*EUT_OF_EUC(euc)*	Subsets of EUD types regrouped into categories
Resources		
RESOURCES	*RES*	Energy resources
RE_RESOURCES	RES_{re}	Subset grouping renewable resources
RES_IMPORT_CST	RES_{cst}	Subset grouping resources with a constant import over the year
EXCHANGE_R	*ER*	Subset of resources considered for energy exchanges
NOEXCHANGES	*NOEXCHANGES*	Subset of resources not considered for exchanges
EXCHANGE_NETWORK_R	*NER*	Subset of *ER* for resources exchanged through a network
EXCHANGE_FREIGHT_R	*FER*	Subset of *ER* for resources exchanged through freight
Layers		
LAYERS	*L*	Set of layers balanced at each time step, regroups *EUT* and *RES*
Technologies		
TECHNOLOGIES	*TECH*	Technologies
TECH_OF_EUC(euc)	*TECH_OF_EUC(euc)*	Subsets of technologies supplying each EUD category
TECH_OF_EUT(eut)	*TECH_OF_EUT(eut)*	Subsets of technologies supplying each EUD type
STORAGE_TECH	*STO*	Subset grouping the storage tech.
STORAGE_DAILY	*STO_DAILY*	Subset of daily storage technologies
STO_OF_EUT(eut)	*STO_OF_EUT(eut)*	Subset of storage technologies related to each EUD type
TS_OF_DEC_TECH(tech)	*TS_OF_DEC_TECH(tech)*	Subset of thermal storage technologies linked with each decentralised heating technology
V2G	*V2G*	Set of electric vehicles (EVs) which can be used for vehicle-to-grid (V2G)
EVs_BATT	*EVs_BATT*	Set of batteries of EVs
EVs_BATT_OF_V2G	*EVs_BATT_OF_V2G*	Set linking EVs batteries with their EVs
NETWORK_TYPE(ner)	*NT(ner)*	Subsets of network types for each resource exchanged through networks

Table 1.3: Time series parameters

Parameter	Units	Description
$\%_{elec}(reg, h, td)$	[-]	Yearly time series (adding up to 1) of electricity end-uses
$\%_{sh}(reg, h, td)$	[-]	Yearly time series (adding up to 1) of space heating (SH) end-uses
$\%_{sc}(reg, h, td)$	[-]	Yearly time series (adding up to 1) of space cooling (SC) end-uses
$\%_{pass}(reg, h, td)$	[-]	Yearly time series (adding up to 1) of passenger mobility end-uses
$\%_{fr}(reg, h, td)$	[-]	Yearly time series (adding up to 1) of freight mobility end-uses
$c_{p,t}(tech, reg, h, td)$	[-]	Hourly maximum capacity factor for each technology (default 1)
$soc_{ev}(v2g, h)$	[-]	Minimum state of charge of EVs battery at each hour of the day

Table 1.4: List of parameters (except time series, part 1).

Parameter	Units	Description
$\tau(reg,\ tech)$	[-]	Investment cost annualization factor
i_{rate}	[-]	Real discount rate
$endUses_{year}(reg, eui, s)$	[GWh/y][a]	Annual end-uses in energy services per sector
$endUsesInput(reg, eui)$	[GWh/y][a]	Total annual end-uses in energy services
$f_{min}, f_{max}(reg,tech)$	[GW][bc]	Min./max. installed size of the technology
$f_{min,\%}, f_{max,\%}(reg,tech)$	[-]	Min./max. relative share of a technology in a layer
$avail_{local}(reg,res)$	[GWh/y]	Resource yearly total local availability in each region
$avail_{ext}(reg,res)$	[GWh/y]	Resource yearly total availability for import from the exterior of the overall system in each region
$c_{op,local}(reg,res)$	[M€$_{2015}$/GWh]	Specific cost of local resources in each region
$c_{op,ext}(res)$	[M€$_{2015}$/GWh]	Specific cost of resources coming from the exterior
$veh_{capa}(tech)$	[km-pass/h/veh.]	Mobility capacity per vehicle (veh.).
$\%_{Peak_{sh}}(reg)$	[-]	Ratio peak/max. space heating demand in typical days
$\%_{Peak_{sc}}(reg)$	[-]	Ratio peak/max. space cooling demand in typical days
$f(res \cup tech \setminus sto, l)$	[GW][c]	Input from (< 0) or output to (> 0) layers. $f(i, j) = 1$ if j is main output layer for technology/resource i
$c_{inv}(reg,tech)$	[M€$_{2015}$/GW][bc]	Technology specific investment cost
$c_{maint}(reg,tech)$	[M€$_{2015}$/GW/y][bc]	Technology specific yearly maintenance cost
$lifetime(reg,tech)$	[y]	Technology lifetime
$gwp_{constr}(reg,tech)$	[ktCO$_2$-eq./GW][bc]	Technology construction specific GHG emissions
$gwp_{op,local}(reg,res)$	[ktCO$_2$-eq./GWh]	Specific GHG emissions of local resources

[a] Instead of [GWh], we have [Mpkm] (millions of passenger-km) for passenger mobility and aviation, [Mtkm] (millions of ton-km) for freight mobility and shipping end-uses

[b] Instead of [GW], we have [GWh] if $tech \in STO$.

[c] Instead of [GW], we have [Mpkm/h] for passenger mobility and aviation end-use technologies, and [Mtkm/h] for freight mobility and shipping end-use technologies.

Table 1.5: List of parameters (except time series, part 2).

Parameter	**Units**	**Description**
$re_{share}(reg)$	[-]	Minimum share [0;1] of primary renewable energy (RE)
$gwp_{limit}(reg)$	[ktCO$_{2\text{-eq}}$/y]	Higher CO$_{2\text{-eq}}$ emissions limit for each region
$gwp_{limit,overall}$	[ktCO$_{2\text{-eq}}$/y]	Higher CO$_{2\text{-eq}}$ emissions limit for the overall system
$\%_{public,min}(reg), \%_{public,max}(reg)$	[-]	Lower and upper limit to $\boldsymbol{\%_{Public}}$
$\%_{av,short,min}(reg), \%_{av,short,max}(reg)$	[-]	Lower and upper limit to $\boldsymbol{\%_{Av,Short}}$
$\%_{fr,rail,min}(reg), \%_{fr,rail,max}(reg)$	[-]	Lower and upper limit to $\boldsymbol{\%_{Fr,Rail}}$
$\%_{fr,boat,min}(reg), \%_{fr,boat,max}(reg)$	[-]	Lower and upper limit to $\boldsymbol{\%_{Fr,Boat}}$
$\%_{fr,road,min}(reg), \%_{fr,road,max}(reg)$	[-]	Lower and upper limit to $\boldsymbol{\%_{Fr,Road}}$
$\%_{dhn,min}(reg), \%_{dhn,max}(reg)$	[-]	Lower and upper limit to $\boldsymbol{\%_{Dhn}}$
$\%_{ned}(reg, eut\_of\_euc(NED))$	[-]	Share of the different feedstocks for the NED
$t_{op}(h, td)$	[h]	Time period duration (default 1h)
$gwp_{op,ext}(res)$	[ktCO$_2$-eq./GWh]	Specific GHG emissions of resources from the exterior
$co2_{net}(res)$	[ktCO$_2$-eq./GWh]	Specific net GHG emissions of resources
$c_p(reg, tech)$	[-]	Yearly capacity factor
$\eta_{sto,in}, \eta_{sto,out}(sto, l)$	[-]	Efficiency [0;1] of storage input from/output to layer. Set to 0 if storage not related to layer.
$\%_{sto_{loss}}(sto)$	[1/h]	Losses in storage (self discharge)
$t_{sto_{in}}, t_{sto_{out}}(reg, sto)$	[h]	Time to charge/discharge storage (Energy to power ratio)
$\%_{sto_{avail}}(sto)$	[-]	Storage technology availability to charge/discharge
$\%_{net_{loss}}(eut)$	[-]	Losses coefficient [0; 1] in the networks (grid and DHN)
$ev_{batt,size}(v2g)$	[GWh]	Battery size per V2G car technology
$c_{grid,extra}$	[M€$_{2015}$/GW]	Cost to reinforce the grid per GW of intermittent renewable
$elec_{import,max}(reg)$	[GW]	Maximum net transfer capacity
$solar_{area,rooftop}(reg)$	[km^2]	Available area for solar panels on rooftop in each region
$solar_{area,ground}(reg)$	[km^2]	Available area for solar panels on the ground in each region
$solar_{area,ground,csp}(reg)$	[km^2]	Available area for CSP in each region
$power\_density_{pv}$	[GW/km^2]	Peak power density of PV
$power\_density_{solar\ thermal}$	[GW$_{th}$/km^2]	Peak power density of solar thermal
$power\_density_{pt}$	[GW$_{th}$/km^2]	Peak power density of solar parabolic trough (pt) power plants
$power\_density_{st}$	[GW$_{th}$/km^2]	Peak power density of solar tower (st) power plants
sm_{max}	[-]	Maximum solar multiple for CSP plants
$exch_{loss}(er)$	[-]	Exchanges losses
$tc_{min}, tc_{max}(reg,reg,ner,nt(ner))$	[GW]	Min./max. transfer capacity for each network type of each network exchange resource
$ch4toh2$	[-]	Diminution of transfer capacity when retrofitting methane to hydrogen pipelines
$lhv(fer)$	[GWh/t]	Energy density of freight exchanged resources
$dist\ (reg_1, reg_2)$	[km]	Typical distance between two regions, set to 0 for non-neighbouring regions

Table 1.6: Independent variables. All variables are continuous and non-negative.

Variable	Units	Description
$\mathbf{\%_{Public}}$ *(reg)*	[-]	Ratio [0; 1] public mobility over total passenger mobility
$\mathbf{\%_{Av,Short}}$ *(reg)*	[-]	Ratio [0; 1] short-haul aviation over total passenger mobility
$\mathbf{\%_{Fr,Rail}}$ *(reg)*	[-]	Ratio [0; 1] rail transport over total freight transport
$\mathbf{\%_{Fr,Boat}}$ *(reg)*	[-]	Ratio [0; 1] boat transport over total freight transport
$\mathbf{\%_{Fr,Road}}$ *(reg)*	[-]	Ratio [0; 1] road transport over total freight transport
$\mathbf{\%_{Dhn}}$ *(reg)*	[-]	Ratio [0; 1] centralized over total low-temperature heat
$\mathbf{F}(reg, tech)$	[GW][a]	Installed capacity for main output
$\mathbf{F_t}(reg, tech, h, td)$	[GW][a]	Operation in each period
$\mathbf{R_{t,local}}(reg, res, h, td)$	[GW]	Use of local resources
$\mathbf{R_{t,ext}}(reg, res, h, td)$	[GW]	Use of resources imported from the exterior
$\mathbf{Sto_{in}}, \mathbf{Sto_{out}}(reg, sto, l, h, td)$	[GW]	Input to/output from storage units
$\mathbf{Tc}(reg_1, reg_2 ner, nt(ner))$	[GW]	Installed transfer capacity between two regions
$\mathbf{Exch_{imp}}, \mathbf{Exch_{exp}}(reg_1, reg_2, er, h, td)$	[GW]	Import/export of exchanged resources to/from region 1 from/to region 2
$\mathbf{P_{Nuclear}}(reg)$	[GW]	Constant load of nuclear
$\mathbf{\%_{PassMob}}(reg, TECH\_OF\_EUC(PassMob))$	[-]	Constant share of passenger mobility
$\mathbf{\%_{FreightMob}}(reg, TECH\_OF\_EUC(FreightMob))$	[-]	Constant share of freight mobility
$\mathbf{\%_{Shipping}}(reg, TECH\_OF\_EUC(Shipping))$	[-]	Constant share of shipping
$\mathbf{\%_{HeatDec}}(reg, TECH\ OF\ EUT((HeatLowTDEC) \setminus \{Dec_{Solar}\})$	[-]	Constant share of low temperature heat decentralised supplied by a technology plus its associated thermal solar and storage
$\mathbf{F_{sol}}(reg, TECH\_OF\_EUT((HeatLowTDEC) \setminus \{Dec_{Solar}\})$	[GW]	Solar thermal installed capacity associated to a decentralised heating technology
$\mathbf{F_{t_{sol}}}(reg, TECH\ OF\ EUT((HeatLowTDEC) \setminus \{Dec_{Solar}\})$	[GW]	Solar thermal operation in each period

[a] [Mpkm] (millions of passenger-km) for passenger mobility and aviation, [Mtkm] (millions of ton-km) for freight mobility and shipping end-uses, [GWh] if *tech* ∈ *STO*.

Table 1.7: Dependent variable. All variables are continuous and non-negative.

Variable	Units	Description
$\mathbf{EndUses}(reg, l, h, td)$	[GW][a]	End-uses demand. Set to 0 if $l \notin EUT$
$\mathbf{C_{tot}}(reg)$	[M€$_{2015}$/y]	Total annual cost of the energy system
$\mathbf{C_{inv}}(reg, tech)$	[M€$_{2015}$]	Technology total investment cost
$\mathbf{C_{maint}}(reg, tech)$	[M€$_{2015}$/y]	Technology yearly maintenance cost
$\mathbf{C_{op}}(reg, res)$	[M€$_{2015}$/y]	Total cost of resources
$\mathbf{GWP_{tot}}(reg)$	[ktCO_2-eq./y]	Total yearly GHG emissions of the energy system
$\mathbf{GWP_{constr}}(reg, tech)$	[ktCO_2-eq.]	Technology construction GHG emissions
$\mathbf{GWP_{op}}(reg, res)$	[ktCO_2-eq./y]	Total GHG emissions of resources
$\mathbf{CO2_{net}}(reg, res)$	[ktCO_2-eq./y]	Total net GHG emissions of resources
$\mathbf{Curt}(reg, tech, h, td)$	[GW]	Curtailment of technologies
$\mathbf{Net_{loss}}(reg, eut, h, td)$	[GW]	Losses in the networks (grid and DHN)
$\mathbf{Sto_{level}}(reg, sto, t)$	[GWh]	Energy stored over the year
$\mathbf{R_{t,imp}}, \mathbf{R_{t,exp}}(reg, res, h, td)$	[GW]	Import/Export of resources from neighbouring regions
$\mathbf{Imp_{cst}}(reg, res_{cst})$	[GW]	Constant import from the rest of the world
$\mathbf{Freight_{exch,b}}(reg_1, reg_2)$	[Mtkm]	Additional yearly freight due to exchanges across each border
$\mathbf{Freight_{exch}}(reg)$	[Mtkm]	Additional yearly freight due to exchanges

[a] [Mpkm] (millions of passenger-km) for passenger mobility and aviation, [Mtkm] (millions of ton-km) for freight mobility and shipping end-uses.

1.1.2 Objective and constraints

Eqs. (1.1)-(1.64) presented and described below regroup the objective function and the constraints of the optimisation model.

Objective function: total annualised system cost

The objective is the minimisation of the sum of the total annual cost of the energy system of each region($\mathbf{C_{tot}}$):

$$\min \sum_{r \in REG} \mathbf{C_{tot}}(r). \tag{1.1}$$

The total annual cost is defined as the sum of the annualized investments cost of the technologies (τ $\mathbf{C_{inv}}$), the operating and maintenance costs of the technologies ($\mathbf{C_{maint}}$) and the operating cost of the resources ($\mathbf{C_{op}}$). The three elements of cost are computed for each region:

$$\mathbf{C_{tot}}\ (\mathbf{r}) = \sum_{j \in TECH} \left(\tau(r,j)\mathbf{C_{inv}}(r,j) + \mathbf{C_{maint}}(r,j) \right) + \sum_{i \in RES} \mathbf{C_{op}}(r,i) \qquad \forall r \in REG. \quad (1.2)$$

The investment cost ($\mathbf{C_{inv}}$) is annualised with the factor τ, calculated based on the discount rate (i_{rate}) and the technology lifetime (*lifetime*), Eq. (1.3). The discount rate is set by default in EnergyScope to 1.5%. This value is low compared to other studies with typical values of 7.5 to 12% [60, 119, 120]. This low value is chosen to represent the fact that we place ourselves as a central public investor. Having a low value gives a lower weight to investments in the total annualised cost and thus encourages the investments. This is further discussed in the model's documentation [116].

$$\tau(r,j) = \frac{i_{rate}(i_{rate}+1)^{lifetime(r,j)}}{(i_{rate}+1)^{lifetime(r,j)} - 1} \qquad \forall r \in REG, j \in TECH. \quad (1.3)$$

The total investment cost ($\mathbf{C_{inv}}$) of each technology results from the multiplication of its specific investment cost (c_{inv}) and its installed size ($\mathbf{F}$)[1]:

$$\mathbf{C_{inv}}(r,j) = c_{inv}(r,j)\mathbf{F}(r,j) \qquad \forall r \in REG, j \in TECH. \quad (1.4)$$

The total maintenance cost is calculated similarly:

$$\mathbf{C_{maint}}(r,j) = c_{maint}(r,j)\mathbf{F}(r,j) \qquad \forall r \in REG, j \in TECH. \quad (1.5)$$

The operational cost of the resources is the sum of the operational cost for local resources and the operational cost of imported resources from the exterior of the overall system. In this mathematical formulation, the same resource can be both produced locally and imported from the exterior. For both, it is calculated as the sum of their use ($\mathbf{R_{t,local}}$ and $\mathbf{R_{t,ext}}$, respectively) over the different periods multiplied by the period duration (t_{op}) and the specific cost of the resource which is different for local and exterior sources ($c_{op,\ local}$ and $c_{op,\ ext}$):

[1] Some technologies have several outputs, such as a cogeneration of heat and power (CHP). Thus, the installed size must be defined for one of these outputs. For example, CHPs are defined based on the thermal output rather than the electrical one.

$$\mathbf{C_{op}}(r,i) = \sum_{t(h,td)\in T} \big(c_{op,local}(r,i)\mathbf{R_{t,\,local}}(r,i,h,td)\, t_{op}(h,td) + c_{op,ext}(r,i)\mathbf{R_{t,\,ext}}(r,i,h,td)\, t_{op}(h,td) \big) \quad \forall r \in REG, i \in RES. \quad (1.6)$$

Note that, in Eq. (1.6), hourly quantities are summed over the entire year (8760h). As we solve the system operation on typical days, the value at each hour of the year is obtained through a mapping on typical days. To simplify the reading, the formulation $t(h,td) \in T$ is used. However, the formulation in the code is more complex and requires two additional *SETS*: *HOUR_OF_PERIOD(t)* and *TYPICAL_DAY_OF_PERIOD(t)*. These *SETS* link each hour of the year with its corresponding typical day and hour in the typical day. Hence, we have: $t(h,td) \in T$, which is equivalent in the code to $t \in T | h \in$ *HOUR_OF_PERIOD(t)*, $td \in$ *TYPICAL_DAY_OF_PERIOD(t)*.

Emissions

Similarly to the cost, greenhouse gas (GHG) emissions can be computed from the installation of technologies and the use of resources. The global annual GHGs emissions are calculated using a life cycle assessment (LCA) approach, i.e. taking into account emissions of the technologies and resources '*from cradle to grave*'. For climate change, the natural choice as an indicator is the global warming potential (GWP), expressed in ktCO_2-eq./year. In Eq. (1.7), the total yearly emissions of the system ($\mathbf{GWP_{tot}}$) are defined as the sum of the emissions related to the construction and end-of-life of the energy conversion technologies ($\mathbf{GWP_{constr}}$), allocated to one year based on the technology lifetime (*lifetime*), and the emissions related to resources ($\mathbf{GWP_{op}}$):

$$\mathbf{GWP_{tot}}(r) = \sum_{j\in TECH} \frac{\mathbf{GWP_{constr}}(r,j)}{lifetime(r,j)} + \sum_{i\in RES} \mathbf{GWP_{op}}(r,i) \quad \forall r \in REG. \quad (1.7)$$

The total emissions related to the construction of technologies are the product of the specific emissions (gwp_{constr}) and the installed size ($\mathbf{F}$):

$$\mathbf{GWP_{constr}}(r,j) = gwp_{constr}(r,j)\mathbf{F}(r,j) \quad \forall r \in REG, j \in TECH. \quad (1.8)$$

The total emissions of the resources are the emissions, from cradle to use, associated with resources locally produced and imported from the exterior of the overall system (gwp_{op})

multiplied by the period duration (t_{op}):

$$\mathbf{GWP_{op}}(r,i) = \sum_{t(h,td)\in T} \big(gwp_{op,\,local}(r,i)\mathbf{R_{t,\,local}}(r,i,h,td)\, t_{op}(h,td) + gwp_{op,\,ext}(r,i)\mathbf{R_{t,\,ext}}(r,i,h,td)\, t_{op}(h,td)\big) \quad \forall r \in REG, i \in RES. \tag{1.9}$$

GHGs emissions accounting can be conducted in different manners. The European Commission and the International Energy Agency (IEA) mainly use resource-related emissions ($\mathbf{CO_{2,net}}$) while neglecting indirect emissions related to the extraction of those resources ($\mathbf{GWP_{op}}$) or the construction of technologies ($\mathbf{GWP_{constr}}$). To facilitate the comparison with their results, a similar implementation is proposed:

$$\mathbf{CO_{2,\,net}}(r,i) = \sum_{t(h,td)\in T} co2_{net}(i)\big(\mathbf{R_{t,\,local}}(r,i,h,td)\, t_{op}(h,td) + \mathbf{R_{t,\,ext}}(r,i,h,td)\, t_{op}(h,td)\big) \quad \forall r \in REG, i \in RES. \tag{1.10}$$

End-use demand

As explained before, this model uses a end-use demand (EUD) approach to define the demand. The hourly end-use demands (**EndUses**) are computed based on the yearly end-use demands (*endUsesInput*), distributed according to their time series (listed in Table 1.3). Figure 1.3 graphically presents the constraints associated with the hourly end-use demands (**EndUses**), e.g. the public mobility demand at time t is equal to the hourly passenger mobility demand times the public mobility share ($\mathbf{\%_{Public}}$). This computation is made for each region.

Specific electricity end-use is distributed across the periods according to its time series ($\%_{elec}$) and is augmented by the network losses onto the regional grid ($\mathbf{Net_{loss}}(r, ELEC, h, td)$). Low-temperature heat demand results from the sum of the yearly demand for hot water, evenly shared across the year, and space heating, distributed across the periods according to $\%_{sh}$. The percentage repartition between centralized (district heating network (DHN)) and decentralized heat demand is defined by the variable $\mathbf{\%_{Dhn}}$. The demand for low-temperature heat on the DHN is augmented by the losses on this network ($\mathbf{Net_{loss}}(r, DHN, h, td)$). The space cooling is distributed across the periods according to $\%_{sc}$. High-temperature process heat and process cooling demands are evenly distributed across the periods. Passenger mobility and long-haul aviation demands are distributed across

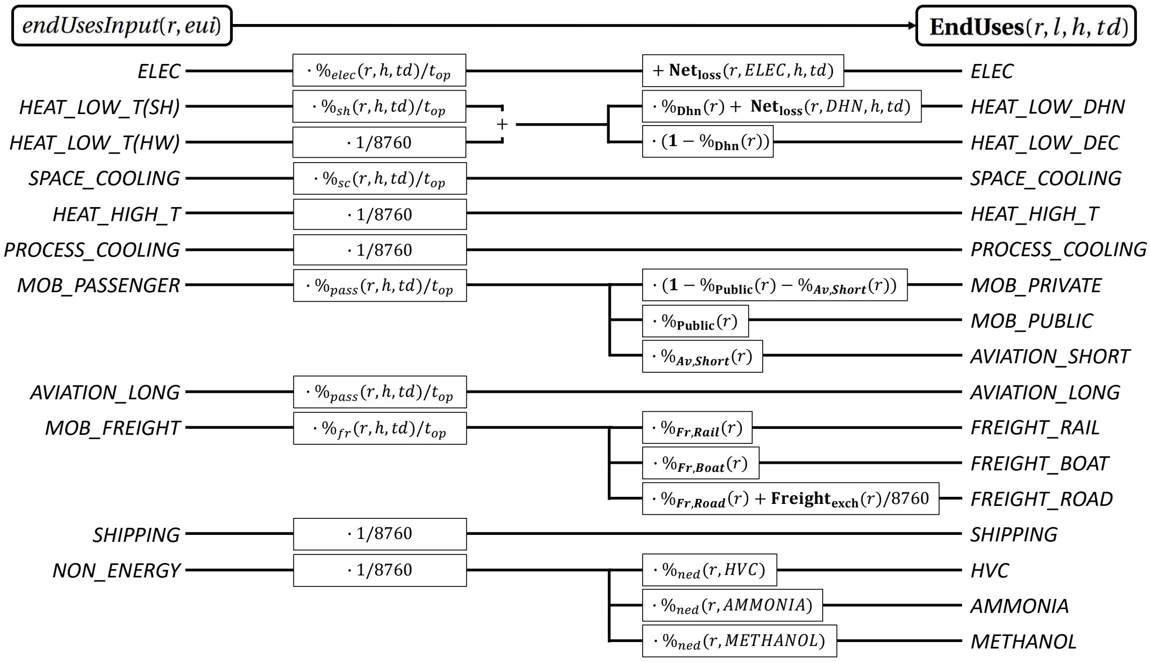

Figure 1.3: Hourly end-uses demands ($\mathbf{EndUses}(r,l,h,td)$, $\forall r \in REG, l \in EUT, h \in H, td \in TD$) calculation starting from yearly demand inputs ($endUsesInput(r, eui)$, $\forall r \in REG, eui \in EUI$). Two main operations occur: (i) the yearly demands are dispatched into hourly demands according to their time series or uniformly if the demand input does not have a time series (left operation column); (ii) the demands are dispatched into end-uses types according to the end-uses technologies that can supply them (right operation column). Abbreviations: aviation (Av), district heating network (DHN), freight (fr), high-value chemicals (HVC), hot water (HW), non-energy demand (ned), passenger (pass), space cooling (SC), and space heating (SH). Adapted from [99].

the periods according to $\%_{pass}$. They are expressed in millions of passenger-kilometers (Mpkm). The variable $\mathbf{\%_{Public}}$ defines the penetration of public transportation in the passenger mobility sector and $\mathbf{\%_{Av,Short}}$ the share done by short-haul aviation. Short- and long-haul aviation are considered in a separate way as they don't use the same type of aircraft. Furthermore, short-haul aviation could be replaced by private or public mobility (e.g. cars or trains) but not long-haul aviation. Freight transportation and international shipping demand are expressed in millions of ton-kilometers (Mtkms). Freight mobility is distributed across the periods according to $\%_{fr}$ time series. The variables $\mathbf{\%_{Rail}}$, $\mathbf{\%_{Boat}}$ and $\mathbf{\%_{Road}}$ define the share of rail, boat and road for freight mobility, respectively. The freight due energy exchanges also augment the freight mobility demand ($\mathbf{Freight_{exch}}(r)/8760$)[2].

[2]This variable is added to the road freight demand to keep a linear formulation. Furthermore, as rail and boat freight are always more efficient than road freight, their maximum capacity is already reached with the freight demand of the region. Therefore, adding the additional freight due to exchanges to the road freight

The shipping and non-energy demands are distributed uniformly across the periods. The non-energy demand is dispatched into its three main feedstocks according to their share, $\%_{ned}(r,HVC)$, $\%_{ned}(r,AMMONIA)$ and $\%_{ned}(r,METHANOL)$. This subdivision is adapted from [101].

System design and operation

Sizing of technologies

In each region, the installed capacity of a technology (**F**) is constrained between upper and lower bounds (f_{max} and f_{min}):

$$f_{min}(r,j) \leq \mathbf{F}(r,j) \leq f_{max}(r,j) \qquad \forall r \in REG, j \in TECH. \quad (1.11)$$

This formulation allows accounting for old technologies still existing in the target year (lower bound), but also for the maximum deployment potential of a technology. As an example, for offshore wind turbines, f_{min} represents the existing installed capacity (which will still be available in the future), while f_{max} represents the maximum potential.

Capacity factors and curtailment

The operation of technologies at each period is determined by the decision variable $\mathbf{F_t}$. The capacity factor of technologies is conceptually divided into two components, see Eqs. (1.12) and (1.13): a capacity factor for each period ($c_{p,t}$) depending on resource availability (e.g. renewables) and a yearly capacity factor (c_p) accounting for technology downtime and maintenance. For a given technology, the definition of only one of these two is needed, the other being fixed to the default value of 1. For example, intermittent renewables are constrained by an hourly capacity factor ($c_{p,t} \in [0;1]$) while CCGTs are constrained by an annual capacity factor (c_p, in that case 96%). When the hourly operation is lower than its bound set by the hourly capacity factor, it is curtailed. This curtailment (**Curt**) only makes sense for technologies with defined hourly capacity factors (e.g. renewables).

Eqs. (1.12) and (1.13) link the installed size of a technology to its actual use in each period (F_t) via the two capacity factors:

demand is equivalent to directly adding it to the whole freight mobility demand. This does not mean that the transportation of energy goods will always be done by truck in practice. Some of the energy goods might be more interesting to transport by train or boat than other goods, which will then be transported by truck.

$$\mathbf{F_t}(r,j,h,td) + \mathbf{Curt}(r,j,h,td) = \mathbf{F}(r,j)c_{p,t}(r,j,h,td) \quad \forall r \in REG, j \in TECH, h \in H, td \in TD, \tag{1.12}$$

$$\sum_{t(h,td)\in T} \mathbf{F_t}(r,j,h,td)t_{op}(h,td) \leq \mathbf{F}(r,j)c_p(r,j)t_{tot} \quad \forall r \in REG, j \in TECH. \tag{1.13}$$

Availability of resources

At each period (t_{op}) and in each region ($r \in REG$), each resource ($i \in RES$) can be produced locally ($\mathbf{R_{t,local}}$) and/or imported from the exterior of the overall energy system ($\mathbf{R_{t,ext}}$). In both cases, the total use of resources is limited by a yearly availability ($avail_{local}$ and $avail_{ext}$, respectively):

$$\sum_{t(h,td)\in T} \mathbf{R_{t,local}}(r,i,h,td)t_{op}(h,td) \leq avail_{local}(r,i) \quad \forall r \in REG, i \in RES, \tag{1.14}$$

$$\sum_{t(h,td)\in T} \mathbf{R_{t,ext}}(r,i,h,td)t_{op}(h,td) \leq avail_{ext}(r,i) \quad \forall r \in REG, i \in RES. \tag{1.15}$$

For resources such as gaseous and liquid fuels ($r \in RES_{cst}$), we assume that their import is constant ($\mathbf{Imp_{cst}}$) at each hour of each typical day:

$$\mathbf{R_{t,ext}}(r,i,h,td)t_{op}(h,td) = \mathbf{Imp_{cst}}(r,i) \quad \forall r \in REG, i \in RES_{cst}, h \in H, td \in TD. \tag{1.16}$$

This equation simulates the fact that to import these resources, the region ($r \in REG$) must install infrastructures, and these infrastructures have a certain capacity (e.g. gasoduct, oleoduct or a port with infrastructures to inject it into the local distribution system). We don't model the import infrastructure and their cost but simulate the fact that to amortize the investment, they must be used as continuously as possible. To compensate for the fluctuating demand of the local energy system, the model has to install storage capacity for these resources.

Layer balance

The hourly layer balance equation generalises the energy and mass balance to any energy commodity or service:

$$
\begin{aligned}
&\sum_{i\in RES} f(i,l)\Big(\mathbf{R_{t,local}}(r,i,h,td)+\mathbf{R_{t,ext}}(r,i,h,td)+\mathbf{R_{t,imp}}(r,i,h,td)-\mathbf{R_{t,exp}}(r,i,h,td)\Big)\\
&+\sum_{j\in TECH\setminus STO} f(j,l)\mathbf{F_t}(r,j,h,td)\\
&+\sum_{k\in STO}\Big(\mathbf{Sto_{out}}(r,k,l,h,td)-\mathbf{Sto_{in}}(r,k,l,h,td)\Big)\\
&=\mathbf{EndUses}(r,l,h,td)\\
&\qquad\qquad\forall r\in REG, l\in L, h\in H, td\in TD. \qquad (1.17)
\end{aligned}
$$

For energy commodities, as they can be measured in terms of energy, it is indeed an energy balance. For energy services that are not directly measured as an energy quantity (e.g. passenger mobility measured in Mpkm/h), it expresses the fact that when energy is converted to produce those services, they have to be used directly. For instance, if some methane is used in buses at some hour, the public mobility "produced" must be consumed by the public mobility demand at the same hour. Similarly, there is a layer for captured carbon dioxyde (CO_2). This layer ensures to have a mass balance for this commodity at each hour. If a process needs CO_2 to produce a synthetic fuel, this CO_2 must be captured from another process with carbon capture.

The matrix f defines, for all technologies and resources, the ratio between consumption on input layers (negative) and production on output layers (positive). For instance, a synthetic methanation plant consumes 1.2 GW of hydrogen and 0.2 ktCO_2 to produce 1 GW of methane and 0.295 GW of DHN heat as a co-product. Eq. (1.17) expresses the balance for each layer: all outputs from resources and technologies (including storage) are used to satisfy the EUD or as inputs to other resources and technologies. Resources have four different source terms, they can be : (i) produced locally ($\mathbf{R_{t,local}}$), (ii) imported from the exterior of the system, i.e. the global market ($\mathbf{R_{t,ext}}$), (iii) imported from neighbouring regions considered in the model scope ($\mathbf{R_{t,imp}}$), (iv) exported to neighbouring regions considered in the model scope ($\mathbf{R_{t,exp}}$). Similarly, storage technologies can withdraw energy from a layer to store it ($\mathbf{Sto_{in}}$) or deliver energy from its storage to the layer ($\mathbf{Sto_{out}}$).

Storage

The storage level ($\mathbf{Sto_{level}}$) at a time step (t) is equal to the storage level at $t-1$, minus the self-discharge losses ($\%_{sto_{loss}}$), plus the inputs to the storage, minus the outputs from the storage (accounting for input/output efficiencies), see Eq. (1.18). In the code, for the first period of the year, this equation is slightly modified to set the storage level at the beginning of the year according to the one at the end of the year. Hence, if $t = 1$, we set $t-1$ to the last period of the year (8760).

$$\mathbf{Sto_{level}}(r,j,t) = \mathbf{Sto_{level}}(r,j,t-1)\cdot\left(1-\%_{sto_{loss}}(j)\right) +$$
$$t_{op}(h,td)\cdot\Big(\sum_{l\in L|\eta_{sto,in}(j,l)>0}\mathbf{Sto_{in}}(r,j,l,h,td)\eta_{sto,in}(j,l) - \sum_{l\in L|\eta_{sto,out}(j,l)>0}\mathbf{Sto_{out}}(r,j,l,h,td)/\eta_{sto,out}(j,l)\Big)$$
$$\forall r\in REG, j\in STO, t(h,td)\in T. \quad (1.18)$$

The storage systems which can only be used for short-term (daily) applications are included in the daily storage set (*STO_DAILY*). For these units, Eq. (1.19) imposes that the storage level be the same at the end of each typical day[3]. Adding this constraint drastically reduces the computational time. Indeed, this constraint reduces the number of variables by forcing the storage level of daily storage technologies to be defined on typical days and not over the entire year as the other storage technologies.

$$\mathbf{Sto_{level}}(r,j,t) = \mathbf{F_t}(r,j,h,td) \qquad \forall j\in STO\_DAILY, t(h,td)\in T. \quad (1.19)$$

For the other storage technologies, which can also be used for seasonal storage, the storage level is bounded by Eq. (1.20). For these units, the storage behaviour is thus optimized over 8760h.

$$\mathbf{Sto_{level}}(r,j,t) \leq \mathbf{F}(r,j) \qquad \forall j\in STO\setminus STO\_DAILY, t\in T. \quad (1.20)$$

Eq. (1.21) limits the power input/output of a storage technology based on its installed capacity (**F**) and three specific characteristics. First, storage availability ($\%_{sto_{avail}}$) is defined as the ratio between the available storage capacity and the total installed capacity (default value is 100%). Second and third, the charging/discharging time ($t_{sto_{in}}$, $t_{sto_{out}}$), which are the time to complete a full charge/discharge from empty/full storage. As an example, a daily thermal storage needs at least 4 hours to discharge ($t_{sto_{out}} = 4$[h]), and another 4 hours to charge ($t_{sto_{in}} = 4$[h]). These two parameters are defined in each region as for some

[3] In most cases, the activation of the constraint stated in Eq. (1.19) will have as a consequence that the level of storage is the same at the beginning and the end of each day — hence the use of the terminology '*daily storage*'. Note, however, that this constraint does not always guarantee such daily storage behaviour. Thus, depending on the typical days sequence, a daily storage behaviour might need to be explicitly enforced.

specific storage technologies (e.g. PHS), the discharging and charging power depends on the location. However, these parameters generally are intrinsic characteristics of a storage technology and are identical in all regions. Note that, in this linear formulation, storage technologies can charge and discharge simultaneously. On the one hand, this avoids the need for integer variables; on the other hand, it has no physical meaning. However, in a cost minimization problem, the cheapest solution identified by the solver will always choose to either charge or discharge at any given time, as long as cost and efficiencies are defined. Hence, we recommend always verifying numerically the fact that only storage inputs or outputs are activated at each hour, as we do in all our implementations.

$$\Big(\mathbf{Sto_{in}}(r,j,l,h,td)\, t_{sto_{in}}(r,j) + \mathbf{Sto_{out}}(r,j,l,h,td)\, t_{sto_{out}}(r,j)\Big) \leq \mathbf{F}(r,j)\%_{sto_{avail}}(j)$$
$$\forall r\, in REG, j \in STO \setminus EVs\_BATT, l \in L, h \in H, td \in TD. \quad (1.21)$$

Eqs. (1.22)-(1.23) force the power input and output to zero if the layer is incompatible. As an example, a PHS will only be linked to the electricity layer (input/output efficiencies > 0). All other efficiencies will be equal to 0, to impede that the PHS exchanges with incompatible layers (e.g. mobility, heat, etc).

$$\mathbf{Sto_{in}}(r,j,l,h,td) \cdot \Big(\lceil \eta_{sto,in}(j,l) \rceil - 1\Big) = 0 \qquad \forall r \in REG, j \in STO, l \in L, h \in H, td \in TD, \quad (1.22)$$

$$\mathbf{Sto_{out}}(r,j,l,h,td) \cdot \Big(\lceil \eta_{sto,out}(j,l) \rceil - 1\Big) = 0 \qquad \forall r \in REG, j \in STO, l \in L, h \in H, td \in TD. \quad (1.23)$$

Exchanges

The exchanges are modelled into two distinct categories according to the means of transportation: (i) exchanges through a network and (ii) exchanges through freight. The resources in each category are defined by the sets *NER* and *FER*, respectively. Those two categories share equations ensuring the energy and mass balance of exchanges (Eqs. (1.24)-(1.28)) but differ in terms of losses and cost constraints. Table 1.8 summarizes conceptually those constraints, which are then fully described (Eqs. (1.29)-(1.37)). On the one side, energy carriers exchanged through a network experience some losses during transportation. They require a transmission infrastructure whose design is optimised between certain bounds. These optimised transfer capacities limit the quantity that can be transported across each border. On the other side, energy carriers' exchanges through freight increase the freight demand in each region involved in the exchange. This freight demand increase implies buying more freight vehicles. Here, the exchange is only constrained by the amount that the exporting region can provide.

Table 1.8: Exchanges modelling into two main categories: network exchanges and freight exchanges. They differ in the way their energetic cost, investment cost and quantity constraint are formulated.

	Network exchanges	**Freight exchanges**
Energetic cost	Network losses	Additional freight demand
Investment cost	Transmission infrastructure	More freight vehicles
Quantity constraint	Transfer capacity	Availability of resources
Examples	*Electricity, methane*	*Methanol, woody biomass*

Exchanges balance

Eq. (1.24) defines the energy balance of the exchanges between two regions considering the losses during exchanges ($exch_{loss}$). As exchanges have an energy cost (i.e. losses for network exchanges or additional demand for freight exchanges), the optimisation model never considers exchanges in both directions between two regions simultaneously. Hence, when one region imports a certain quantity at a certain time ($\mathbf{Exch_{imp}}$), the corresponding region exports ($\mathbf{Exch_{exp}}$) this quantity increased by the exchanges losses:

$$\begin{aligned}&\mathbf{Exch_{imp}}(r_1, r_2, i, h, td) \cdot \Big(1 + exch_{loss}(i) \cdot dist(r_1, r_2)/1000\Big) - \mathbf{Exch_{exp}}(r_1, r_2, i, h, td)\\&= -\mathbf{Exch_{imp}}(r_2, r_1, i, h, td) \cdot \Big(1 + exch_{loss}(i) \cdot dist(r_2, r_1)/1000\Big) + \mathbf{Exch_{exp}}(r_2, r_1, i, h, td)\\&\qquad \forall r_1, r_2 \in REG, i \in RES, h \in H, td \in TD. \quad (1.24)\end{aligned}$$

Eq. (1.25) ensures that exchanges occur only between adjacent regions. The distance parameter ($dist$) is set by default to 0 and is only defined for adjacent regions where direct exchanges are considered. Nevertheless, two non-adjacent regions can exchange energy commodities with the help of one or several other regions that link them.

$$\begin{aligned}&\mathbf{Exch_{imp}}(r_1, r_2, i, h, td) = \mathbf{Exch_{exp}}(r_1, r_2, i, h, td) = 0\\&\qquad \forall r_1, r_2 \in REG | dist(r_1, r_2) = 0, i \in RES, h \in H, td \in TD. \quad (1.25)\end{aligned}$$

The exchanges of each region with its adjacent regions are regrouped into total imported

($\mathbf{R_{t,imp}}$) and exported ($\mathbf{R_{t,exp}}$) quantities, see Eqs. (1.26) and (1.27). Those are then included in the layer balance of each region Eq. (1.17).

$$\mathbf{R_{t,imp}}(r_1, i, h, td) = \sum_{r_2 \in REG} \mathbf{Exch_{imp}}(r_1, r_2, i, h, td) \qquad \forall r_1 \in REG, i \in RES, h \in H, td \in TD, \tag{1.26}$$

$$\mathbf{R_{t,exp}}(r_1, i, h, td) = \sum_{r_2 \in REG} \mathbf{Exch_{exp}}(r_1, r_2, i, h, td) \qquad \forall r_1 \in REG, i \in RES, h \in H, td \in TD. \tag{1.27}$$

Eq. (1.28) forces to have no exchanges for resources if it does not make sense. For instance, one region cannot directly exchange its solar or wind resources. It must first convert it into electricity or another carrier to exchange it.

$$\mathbf{R_{t,imp}}(r, i, h, td) = \mathbf{R_{t,exp}}(r, i, h, td) = 0 \quad \forall r \in REG, i \in NOEXCHANGES, h \in H, td \in TD. \tag{1.28}$$

Network exchanges

For energy carriers exchanged through a network (*NER*, e.g. electricity, methane, hydrogen), at each period, the exchanges ($\mathbf{Exch_{imp}}$ and $\mathbf{Exch_{exp}}$) are bounded by the installed transfer capacity linking the two regions (**Tc**) for all network types related to this resource (*NT(i)*), see Eqs. (1.29) and (1.30). The network type allows us to consider different onshore and offshore interconnections. For instance, two regions can be interconnected by a hydrogen network made of four different network types: (i) underground pipelines retrofitted from existing methane pipelines, (ii) new underground pipelines, (iii) subsea pipelines retrofitted from existing methane pipelines, (iv) new subsea pipelines. The total hydrogen transfer capacity between the two regions equals the sum of the transfer capacity of all these network types.

$$\mathbf{Exch_{imp}}(r_1, r_2, i, h, td) \leq \sum_{n \in NT(i)} \mathbf{Tc}(r_2, r_1, i, n) \qquad \forall r_1, r_2 \in REG, i \in NER, h \in H, td \in TD, \tag{1.29}$$

$$\mathbf{Exch_{exp}}(r_1, r_2, i, h, td) \leq \sum_{n \in NT(i)} \mathbf{Tc}(r_1, r_2, i, n) \qquad \forall r_1, r_2 \in REG, i \in NER, h \in H, td \in TD. \tag{1.30}$$

The model can optimise the transfer capacities (**Tc**) between all regions and for each network type of each resource. For all resources exchanged through a network, these transfer capacities are limited by the parameters defining the lower and upper bounds (tc_{min} and tc_{max}), see Eq. (1.31). The lower bound expresses the fact that there is an existing network that will stay in place. The upper bound allows the expansion of this existing network.

$$tc_{min}(r_1, r_2, i, n) \leq \mathbf{Tc}(r_1, r_2, i, n) \leq tc_{max}(r_1, r_2, i, n) \qquad \forall r_1, r_2 \in REG, i \in NER \setminus Methane, n \in NT(i). \tag{1.31}$$

For the methane network, specific equations are defined to consider that the existing network can be retrofitted to a hydrogen network, see Eqs. (1.32) and (1.33). These equations ensure that the methane network transfer capacity and the methane capacity retrofitted to hydrogen are within the bounds of the methane network. Hydrogen is less dense than methane. Thus, when retrofitting a methane pipeline to a hydrogen pipeline, we lose 37% of the transfer capacity [121]. This is expressed by the ratio *ch4toh2*. There are two network types for methane: underground pipelines and subsea pipelines. Therefore, we have two equations:

$$\begin{aligned} & tc_{min}(r_1, r_2, Methane, MethanePipeline) \\ & \quad \leq \mathbf{Tc}(r_1, r_2, Methane, MethanePipeline) + \mathbf{Tc}(r_1, r_2, H2, H2Retro) / ch4toh2 \leq \\ & tc_{max}(r_1, r_2, Methane, MethanePipeline) \\ & \qquad \forall r_1, r_2 \in REG, \end{aligned} \tag{1.32}$$

$$\begin{aligned} & tc_{min}(r_1, r_2, Methane, MethaneSubsea) \\ & \quad \leq \mathbf{Tc}(r_1, r_2, Methane, MethaneSubsea) + \mathbf{Tc}(r_1, r_2, H2, H2SubseaRetro) / ch4toh2 \leq \\ & tc_{max}(r_1, r_2, Methane, MethaneSubsea) \\ & \qquad \forall r_1, r_2 \in REG. \end{aligned} \tag{1.33}$$

In this model, it is assumed that all network transfer capacities between regions are bidirectional:

$$\mathbf{Tc}(r_1, r_2, i, n) = \mathbf{Tc}(r_2, r_1, i, n) \qquad \forall r_1, r_2 \in REG, i \in NER, n \in NT(i). \tag{1.34}$$

Installed transfer capacities between two regions imply an investment into the corresponding technology in each region. This investment is proportional to the typical distance between the region pair. Each region of the pair pays for half of the installation:

$$\mathbf{F}(r_1, n) = \sum_{r_2 \in REG} \left(dist(r_1, r_2) \cdot \mathbf{Tc}(r_2, r_1, i, n)/2 \right) \qquad \forall r_1 \in REG, i \in NER, n \in NT(i). \quad (1.35)$$

Freight exchanges

The resources that can be exchanged by freight are defined by the set *FER* (i.e. ammonia, methanol, Fischer-Tropsch (FT) fuels, woody biomass and CO_2). The annual freight to transport these resources across each border ($\mathbf{Freight_{exch,b}}$) is computed in two steps, see Eq. (1.36). First, the energy exchanged is converted into tonnes thanks to the lower heating value (LHV) of each resource (*lhv*). Second, these tonnes are converted into ton-kilometers with the typical distance between the region pair (*dist*).

$$\begin{aligned} &\mathbf{Freight_{exch,b}}(r_1, r_2) \\ &\quad = dist(r_1, r_2) \sum_{i \in FER, t(h,td) \in T} \left(\left(\mathbf{Exch_{imp}}(r_1, r_2, i, h, td) + \mathbf{Exch_{exp}}(r_1, r_2, i, h, td) \right) / lhv(i) \right) \\ &\qquad\qquad \forall r_1, r_2 \in REG. \quad (1.36) \end{aligned}$$

The additional freight across each border is shared evenly between the two regions of the pair to compute the total additional freight of each region, see Eq. (1.37). This additional demand is directly added to the freight demand of each region, see Figure 1.3.

$$\mathbf{Freight_{exch}}(r_1) = \sum_{r_2 \in REG} \mathbf{Freight_{exch,b}}(r_1, r_2)/2 \qquad \forall r_1 \in REG. \quad (1.37)$$

Local networks

Eq. (1.38) calculates network losses as a share ($\%_{net_{loss}}$) of the total energy transferred through the local network of each region. As an example, losses in the electricity grid in Belgium are estimated to be 4.7% of the energy transferred in 2015[4].

[4]This is the ratio between the losses in the grid and the total annual electricity production in Belgium in 2015 [122].

$$\mathbf{Net_{loss}}(r, eut, h, td) =$$
$$\Big(\sum_{j \in TECH \setminus STO | f(j,eut)>0} f(j, eut)\mathbf{F_t}(r, j, h, td) + \sum_{i \in RES | f(i,eut)>0} f(i, eut)\mathbf{R_{t,imp}}(r, i, h, td)\Big)\%_{net_{loss}}(eut)$$
$$\forall r \in REG, eut \in EUT, h \in H, td \in TD. \quad (1.38)$$

Eq. (1.39) defines the extra investment for the local electricity network. Integration of intermittent RE implies additional investment costs for the electricity grid ($c_{grid,extra}$). As an example, the reinforcement of the electricity grid is estimated to be 368 million €$_{2015}$ per Gigawatt of intermittent renewable capacity installed (see Limpens [99] for more details).

$$\begin{aligned}\mathbf{F}(r, Grid) = 1 + \frac{c_{grid,extra}}{c_{inv}(r, Grid)}\Bigg(&\big(\mathbf{F}(r, Wind_{onshore}) - f_{min}(c, Wind_{onshore})\big)\\ &+ \big(\mathbf{F}(r, Wind_{offshore}) - f_{min}(c, Wind_{offshore})\big)\\ &+ \big(\mathbf{F}(r, PV_{utility}) - f_{min}(c, PV_{utility})\big)\\ &+ \big(\mathbf{F}(r, PV_{rooftop}) - f_{min}(c, PV_{rooftop})\big)\Bigg)\end{aligned}$$
$$\forall r \in REG. \quad (1.39)$$

Eq. (1.40) links the size of DHN to the total size of the installed centralized energy conversion technologies:

$$\mathbf{F}(r, DHN) = \sum_{j \in TECH\_OF\_EUT(HeatLowTDHN)} \mathbf{F}(r, j) \qquad \forall r \in REG. \quad (1.40)$$

Mobility shares

The share of the different technologies for passenger mobility ($j \in TECH\_OF\_EUC(PassMob)$) stays constant at each time step ($\mathbf{\%_{PassMob}}$):

$$\mathbf{F_t}(r, j, h, td) = \mathbf{\%_{PassMob}}(r, j) \cdot \big(\%_{pass}(r, h, td) \cdot endUsesInput(PassMob)\big)$$
$$\forall r \in REG, j \in TECH\_OF\_EUC(PassMob), h \in H, td \in TD. \quad (1.41)$$

In other words, if 20% of the passenger mobility is supplied by train, this share remains constant in the morning or the afternoon. But the total amount changes according to the passenger mobility time series ($\%_{pass}$). This equation approximates the fact that, in reality, there is an entire fleet of vehicles.

Similarly, we impose that the share of the different technologies for freight mobility ($j \in$ *TECH_OF_EUC*(*FreightMob*)) and for shipping ($j \in$ *TECH_OF_EUC*(*Shipping*)) stays constant at each time step ($\mathbf{\%_{FreightMob}}$ and $\mathbf{\%_{Shipping}}$, respectively):

$$\mathbf{F_t}(r,j,h,td) = \mathbf{\%_{FreightMob}}(r,j) \cdot \big(endUsesInput(FreightMob)/8760\big)$$
$$\forall r \in REG, j \in TECH\_OF\_EUC(FreightMob), h \in H, td \in TD, \quad (1.42)$$

$$\mathbf{F_t}(r,j,h,td) = \mathbf{\%_{Shipping}}(r,j) \cdot \big(endUsesInput(Shipping)/8760\big)$$
$$\forall r \in REG, j \in TECH\_OF\_EUC(Shipping), h \in H, td \in TD. \quad (1.43)$$

For freight mobility, we ensure that the freight technologies supply the overall freight demand by forcing the sum of shares of rail freight ($\mathbf{\%_{Fr,Rail}}$), boat freight ($\mathbf{\%_{Fr,Boat}}$) and road freight ($\mathbf{\%_{Fr,Road}}$) to be equal to one:

$$\mathbf{\%_{Fr,Rail}}(r) + \mathbf{\%_{Fr,Boat}}(r) + \mathbf{\%_{Fr,Road}}(r) = 1 \qquad \forall r \in REG. \quad (1.44)$$

Vehicle-to-grid

Vehicle-to-grid dynamics are included in the model via the *V2G* set. For each vehicle $i \in V2G$, a battery ($j \in EVs\_BATT$) is associated using the set *EVs_BATT_OF_V2G* ($j \in EVs\_BATT\_OF\_V2G(i)$). Each type i of *V2G* has a different size of battery per car ($ev_{batt,size}(i)$), e.g. typical plug-in hybrid electric vehicle (PHEV) and battery electric vehicle (BEV) have different size of batteries. A set of equations links the electric vehicles with their batteries for both sizing and operation, see Eqs. (1.45-1.48).

The general working principle is illustrated in Figure 1.4. It is an example of BEVs supplying some passenger mobility. In this illustration, a battery technology is associated with a BEV. The battery can either supply the BEV needs or send electricity back to the grid. It can also be charged smartly, i.e. according to the grid flexibility needs.

Eq. (1.45) forces batteries of electric vehicles to supply, at least, the energy required by each associated electric vehicle technology. This constraint is not an equality, as batteries can also be used to support the grid. There is a minus sign on the right side of the equation as the car consumes electricity, and thus, the f parameter is negative.

$$\mathbf{Sto_{out}}(r,j,Elec,h,td) \geq -f(i,Elec)\mathbf{F_t}(r,i,h,td)$$
$$\forall r \in REG, i \in V2G, j \in EVs\_BATT\_OF\_V2G(i), h \in H, td \in TD. \quad (1.45)$$

The number of vehicles of a given technology is calculated by the ratio of the installed capacity (**F**) in [Mkm-pass/h] with the capacity per vehicle (veh_{capa}) in [km-pass/h/veh.]. Thus, the energy that can be stored in batteries is this ratio times the size of battery per car ($ev_{batt,\,size}(i)$), see Eq. (1.46). As an example, if this technology of cars covers 10 Mpass-km/h, and the capacity per vehicle is 50.4 pass-km/car/h (which represents an average speed of 40km/h and occupancy of 1.26 passengers per car), the amount of BEV cars are 0.198 million cars. Thus, if a BEV has a 50kWh battery, the equivalent battery has a capacity of 9.92 GWh.

$$\mathbf{F}(r,j) = \frac{\mathbf{F}(r,i)}{veh_{capa}(i)} ev_{batt,size}(i) \qquad \forall r \in REG, i \in V2G, j \in EVs\_BATT\_OF\_V2G(i). \quad (1.46)$$

Eq. (1.47) limits the availability of batteries for charging and discharging to the number of vehicles connected to the grid. This equation is similar to the one for other types of storage, see Eq. (1.21), except that a part of the batteries are not connected to the grid, i.e. the batteries of the cars on the move. Therefore, the available output is corrected by removing the electricity powering the running car (here, $f(i,Elec) \leq 0$) and the available batteries are corrected by removing the number of electric cars on the move ($\frac{\mathbf{F_t}(r,i,h,td)}{veh_{capa}(i)} ev_{batt,size}(i)$). Furthermore, not all the stationed cars are connected to a smart charging station. Only a share (20%) is available for charging or discharging ($\%_{sto_{avail}}(j)$).

$$\Big(\mathbf{Sto_{in}}(r,j,l,h,td)\, t_{sto_{in}}(r,j) + \big(\mathbf{Sto_{out}}(r,j,l,h,td) + f(i,Elec)\mathbf{F_t}(r,i,h,td)\big)\, t_{sto_{out}}(r,j)\Big)$$
$$\leq \Big(\mathbf{F}(r,j) - \frac{\mathbf{F_t}(r,i,h,td)}{veh_{capa}(i)} ev_{batt,size}(i)\Big)\%_{sto_{avail}}(j)$$
$$\forall r \in REG, i \in V2G, j \in EVs\_BATT\_OF\_V2G(i), l \in L, h \in H, td \in TD. \quad (1.47)$$

For each EV, a minimum state of charge is imposed for each hour of the day ($soc_{ev}(i,h)$). By default, we impose that the state of charge of the EVs fleet is 60% at 7 a.m. to ensure that cars can be used to go to work. Eq. (1.48) imposes, for each type of V2G, that the level of

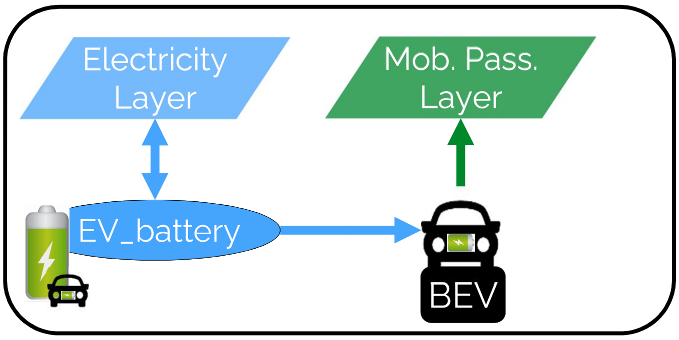

Figure 1.4: Illustrative example of a vehicle-to-grid implementation. The battery (EV_battery) can interact with the electricity layer and the battery electric vehicle (BEV). The link with the electricity layer goes in both directions as the battery can be charged or discharged flexibly according to the grid needs and respecting both the availability of the vehicle connected to the grid and the minimum state of charge required. The link with the BEV only goes in one direction as the battery is discharged to supply these vehicles with power according to the demand in the passenger mobility (Mob. Pass.) layer. This figure is taken from [99].

charge of the EV batteries is greater than the minimum state of charge times the storage capacity.

$$\mathbf{Sto_{level}}(r,j,t) \geq \mathbf{F}(r,j) soc_{ev}(i,h)$$
$$\forall r \in REG, i \in V2G, j \in EVs\_BATT\_OF\_V2G(i), t(h,td) \in T. \quad (1.48)$$

Hydro dams

The hydro dams are implemented as the combination of two components, see Figure 1.5: a storage unit (the reservoir or dam storage (*DamSto*)) and a power production unit (*HydroDam*).

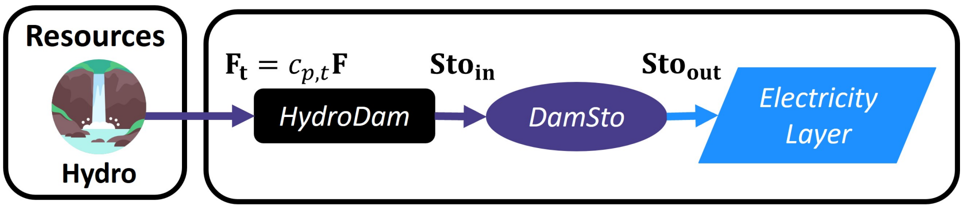

Figure 1.5: Visual representation of hydro dam modelling. This figure is adapted from [123].

We differentiate between PHS and the storage unit with river inflow, *DamSto*. PHS has a lower and upper reservoir without an inlet source; *DamSto* has an inlet source, i.e. a river inflow, but cannot pump water from the lower reservoir.

The technology *HydroDam* accounts for all the dam hydroelectric infrastructure costs and emissions. Eqs. (1.49)-(1.51) regulate the reservoir (*DamSto*) based on the production (*HydroDam*). Eq. (1.49) linearly relates the reservoir size with the power plant size ($\mathbf{F}(r, HydroDam)$).

$$\begin{aligned}
&\mathbf{F}(r, DamSto) \leq f_{min}(r, DamSto) \\
&+ \Big(f_{max}(r, DamSto) - f_{min}(r, DamSto)\Big) \cdot \left(\frac{\mathbf{F}(r, HydroDam) - f_{min}(r, HydroDam)}{f_{max}(r, HydroDam) - f_{min}(r, HydroDam)}\right) \\
&\qquad\qquad \forall r \in REG \setminus RWITHOUTDAM. \quad (1.49)
\end{aligned}$$

Eq. (1.50) imposes the storage input power ($\mathbf{Sto_{in}}$) to be equal to the water inflow of the dam ($\mathbf{F_t}(r, HydroDam, h, td)$). This water inflow is constrained by the hourly capacity factor equation, see Eq. (1.12).

$$\mathbf{Sto_{in}}(r, DamSto, Elec, h, td) = \mathbf{F_t}(r, HydroDam, h, td) \qquad \forall r \in REG, h \in H, td \in TD. \quad (1.50)$$

Eq. (1.51) ensures that the storage output ($\mathbf{Sto_{out}}$) is lower or equal to the installed capacity ($\mathbf{F}(r, HydroDam)$). Furthermore, the dam storage is constrained by the storage equations, see Eqs. (1.18) and (1.20).

$$\mathbf{Sto_{out}}(r, DamSto, Elec, h, td) \leq \mathbf{F}(r, HydroDam) \qquad \forall r \in REG, h \in H, td \in TD. \quad (1.51)$$

Concentrated solar power

The CSP technologies are modelled into 3 elements, see Figure 1.6: collectors, storage and power block. The solar irradiance converted into heat is given by a time series and constrained by Eq (1.12). This heat goes onto a specific layer where it is either stored in the CSP heat storage or converted into electricity through the power block.

Two different CSP technologies are considered: solar tower (ST) and parabolic trough (PT). Each CSP technology also has its own layer representing the heat produced and stored on

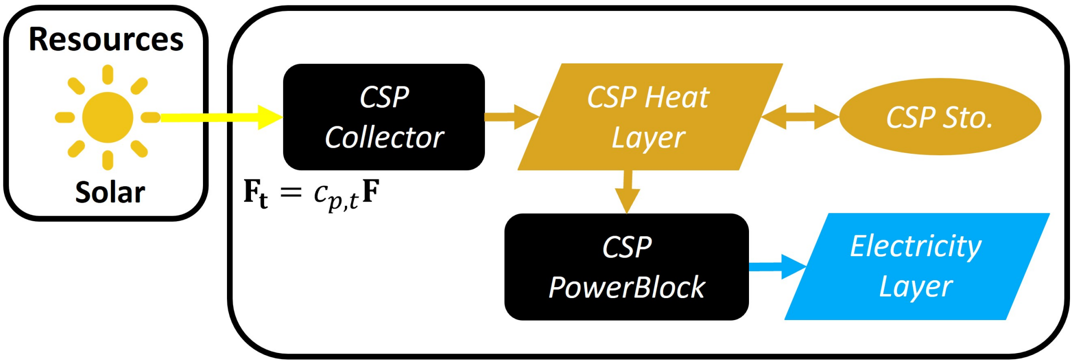

Figure 1.6: Visual representation of concentrated solar power (CSP) modelling.

the CSP plant. Eqs. (1.52) and (1.53) ensure that the link between the size of the collector field $\left(\mathbf{F}(r, ST_{collector}) \text{ or } \mathbf{F}(r, PT_{collector})\right)$ and the size of the power block $\left(\mathbf{F}(r, ST_{powerblock}) \text{ or } \mathbf{F}(r, PT_{powerblock})\right)$ are kept within a realistic range. In these equations, the size of the collector field defined in [GW_{th}] is converted into equivalent electrical power (i.e. [GW_{el}]) thanks to an efficiency of the power block $\left(\frac{-1}{f(ST_{powerblock}, ST_{Heat})} \text{ or } \frac{-1}{f(PT_{powerblock}, PT_{Heat})}\right)$. There is a minus sign as the power block consumes heat ($f < 0$). The link between this equivalent electrical power and the power block size is bounded by the maximum solar multiple (sm_{max}). A typical maximum solar multiple of 4 is taken [124].

$$-\frac{\mathbf{F}(r, ST_{collector})}{f(ST_{powerblock}, ST_{Heat})} \leq sm_{max}\mathbf{F}(r, ST_{powerblock}) \qquad \forall r \in REG, \quad (1.52)$$

$$-\frac{\mathbf{F}(r, PT_{collector})}{f(PT_{powerblock}, PT_{Heat})} \leq sm_{max}\mathbf{F}(r, PT_{powerblock}) \qquad \forall r \in REG. \quad (1.53)$$

Solar area

As several solar-based technologies are competing for the same locations, the upper limit for those is calculated based on the available land area ($solar_{area}$) and power densities of PV ($power\_density_{pv}$), solar thermal ($power\_density_{solar\ thermal}$) and CSP ($power\_density_{pt}$ and $power\_density_{st}$), see Eqs. (1.54)-(1.56). The equivalence between an installed capacity (in gigawatt peaks, GWp) and the land use (in km^2) is calculated based on the peak power density (GWp/km^2). In other words, it represents the peak power of one square meter of solar technology, considering also the spacing needed between panels.

Rooftop PV and solar thermal decentralised and centralised are competing for rooftop area

($solar_{area,rooftop}$):

$$\frac{\mathbf{F}(r, PV_{rooftop})}{power\_density_{pv}} + \frac{\left(\mathbf{F}(r, Dec_{Solar}) + \mathbf{F}(r, DHN_{Solar})\right)}{power\_density_{solar\ thermal}} \leq solar_{area,rooftop}(r) \qquad \forall r \in REG. \tag{1.54}$$

The utility PV and CSP technologies compete for ground area ($solar_{area,ground}$):

$$\frac{\mathbf{F}(r, PV_{utility})}{power\_density_{pv}} + \frac{\mathbf{F}(r, PT_{collector})}{power\_density_{pt}} + \frac{\mathbf{F}(r, ST_{collector})}{power\_density_{st}} \leq solar_{area,ground}(r) \quad \forall r \in REG. \tag{1.55}$$

Additionally, CSP technologies can only be installed on locations with annual direct normal irradiance (DNI) above 1800 kWh/m^2 and a maximum slope of 2.1°[110]. The two different CSP technologies compete for that high irradiance ground area ($solar_{area,ground,\ high\ irr}$), which is a subset of the total solar ground area ($solar_{area,ground}$):

$$\frac{\mathbf{F}(r, PT_{collector})}{power\_density_{pt}} + \frac{\mathbf{F}(r, ST_{collector})}{power\_density_{st}} \leq solar_{area,ground,high\ irr}(r) \qquad \forall r \in REG. \tag{1.56}$$

Decentralised heat production

Figure 1.7 shows, through an example with two technologies (a methane boiler and a HP), how decentralised heat production, thermal storage and thermal solar are implemented. Each heating technology can be linked with a thermal solar panel installation and thermal storage. Together, they must supply a constant share of the decentralised heat demand.

Thermal solar, when implemented as a decentralized technology, is always installed together with another decentralized technology, which serves as a backup to compensate for the intermittency of solar thermal. Thus, we define the total installed capacity of solar thermal ($\mathbf{F}(r,Dec_{Solar})$) as the sum of the solar thermal capacity associated with each backup technology ($\mathbf{F_{sol}}(r, j)$):

$$\mathbf{F}(r, Dec_{Solar}) = \sum_{j \in TECH\_OF\_EUT(HeatLowTDec) \setminus \{Dec_{Solar}\}} \mathbf{F_{sol}}(r, j) \qquad \forall r \in REG. \tag{1.57}$$

Eq. (1.58) links the installed size of each solar thermal capacity ($\mathbf{F_{sol}}(r, j)$) to its actual

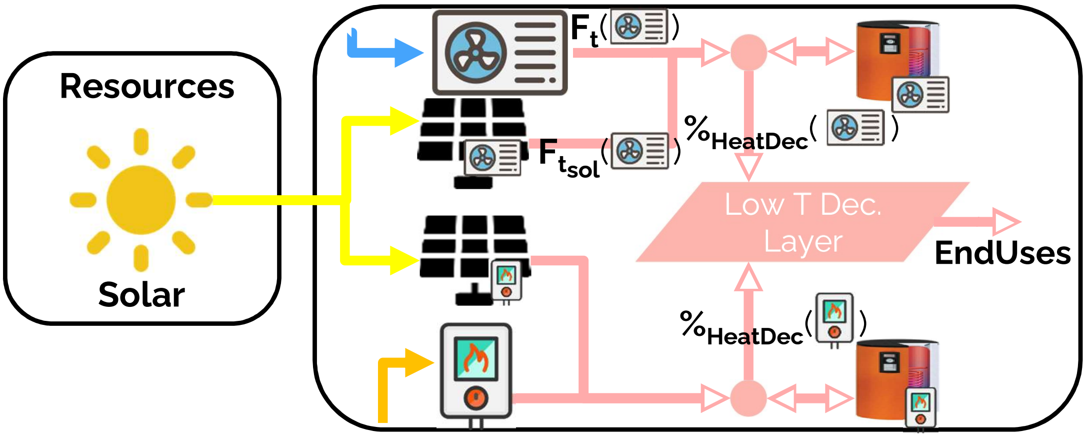

Figure 1.7: Illustrative example of a decentralised heating layer in one region with thermal storage, solar thermal and two conventional production technologies, methane boilers and electrical heat pumps (HP). In this case, Eq. (1.59) applied to the electrical HPs becomes the equality between the two following terms: the left term is the heat produced by: the eHPs ($\mathbf{F_t}(eHPs)$), the solar panel associated to the eHPs ($\mathbf{F_{t_{sol}}}(eHPs)$) and the storage associated to the eHPs; the right term is the product between the share of decentralised heat supplied by eHPs ($\mathbf{\%_{HeatDec}}(eHPs)$) and heat low-temperature decentralised demand ($\mathbf{EndUses}(r, HeatLowT, h, td)$). This figure is taken from [99].

production ($\mathbf{F_{t_{sol}}}(r, j, h, td)$) via the solar capacity factor ($c_{p,t}(r,Dec_{Solar},h,td)$).

$$\mathbf{F_{t_{sol}}}(r, j, h, td) \leq \mathbf{F_{sol}}(r, j) c_{p,t}(r, Dec_{Solar}, h, td)$$
$$\forall r \in REG, j \in TECH\_OF\_EUT(HeatLowTDec) \setminus \{Dec_{Solar}\}, h \in H, td \in TD. \quad (1.58)$$

A thermal storage i is defined for each decentralised heating technology j, to which it is linked via the set *TS_OF_DEC_TECH*. Each thermal storage i can store heat from its technology j and the associated thermal solar $\mathbf{F_{sol}}(r,j)$. Similarly to passenger mobility, Eq. (1.59) makes the model more realistic by defining the operating strategy for decentralized heating. In fact, in the model, we represent decentralized heat in an aggregated form; however, in a real case, residential heat cannot be aggregated. A house heated by a decentralised methane boiler and solar thermal panels should not be able to be heated by the electrical heat pump and thermal storage of the neighbours, and vice-versa. Hence, Eq. (1.59) imposes that the use of each technology ($\mathbf{F_t}(r, j, h, td)$), plus its associated thermal solar ($\mathbf{F_{t_{sol}}}(r, j, h, td)$), plus its associated storage outputs ($\mathbf{Sto_{out}}(r, i, l, h, td)$), minus its associated storage inputs ($\mathbf{Sto_{in}}(r, i, l, h, td)$) should keep a constant share ($\mathbf{\%_{HeatDec}}(r,j)$) of the heat demand ($\mathbf{EndUses}(r, HeatLowT, h, td)$) throughout the year. This work presents Eq. (1.59) in a non-linear compressed form for clarity and conciseness. In the model implementation, it is linearized by directly replacing the demand variable (**EndUses**) with the parameters that define it: the end-use inputs and the time series.

$$\mathbf{F_t}(r,j,h,td) + \mathbf{F_{t_{sol}}}(r,j,h,td) + \sum_{l \in L}\Big(\mathbf{Sto_{out}}(r,i,l,h,td) - \mathbf{Sto_{in}}(r,i,l,h,td)\Big)$$
$$= \mathbf{\%_{HeatDec}}(r,j)\mathbf{EndUses}(r, HeatLowT, h, td)$$
$$\forall r \in REG, j \in TECH\_OF\_EUT(HeatLowTDec) \setminus \{Dec_{Solar}\},$$
$$i \in TS\_OF\_DEC\_TECH(j), h \in H, td \in TD. \quad (1.59)$$

Peak demand

Eqs. (1.60)-(1.62) constrain the installed capacity of low-temperature heat supply and space cooling supply. Based on the selected TDs, the ratio between the yearly peak demand and the TDs peak demand is defined for space heating and space cooling in each region($\%_{Peak_{sh}}(r)$ and $\%_{Peak_{sc}}(r)$). These equations force the installed capacity to meet the peak demand, i.e. which represents, somehow, the network adequacy [5].

Eq. (1.60) imposes that the installed capacity for decentralised heating technologies covers the real peak over the year. This work expresses it in a non-linear form for clarity and conciseness. In the actual model implementation, it is linearized by dividing it into two equations.

$$\mathbf{F}(r,j) \geq \%_{Peak_{sh}}(r) \max_{h \in H, td \in TD}\{\mathbf{F_t}(r,j,h,td)\}$$
$$\forall r \in REG, j \in TECH\_OF\_EUT(HeatLowTDEC) \setminus \{Dec_{Solar}\}. \quad (1.60)$$

Similarly, Eq. (1.61) forces the centralised heating system to have a supply capacity (production plus storage) higher than the peak demand.

[5] The model resolution of the dispatch is not accurate enough to verify the adequacy. As one model cannot address all the issues, another approach has been preferred: couple the model to a dispatch one and iterate between them. This was tested by Pavicevic et al.[125] on the regional version of the EnergyScope model by coupling it with a dispatch model (Dispa-SET [126]). Based on a feedback loop, they iterated on the design to verify the power grid adequacy and the strategic reserves. Results show that the backup capacities and storage needed to be slightly increased compared to the results of the design model alone.

$$\sum_{i,j}\left(\mathbf{F}(r,j)+\frac{\mathbf{F}(r,i)}{t_{sto_{out}}(r,i)}\right)\geq \%_{Peak_{sh}}(r)\max_{h\in H, td\in TD}\left\{\mathbf{EndUses}(r, HeatLowTDHN, h, td)\right\}$$

where $j \in TECH\_OF\_EUT(HeatLowTDHN), i \in STO\_OF\_EUT(HeatLowTDHN),$

$$\forall r \in REG. \quad (1.61)$$

Eq. (1.62) imposes that the installed capacity for space cooling technologies covers the real peak over the year.

$$\mathbf{F}(r,j)\geq \%_{Peak_{sc}}(r)\max_{h\in H, td\in TD}\left\{\mathbf{F_t}(r,j,h,td)\right\}$$

$$\forall r \in REG, j \in TECH\_OF\_EUT(SpaceCooling). \quad (1.62)$$

Additional Constraints

Conventional nuclear power plants are assumed to have no power variation over the year, see Eq. (1.63). If needed, this equation can be replicated for all other technologies for which a constant operation over the year is desired.

$$\mathbf{F_t}(r, Nuclear, h, td) = \mathbf{P_{Nuclear}}(r) \qquad \forall r \in REG, h \in H, td \in TD. \quad (1.63)$$

To account for efficiency measures from today to the target year, Eq. (1.64) imposes their cost. The EUD is based on a scenario detailed in Section 1.2 and has a lower energy demand than the "business as usual" scenario, which has the highest energy demand. Hence, the energy efficiency cost accounts for all the investment required to decrease the demand from the "business as usual" scenario and the implemented one. As the reduced demand is imposed over the year, the required investments must be completed before this year. Therefore, the annualisation cost has to be deducted from one year. This mathematically implies to define the capacity of efficiency measures deployed to $1/(1+i_{rate})$ rather than 1.

$$\mathbf{F}(r, Efficiency) = \frac{1}{1+i_{rate}} \qquad \forall r \in REG. \quad (1.64)$$

Adaptations for the case study

Additional constraints are coded to implement scenarios. They are not used in all scenarios, and scenarios can be set in other ways, but they facilitate setting certain typical scenario constraints.

To go into the direction of the energy transition, there are three possible levers. The first lever, using Eq. (1.65), imposes a maximum yearly emissions threshold on the overall GWP ($gwp_{limit,overall}$):

$$\sum_{r \in REG} \mathbf{GWP_{tot}}(r) \leq gwp_{limit,overall}. \tag{1.65}$$

The second lever, using Eq. (1.66), fixes the minimum renewable primary energy share in each region. The third lever, using Eq. (1.15), can force regions to use less fossil resources by reducing their availability ($avail_{ext}$).

$$\begin{aligned} &\sum_{j \in \mathrm{RES_{re}}, t(h,td) \in T} \left(\mathbf{R_{t,local}}(r,j,h,td) + \mathbf{R_{t,ext}}(r,j,h,td) + \mathbf{R_{t,imp}}(r,j,h,td)\right) \cdot t_{op}(h,td) \\ &\quad \geq re_{\mathrm{share}}(r) \sum_{j \in RES, t(h,td) \in T} \left(\mathbf{R_{t,local}}(r,j,h,td) + \mathbf{R_{t,ext}}(r,j,h,td) + \mathbf{R_{t,imp}}(r,j,h,td)\right) \cdot t_{op}(h,td) \\ &\qquad \forall r \in REG. \end{aligned} \tag{1.66}$$

The model also has the ability to represent a historical energy system of the regions studied. This is done thanks to Eq. (1.67), which imposes the relative technology share in its sector. Eq. (1.67) is complementary to Eq. (1.11) which bounds the capacity of technologies, as it expresses the minimum ($f_{min,\%}$) and maximum ($f_{max,\%}$) yearly output shares of each technology for each end-use type. In fact, for a given technology, assigning a relative share (e.g. boilers providing at least a given percentage of the total heat demand) is more intuitive and closer to the energy planning practice than limiting its installed size. By default, for all technologies, $f_{min,\%}$ and $f_{max,\%}$ are fixed to 0 and 1, respectively, unless otherwise indicated.

$$\begin{aligned} f_{min,\%}(r,j) \sum_{j' \in TECH\_OF\_EUT(eut), t(h,td) \in T} \mathbf{F_t}(r,j',h,td) \cdot t_{op}(h,td) &\leq \sum_{t(h,td) \in T} \mathbf{F_t}(r,j,h,td) \cdot t_{op}(h,td) \\ &\leq f_{max,\%}(r,j) \sum_{j'' \in TECH\_OF\_EUT(eut), t(h,td) \in T} \mathbf{F_t}(r,j'',h,td) \cdot t_{op}(h,td) \end{aligned}$$

$$\forall r \in REG, eut \in EUT, j \in TECH\_OF\_EUT(eut). \quad (1.67)$$

Eq. (1.68) limits the power grid import capacity from neighbouring regions that are outside of the modelled regions, based on a net transfer capacity ($elec_{import,max}$). This equation can be used with Eq. (1.15), which defines the total quantity of electricity that can be imported. If this quantity is 0, then no imports from outside of the modelled area are considered, and Eq. (1.68) can be neglected.

$$\mathbf{R_{t,ext}}(r, Electricity, h, td)) \leq elec_{import,max}(r) \qquad \forall r \in REG, h \in H, td \in TD. \quad (1.68)$$

1.2 Representing a fossil-free European whole-energy system

The optimisation model described in the previous section is suitable to model any multi-regional whole-energy system. This section presents how we modelled a fossil-free European whole-energy system in 2050. This study's environmental constraint is to eliminate all fossil fuels. The aim is to analyze the design and the technical challenges of energy systems without these fuels. Therefore, we do not fix any constraint onto the GHG emissions (Eq. (1.65) is not used and thus Eqs. (1.7)-(1.10) only serve for accounting but not for constraining the system). However, the fossil-free constraint is more ambitious than a net-zero constraint as it forces Europe to have no fossil emissions at all in its whole-energy system. We model 34 European countries, each one modelled as one cell, see Figure 1.8: the 28 European Union countries minus Cyprus and Malta[6], plus the United Kingdom, Norway, Switzerland, Albania, Bosnia and Herzegovina, Montenegro, North Macedonia, Serbia and Kosovo. The list of countries considered and their two-letter code can be found in Appendix B.

Following the whole-energy system approach, our model of the European energy system considers 28 energy resources converted through 167 technologies to supply demands in 17 end-use layers, see Figure 1.9[7]. The resources provide some energy fluxes at a certain cost

[6] Cyprus and Malta are not considered because they are islands with small energy demands compared to the rest of Europe. Adding those two nodes increases the computational burden without changing the global trends at the European level.

[7] Abbreviations for the figure: atmospheric (Atm.), battery electric vehicle (BEV), biomass (biom.), biomethanisation (Biometh.), compressed air energy storage (CAES), carbon capture (CC), combined cycle gas turbine (CCGT), cogeneration of heat and power (CHP), carbon dioxyde (CO_2), collector (Coll.) concentrated solar power (CSP), decentralised heat (Decen. or Dec.), district heating network (DHN), electricity (Elec.),

Figure 1.8: Our model represents 34 European countries. In the model, each country is one cell with its own energy system interconnected with other cells through energy exchanges.

and with a certain availability (e.g. the wood resource provides energy in the form of woody biomass at a certain cost and is limited by its potential). The renewable energy potentials are evaluated for each country. Additionally, certain resources can be imported from the exterior of the system. Then, the technologies convert one or several fluxes as input into one or several fluxes as output with a certain efficiency (e.g. an industrial wood CHP converts 1.9 GW of woody biomass into 1 GW of high-temperature heat and 0.34 GW of electricity and produces 0.74 Mt of industrial CO_2 that can be captured with additional investments). Finally, the different EUDs consume specific fluxes which are provided by corresponding end-use technologies (e.g. the high-temperature heat demand consumes GW of heat produced by industrial furnaces, whereas the private mobility consumes Mpkm/h supplied by cars). The EUDs are forecasted for each country in 2050. Additionally, the networks and exchange possibilities are modelled between neighbouring countries. All those input data

Fischer-Tropsch (FT) geothermal (Geoth.), hydrogen (H2), high-temperature (High T), high value chemical (HVC), internal combustion engine (ICE), industrial (Ind.), low-temperature (Low T), methanation (Methan.), methanolation (Methanol.), offshore (Off.), onshore (On.), power block (PB), plug-in hybrid electric vehicle (PHEV), pumped hydro storage (PHS), photovoltaic (PV), renewable (Re.), thermal (Th.)

define the environment in which the energy system is optimised.

This section summarizes the main assumptions into four categories: (i) Energy conversion technologies, (ii) Energy demand evaluation and projection, (iii) Resources and renewable energy potentials, and (iv) Interconnections and exchanges. All the numerical values and assumptions can be found in the online documentation of the model [116]. The full datasets and the preprocessing scripts are open-source. The up-to-date version that can still evolve is accessible on the GitHub of the model [115], and the frozen version used for this work is stored on Zenodo [117].

1.2.1 Energy conversion technologies

The system can choose between 167 different energy conversion technologies to transform the energy sources to supply the end-use demands, see Figure 1.9. For each technology, 10 characteristics are quantified: investment cost (c_{inv}), maintenance cost (c_{maint}), construction emissions (gwp_{constr}), lifetime (*lifetime*), capacity factor (c_p), efficiency (f), lower and upper bound on capacity(f_{min} and f_{max}), and lower and upper bound on their share of production on their output layer ($f_{min,perc}$ and $f_{max,perc}$). Similarly to the previous version of the model, we use the Danish energy agency's database [127] to characterise the different energy conversion technologies. This agency gathered different reports to estimate the evolution of the cost and efficiency of energy technologies. We use the following three reports: *'Technology Data for Energy Plants for Electricity and District heating generation'* [114], *'Technology data for Energy storage'* [128], and *'Technology Data for Renewable Fuels'* [129]. These reports provide information on all the characteristics except the lower and upper bounds and capacity and production. For most technologies, the lower bound on the capacity is set to 0, and the upper bound to an infinite value. Only nuclear and renewable energy technologies are bound. In this scenario, nuclear is forced to 0. For renewable energy technologies, we assume that Europe will keep at least the current capacity, which fixes the lower bound. The upper bound is set to the socio-technical potential evaluated in Section 1.2.3. For most technologies, the share of production on their output layer is not bound. Only three technologies related to end-use demands have an upper bound: i) metro, tramway and trolley bus (≤30% of public mobility); (ii) passenger train (≤50% of public mobility); (iii) electrical heating for industrial processes (≤60% of the high-temperature heat). The other details of the technologies' characteristics are presented in the online documentation of the model [116].

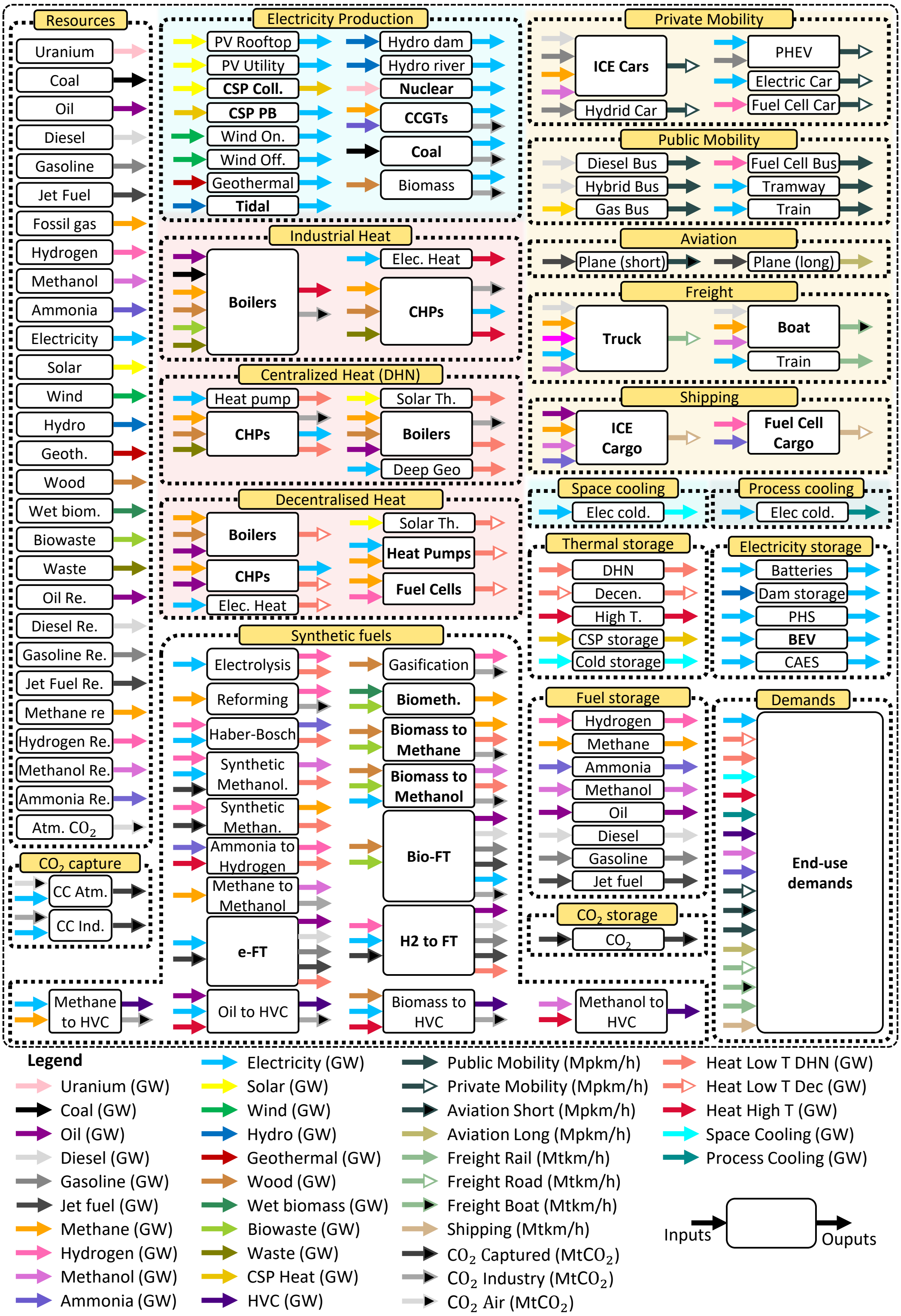

Figure 1.9: The European energy system modelled with EnergyScope Multi-Cells implements in each country: 28 energy resources converted through 167 technologies to supply demands in 17 end-use layers. Technologies (in bold) represent groups of technologies with different energy inputs (e.g. Boilers include methane boilers, oil boilers ...).

1.2.2 Energy demand evaluation and projection

We characterise energy demands in two steps. First, we evaluate and project each country's annual end-use demands for 2050. Second, we compute hourly time series to represent the temporal variability of demands.

Annual end-use demands evaluation and projection

The energy demand projection is based on the *EU Reference Scenario 2020* [130]. This work provides a unified projection of the final energy consumption in each country of the European Union. In this report, the year 2015 is used as historical data from which the demand is projected every five years up to 2050. We chose this work for our Reference scenario for several reasons: (i) unified projection for 25 of the 34 countries considered; (ii) done by an official instance, the European Commission; (iii) compatibility with other and previous versions of EnergyScope.

However, for most sectors, this report only provides a projection of the final energy consumption with no further details. In our model, we consider the end-use demand (EUD), which is much closer to the energy service. The goal is to capture the sector-coupling and flexibility opportunities that lie between the final energy consumed and the end-use demand. For instance, to supply low-temperature heat for space heating and hot water, considering the final energy consumption only gives information about energy carriers to provide, such as methane or electricity. But it misses the opportunity to change the end-use technology from a methane boiler to a heat pump, for instance, and both gain efficiency and change the final energy to supply. Furthermore, if the demand is defined in terms of end-use demand, the model can add a storage tank between the heat production and consumption. Then, the heat pump can provide flexibility for the electrical grid.

We make different assumptions using different datasets to split the final consumption projected by the *EU Reference Scenario 2020* into different end-uses; see Table 1.9.

For the residential and tertiary sectors, the *EU Reference Scenario* projections of the final energy consumption are combined with the fitting of the EUCalc model on this scenario [132]. The EUCalc model provides additional information on energy consumption in buildings and agriculture. The information on buildings allows us to split the final energy consumption in those sectors into specific electricity, space heating, hot water and space cooling. All the cooking is assumed to be electrified and is converted into electricity demand and included in the specific electricity. For space heating and hot water, when done with

Table 1.9: Evaluation and projection of end-use demands. The projection of the final energy consumption by sector (columns) from the *EU Reference Scenario 2020* is split into end-use types (rows) thanks to other studies.

	Residential	Tertiary	Industry	Transportation
Specific electricity	EUCalc[a]	EUCalc[a]	HRE4[b]	X
Space heating	EUCalc[a]	EUCalc[a]	HRE4[b]	X
Hot water	EUCalc[a]	EUCalc[a]	HRE4[b]	X
Space cooling	EUCalc[a]	EUCalc[a]	HRE4[b]	X
High-temperature heat	X	X	HRE4[b]	X
Process cooling	X	X	HRE4[b]	X
Non-energy	X	X	Rixhon et al.[c]	X
Passenger mobility	X	X	X	EUref[d]
Long-haul aviation	X	X	X	Eurostat[e] EUROCONTROL[f]
Freight	X	X	X	EUref[d]
Shipping	X	X	X	EUref[d]

[a]EUcalc is a Transition Pathways Explorer fitted on 31 decarbonization pathways from different projects [131]. We use the fitting the *EU Reference Scenario 2020* [132].

[b]We use the *Delivrable 3.1: Profile of heating and cooling demand in 2015* [133] from the Heat Roadmap Europe (HRE4) project [134].

[c]We adapt the method proposed by Rixhon et al. [101] for Belgium to all European countries using data from the Eurostat energy balances [1], Eurostat *Prodcom* database [135], the *National Inventory Submission* of the UNFCCC [136] and the *World Integrated Trade Solution* of the World Bank [137].

[d]For passenger mobility, freight and shipping, the *EU Reference Scenario 2020* contains data about mobility activity in end-use demand unit (Mpkm and Mtkm). No other data source is necessary.

[e]We compute the current aviation activity (Mpkm) from the Eurostat database on air transport measurement for passengers[138].

[f]We project the demand to 2050 using the data of the *Aviation Outlook 2050* report of EUROCONTROL [139].

heat pumps, EUCalc provides the ambient heat used. Thus, the sum of this ambient heat and the electricity consumption of the electrical heat pump equals the end-use demand. For heat provided by boilers, we keep the final energy consumption as end-use demand. This assumption overestimates this demand slightly as the efficiency of a boiler is close to 1. The final energy consumed for space cooling is converted into end-use demand using the coefficient of performance of space cooling units in our model.

In the industrial sector, the EUCalc model does not provide enough information to convert the final energy consumption into end-use demand. Hence, the final energy consumption is split into specific electricity, space heating, hot water, space cooling, high-temperature heat and process cooling according to the shares computed in the Heat Roadmap Europe

(HRE4) project [133]. Those shares are computed on the real consumption of the industry of European countries in 2015. We assume that these shares stay constant in 2050. This implies assuming that the European industry stays similar to the actual one in each country.

The non-energy demand (NED) is modelled separately from the rest of the industrial demand. We adapt the method proposed by Rixhon et al. [101] for Belgium to all the European countries. To decarbonize this demand, it will no longer be supplied with petroleum products and other fossil fuels. Therefore, Rixhon et al. propose quantifying the non-energy demand as three main feedstocks rather than one final energy consumption of petroleum products. The three feedstock are high value chemical (HVC), methanol and ammonia. Together, they cover 90% of the total non-energy demand worldwide [140]. For each feedstock, we chose a database based on its completeness across Europe. For the HVC, we assume that the production sites remain where they are currently and quantify their current production based on the Eurostat energy balances [1]. For methanol and ammonia, we assume that they become highly traded fuels, and thus, the production sites can change with the change in the topology of the energy system. Therefore, we quantify the local consumption of those fuels by subtracting exports from local production and imports. For methanol, these data are taken from the *Prodcom* dataset of Eurostat [135]. For ammonia, the trade data come from the *World Integrated Trade Solution* database of the World Bank [137] and the local production from *National Inventory Submission* of the UNFCCC [136] and is completed with *Indexmundi* database for Switzerland and Hungary [141]. These computations provide demands for kilo-tonnes of HVC, methanol and ammonia in 2019 in each European country. These quantities are converted into equivalent energy based on their LHV. We assume their respective shares in non-energy demand are constant up to 2050. We project their total non-energy demand to 2050 by assuming the same growth as the final energy demand for non-energy in the *EU Reference Scenario 2020*.

For the transportation sectors, the *EU Reference Scenario 2020* provides information about the transport activity for passenger mobility in Mpkm/y and inland freight in Mtkm/y. These are the same definition as our end-use demands. For international shipping, the end-use demand is computed thanks to the total freight energy consumption and energy intensity. Their ratio provides the total freight activity, including inland freight and shipping, in Mtkm/y. By subtracting the activity of inland freight, we obtain the international shipping activity. For passenger aviation, the current demand in Mpkm/y is computed with the method proposed in [107]. Based on Eurostat datasets of passengers boarding planes departing each European country [138], both intra-European and extra-European demands are computed in Mpkm/y for the year 2019. The evolution of those demands is projected to 2050 using the growth rates predicted by EUROCONTROL [139]. The intra-European aviation is considered as short-haul flights and is represented in the model as a minimal and maximal share of passenger mobility. Here, we assume this share cannot be changed and fix the minimal and maximal values to the same amount. The extra-European aviation is considered as long-haul aviation and is defined as an end-use demand as such into Mpkm/y.

We only consider jet-fueled planes for short- and long-haul aviation demands. Other types of motorization are highly uncertain and will most likely not play an important role [68, 142]. To decarbonize them, they are fueled with renewable fuels. We assume that all shipping is supplied with cargo ships of 4000 twenty equivalent units. It is the second type of cargo the most handled in Europe in terms of weight after liquid bulk [143]. However, as they serve mainly for fossil fuel imports, liquid bulk cargo is likely to decrease significantly in a fossil-free energy system. From the literature, we model different potential motorizations for these boats: internal combustion engines or fuel cells. The internal combustion engine boats are further divided according to their fuel: (i) oil-fueled cargos [144]; (ii) methane-fueled cargos [69]; (iii) methanol-fueled cargos [69]; (iv) ammonia-fueled cargos [145]. Similarly, two types of fuel-cell cargo ships use two different fuels [70]: (i) hydrogen and (ii) ammonia.

Similarly to the short-haul aviation share in passenger mobility, other shares are applied to the demands: (i) share of low-temperature heat, that is, space heating plus hot water, supplied with DHNs; (ii) share of freight mobility supplied by boats on rivers, by trains and by trucks; (iii) share of passenger mobility provided by public mobility. For each of them, the share is optimized by the model within maximum and minimum bounds. These bounds are kept equal to the ones of Belgium in the original version of EnergyScope [99].

Additionally, some specific end-use technologies are constrained in the maximum share of their end-use they can supply: (i) metro, tramway and trolley bus (<30% of public mobility); (ii) passenger train (<50% of public mobility); (iii) electrical heating for industrial processes (<60% of the high-temperature heat). In the model, these technologies are efficient and cost-competitive options to supply the demand. However, they have practical limitations that keep them from supplying a part of that demand. Due to their high infrastructure, which is not modelled here, metro, tramway, trolley bus, and trains cannot be installed in all locations with a public mobility service. The maximum shares are kept as in the previous version of EnergyScope for Belgium [99]. In this previous version, all assumptions related to the share of mobility were fixed arbitrarily based on historical data in 2015 such that they are ambitious and realistic. However, Rixhon et al. [8] showed that the uncertainty on the maximum share of public mobility is not among the most impactful uncertain parameters for the Belgian energy system. This result most likely also applies to a European energy system. The limit on electrification of high-temperature heat is added in this model version. It models the fact that between 33 and 51% of the process heat demand is unsure of being suitable for electrification [44, 45].

The *EU Reference Scenario 2020*, which is at the heart of our quantification of the energy demand, covers only 25 out of the 34 modelled countries. The nine remaining countries are split into 4 categories according to the data found and the method to approximate their demand: (i) the United Kingdom; (ii) Switzerland; (iii) Norway; (iv) non-EU Balkan countries: Albania, Bosnia-Herzegovina, Kosovo, Montenegro, North Macedonia and Serbia.

At the time of the previous *EU Reference Scenario*, in 2016, the United Kingdom was a European Union member. This is no longer true in the 2020 version of the *EU Reference Scenario*. Hence, the projection of the previous report is used, and the rest of the demand quantification is identical to other countries.

Switzerland is already modelled in a previous version of EnergyScope for 2035. The demand is completed with demand not present in this version of EnergyScope: aviation, shipping, space cooling and process cooling. Aviation is computed based on the same method as the other countries. As Switzerland has no coast, it does not have any shipping demand. Space cooling and process cooling are extrapolated from data from Austria, assuming that they are proportional to space heating and high-temperature heat, respectively. Then, the energy demand is projected to 2050, assuming the same growth as in Austria.

For Norway, historical data can be found for several demands: passenger mobility, freight mobility, aviation and non-energy demand. The Norwegian National Statistical Department provides data on passenger mobility and freight [146, 147]. The aviation and non-energy demand computations are done in the same way as the other countries. Then, we assume the same growth of those demands as in Sweden. For the other demands, we assume the same demand per capita as in Sweden and verify the total demand per sector by comparison with Odyssee [148] and International Energy Agency [149] reports.

For the non-EU Balkan countries, the extrapolation is based on final energy consumption data per sector from Eurostat [1]. Each of these countries is linked with a neighbouring used for the mapping, see Table 1.10. The ratio of the end-use demands of each sector to the final energy consumption of this sector is computed for each mapping country for 2015. Then, the end-use demands in 2015 for each non-EU Balkan country are computed assuming the same ratio between EUD and FEC as in its mapping country for each category. Afterwards, the end-use demand per capita in 2015 is computed for each country. We assume that this demand per capita evolve like the one of its mapping country up to 2050. Finally, the end-use demands per capita are multiplied by the population projection of each country in 2050 [150, 151]. The underlying hypothesis is that those countries will have a similar evolution of energy services per capita as their mapping country.

Table 1.10: European Union (EU) mapping countries for non-EU countries.

Non-EU country	**EU mapping country**
Albania	Greece
Bosnia and Herzegovina	Croatia
Kosovo	Bulgaria
Montenegro	Croatia
North Macedonia	Bulgaria
Serbia	Romania

The end-use demand obtained from the *EU Reference Scenario 2020* experiences a general increase in Europe, Figure 1.10. Six end-uses types increase significantly: space cooling, freight, shipping, long-haul aviation, passenger mobility and non-energy. Five other end-use types decrease slightly: hot water, process cooling, high-temperature heat, space heating and electricity. The end-use type with the highest increase is space cooling. On average, at the European level, it increases by 286% from 2015 to 2050. However, space cooling is small compared to other demands and is supplied with efficient technologies. All the mobility demands are multiplied by 1.3 to 1.5. This means that people will travel more and more goods will be transported. The non-energy demand increases by 13%, which means more production of plastics, fertilizers and other products. Five decreasing end-use types profit from gains in efficiency between the end-use and the energy service: electricity, space heating, high-temperature heat, process cooling and hot water. For instance, renovation improves the insulation and decreases the heat needed to keep the same indoor thermal comfort. Led lighting provides the same lighting service with less electricity consumption than other lights.

The energy demand is not uniformly dispatched across Europe. Two main factors explain this difference: the country's population and the energy consumption intensity per capita. For each end-use type in each country, Figure 1.11 presents the total demand and Figure 1.12 presents the demand per capita.

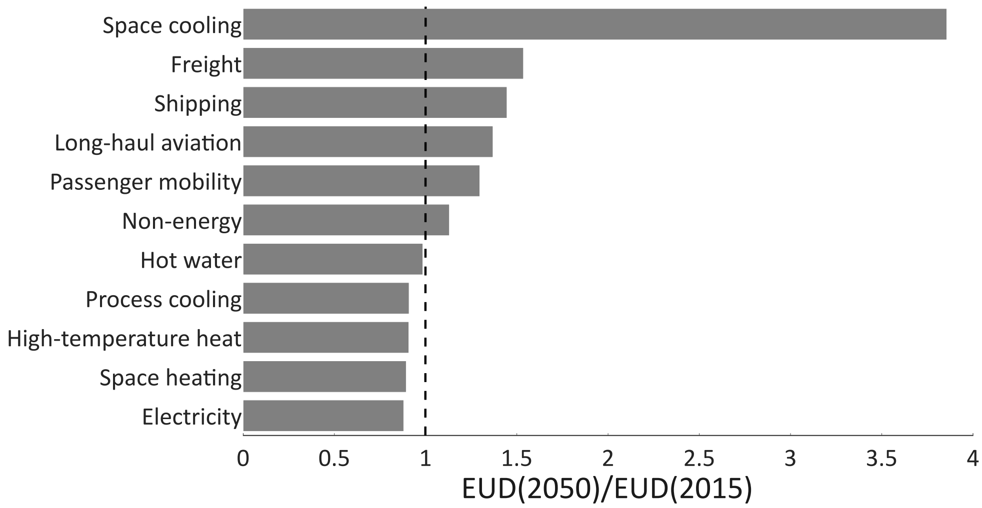

Figure 1.10: In the *EU Reference Scenario*, the energy demand increases from 2015 to 2050. However, four types of end-use demands EUDs decrease thanks to efficiency improvements such as efficient appliances and renovation.

The maps of the total demand show which cells have the largest demands for each end-use type as the model sees it. For instance, Germany has a high population and an intensive industry. It is the largest consumer in many end-use types: specific electricity, hot water, space heating, etc. In general, the big countries are the largest consumers, but some smaller countries stand out for specific end-use types. For instance, the Netherlands and Belgium are among the largest consumers of shipping and non-energy.

The maps of the demand per capita provide more information on the way of life and the industry intensity in each country. For instance, Finland is the largest consumer per capita in many end-use types: electricity, hot water, space heating and high-temperature heat. This is due to its energy-intensive industry that drives the consumption of those end-use types. In these maps, the important demands for shipping and non-energy in the Netherlands and Belgium pop out even stronger than in the total demands maps. Some demands, such as passenger mobility, have low variations from one country to another, whereas others have very big variations. These bigger variations can be due to: climatic conditions such as space cooling; economic activities such as non-energy demand linked with the chemical industry; or life standards such as long-haul aviation.

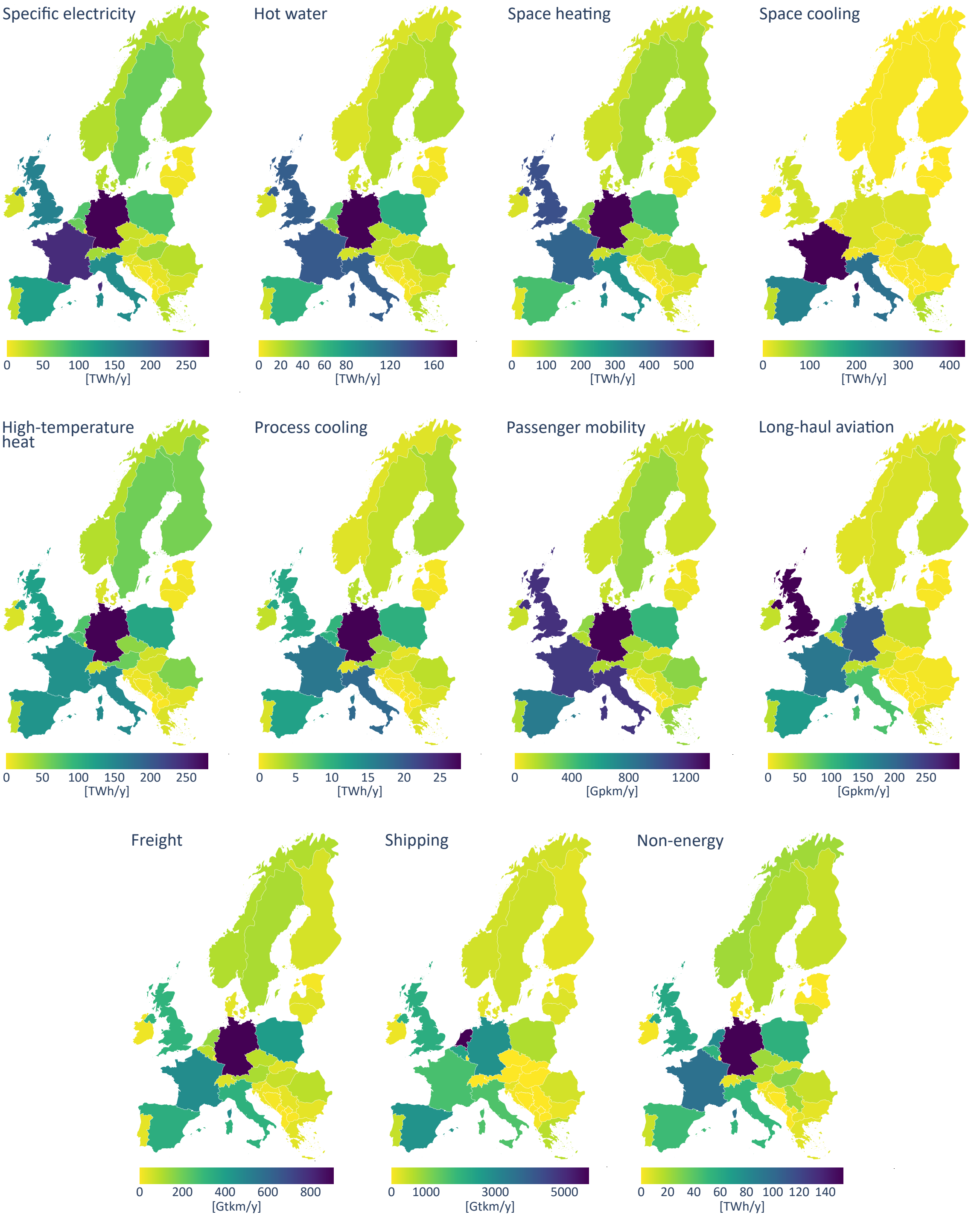

Figure 1.11: Map of the end-use demands in Europe in 2050.

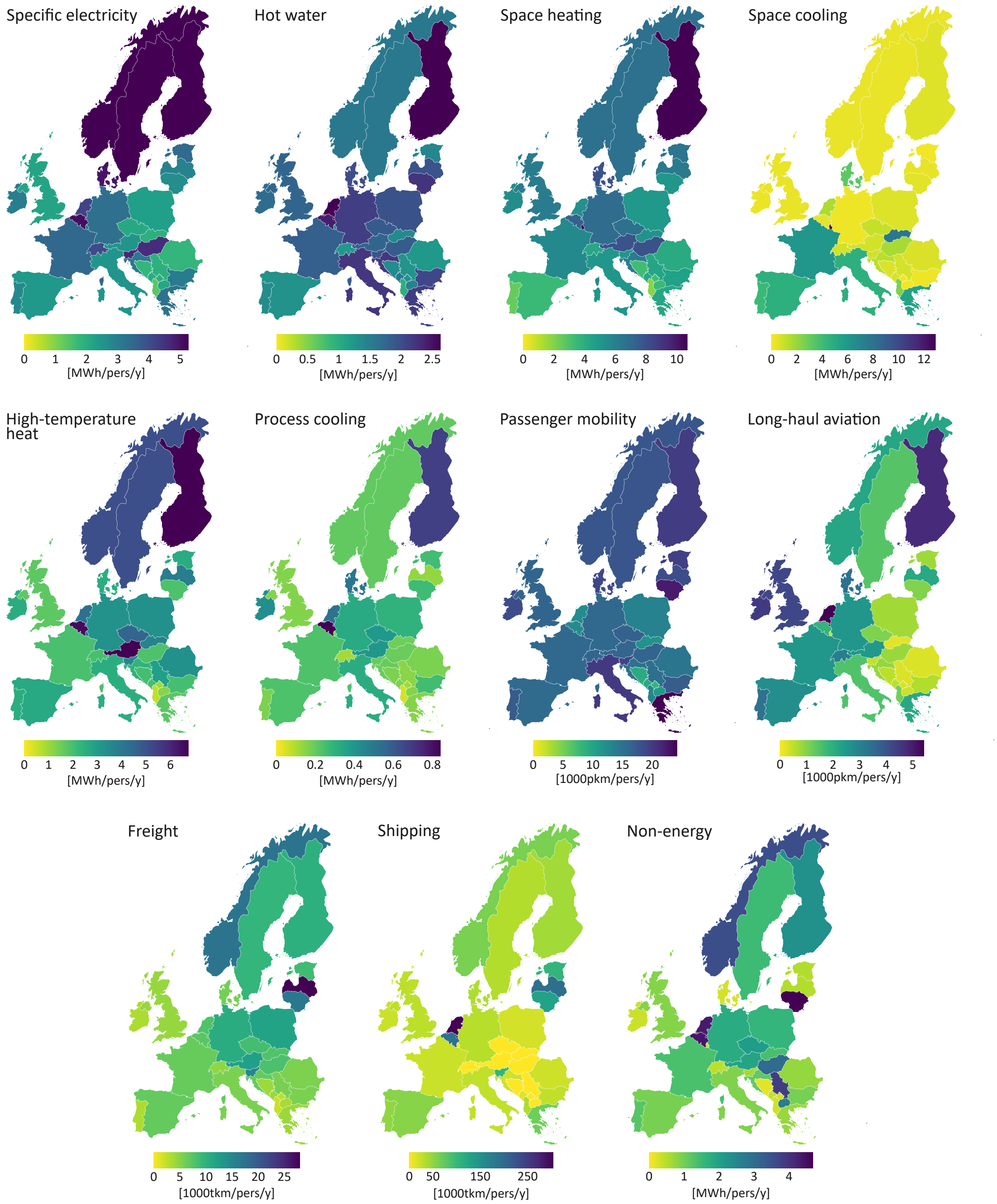

Figure 1.12: Map of the end-use demands per capita in Europe in 2050.

Time series of end-use demands

In addition to the spatial repartition of the demand, it varies in time. Time series describe this variation. They provide the share of the total energy demand at each hour of the year and are computed in each country for several demands: specific electricity, space heating, space cooling and mobility passenger. Table 1.11 summarizes the data source and the method to compute those time series. The same historical year is taken for the different time series to ensure their synchronicity. The year 2017 was chosen as it is the historical year with the most complete data (i.e. the lowest number of hours with missing data). For the hours with missing data, we fulfil them with the value at the same time during the previous or next week.

Table 1.11: The time series of specific electricity, space heating, space cooling and passenger mobility come from different data sources and undergo different data processing.

Time series name	Data sources	Data processing
Specific electricity	ENTSOE [152]	*Load actual ENTSOE transparency*, subtract heating and cooling with electricity
Space heating	MERRA-2 [153]	*Hourly geographically aggregated weather data, temperature*, computing heating degree hours
Space cooling	MERRA-2 [153]	*Hourly geographically aggregated weather data, temperature*, computing cooling degree hours
Mobility passenger	NHTS [154]	*Hourly time series of passenger mobility*

Specific electricity time series is computed based on the historical load to which we subtract heating and cooling done with electricity. The historical load comes from the European Network of Transmission System Operators for Electricity (ENTSOE) Transparency platform [152] and is gathered into an extractable format in the open power system data (OPSD) platform [155]. The annual heating and cooling with electricity is computed based on the data of the HRE4. It is dispatched over the year based on their time series in the model and subtracted to the electrical load. Finally, the specific electricity time series is normalized such that its sum over the year is equal to 1.

For the space heating and space cooling demands, heating and cooling degree hours are computed and normalized over the year. The OPSD platform provides hourly profiles for geographically aggregated temperature in each country based on Modern-Era Retrospective analysis for Research and Applications, version 2 (MERRA-2) data [153]. Staffell et al. [156] gives an outdoor temperature threshold below which we need to heat (14°C) and above which we need to cool (20°C). The heating degree hours are computed as the difference between the heating threshold and outdoor temperature when the outdoor temperature is above the threshold. Similarly, cooling degree hours are computed as the difference between the outdoor temperature and cooling threshold when the outdoor temperature is above the cooling threshold. Then, the two time series are normalized such that their sum over the year is equal to 1. Finally, the two time series undergo a moving average with a time window of 24 hours to simulate the thermal inertia of the fleet of buildings, and to avoid unrealistic peaks in the demand that would lead to oversizing. The passenger mobility time series is kept as in EnergyScope TD for Belgium, see Figure 1.13. As in EnergyScope TD, we assume this time series is the same every day of the year, using the daily time series of the National Household Travel Survey (NHTS) [154]. The same time series is used for every country, mapping it according to the time zone.

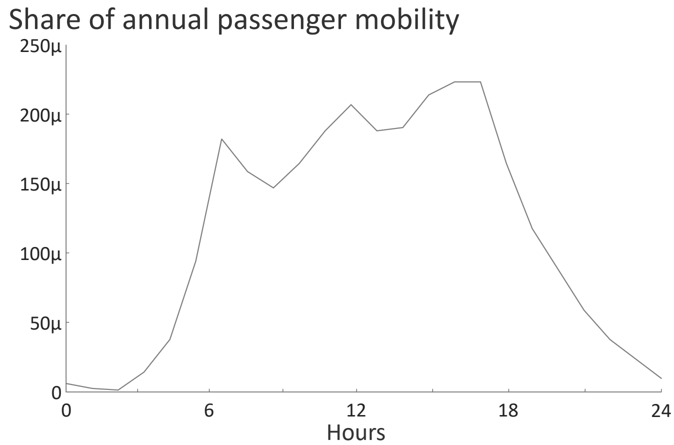

Figure 1.13: Passenger mobility time series is defined on a daily scale.

Specific electricity, space heating and space cooling time series have very different profiles. Figure 1.14 presents these time series for three European countries: Finland, the Netherlands and Romania. As the time series are normalized such that their sum over the year equals 1, the value at each hour is very small (<1.5e-3). In the three countries, the specific electricity time series have a small seasonal variation with lower demands during the summer. They have two daily peaks, one in the morning and the other in the evening. The space heating time series has a strong seasonal variability, with null values in the hot season (middle of the graph) and peaks during the cold season (extreme left and right). This variability is the strongest in Finland and the weakest in Romania. The space cooling has the opposite variability, with peaks during the hot season and null values during the cold season. This variability is the strongest in Romania and the weakest in Finland.

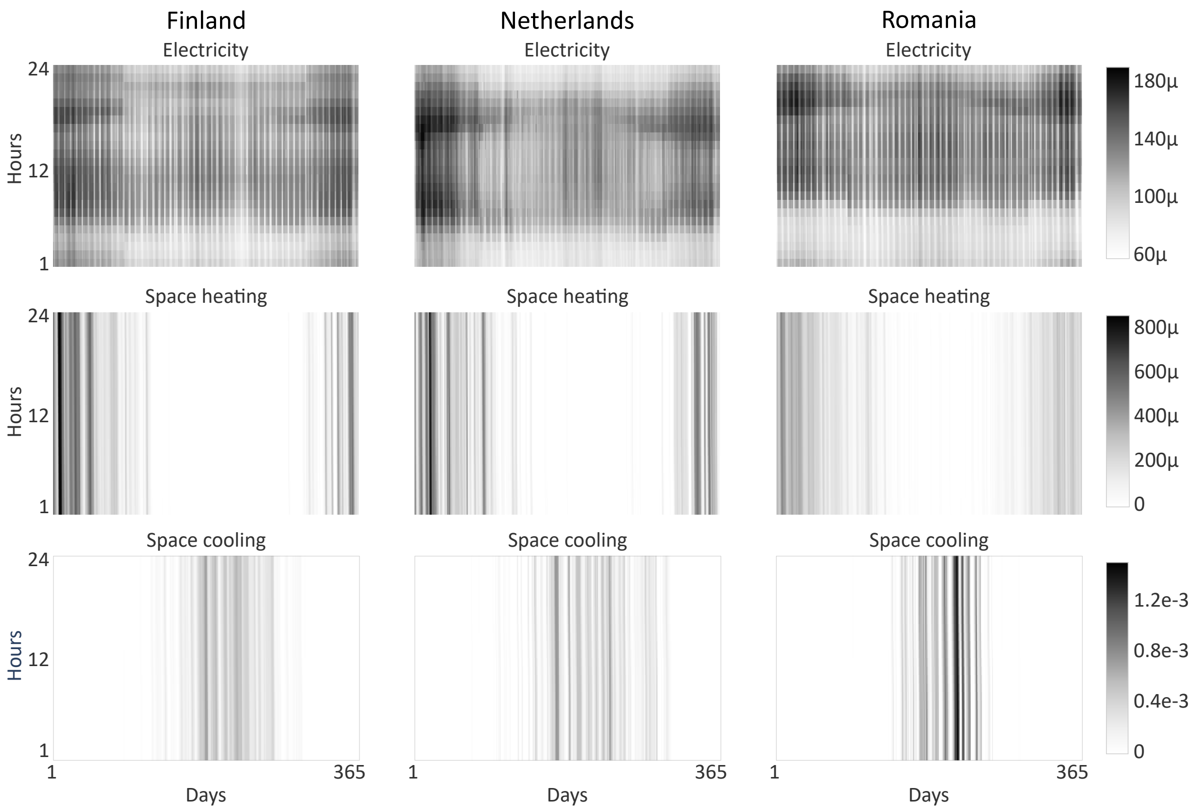

Figure 1.14: Example of time series for end-use demands in Finland, the Netherlands and Romania. The hours of the day are plotted along the vertical axis, and the days of the year are plotted along the horizontal axis. All time series are plotted in coordinated universal time (UTC) time zone.

1.2.3 Resources and renewable energy potentials

The resources are the model's energy inputs. They can be produced locally or imported from the rest of the world. This section describes how the local renewable energy sources are evaluated. Then, it compares them to the energy demand in each region. Finally, it describes the energy imports considered and their cost.

Local renewable resources

To phase out fossil fuels, Europe needs to exploit its renewable energy sources. However, those sources encounter socio-technical limits. Furthermore, some renewables, such as solar and wind, have production that is influenced by meteorological conditions and must be described with a time series.

The socio-technical limits to renewables deployment are related to various factors: (i) natural phenomena, such as wind speed for wind turbines; (ii) technology characteristics; (iii) land use and societal constraints, such as the impossibility of installing a wind turbine too close from houses. Therefore, many studies have evaluated the socio-technical potential of renewable energy sources using geographic information system (GIS)-based approach [110, 124, 157–168]. These studies superpose maps defining the profitable zones for renewable energy sources according to meteorological conditions (e.g. solar irradiance, wind speed) and maps defining exclusion zones according to societal constraints (e.g. protected areas, settlements). Based on this superposition, they evaluate the locations and potential power and production of renewables. Table 1.12 presents the data sources, selected scenarios in these databases and data processing to define the renewable energy sources potential for each European country. For all renewable energy sources, except biomass, the renewable energy potential is integrated into the model by setting the upper bound on the installed capacity (parameter f_{max}). For biomass, the potential is set by the local annual availability of the resource (parameter $avail_{local}$).

For wind, solar and hydro technologies, the lower bound of installable capacity (f_{min}) is set to their current capacity. For wind and solar, the current capacity is computed from Eurostat [169]. For hydro, the current capacity is computed from the Joint Research Center (JRC) Hydropower database [170]. We assume that in 2050, at least these capacities should be installed. These technologies and the cross-border transmission network capacities are the only ones where we consider the legacy capacity. For all the other technologies, the model can choose to install any quantity (down to zero).

For the three main renewable energy sources (solar, wind and biomass), we use the JRC ENSPRESO database as it provides a coherent evaluation of potentials across all European Union. In each case, we select the reference or median scenario for ENSPRESO. The regional data (NUTS2 scale) are regrouped at the country scale (NUTS0).

For wind energy, the ENSPRESO scenario *Reference - Large turbines* is used with a cut-off at a capacity factor of 20%, see Table 1.12. Furthermore, for offshore wind turbines, the potential proposed by ENSPRESO is outdated, as the sector has seen intense development in recent years [171]. For instance, ENSPRESO evaluates a potential of 1.85 GW for Belgium whereas it has already installed 2.26 GW [169]. This is especially true for the North Sea region, which has the highest potential for this energy source. Therefore, the ENSPRESO wind offshore potentials were updated with the Ostend Declaration [172], which is a political statement of countries of the North Sea region to collaborate in order to reach certain objectives in terms of installed capacities of offshore wind in the North Sea.

Table 1.12: Renewable energy potentials: data sources and processing.

Renewable energy	Data sources	*Selected scenario* and data processing
Onshore wind	ENSPRESO[a]	*Reference - Large turbines* with $c_p \geq 0.2$
Offshore wind	ENSPRESO[a], Ostend Declaration[b]	*Reference - Large turbines* with $c_p \geq 0.2$, updated with Oostende Declaration
Rooftop solar	ENSPRESO[a]	*MS 170 W per m2 and 3%*, all rooftop areas converted into PV and solar thermal capacity
Utility PV	ENSPRESO[a]	*MS 170 W per m2 and 3%*, all ground areas
CSP	ENSPRESO[a]	*MS 170 W per m2 and 3%*, high irradiance ground areas
Biomass	ENSPRESO[a]	*ENS_Med* regrouped into five categories[c]
Hydro river	JRC Hydropower[d], e-Highway[e]	Maximum between current capacity from JRC, and potential in *e-Highway - 100% RES*
Hydro dam	JRC Hydropower[d], e-Highway[e]	Maximum between current capacity from JRC, and potential in *e-Highway - 100% RES*
PHS	JRC Hydropower[d], JRC PHS potentials[f]	Maximum between current capacity from JRC, and JRC PHS potentials (*T2 - Realisable potential, 10km*)
Tidal	Hammons[g]	*Parametric Modelling*
Geothermal	Chamorro et al.[h]	*EGS sustainable potential (>150 °C), 3-10km*
Waste	Elbersen et al.[i]	Method of Dommisse and Tychon

[a] For the three main renewable energy sources (solar, wind and biomass), we use the JRC ENSPRESO database [110] as it provides a coherent evaluation of potentials across all European Union. For biomass, the detailed assumptions can be found in [159].

[b] For offshore wind, the outdated data of ENSPRESO are updated with the Ostend Declaration [172].

[c] More details for each category of biomass in Table 1.14. The five categories are woody biomass, second-generation energy crops, wet biomass, biowaste and biomass residues.

[d] The Joint Research Center (JRC) maintains a dataset with all the hydropower plants and storage plants in Europe [170].

[e] The e-Highway projects studies a *Modular Development Plan of the Pan-European Transmission System 2050* [173] and provide data for future capacity in each European country [112]

[f] The JRC produced a dataset of potential new PHS capacity by linking existing reservoirs [174]. This dataset is based on a paper that develops the GIS-based methodology [113].

[g] Hammons [161] evaluates the reasonably exploitable sites for tidal energy in Europe.

[h] Chamorro et al. [160] evaluate the sustainable potential for enhanced geothermal system (EGS) in Europe.

[i] The waste is not a renewable energy. However, we consider it a local resource. Some waste is better valorised as energy than stored in landfills. Its potential is evaluated from [175] with the method of Dommisse and Tychon [109].

For solar energy, the ENSPRESO scenario *MS 170 W per m2 and 3%* is used, see Table 1.12. This scenario assumes that 3% of the available non-artificial areas can be used to install solar panels with a density of 170 W/m^2. For all solar technologies, the potentials are primarily defined by the suitable area. Different solar technologies compete for the same areas and their installed power is converted into area used thanks to their power density, Table 1.13. Hence, the upper bound on installable capacity (f_{max}) of one solar technology can be installed only if the solar technologies competing for the same area are not installed at all.

We divide the suitable areas into three types of categories: (i) rooftop areas ($solar_{area,\ rooftop}$); (ii) ground areas ($solar_{area,\ ground}$); (iii) ground areas with high-irradiance (>1800 kWh/m^2) and low slope (<2.1°) ($solar_{area,\ ground,\ csp}$). Rooftop PV, decentralised solar thermal and DHN solar thermal compete for rooftop area. Utility PV and CSP technologies compete for ground area. However, CSP technologies can only be installed on ground areas with high solar irradiance and a low slope. Therefore, they are further constrained by the high irradiance area with competition between parabolic trough (PT) and solar tower (ST). Those technologies comprise three components in the model: the collectors, the storage tanks and the power block. The collectors are constrained by the available area, assuming a power density that includes the rest of the plant. The solar multiple links the storage tanks and the power block with the collectors. It is defined as the ratio of the collectors' thermal power and the power block's thermal power input at full load. It is constrained by a maximum value of 4 [124].

Table 1.13: Power density of solar technologies.

Solar technology	**Power density** [GW/km^2]
Rooftop PV [110]	0.17
Utility PV [110]	0.17
Decentralised solar thermal [176]	0.70
DHN solar thermal [176]	0.70
Parabolic trough (CSP)[a] [110]	0.395
Solar tower (CSP)[a] [110]	0.355

[a] The power density of CSP technologies are derived from ENSPRESO. It gives the power density in electrical power of the power block for a plant with a solar multiple of 1. This plant has a thermal power of the collectors equal to the thermal power input of the power block at full load. In our model, we convert this density in terms of thermal power and associate it with the collectors as we allow the model to optimise the solar multiple.

The biomass potential is derived from the *ENS_Med* scenario of ENSPRESO, Table 1.12. We regroup their 17 commodity into five categories: woody biomass, second generation energy crops, wet biomass, biowaste and biomass residues. Table 1.14 describes those categories. The energy commodities of ENSPRESO are regrouped according to their feedstock characteristic and origin and their production cost. Furthermore, the three commodities related to first generation energy crops (e.g. bioethanol) that compete with food production are rejected in this work. We aggregated the annual potentials and costs of energy commodities at regional level (NUTS2) to each category at national level. The woody biomass and second generation energy crops supply both the wood layer in the model. They have different costs and origin but can be used in the same conversion technologies. Similarly, the biowaste and biomass residues feed the biowaste layer at different costs.

This version of the model develops a more refined representation of biomass. As explained above, the biomass feedstocks are separated into five categories. Those categories feed three layers at different costs and the full conversion chain for these layers is updated. The objective is to represent all the competing uses for these dispatchable renewable energy sources and to let the model optimize their use. Figure 1.9 presents all the conversion technologies using the different biomass feedstocks. The wood layer can be used in technologies producing electricity, electricity and heat (high- or low-temperature), heat (high- or low-temperature) and renewable fuels. We model the biowaste conversion chain by duplicating the woody biomass centralised conversion units (e.g. industrial boiler) with an increase in maintenance cost (+22%) and a decrease in efficiency (-7%). These changes model the fact that a more diverse and lower-quality feedstock induces more maintenance and lower efficiency. These changes are evaluated by comparing industrial boiler technologies for each of these feedstock in the Danish Energy Agency Technology Catalogue [114]. We assume that similar changes in characteristics are experienced in other conversion technologies. The wet biomass is always transformed into biomethane, which can be used in many applications.

For hydro dam and hydro river, the potential is the maximum between the current capacity from the JRC Hydropower database and the potential in *100% RES* scenario of e-Highway [112, 173]. Similarly, the PHS potential is the maximum between the current capacity from the JRC Hydropower database and the potentials *T2 - Realisable potential, 10km* assessed by Gimeno-Gutiérez and Lacal-Arántegui [113]. They use a GIS-based method to evaluate the potential for new PHS capacity by linking existing reservoirs. The T2 potential means that they consider two types of topology: (i) an existing pair of reservoirs to be connected and (ii) an existing reservoir with a site suitable for a second reservoir. Furthermore, they consider sites with less than *10km* distance and restrain the theoretical potential with land use restrictions to get a *Realisable potential.* Their assessment is regrouped into a JRC report and dataset [174].

The tidal potential is taken from parametric modelling. Hammons [161] evaluates the technically available tidal energy resource by applying a tidal power plant model to assess all exploitable sites in Europe. Then, they discard sites according to environmental constraint such as protected areas. The geothermal potential comes from *EGS sustainable potential (>150°C), 3-10km.* Chamorro et al. [160] evaluate the sustainable potential for enhanced geothermal system (EGS) in Europe. They consider sites as suitable if they reach at least

150°C at a depth between 3 and 10 km. From those sites, they discard natural protection areas and apply a sustainable criterion to geothermal energy: the heat removed from the resource is replaced on a similar time scale [177, 178]. The waste potential is computed from [175] using the method of Dommisse and Tychon [109].

For non-EU countries, all the potentials except solar and wind are found in the same database as those of EU countries. For solar and wind, we computed the potentials with the model of Dupont [158, 179, 180] both for those countries and their neighbouring EU member. The potentials obtained for their neighbouring EU member with this model are compared to the ones of ENSPRESO. If they differ by more than 20%, the potential computed with Dupont's model for the corresponding non-EU country is rescaled proportionally to this difference.

Table 1.14: Biomass categories and potential.

Category	**Layer**	**Description**	**ENSPRESO commodity codes**
Woody biomass	Wood	Lignocellulosic biomass from stemwood, logging residues, sawdust, woodchips and pellets, residues from landscape care	MINBIOWOO, MINBIOWOOa, MINBIOWOOW1, MINBIOWOOW1a, MINBIOFRSR1, MINBIOFRSR1a
Second generation energy crops	Wood	Lignocellulosic biomass from second generation energy crops: miscanthus, switchgrass, reed canary grass, willow, poplar	MINBIOCRP31, MINBIOCRP41, MINBIOCRP41a
Wet biomass	Wet biomass	Biomethane from wet biomass: solid and liquid manure, sludge	MINBIOGAS1, MINBIOSLU1
Biowaste	Biowaste	Municipal waste	MINBIOMUN1
Biomass residues	Biowaste	Agricultural waste	MINBIOAGRW1

In addition to their limited potential, several renewable energy sources have variable production over the year. This characteristic is described by hourly times series of the capacity factor (GW/GW_p) at each hour of the year in each country. Table 1.15 presents the eight time series describing renewable energy sources production. Each time series applies to one or two technologies and extracted and processed from specific data sources. In general, the time series regroup country-aggregated data as the temporal production of renewables varies from location to location. Ideally, this aggregation should be done with the same assumptions and locations as for the evaluation of the potential. However, no work providing such data has been found and we use other data sources with similar assumptions.

The wind turbine and PV time series are obtained on the OPSD platform [155] that gathers *hourly country-aggregated capacity factors* from the Renewable ninja project [181–184]. For onshore wind and PV, no further data processing is necessary. The PV time series is used for utility and rooftop PV. For offshore wind, the historical data for some countries are missing. They didn't install offshore wind turbines yet but have a non-null potential. For Estonia, Spain, Lithuania, Poland and Portugal, the Renewable ninja project mapped potential future installed offshore wind turbines onto historical wind speed data to rebuild time series for historical years. For Croatia and Latvia, no data is available. We take the capacity factors of neighbouring country with a common sea: Italy and Lithuania, respectively. For Bulgaria and Romania, non of the above is feasible. We choose a location point from an offshore wind parc feasibility study [185] and use its time series [181] as representative of the entire fleet for those countries.

The solar thermal time series is derived from the global horizontal irradiance (GHI) from the *hourly geographically aggregated weather data* gathered on the OPSD platform [155] and computed from MERRA-2 dataset [153]. This time series is used for decentralised solar thermal and DHN solar thermal.

For the CSP time series, we use the Oemof thermal model [186, 187] to compute the thermal output of the collector field. The main input for this model is the DNI time series at a point location. We use the pvlib library [188] to extract it from the PVGIS dataset [189, 190]. The point location is chosen at the location of an exiting CSP plant for each country with a CSP potential. The obtained CSP time series is used for parabolic trough and solar tower collectors. This is an approximation as the Oemof model is for parabolic trough plant.

The hydro river generation is obtained by an hourly interpolation of *daily run-of-river generation* from JRC-EFAS [191, 192] and ENTSOE-PECD [193, 194] datasets. The JRC-EFAS dataset is used by default but the data for some countries are missing. These data are completed with the ENTSOE-PECD dataset. The hourly generation is normalized by it maximum value to obtain the capacity factor.

The hydro dam inflow is obtained by an hourly interpolation of *weekly hydropower inflow* from JRC-EFAS [191, 192] and ENTSOE-PECD [193, 194] datasets. The JRC-EFAS dataset is used by default but the data for some countries are missing. These data are completed with the ENTSOE-PECD dataset. The hourly generation is normalized by it maximum value to obtain the capacity factor. The inflow data is used for this time series to allow the model to choose when to produce according to the dam level and the power production of other assets.

The tidal time series are taken from Dommisse and Tychon [109] and are rescaled to have the same average capacity factor as in Hammons [161]. The same time series is used for all countries with tidal potentials as no better data has been found. However, tidal energy is a small energy source and errors on input data has low impact on the energy system design.

Table 1.15: Time series of renewable energy sources.

Time series name	Renewable technologies	Data sources	Data processing
Onshore wind	Onshore wind	Renewable.ninja [181]	*Renewable ninja hourly country-aggregated onshore wind capacity factor*
Offshore wind	Offshore wind	Renewable.ninja [181]	*Renewable ninja hourly country-aggregated offshore wind capacity factor*
PV	Utility PV, Rooftop PV	Renewable.ninja [181]	*Renewable ninja hourly country-aggregated PV capacity factor*
Solar thermal	Decentralised solar thermal, DHN solar thermal	MERRA-2 [153]	*Hourly geographically aggregated weather data, GHI*
CSP	Parabolic trough collectors, Solar tower collectors	PVGIS [189]	Collectors' thermal output modelled with Oemof thermal [186], using the *DNI* at the location of an existing CSP plant
Hydro river	Hydro river	JRC-EFAS [191], ENTSOE-PECD [193]	Hourly interpolation of *daily run-of-river generation*
Hydro dam	Hydro dam	JRC-EFAS [191], ENTSOE-PECD [193]	Hourly interpolation of *weekly hydropower inflow*
Tidal	Tidal stream, tidal range	Dommisse et al. [109], Hammons [161]	Time series of Dommisse et al., rescaled to average capacity factor of Hammons

The variable energy sources have very different capacity factors over the year, see Figures 1.15 and 1.16 for examples in Norway, the United Kingdom and Spain. The wind turbines have strong variations in their production, with peaks and valleys happening during any season and hour of the day. However, the occurrence and intensity of peaks is higher during the cold season (extreme left and right of the graph). The solar technologies have peaks during the day and null production at night. They also have a seasonal variability with less hours of production and lower peaks during the cold season than during the warm season. This seasonal variability is less strong in Spain which keeps more hours and higher peaks even during the cold season. Furthermore, among these three countries, only Spain can install CSP. Thus it is the only one with a CSP time series. This time series is more scattered than the other solar time series as it only relies on direct irradiation. The hydro time series in Norway and Spain are influenced by the ice melting. This occurs much earlier in the year in Spain than in Norway. In the United Kingdom, the hydro time series are more uniformly dispatched over the year as the are mostly influence by rain regimes. Among these three countries, the United Kingdom is the only one with a tidal potential and time series. This time series has four cycles per day as the four tides and has variation of time amplitude from one day to another.

The renewable energy potentials are not uniformly distributed across Europe, Figure 1.17. For instance, the solar potential is the largest in the big southern countries such as Spain and France. The onshore wind potential is consequent in France, Spain, the United Kingdom and Norway. The offshore wind potential is mainly located in the North Sea region. Waste

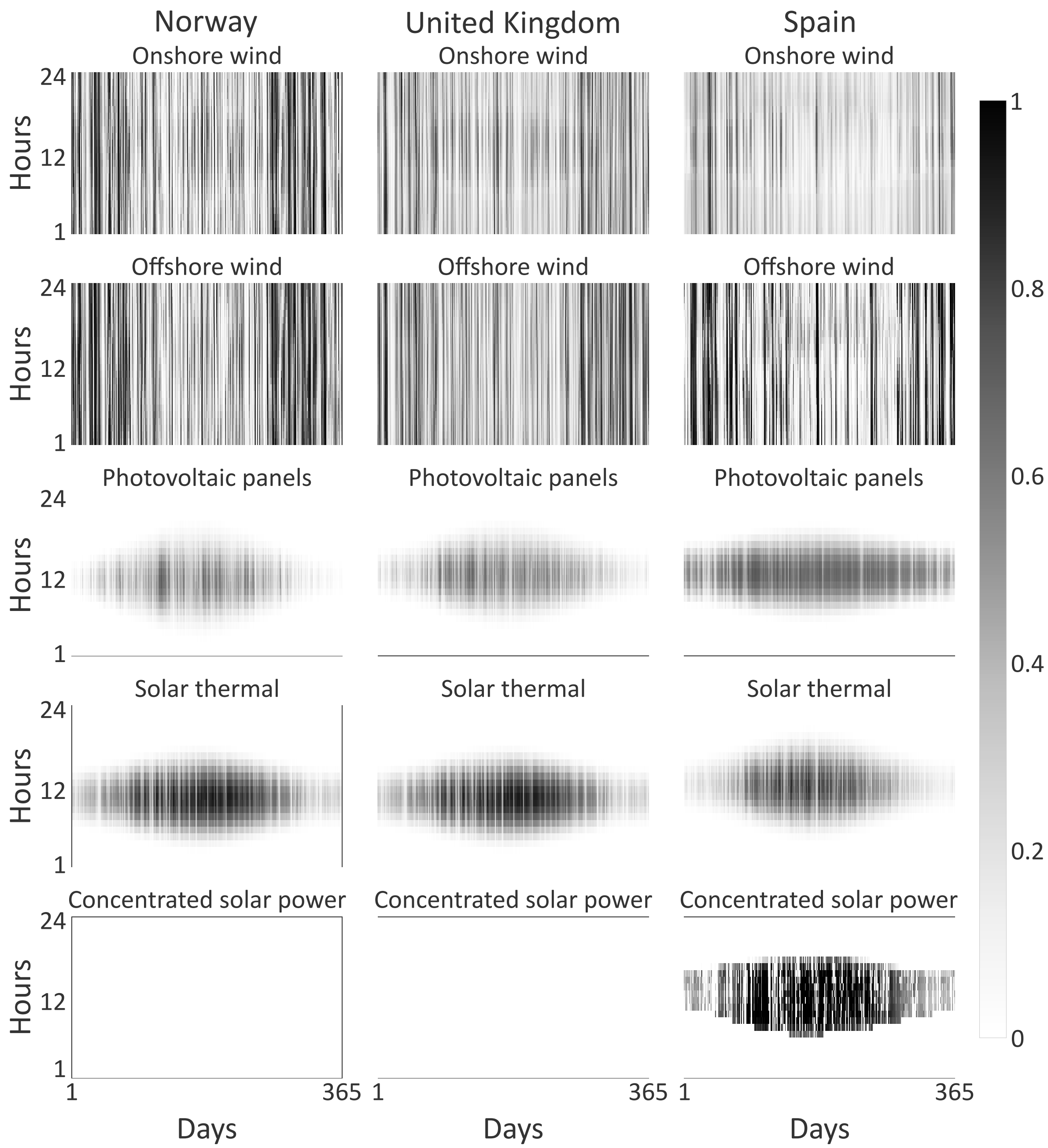

Figure 1.15: Example of time series for renewable energy sources in Norway, the United Kingdom and Spain (part1). The hours of the day are plotted along the vertical axis and the days of the year along the horizontal axis. All time series are plotted in UTC time zone.

potential is directly related to population and is high in countries with high population. Norway has the main hydro potentials both in terms of energy produced and storage capacity. Geothermal energy is high in France, Spain and Germany. Tidal energy is mainly present in the United Kingdom.

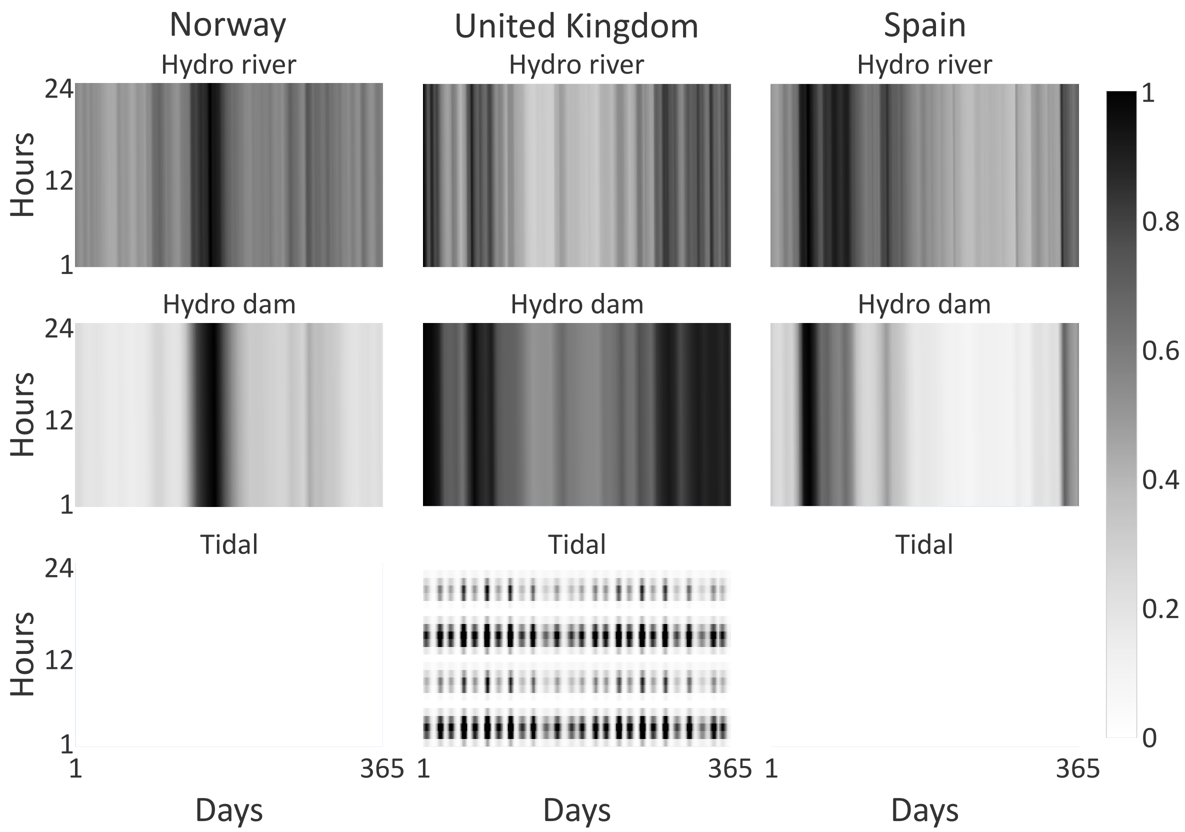

Figure 1.16: Example of time series for renewable energy sources in Norway, the United Kingdom and Spain (part2). The hours of the day are plotted along the vertical axis and the days of the year along the horizontal axis. All time series are plotted in UTC time zone.

The biomass potential is important in countries such as France, Germany, Poland, Sweden, Spain and Romania. Figure 1.18 illustrates how the different biomass categories are distributed across Europe. In general, France and Germany have high biomass potentials. However, some countries stand out for specific categories. For instance, Sweden, Finland and Poland have woody biomass potentials above 110 TWh/y. Spain and Romania have second-generation energy crop potentials above 83 TWh/y.

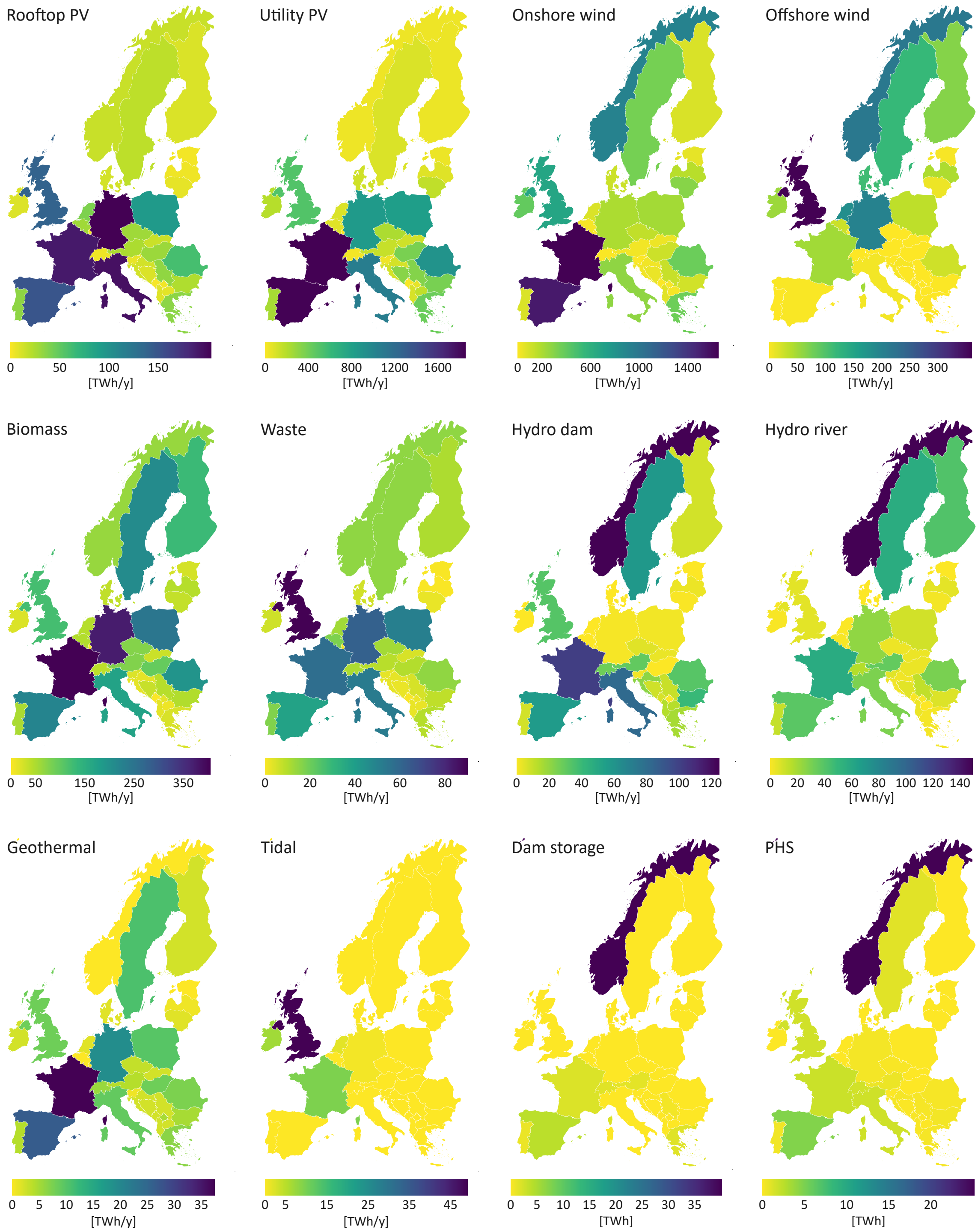

Figure 1.17: Map of the renewable energy potentials in Europe in 2050.

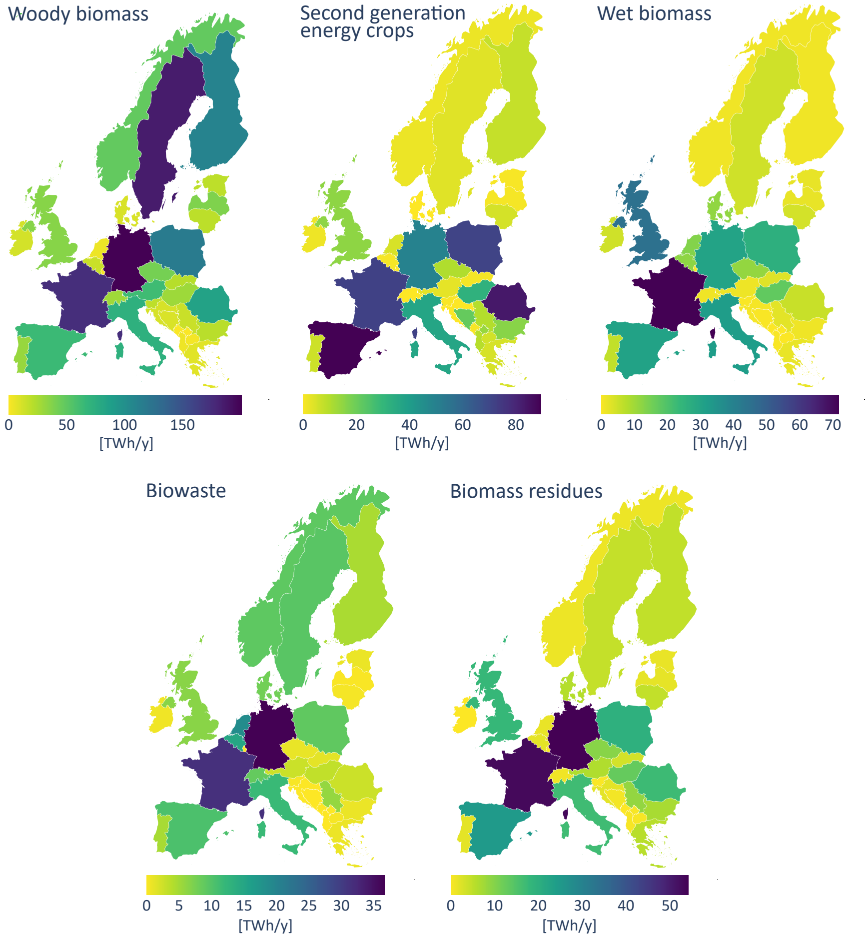

Figure 1.18: Map of the biomass potentials in Europe in 2050.

Comparison of renewable energy potentials and energy demand

The different countries in Europe have very different sizes, population and resources. This leads to very different energy demands and renewable energy potentials. Figure 1.19 depicts the ratio between the energy demand and the renewable energy potentials in each country. To compute this ratio, the end-use demands are converted into final energy with the following assumptions. If not said otherwise, the efficiencies are the ones of technologies in the model: (i) the low-temperature heat is provided with heat-pumps with a coefficient of performance (COP) of 3.17; (ii) the space cooling supply has a COP of 4; (iii) the high temperature heat has a fictive efficiency of 1; (iv) the process cooling has a COP of 2.86; (v) the passenger mobility supply has the average efficiency of the *EU Reference Scenario* in 2050, i.e. 0.158 GWh/Mpkm; (vi) the freight mobility supply has the average efficiency of the *EU Reference Scenario* in 2050, i.e. 0.055 GWh/Mtkm; (vii) the long-haul plane has an efficiency of 0.42 GWh/Mpkm; (viii) the shipping is supplied with oil-fueled cargo ships with an efficiency of 0.02 GWh/Mtkm.

The comparison of renewable energy sources and energy demand gives a qualitative intuition of which countries would be in deficit in a 100% renewable energy system: Belgium, the Netherlands, Switzerland and Germany. On the contrary, many countries are able to produce more renewable energy than their energy demand. Other countries, such as Austria, Slovenia, Finland the United Kingdom, and Italy, lie in between. We do not know beforehand whether they will be in deficit or in excess. These intuitions are verified with the results of the model presented in Chapter 3.

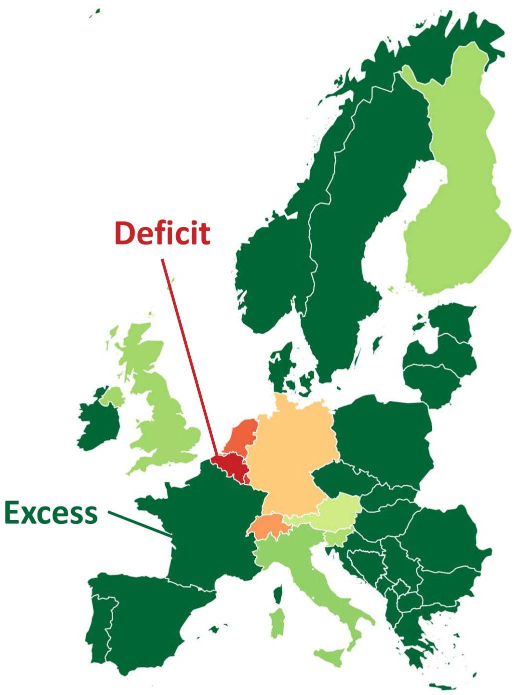

Figure 1.19: Comparison of renewable energy potentials and energy demand in European countries.

Imported resources

In this scenario, we model a fossil-free and nuclear-free European energy system. Therefore, we consider only imports of renewable fuels. Each European country can import renewable fuels from the rest of the world at a certain cost, see Table 1.16. We take these costs from a review estimating the supply cost of green chemical energy carriers at the European border using a dataset of 1050 data points from 30 studies [195]. They are aligned with the cost taken in the previous version of the model from the Hydrogen Import Coalition report [196]. In all these studies, the renewable fuels are all produced from renewable electricity. We don't consider the import of advanced fuels from biomass in this work.

In our model, the FT fuels are further divided into four categories that represent synthetic fuels replacing typical fossil fuels: (i) light fuel oil, (ii) diesel, (iii) gasoline, and (iv) jet fuel. They can be imported at a given cost or produced locally. The Fischer-Tropsch technology is taken as the representative for the production of those complex synthetic fuels [129]. Different plants with different feedstock are considered: woody biomass, biowaste, electricity and hydrogen. These technologies always produce a mix of different fuels. To represent that in the model, for each feedstock, we model one FT plant that has as main output one of the FT fuels and as secondary output another one. We assume that the plant produces two third of the main output and one third of the secondary output. The secondary output is light fuel oil for all plant except when it is the primary output. Then, the secondary output is jet fuel. In total, as we have four possible feedstock and four possible main output, we model 16 different FT plants that the model can install.

Table 1.16: Cost of renewable fuels imports.

Renewable fuel	**Cost [€/MWh]** [195]
Hydrogen	100.63
Methane	104.31
Ammonia	70.90
Methanol	100.15
FT fuels[a]	128.63

[a]FT fuels regroups four types of fuels produced with the Fischer-Tropsch process. In the model, these fuels are synthetic substitutes for fossil fuels: gasoline, diesel, jet fuel and light fuel oil.

The other resources, such as fossil fuels and uranium, are not considered for import in this scenario ($avail_{ext} = 0$). However, as in the previous versions of EnergyScope, their cost and emissions are quantified. It allows the user to add these imports in other scenarios.

1.2.4 Interconnections and exchanges

The energy exchanges are modelled into two categories, see Table 1.17: network exchanges and freight exchanges. We consider three resources for network exchanges: electricity, methane and hydrogen. Electricity and methane already have a European network. Nowadays, there is no European hydrogen network, but this idea has seen growing interest in recent years in the academia [40, 52, 197–200], in the industry [121, 201–204] and in the political institutions [205, 206]. We consider five resources for freight exchanges: ammonia, methanol, FT fuels, woody biomass and CO_2. All these resources have a high energy density and can be transported in trucks, trains, and boats. Although a network could be built for some of these resources, such as CO_2 or liquid fuels, we only consider freight exchanges in this work.

Table 1.17: The resources exchanged are categorized into two different types of exchanges: network exchanges and freight exchanges.

	Network exchanges	**Freight exchanges**
Resources	Electricity	Ammonia
	Methane	Methanol
	Hydrogen	FT fuels
		Woody biomass
		CO_2

The modelling of both types of exchanges relies on the typical distance between two neighbouring countries. It is computed as the distance between the centroid of each region. It is assumed to be the mean distance of all energy exchanges between the two countries. For network exchanges, this distance is longer than the actual length of the cross-border transmission line or pipeline to account for the need to reinforce the network around it.

Network exchanges

For network exchanges, we evaluate the current transfer capacity and the potential expansion of the transmission network, see Table 1.18. For all networks, we assume that Europe keeps at least the current installed capacity. For the methane networks a part of this capacity can be retrofitted to hydrogen network.

The electricity network topology is evaluated based on the European resource adequacy assessment (ERAA) [207] and the Ten-Year Network Development Plan (TYNDP) [208] of the ENTSOE. The lower bound on the transfer capacity (tc_{min}) of the cross-border electricity transmission network is taken as the current capacity, and the lines under construction for the ERAA report of the ENTSOE [207]. From this topology, the upper bound on the transfer capacity (tc_{max}) at each border is computed as the maximum between three options: (i) installing a 4-wire 380kV overhead line with a typical capacity of 1.5 GW [209]; (ii) extending of 50% of the lower bound [67]; (iii) following the *2040 economical needs* for the TYNDP of the ENTSOE [208].

The topology of the methane network is based on the system development map (2021-2022) of the European Network of Transmission System Operators for Gas (ENTSOG) [210]. The lower bound corresponds to the current capacity. We assume that the upper bound is the maximum between two options: (i) installing a 48-inch methane pipeline with a capacity of 20 GW [121]; (ii) extending the current network of 50%.

The potential for a hydrogen network is derived from publications of the European Hydrogen Backbone (EHB) [121, 201, 202, 204]. As no European hydrogen network exists nowadays, the lower bound is set to 0. The upper bounds evaluation differs for retrofitted or new pipelines. The EHB affirms that it is feasible to retrofit the current methane pipelines to hydrogen ones. This induces a retrofitting cost and a loss in the quantity of energy that can be transported through the same pipeline. This loss is expressed by the *ch4toh2* ratio (0.63) [121]. The upper bound on the retrofitted hydrogen network is computed from the current methane network capacity ($tc_{min}(Methane)$) multiplied by the conversion ratio. For the new hydrogen pipeline, we assume an upper bound corresponding to installing a 48-inch hydrogen pipeline (13 GW) [121].

Table 1.18: The maximum bound on transmission networks topology (tc_{max}) is computed based on already existing and under construction lines/pipelines (tc_{min}).
Abbreviations: European Hydrogen Backbone (EHB), European Network of Transmission System Operators for Electricity (ENTSOE), European Network of Transmission System Operators for Gas (ENTSOG), conversion ratio of retrofitting methane to hydrogen (*ch4toh2*), upper bound on transfer capacity (tc_{max}), lower bound on transfer capacity (tc_{min}).

Network	**Source**	tc_{max} [GW]
Electricity	ENTSOE	Max(1.5 GW, 1.5 tc_{min}, TYNDP)
Methane	ENTSOG	Max(20 GW, 1.5 tc_{min})
Retrofitted hydrogen	EHB	$ch4toh2 \cdot tc_{min}(Methane)$
New hydrogen	EHB	13 GW

In addition to their lower and upper bound, the networks are characterised by a cost for their infrastructure and exchange losses, see Table 1.19. The cost of infrastructure includes an investment (c_{inv}) and a maintenance cost (c_{maint}). They differ according to the resource and the network type. For the electricity network, these costs include the cost of the line or cable and the cost of the station. We consider only high voltage alternating current (HVAC) line for inland electricity transmission network and high voltage direct current (HVDC) cables for subsea transmission network. The cost of the methane and hydrogen networks includes the cost of pipelines and compressor stations. The cost of retrofitted hydrogen pipelines includes the cost of the previously built methane pipeline and the retrofitting cost. Indeed, in the model, when retrofitted hydrogen pipelines are installed, they replace the methane ones. For hydrogen and methane subsea pipelines, we use the assumption of the EHB: subsea pipelines are 1.7 times more expansive than underground pipelines. In opposition to cost, in our model, exchange losses are characterised only by the type of resource used.

Table 1.19: Characteristics of transmission network technologies. Abbreviations: specific investment cost (c_{inv}), specific maintenance cost (c_{maint}), exchanges losses ($exch_{loss}$), high voltage alternating current (HVAC), high voltage direct current (HVDC), retrofitted (retro.).

Resource	**Network type**	c_{inv} [M€/GWkm]	c_{maint} [M€/GWkm/y]	*lifetime* [y]	$exch_{loss}$ [%/1000km]
Electricity [211]	HVAC line	2.0	0.04	40	7.5
	HVDC subsea cable	3.24	0.06	40	7.5[a]
Methane [121, 212]	Underground pipeline	0.134	0.001	55	1.0
	Subsea pipeline	0.208	0.002	55	1.0
Hydrogen [121]	Retro. underground pipeline[b]	0.356	0.005	40	2.3
	Retro. subsea pipeline[b]	0.533	0.007	40	2.3
	New underground pipeline	0.452	0.005	40	2.3
	New subsea pipeline	0.726	0.005	40	2.3

[a] In the model, the losses are defined according to the resource and not the network type. For electricity, we choose to take the losses of the HVAC lines for all transmission networks.

[b] The cost of the retrofitted pipeline includes the cost of the previously built methane pipeline and the retrofitting cost.

Freight exchanges

To compute the additional freight due to freight exchanges, the energy quantity exchanged (GWh) must be converted into freight to transport (Mtkm). First, the energy quantity is converted in mass (Mt) thanks to the LHV of the fuel, see Table 1.20. Then, this mass is multiplied by the typical distance between the two exchanging countries to compute the additional freight. The term LHV is correct for all freight exchanged resources except for CO_2, which is not a fuel. In this case, the ratio converts the units of the CO_2 captured layer (t) to the mass units for freight (Mt).

Table 1.20: The freight exchanged resources are converted into millions of tonnes to transport thanks to their lower heating value (LHV).

Resource	**LHV** [213] [GWh/Mt]
Ammonia	5170
Methanol	6390
Gasoline[a]	12890
Diesel[a]	12670
Oil[a]	12220
Jet fuel[a]	12830
Woody biomass	3500
CO_2[b]	1e6

[a] In the model, the synthetic substitute for gasoline, diesel, oil and jet fuel can be produced with the Fischer-Tropsch process, or imported from the international market. They are modelled separately but to simplify the analysis, they are regrouped under FT fuels.

[b] By definition, the CO_2 does not have a LHV. The conversion ratio is to go from tonnes of CO_2 captured to Mt to be transported.

1.3 Summary of the European whole-energy system model

This chapter presents the multi-regional whole-energy system optimization model EnergyScope Multi-Cells. This model is a linear programming model that proposes cost-optimal designs. It is suitable for any multi-regional energy system. It has the specificity of having a whole-energy system approach: it models all energy carriers and all energy demands up to the end-use demand. This allows to reveal all the potential sector-coupling levers to integrate high share of renewable energies.

In addition, this chapter details the assumptions to apply this model to find a cost-optimal fossil-free and nuclear-free European energy system. This energy system representation has a technology-rich catalogue of 167 conversion technologies which can convert 28 energy resources to supply 17 layers of end-use demands. The European energy system is modelled with 34 interconnected countries. Each country is represented as one cell with its own resources, demands and energy conversion system. It is interconnected with other European countries through network exchanges (electricity, methane and hydrogen) and through freight exchanges (ammonia, methanol, FT fuels, woody biomass and CO_2). In addition, each European country can import renewable fuels from the rest of the world at a certain cost.

2 Representing spatio-temporal variability through typical days

Any intelligent fool can make things bigger, more complex, and more violent. It takes a touch of genius — and a lot of courage to move in the opposite direction.
E.F. Schumacher

Chapter overview

- Typical days integration in EnergyScope Multi-Cells.
- Evaluation of design error due to temporal aggregation.
- A priori method to select the number of typical days.

This chapter is built on the peer-reviewed journal publication by Thiran et al. [105].

As explained in the introduction, optimal planning of fossil-free energy systems requires complex models [6] with a whole-energy system approach [66] and an hourly time resolution [50]. With the rising model's size and complexity, keeping good computational tractability is challenging. This tractability is essential to perform several model evaluations and propose different options for the energy transition.

To limit the computational burden of these complex models, several performance enhancement techniques have been developed [79]. They are solver-based or model-based. The first category consists of selecting the best modelling approach and solver. In general, for complex energy system optimisation models (ESOMs), a linear or integer optimisation problem is formulated [39]. The model-based category includes the following: (i) exact mathematical decomposition [214–217]; (ii) heuristic decomposition [218–220]; and (iii) model reduction techniques [78, 221]. The two types of decomposition techniques take advantage of the mathematical structure of the problem to separate it into linked sub-problems. They are less often used than model reduction for integrated energy system models because of the size, complexity and linked nature of the optimisation problem [79].

The model reduction techniques consist of aggregating the data to simplify the model evaluation. This aggregation must be performed wisely to improve performance while maintaining correct accuracy. It can be performed on a temporal level [80, 222–224], a spatial level [225–230] or a technological level [231–233]. Temporal aggregation is the most commonly used and regroups a set of different techniques: from the simple down-sampling that can provide a reduction in computational time of 80% but loses a significant part of the dynamic of variable renewable energy sources [234] to the more complex TDs clustering which relies on recurrent patterns in variable production and demands. This technique has become the most studied temporal aggregation technique in the last few years [80]. Different TDs selection approaches have been applied and compared: heuristics [234–237], random selection [235], k-means clustering [238–243], k-medoid clustering [41, 238–240, 244, 245], hierarchical clustering [235, 238, 239, 242, 246, 247], chronological clustering [242, 248] and hybrid methods [234, 235]. In addition, some authors have underlined the importance of considering extreme days [234, 249, 250] and inter-annual variability [234, 251] in the clustering of TDs.

To evaluate the selected TDs and choose the "best" number of TDs, a diversity of evaluation metrics is proposed in the literature. Most papers look at *a priori* metrics, that is, without running the energy system model. The most common ones are the errors on the time series and their duration curve [223, 242, 244, 246, 252]. Some also consider the error in the correlation between time series [246]. However, the impact on the accuracy of the energy system optimisation results is rarely studied [79]. When it is, most authors limit themselves to evaluating the error on the objective function [223, 239, 241, 246, 248, 252, 253]. In this objective function, some parts of the system, very insensitive to the temporal resolution, hide errors on other key elements. Hence, as shown later in this study, analysing the objective function tends to underestimate the impact of the number of TDs. Some studies consider, in addition, summarized results of their optimisation, such as power generators, storage assets and transmission lines [79, 234, 242, 243, 254]. However, in all these cases, the model focuses on the electricity sector, and their method is hard to extend to a whole-energy system approach because a multitude of different technologies, resources and energy fluxes (e.g., electricity, heat, synthetic molecules) are present and cannot be compared directly (e.g., 1 GWh of low-temperature heat does not have the same value as 1 GWh of synthetic methane). Limpens et al. [41] proposed a first approach for whole-energy system models. They chose 12 TDs with a k-medoid clustering algorithm. This leads, in their case, in the Swiss energy system, to an under-sizing of 74.8% of seasonal thermal storage.

Their work cannot be directly extended to a multi-regional whole-energy system. Indeed, considering multi-regional cases multiplies the number of time series and complexifies the TDs clustering. Furthermore, it is impossible to predict a priori if the results observed in the 1-region Swiss case extend to multi-regional cases. To the best authors' knowledge, no method exists suitable to evaluate the impact on a multi-regional whole-energy system. Furthermore, no study linked the *a priori* evaluation of TDs clustering and the impact on the energy system results.

The objective of this chapter is to fill these two gaps: (i) developing an error metric to evaluate the sensitivity of energy system results to the number of TDs, suitable for any ESOM and any case study; (ii) comparing this *a posteriori* metric with the classical *a priori* metrics to find out which one of these a priori metrics gives a good estimation of the impact of the number of TDs on the energy system results. To carry this out, the methodology is developed and tested on nine cases with different typologies and numbers of regions. For each case, the clustering of TDs is evaluated in a classical way by computing the error on the time series, on their duration curve and on the correlation between the time series. Then, the open-source, multi-regional whole-energy system model, EnergyScope Multi-Cells [115, 116], is applied for different numbers of TDs with a 90% reduction in direct CO_2 emissions. Its sensitivity to the number of TDs is studied, and a *DE* is developed based on the sizing of the technologies and the use of primary energy resources. A strong correlation between the *TSE* and design error (*DE*) is underlined, and a generalized method is proposed for any new case study.

> The chapter is structured as follows. First, Section 2.1 the TDs clustering algorithm, how the TDs are integrated into the model formulation and how their impact is evaluated *a priori* and *a posteriori*. Then, Section 2.2 presents and motivates the studied cases. Afterwards, Section 2.3 presents, compares and discusses the *a priori* and *a posteriori* evaluation of TDs clustering. From this, an *a priori* method to choose the number of TDs is proposed. Finally, Section 2.4 underlines the key findings, their limitations and how they fill the gap in the literature.

2.1 Methods

This Section presents how the TDs are included in the EnergyScope Multi-Cells model. Then, it explains the methods to evaluate this clustering of TDs and its impact on the energy system results.

2.1.1 Typical Days Clustering Method

As illustrated in Figure 2.1a, a multi-regional whole-energy system approach induces the need to consider several time-dependent attributes for each region: electricity demand, space heating demand, space cooling demand, mobility demand and weather-dependent renewable energy sources (RES) (i.e., 7 resources per cell in this model). Each of them is represented by an hourly time series, increasing the complexity of the clustering. For variable demands, the time series represents the share at each hour of the total demand over the year ($\%year$). For weather-dependent RES, the time series gives the production per peak unit installed (GW/GW_{peak}).

Figure 2.1b presents the TD approach implemented to enhance the performance of the multi-regional whole-energy system optimisation model. It is a simplified conceptual illustration: selecting 3 TDs to represent a week for 2 different regions (A and B). A row represents each region and each day by a square of a different colour. Figure 2.1a is a one-day zoom to present the time series considered.

We use the k-medoid algorithm developed by Dominguez-Muños et al. [244] to cluster the TDs. Limpens et al. [41] have compared several algorithms for this typology of problem and have chosen the one of Dominguez-Muños et al. It has a simple mixed-integer programming formulation, fast convergence and low error on both time series and duration curves. In this study, we will use this algorithm as such. However, based on the approach developed in the following sections, this algorithm could be fine-tuned and compared to other algorithms in the literature. In this algorithm, the days are grouped into clusters to minimise the intra-cluster distance, and the medoid of the cluster is taken as TD. The distance between ($Dist$) between 2 days (i and j) is computed as the L1 norms between each hour (h) for the time series (ts) representing each attribute (a) summed over the 24 h of the day. This gives the distance for each attribute. Then, a weighted sum (with weight, ω_a) of these distances is computed. The number of attributes corresponds to the number of time series considered multiplied by the number of regions studied.

$$Dist(i,j) = \sum_{a\in A} \omega_a \sum_{h=1}^{24} |ts(a,h,i) - ts(a,h,j)|. \tag{2.1}$$

The weights (ω_a) are important hyperparameters of the clustering algorithm. Hence, the metrics developed in this study could help refine them. As a first approach, the weights are defined to reflect the importance of each attribute in the energy system: (i) only the attributes with different time series between the different days are considered. For instance, in this model, the freight is considered constant over the entire year, and the public mobility has the same time series for each day of the year. Hence, they are not considered for the TDs clustering; (ii) the sum of the weights of the different attributes is equal to 1 with 0.5 for the attributes defining the variable demand and 0.5 for the attributes defining the variable production; (iii) among the variable demands, the weight is split according to the total demand over the year, considering Carnot coefficient of performance to scale space heating and space cooling demands; and (iv) among the variable productions, the weight is split according to their yearly production at full potential deployment. As the sum of all the weights is by definition equal to one, the same time series can have a different importance according to the number of regions. For instance, in a case with one region with high solar potential, the PV time series has a large weight and highly influences the choice of TDs. In a different case where this region is grouped with many other regions, or larger regions which have very high renewable energy potentials, this PV time series has a much lower influence on the choice of TDs. However, in this multi-regional case, this PV time series also has a smaller influence on the results of the energy system optimisation as it is only a small source of energy. Thus, this trend reflects well the importance of the time series in the energy system optimisation model.

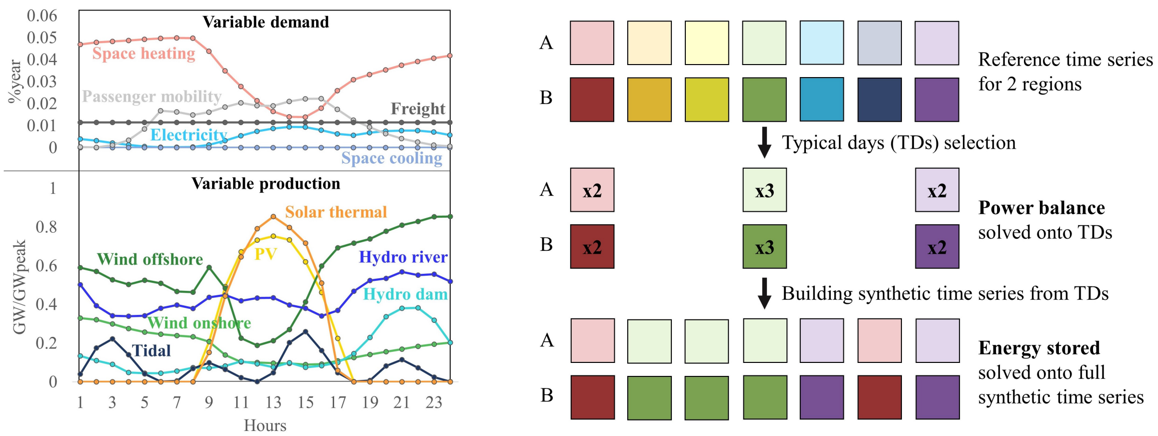

Figure 2.1: Conceptual illustration of the typical day's integration into a multi-regional whole-energy system model: (**a**) Illustration of the time series considered for one day and one region. (**b**) A simplified situation where 3 typical days (TDs) are used to represent a week for 2 different regions (A and B). Each line represents one region, and each colour one day.

The clustering algorithm selects the same days as TDs for all the regions (Figure 2.1b, second step). As these days have different time series in different regions, it ensures the temporal synchronicity of the different regions while considering the spatial disparity of demands and productions. Hence, the TDs selection considers both the intra- and inter-regional relations among the time series. In addition to the clustering algorithm, preprocessing and postprocessing of the time series are performed. During the preprocessing, the time series are normalised such that their sum over the year is equal to 1, while in the postprocessing, the time series of the TDs are rescaled to preserve the average value over the year.

In the optimisation model, the power balance equations are solved on the chosen TDs (Figure 2.1b, second step). This reduces the number of variables and constraints, i.e. the objective of this reduction method. To consider longer-term storage, the storage level equations are solved over the synthetic time series. These synthetic time series are built by replacing each day with its TD (Figure 2.1b, third step). This method was introduced by Gabrielli et al. [243]. In EnergyScope Multi-Cells, the concept illustrated in Figure 2.1 is applied to the entire year.

2.1.2 Sensitivity to the Number of Typical Days

This subsection presents the methods to assess the quality of the representation with TDs and its impact on the energy system results. Therefore, the model is run with different numbers of TDs from 2 to 365: (i) from 2 to 62 with steps of 2; (ii) from 62 to 110 with steps of 4; (iii) from 120 to 180 with steps of 20; (iv) 365. At low numbers of TDs, more model evaluations are performed because more changes occur. The case with the full-year (i.e., 365 TDs) is the reference one. The error due to the number of TDs is assessed *a priori*, i.e., without running the energy system model, and *a posteriori*, i.e., from the energy system optimisation results. Then, the correlation between the metric developed on energy system results and the *a priori* metrics is studied. This analysis gives the best *a priori* metric for the selection of the number of TDs for a new case study.

A Priori Evaluation: Clustering Error

Three different errors are used to evaluate the clustering of TDs. They all compare characteristics of synthetic time series ($\tilde{ts}$) built from the TDs to the original one (ts). The different attributes ($a \in A$) considered are the ones presented in Figure 2.1a. The same weights (ω_a) as in Eq. (2.1) are used.

The time series error (*TSE*) (Eq. (2.2)) evaluates if the value is accurate for each hour of the year and each time series:

$$TSE = \sum_{a \in A} \omega_a \sum_{t=1}^{8760} |\mathrm{ts}(a,t) - \tilde{ts}(a,t)|. \tag{2.2}$$

The duration curve error (*DCE*) (Eq. (2.3)) compares the duration curve of the original time series (dc) and synthetic time series ($\tilde{dc}$) to quantify the error in the statistical distribution:

$$DCE = \sum_{a \in A} \omega_a \sum_{t=1}^{8760} |dc(a,t) - \tilde{dc}(a,t)|. \tag{2.3}$$

The correlation error (*CE*) between attributes across all regions (Eq. 2.4) compares the correlation between each pair of original time series ($corr(ts(a_1,t), ts(a_2,t))$) and the corresponding pair of synthetic time series ($corr(\tilde{ts}(a_1,t), \tilde{ts}(a_2,t))$):

$$CE = \sum_{a_1 \in A} \sum_{a_2 \in A} \omega_{a_1} \omega_{a_2} |corr(ts(a_1,t), ts(a_2,t)) - corr(\tilde{ts}(a_1,t), \tilde{ts}(a_2,t))|. \tag{2.4}$$

A Posteriori Evaluation: Design Error

The error in the whole-energy system design is not trivial to define. Firstly, because it has many elements: 120 technologies and 19 resources per region[1]. All these elements differ in nature and cannot be compared directly. Secondly, it is complex to differentiate the error due to lower temporal resolution from another phenomenon inducing changes in the results. The typology of the problem studied has a flat optimum. It implies that several solutions are as good as the optimal one. They could be the solution to the reference case with nearly no change in cost. In our case, with a decreased temporal resolution, other changes occur due to reduced accuracy. This is the error we want to quantify. For

[1] This paper was published in March 2023 and uses the model version of that period. Since then, some model improvements have been made. For instance, we added the shipping and aviation demands with their end-use technologies and a more refined modelling of the conversion chain of FT fuels. However, the conclusions of this paper/chapter stay valid as no fundamental changes were performed on the model.

specific cases and elements, it is possible to underline the causes of the changes. Still, it is too complex to generalise it to the entire energy system, even more within a sector- and region-coupled energy system. This issue is further presented and explained in Appendix C.1.

To study the sensitivity of this kind of model, it is then relevant to explore and summarize its main results: (i) the annualised total cost of the system (objective function), (ii) the size and cost of energy conversion assets, (iii) the quantity and cost of energy resources and (iv) the size of interconnections and quantity of energy exchanged. As explained before, analysing the objective function is insufficient to detect the impact of TDs on the energy system results. The size of interconnections and quantity of energy exchanged depends directly on the installed technologies and primary energy used in each region. Therefore, we define the size of each conversion technology and the use of each primary energy in each region as an element of interest. From there, we develop a bottom-up approach to quantify the upper bound of the error on all the elements:

1. Compared to the reference case, a threshold of 5% error on an element is arbitrarily defined as acceptable. In Appendix C.2, this computation is also made for 2.5% and 7.5% error thresholds on each element to show that the results are not very sensitive to this value;
2. At each number of TDs (N_{td}), the elements with an error above this threshold are considered as not well represented (set W). The apparent design error (*aDE*) is defined as the share of the total cost these elements represent:

$$aDE(N_{td}, ref) = \frac{\sum_{tech \in W} [\mathbf{C_{inv_{ann}}}(tech) + \mathbf{C_{maint}}(tech)] + \sum_{pe \in W} \mathbf{C_{op}}(pe)}{\mathbf{TotalCost}}, \tag{2.5}$$

   with $\mathbf{C_{inv_{ann}}}(tech)$ being the annualised investment cost of a technology, $\mathbf{C_{maint}}(tech)$ being the maintenance cost of a technology, $\mathbf{C_{op}}(pe)$ being the annual operational cost of a primary energy and **TotalCost** being the annualised total cost of the system;
3. Because of the flat optimum and the oscillating behaviour, this apparent design error is the superposition of the design error ($DE(N_{td}, ref)$) we want to compute and random noise ($\delta(N_{td})$):

$$aDE(N_{td}, ref) = DE(N_{td}, ref) + \delta(N_{td}) \tag{2.6}$$

4. To reduce this noise, the design error is computed for each number of TDs as the

minimum of the apparent design error for a lower or equal number of TDs:

$$DE(N_{td}, ref) = \min_{\forall t \leq N_{td}} aDE(N_{td}, ref) \tag{2.7}$$

2.2 Case Studies

This section describes the cases studied to test the methodology. First, common assumptions for all cases are presented. Then, nine cases with different numbers and typologies of regions are presented. All these cases are examples used to develop and validate the method but are not the main focus of this work.

The following assumptions are common to all cases:

- The weather and consumption data of the year 2015 are used to build the time series of the different attributes [104, 109];
- The target year 2035 is used to forecast costs, efficiency, end-use demands, etc. This year and the regions used are chosen because of data availability from previous studies [104, 109]. The macro-regions are built by merging countries together using the methodology of [104] (e.g., Spain and Portugal are merged to build the Iberian peninsula). This methodology regroups neighbouring countries with similar patterns in terms of demands and resources. From these studies, two main changes have been made. Firstly, the maximum installed capacity for nuclear in France is set to 41.3 GW, taken from [255]. Secondly, the onshore wind potential considered here represents only 50% of the total technical potential used in these studies. This choice was made for two reasons. Firstly, these regions have a very high technical potential for onshore wind. As it is a very cheap renewable energy source, it outcompetes other renewable energy sources. Secondly, the technical potentials are very high compared to what is currently installed and might never be reached because of social acceptance;
- Having a good temporal resolution is especially important to integrate a high share of VRES. Therefore, to obtain systems with high penetration of VRES, we set the greenhouse gas emission reduction to 90% compared to 1990;
- All regions can import fossil or renewable fuels from the rest of the world but not electricity.

The case studies are built by associating six Western Europe macro-regions (Figure 2.2). In all cases, these macro-regions are considered as one cell each. In multi-regional cases, they can exchange energy carriers between them. They are defined as follows:

- AtChIt: Austria, Switzerland and Italy;
- DeBeNeLux: Germany, Belgium, Netherlands and Luxembourg;
- Scandinavia: Denmark and Sweden;
- Iberian Peninsula: Spain and Portugal;
- France;
- British Islands: Ireland and the United Kingdom.

Figure 2.2: The six macro-regions considered to build the nine case studies: six with 1 cell, one with 2 cells, one with 3 cells and one with 6 cells.

From these regions, the nine case studies are selected for their diversity. Four main differences are considered, see Table 2.1: (i) the ratio between renewable energy potentials (REPs) and FECs, providing an informed guess of whether the region will be in deficit or excess in a renewable-based energy system; (ii) the allowed installation of nuclear power plants; (iii) the share of solar in the REPs; (iv) the share of wind in the REPs. Table 2.1 gives a classification of the cases for these criteria in five categories, from the worst/lowest (--) to the best/highest (++). In addition, cases with a different number of interconnected regions are considered: one, two, three and six. Having a multi-regional case complexifies the clustering of TDs and might lead to different results from one- to six-region cases. The code at the beginning of the name of each case gives the number of cells: from one region (1R) to six interconnected regions (6R).

Table 2.1: Diversity of considered cases. Four influential characteristics are compared qualitatively and classified into five categories, from lowest (- -) to the highest (++): (i) ratio between renewable energy potentials (REPs) and final energy consumption (FEC); (ii) investment in nuclear power plants allowed; (iii) share of solar in REPs; (iv) share of wind in REPs.

Test case	**REP/FEC**[a]	**Nuclear**	**Solar**	**Wind**
1R-AtChIt	-	- -	+	-
1R-DeBeNeLux	- -	- -	+ -	+
1R-Scandinavia	++	- -	- -	++
1R-Ib.Peninsula	++	- -	++	+ -
1R-France	+ -	++	+	+ -
1R-Brit.Islands	+ -	- -	+ -	++
2R-DBNL-Fr	-	+	+	+ -
3R-AtlanticEU	+	+	+	+
6R-WesternEU[b]	+ -	+ -	+	+

[a]For all case studies, the renewable energy potentials are derived from [124, 157], and the final energy consumption from [256]. In this column, the symbols indicate ranges of the ratio REP/FEC: (- -) REP/FEC < 1, (-) REP/FEC ∈ [1; 1.25[, (+ -) REP/FEC ∈ [1.25; 1.75[, (+) REP/FEC ∈ [1.75; 2[, (++) REP/FEC ≥ 2. The range at the margin to supply its demand with RES has been chosen to be around 1.5 to account for losses from primary energy to final energy.

[b]For the case with 6 regions, we could not solve the full-year case on our machine due to a lack of memory. The following conservative approach has been used to fill this lack of data: the case with the highest number of TDs (i.e., 180) has been taken as the reference, and the design errors computed have been shifted up by the error at 180 TDs taken from the 3-region case.

From Table 2.1, the cases' characteristics can be summarized as follows:

- 1R-AtChIt: a one-region case with a small deficit of renewable energy source potentials, mostly oriented towards photovoltaic panels;
- 1R-DeBeNeLux: a one-region case with a high deficit of renewable energy source potentials, substantial potential for wind turbines and lower photovoltaic;
- 1R-Scandinavia: a one-region case with a high excess of renewable energy source potentials, especially in terms of wind power;
- 1R-Ib.Peninsula: a one-region case with a high excess of renewable energy source potentials, especially in terms of photovoltaic panels;
- 1R-France: a one-region case at the margin in terms of renewable energy source potentials but allowed to invest in nuclear power;

- 1R-Brit.Islands: a one-region case at the margin in terms of renewable energy source potentials, without nuclear and with its main potential being wind;
- 2R-DBNL-Fr: a two-region case (i.e., DeBeNeLux interconnected with France) with a small deficit of renewable energy sources but with nuclear power allowed in France;
- 3R-AtlanticEU: a three-region case (i.e., Iberian Peninsula, France and British Islands interconnected) with a small excess of renewable energy source potentials, some nuclear in France and good photovoltaic and wind potentials;
- 6R-WesternEU: a six-region case at the margin regarding renewable energy source potentials, some nuclear in France and good photovoltaic and wind potentials.

2.3 Results and Discussion

This section presents and discusses the error evaluations for all cases. First, it illustrates the gain in computational tractability with the number of TDs. Then, it evaluates the *a priori* errors. Afterwards, the sensitivity of the energy system results is studied. Finally, the *a priori* and *a posteriori* metrics are compared, and a method for any new case study is proposed. In all figures, the one-region cases have the same colours as in Figure 2.2, and the multi-region cases have different shades of grey.

2.3.1 Gain in Computational Tractability

Figure 2.3 provides the gain in computational time of each model evaluation compared to the full-year resolution. The optimisation problem is solved using the commercial software IBM CPLEX 12.9 with a barrier algorithm on an Intel®Core™ Quad i9-10980XE CPU @3.0 GHz, with a memory of 128 GB. The oscillation is because the optimisation problem changes slightly by changing the number of TDs. Hence, the polyhedron of the feasible solutions changes, and the algorithm might not always converge faster when slightly decreasing the number of TDs. The optimisation was run several times in the case of the biggest oscillation to ensure it did not come from other causes. However, a general trend can be seen when solving many numbers of TDs. The gain in solving time is mostly significant below 90 TDs, particularly for multi-regional cases. Hence, our range of interest is 2 to 90 TDs. The different errors are studied in this range.

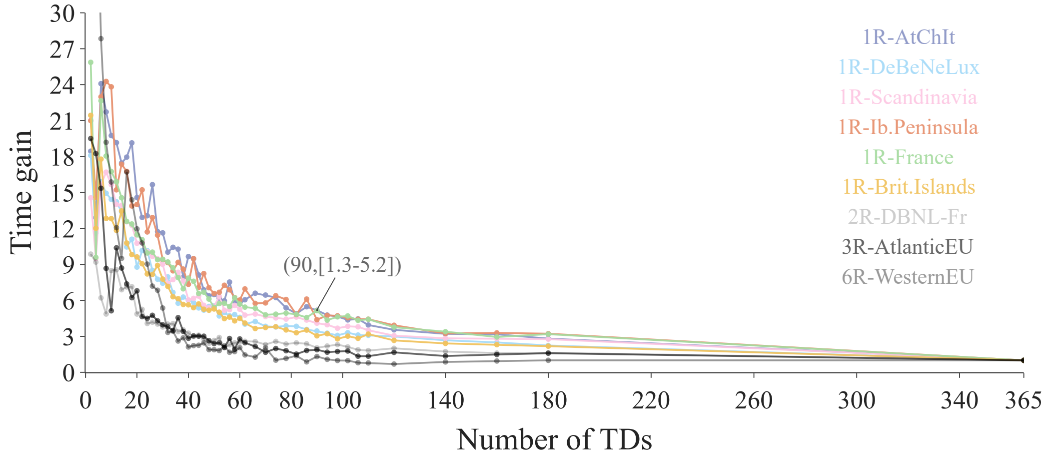

Figure 2.3: Time gain expressed as the ratio of the computational time with the full-year resolution to the one with lower numbers of typical days (TDs) for all case studies.

2.3.2 A Priori Evaluation: Clustering Error

Figures 2.4–2.6 present the evolution of the time series error (*TSE*), duration curve error (*DCE*) and the correlation error (*CE*). They evaluate whether the time series at each hour of the year, their distribution, and the relationship between time series are well represented. These errors are studied as they are the most common in the literature, and they are easy to evaluate *a priori*. Hence, these errors are convenient for choosing the number of TDs at a low cost for a new case study.

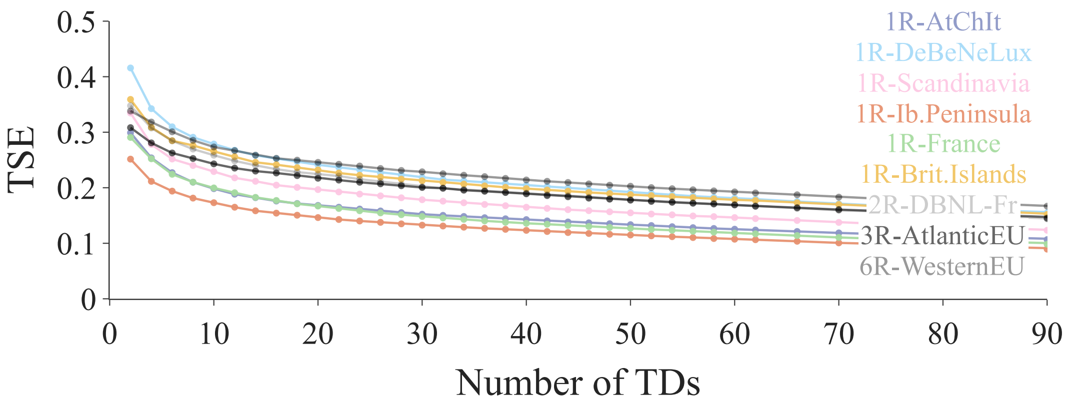

Figure 2.4: Evolution of the time series error (*TSE*) with the number of typical days (TDs) for all case studies.

For all cases, up to 20 TDs, these errors decrease rapidly. At a higher number of TDs, the time series error decreases linearly, whereas the other errors stay very low and are nearly constant. Hence, the time series error is the only *a priori* error that keeps a certain

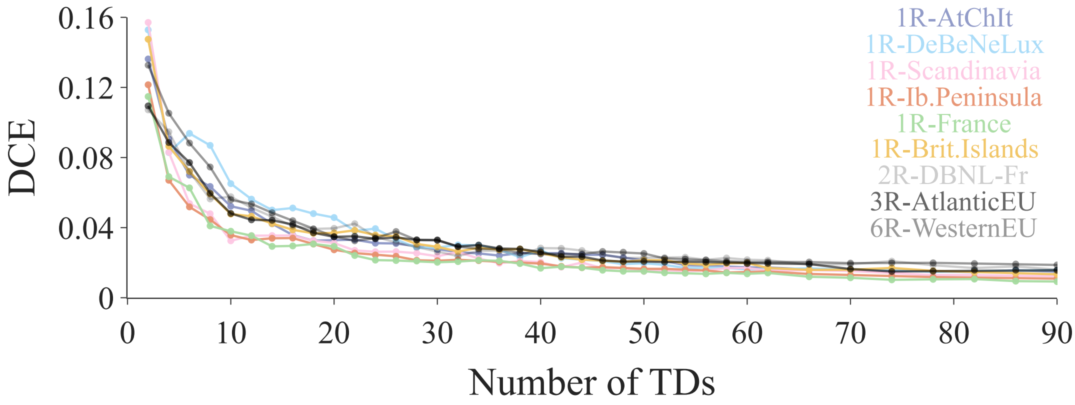

Figure 2.5: Evolution of the duration curve error (*DCE*) with the number of typical days (TDs) for all case studies.

sensitivity to the number of TDs above 20 TDs. At this stage, it is not possible to formally define the acceptable threshold for these errors.

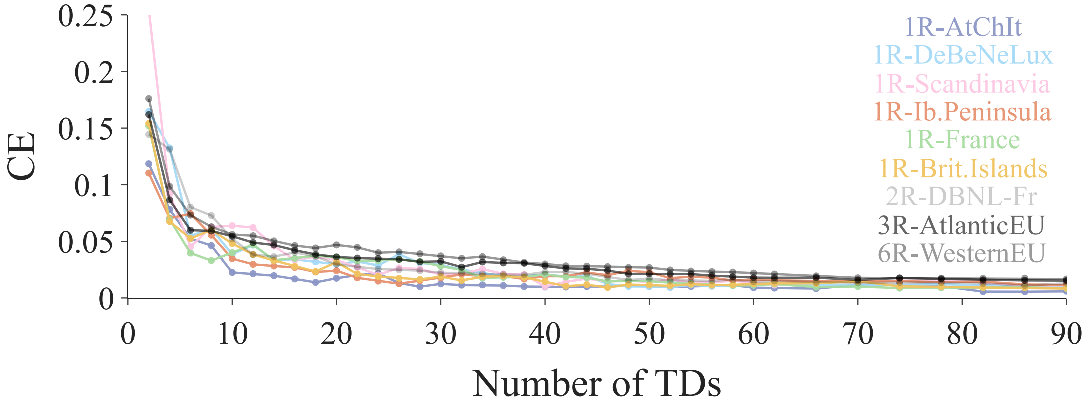

Figure 2.6: Evolution of the correlation error (*CE*) with the number of typical days (TDs) for all case studies.

2.3.3 A Posteriori Evaluation: Sensitivity of Energy System Results

This subsection studies the sensitivity of the energy system optimisation model results to the number of TDs. First, the error on the objective function, i.e., the annualised total cost, is presented. Then, the design error is analysed.

Figure 2.7 presents the relative error on the total annualised cost of the system as a function of the number of TDs. The error decreases rapidly at low numbers of TDs for all cases and then stagnates over the entire range. Above 14 TDs, the error is below 1% for all cases except for 1R-Scandinavia and 1R-Brit.Islands. In these two cases, the total cost is overestimated. In general, the error on the total cost stays very low for any number of TDs. It is thus not the best metric to evaluate the error in the energy system results. Indeed, very expensive technologies (e.g., private cars) are quite insensitive to the temporal resolution. On the contrary, some key technologies for the security of supply (e.g., seasonal thermal storage) might represent a lower share of the total cost and be very sensitive to the number of TDs. A closer look at the error in the asset investments and the primary resources used over the year is necessary.

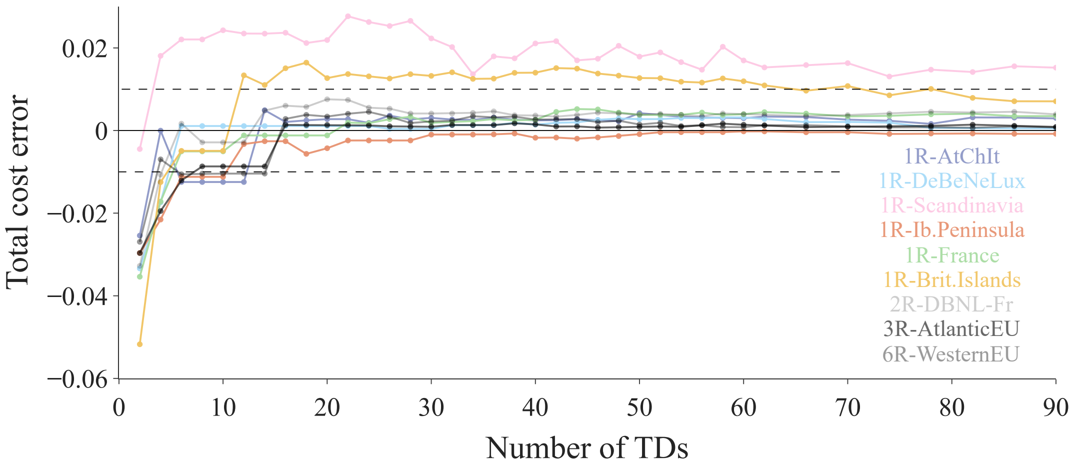

Figure 2.7: Evolution of the error on the annualised total cost (objective function) with the number of typical days (TDs) for all cases. The dashed line represents the threshold of the error at 1%.

Figure 2.8 depicts the design error for all cases. In all cases, except 1R-Brit.Islands, at 10 TDs, most of the gain in accuracy is achieved, and an error below 20% is reached (i.e., $DE \in [7.3;16.1]\%$). Using 10 TDs divides the computational time by 8.6 to 23.8, according to the case. The 1R-Brit.Islands case needs 46 TDs to have a significant gain in accuracy and 66 TDs to reach an error below 20%. However, as described in Table 2.1, this case has particular characteristics that can be detected *a priori*. Indeed, it is the only case with just enough renewable energy potentials to supply its final energy consumption (i.e., $REP/FEC = 1.47$ or "(+ -)" in Table 2.1), and no possibility to install a low-carbon nuclear baseload. Thus, this case study is more sensitive to the quality of the temporal representation. Indeed, a bad temporal representation leads to an underestimation of the intermittency of renewables. Hence, the production of renewables is overestimated and the system needs to import fewer fuels to compensate for their intermittency with dispatchable energy sources. For the other one-region cases, design error can be further reduced by increasing from 10 to 24

TDs, if needed. On the contrary, for the multi-regional cases, only a small reduction in the design error can be achieved above 10 TDs (i.e., at the most, 4.7% by using 90 TDs).

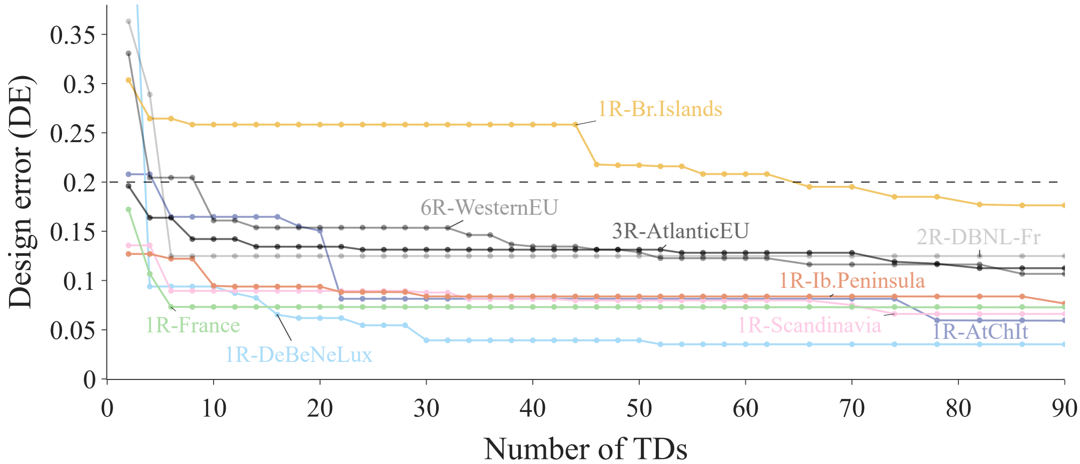

Figure 2.8: Evolution of the design error (*DE*) with the number of typical days (TDs) for all case studies.

Figure 2.9 underlines the trade-off between time gain and design error. It is a combination of Figures 2.3 and 2.8. The more a point is in the upper-left corner of the graph (i.e., high time gain and low design error), the better the trade-off is. Hence, the best trade-offs are at the top of the long vertical section of each curve.

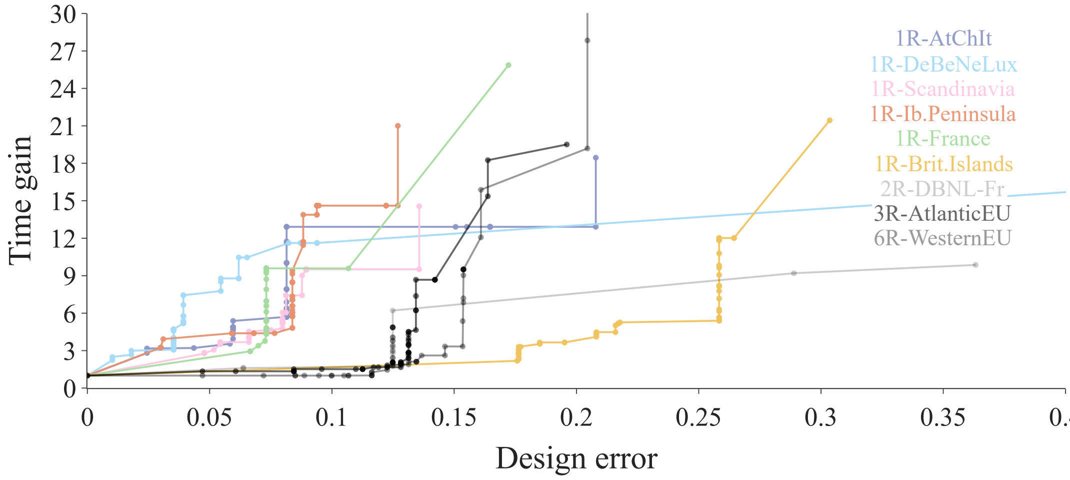

Figure 2.9: Relation between time gain and design error. The more a point is in the upper-left corner, the better it is (i.e., high time gain and low design error). For each curve, the best trade-off lies at the top of the vertical section.

Here, again, the case 1R-Brit.Islands stands out, as it always displays a high design error. To reach a design error below 20%, its time gain falls down to 3.7. Another choice could be to favour time gain (up to 12) at the cost of a higher design error (25.8%). Otherwise, other temporal aggregation techniques could be tested and perform better on this type of case (e.g., adding manually extreme days after the TD clustering). This could be explored in future works using the developed design error.

The other cases can be divided into two categories on this graph: (i) the one-region cases have good trade-offs with a time gain of 9.5 to 14.6 and a design error below 10%; (ii) the multi-regional cases also reach high time gain at the best trade-off (6.2 to 16.1) but have a higher design error (between 12 and 16%). For all these cases, the best trade-offs correspond to the points at 10 TDs already analysed based on Figure 2.8.

2.3.4 Comparison of A Priori and A Posteriori Errors

This subsection studies the correlation between *a priori* and *a posteriori* metrics. *A priori* errors can be evaluated without solving the ESOM. Hence, they could allow the selection of the number of TDs at a low computational cost. Indeed, the clustering of TDs has a low computational cost (i.e., around 10 to 20 seconds), and it only needs to be computed once for many scenarios in the same geographical area.

Table 2.2 reports the significant correlation between the design error and the different *a priori* errors. In particular, the time series error has a correlation above 0.9 in most cases. Hence, it is investigated in further detail.

Table 2.2: Correlation between *a priori* and *a posteriori* errors for all cases.

Test Case	Time Series Error	Duration Curve Error	Correlation Error
1R-AtChIt	0.92	0.85	0.75
1R-DeBeNeLux	0.68	0.83	0.83
1R-Scandinavia	0.94	0.76	0.66
1R-Ib.Peninsula	0.90	0.68	0.70
1R-France	0.69	0.76	0.79
1R-Brit.Islands	0.90	0.64	0.54
2R-DBNL-Fr	0.71	0.77	0.82
3R-AtlanticEU	0.93	0.73	0.69
6R-WesternEU	0.91	0.92	0.94

Figure 2.10 gives more insights into these correlations. It presents the design error and the time series error for all cases and all points evaluated. Discarding the particular case of 1R-Brit.Islands, most of the points (99.5%) are concentrated below the curve $DE = TSE$.

Hence, the time series error can be considered a good prediction of the upper bound of the design error. In addition, the points can be approximated by the linear relationship $DE = 0.75\,TSE$. This relation is still conservative as most of the points (85.7%) lie below this curve.

As discussed previously, the 1R-Brit.Islands case behaves differently than the others. However, this can be detected *a priori* by computing the ratio REP/FEC, and the rule to select the number of TDs based on the time series error can be adapted to a more conservative approach. The points of this case stay close to the curve $DE = TSE$, and for the trade-off at 46 TDs found in Figure 2.8, $DE = TSE + 0.03$.

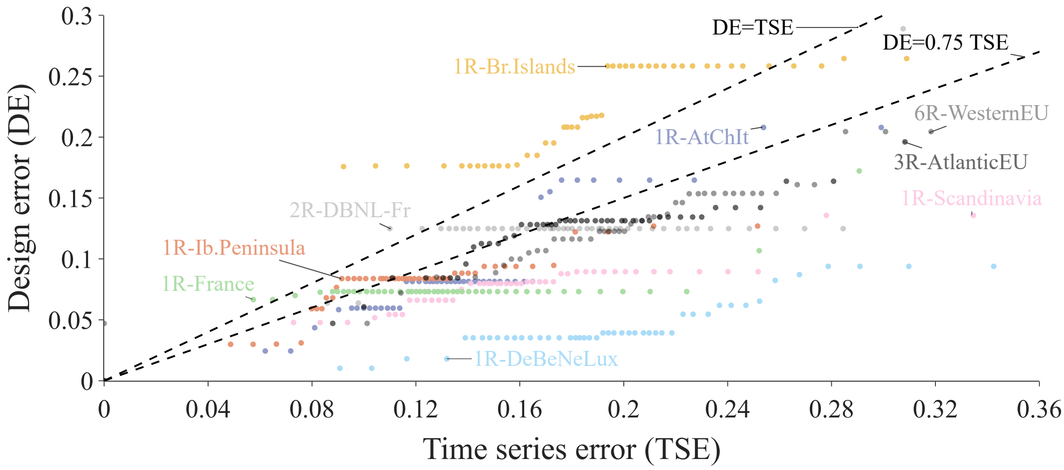

Figure 2.10: Design error (DE) vs. time series error (TSE) for all cases and all numbers of TDs evaluated (i.e., 432 model evaluations). The 1-region cases are depicted in colours, and the multi-region cases are in shades of grey. A line for $DE = TSE$ and a line for $DE = 0.75\,TSE$ are represented to underline that, discarding the particular case 1R-Brit.Islands, (i) all points are located below the first line; (ii) the second line is a good linear approximation of the relation between DE and TSE.

To conclude, the time series error provides a good estimation of the design error that can be expected. Hence, it can be used to select the number of TDs for a new case study. Two different cases have to be considered according to the ratio between renewable energy potential (REP) and final energy consumption (FEC):

1. In most cases, the time series error can be used to select the number of typical days with the relation:

$$DE = 0.75\,TSE \tag{2.8}$$

From the cases studied, a value of $DE = 0.165$ or $TSE = DE/0.75 = 0.22$ gives a good trade-off between accuracy and computational tractability;

2. In the particular cases where REP/FEC $\in$ [1.25; 1.75[and no other low-carbon baseload production is available (e.g., nuclear power), the energy system results are more sensitive to the temporal resolution. The above relation does not work, but the design error and time series error stay close in value. Hence, we can use the following relation:

$$DE = TSE \tag{2.9}$$

For instance, in the case studied that falls into this category (i.e., 1R-Brit.Islands), the best trade-off between accuracy and computational tractability is at $DE = 0.22$ and $TSE = 0.19$.

2.4 Conclusions and Perspectives

Methods to speed up energy system optimisation models (ESOMs) while keeping good accuracy are essential to consider the uncertainty inherent to long-term planning. Typical day (TD) clustering is a well-established method that can significantly improve computational tractability. The clustering error (*a priori*) has been thoroughly studied in the literature, but its impact on the accuracy of the energy system optimisation results (*a posteriori*) is rarely studied in depth. This chapter analyses this impact by applying, for different numbers of TDs, the multi-regional whole-energy system model, EnergyScope Multi-Cells, to nine cases with different typologies and number of regions. A bottom-up design error is developed to evaluate the impact on the results by (i) selecting the elements (i.e., technologies sizes or primary energy uses) with an unacceptable error (i.e., above 5%) and (ii) defining the design error as the share of the total annualised cost that these elements represent. Then, this design error is compared with the commonly used *a priori* errors (i.e., time series, duration curve and correlation errors).

In all cases, we underline a strong correlation between the design error and the time series error. This *a priori* metric gives a good estimation of the upper bound on the design error and can be used to choose the number of TDs in any new case study without having to evaluate the ESOM. However, our analysis reveals that cases can fall into two categories to define the exact relationship between design error and time series error. The first category gathers most of the cases. Here, a trade-off is found at 10 TDs, which is ensured to have a design error lower than 17% and runs 8.6 to 23.8 times faster than the full-year model evaluation according to the case. In those cases, the design error is lower than the time series error in 99.5% of the model evaluations performed, and it can be approximated by the linear relation $DE = 0.75\,TSE$. As an indicative value, the results of this study suggest taking $DE = 0.165$ or $TSE = 0.22$. The second category is a particular case that can be detected *a priori* by looking at the ratio between the renewable energy potentials (REPs) and the final energy consumption (FEC), and the possibility of installing low-carbon baseload (e.g. nuclear power). This particular case corresponds to $\mathrm{REP}/\mathrm{FEC} \in [1.25; 1.75[$ and no low-carbon baseload allowed. It is more sensitive to the temporal resolution than the other cases. For this type of case, this study suggests using a more conservative relation between design error and time series error: $DE = TSE$. In addition, this category does not reach as low a design error as the other, even when increasing the number of TDs. From our results, we advise aiming for $DE = TSE = 0.19$ for this type of case. In our study, this is equivalent to taking 46 TDs, which implies a model evaluation that runs 5.7 times faster than the full-year resolution. All those observations work both for 1-region and multi-regional cases. It proves that the TDs approach can be extended to multi-regional whole-energy systems.

To increase confidence in these conclusions, they should be tested with other models and case studies, with another reference year for the time series, other technologies, etc. In addition, other limitations of this study could lead to future works: (i) To evaluate the accuracy of optimisation results with a lower temporal resolution, they are compared to the full-year model evaluation. It implies that it should be feasible to run this full-year model. Furthermore, due to the flat optimum of the optimisation problem, the design error has an oscillating behaviour that makes it hard to interpret. Another approach to assess the quality of the solutions obtained would be to run a more accurate operation model and evaluate its adequacy. (ii) The clustering algorithm and its hyperparameters were chosen based on the literature. With the newly developed method, it could be fine-tuned and compared to other algorithms. In particular, the ability of the clustering algorithm to include the extreme events was not assessed specifically in this work. (iii) TDs clustering is only one of the performance enhancement techniques. A trade-off between the number of TDs and other techniques, such as spatial aggregation or model decomposition, could exist. Here also, the developed method to evaluate the loss of accuracy in optimisation results could be used to find such a trade-off.

To conclude, this study focuses on developing a relevant *a posteriori* metric (i.e., the design error) to evaluate the impact of TDs clustering on ESOMs results. It compares it with the widely used *a priori* metrics (i.e., time series, duration curve and correlation errors). This comparison reveals that the time series error is a conservative estimation of the design error. Hence, it can be used to select *a priori* the number of TDs to reach a certain accuracy on the ESOM results. In addition, this work paves the way for many other works on performance enhancement techniques. Indeed, with a powerful metric that is easily applicable to any ESOM and any case study, it is possible to compare and assess the best performance enhancement techniques for a specific case.

Using the results of this chapter, we evaluate the time series error for our 34 countries' European scenario and find a compromise at 16 TDs. With 16 TDs, it has a time series error of 0.25 and a model evaluation takes around 20 hours and uses 208GB of memory.

3 The role of renewable fuels in a fossil-free European energy system

Coming together is a beginning; keeping together is progress; working together is success.
Edward Everett Hale

Chapter overview

- Application of EnergyScope Multi-Cells on a fossil-free and nuclear-free European energy system.
- What are the main sources of energy and the main energy carriers?
- What is the role of renewable fuels?
- What are the roles of energy storage and energy exchanges?

The European energy landscape heavily relies on imported fossil and nuclear fuels, accounting for over 80% of its energy supply [1–3]. However, there is an undeniable imperative to transition towards a defossilized energy system, underscored by the European Commission's ambitious target to achieve carbon neutrality by 2050 [257]. Nuclear energy, once regarded as a reliable asset, now faces uncertainties due to its high costs, long construction time, geopolitical implications, and challenges associated with waste management[258, 259]. In light of these considerations, this chapter explores a fossil-free and nuclear-free energy system, aiming to understand its feasibility and challenges. However, the implications of reinvesting in nuclear energy on the European energy system are explored in Chapter 5.

While numerous studies have examined strategies for reducing carbon emissions within the energy sector, most have predominantly focused on the electricity system [85, 260–265] or encompassed a limited range of sectors [51, 55, 67, 266, 267]. Few studies considered all energy-consuming sectors but they quantified them solely as final energy consumed [46, 52, 53, 268, 269]. Consequently, these studies rely on exogenous assumptions about end-use technologies to meet demand. They overlook critical synergies and flexibility necessary for integrating high shares of intermittent renewable energy sources. This chapter aligns with the methodology proposed by Contino et al. [66], advocating for a whole-energy system approach that integrates all energy demands and quantifies them as closely as possible to the energy service.

Within the literature, considerable attention has been directed towards e-hydrogen and its derived fuels [270]. They are promised to have many uses, such as power flexibility, low-carbon fuels for heavy transport, decarbonization of some industrial sectors or even energy trades [202, 271, 272]. However, the exact extent and form of their contributions to decarbonized energy systems remain subjects of ongoing debate. Moreover, there is limited integration of the synergies and competition with biofuels. By encompassing both e-fuels and biofuels under the category of renewable fuels, this chapter aims to elucidate their role within a fossil-free and nuclear-free European whole-energy system.

The chapter presents a comprehensive analysis of a fossil-free and nuclear-free energy system for Europe, encompassing 34 European countries [1]. Each country is represented as a node in the model, with its own resources, demands and energy conversion system. It can exchange energy under various forms (e.g. electricity, hydrogen, methanol) with neighbouring countries and can import renewable fuels from the international market (exterior of the system considered) at a given price [195, 196]. The full description of the case study can be found in Section 1.2.

> Renewable fuels are the focal point of this chapter as they become a cornerstone in the energy system's transition away from fossil fuels. First, Section 3.1 presents and analyzes the results. Its four subsections describe different aspects of the energy system and the key role of renewable fuels: (i) energy supply; (ii) production and uses of renewable fuels; (iii) energy storage; (iv) energy exchanges. Afterwards, Section 3.2 discusses the results, compares them to the related literature and concludes the chapter by presenting the main outcomes, limitations and perspectives.

[1] The 27 countries from the European Union, minus Cyprus and Malta, plus the United Kingdom, Norway, Switzerland, Albania, Bosnia-Herzegovina, Kosovo, Montenegro, North Macedonia, and Serbia.

3.1 Results: A fossil-free and nuclear-free European energy system

This section analyzes the fossil-free and nuclear-free European energy system in four steps. In each step, it underlines the key role of renewable fuels in this system. Firstly, Subsection 3.1.1 presents the general energy supply of this system going from gross available energy to end-use demands. Secondly, Subsection 3.1.2 describes how renewable fuels are produced and for which purposes. Thirdly, Subsection 3.1.3 analyzes the role of storage. Finally, Subsection 3.1.4 illustrates the importance of energy exchanges.

3.1.1 Energy supply: From gross available energy to end-use demands

In a fossil-free and nuclear-free European energy system, renewable energy becomes the main source of energy as illustrated in Figure 3.1(A). Wind and solar energy produce the bulk energy (69%). This represents only 34% of the total technical potential [110] evaluated for those energies in Europe but still requires a significant increase compared to today's production. Wind energy production in 2050 is 8.5 times today's production and solar energy production is 21 times today's production. To reach these objectives, Europe must install every day on average 26 new wind turbines (or 132 MW) and 900 000 new PV panels (or 318 MW). This represents an average increase of installation rates of 164% for wind turbines and 180% for PV panels compared to today [169]. Biomass in diverse forms stands out as the third source of energy with 22%. Here, the increase compared to the current production is low, especially for woody biomass, but 92% of the technical potential [159] is used. Hydro provides only 4% of the energy but offers flexibility, as explained later in Section 3.1.3.

Europe's optimal design for a fossil-free system does not import energy from the exterior of the system. This means that Europe has many untapped potentials for renewables that can be used directly or converted into fuels at a competitive price with the forecasted international market [195, 196]. Furthermore, these resources are key enablers to improve the energy security and energy independence of Europe. These are strategic geopolitical subjects as the recent energy crisis has shown.

The energy system converts the gross available energy to final energy carriers that supply all the end-use demands at each hour of the year in each country. Electricity is the main final energy carrier (52%), see Figure 3.1(B). Indeed, we observe a high electrification of

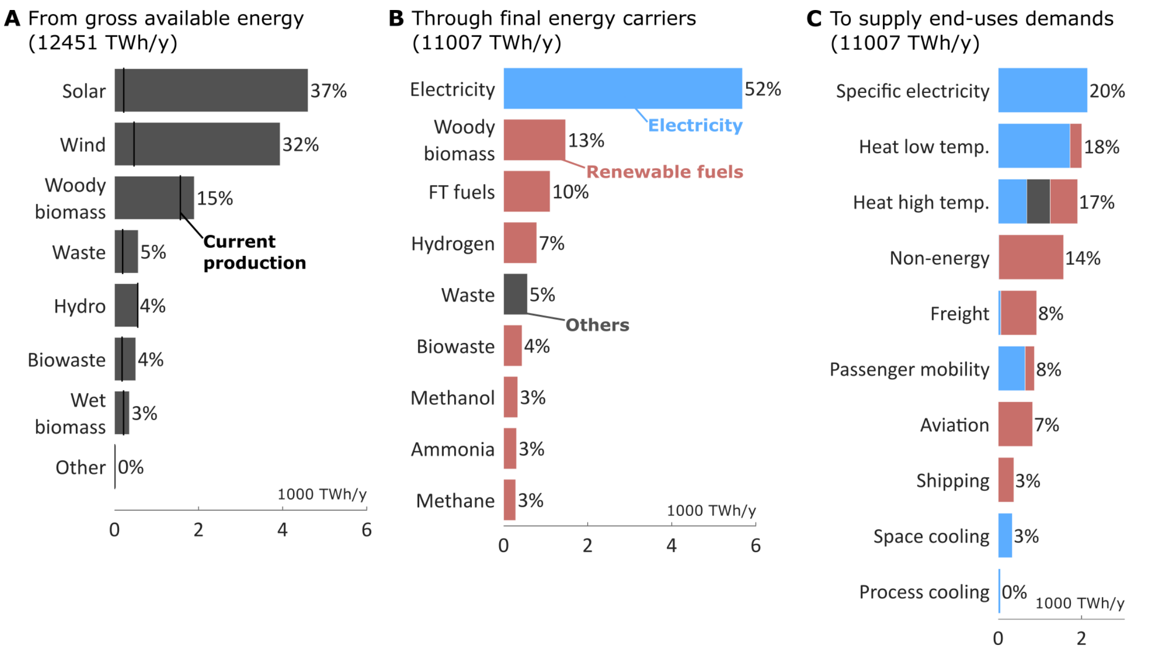

Figure 3.1: **(A)** A fossil-free European energy system by 2050 relies heavily on wind, solar and biomass for its gross available energy. **(B)** Renewable fuels covers 43% of the final energy consumption. The other final energy carriers are electricity (52%) and waste (5%). **(C)** Many end-use demands are electrified (52%) but some still need fuels as input (48%).

the energy system. The specific electricity end-uses (2149 TWh) are augmented by other final electricity consumption for end-use applications, Figure 3.1(C): (i) high-temperature heat for the industry (684 TWh); (ii) domestic and district heat pumps for low-temperature heat (1725 TWh); (iii) electrical cars (649 TWh); (iv) space cooling (343 TWh); (v) other end-uses (133 TWh). In addition, large quantities of electricity are converted into electrofuels (3693 TWh). In total, the electricity produced and consumed is 4.3 times greater than the demand for specific electricity end-uses. The sector-coupling and interconnections between countries allow reaching high shares of variable renewable energy sources while keeping their curtailment as low as 4.3%. However, a part of this electricity might never get onto the main grid as it is converted directly locally (e.g. self-consumption in houses, self-consumption in industries, combined installation of renewable production assets and electrolyzers, etc.).

After electricity, renewable fuels constitute the second-largest category of final energy carriers (43%). Waste incineration (5%) is the last category of final energy carrier. The renewable fuels are either e-fuels or biofuels and are used in a variety of forms according to the application. This underscores a substantial interest in maintaining fuels as the final energy source for various end-uses. Recognizing that not all aspects of the energy system can be electrified, achieving a fossil fuel-free scenario necessitates the substantial production of renewable fuels for final consumption (4760 TWh). The following section provides insights into the value chain to produce each type of fuel and the end-uses they supply.

3.1.2 Production and uses of renewable fuels

As presented earlier, significant amounts of renewable fuels are produced for several end-uses. Figure 3.2 presents the yearly balance of each of the six categories of fuels considered: biomass, hydrogen, FT fuels, methane, methanol and ammonia. In the model, the FT fuels are further divided into more categories. Here, for the sake of clarity, we regroup them and we take the FT process as a representative of the conversion routes to produce these synthetic liquid fuels, either from biomass, from hydrogen or directly from electricity. However, other similar processes can be integrated into the model.

Biomass and hydrogen emerge as the two primary renewable fuels (Figure 3.2(A-B)). They are either used directly for end-use (e.g. biomass furnaces for industrial process heat, hydrogen fuel-cell trucks) or upgraded to more advanced renewable fuels: ammonia, methane, methanol and FT fuels.

Biomass comes from 3 different feedstocks with different costs, availabilities, and potential uses: woody biomass (69%), biowaste (18%) and wet biomass (13%).

A part of the biomass (65%) is directly used to supply end-uses: (i) woody biomass and biowaste transformed into HVCs for the NED; (ii) woody biomass and biowaste burned in industrial furnaces for high-temperature heat. The latter also introduces some flexibility to the system as it is coupled with electrical furnaces. During periods of surplus of renewable electricity, furnaces operate on electricity. Conversely, in electricity-deficient periods, wood supplies the furnaces.

A smaller share of the biomass (35%) is converted into complex liquid and gaseous renewable fuels for uses in specific applications, storage, and transport of energy: (i) methanolation of woody biomass and biowaste; (ii) biomethanation of wet biomass and methanation of wood and biowaste; (iii) synthesis of FT fuels from wood and biowaste.

Hydrogen is derived from renewable electricity through electrolysis. Subsequently, 58% of this hydrogen is directly used in fuel-cell trucks for freight transport. The remaining 38% is upgraded into more advanced fuels for specific applications, storage, and exchanges of

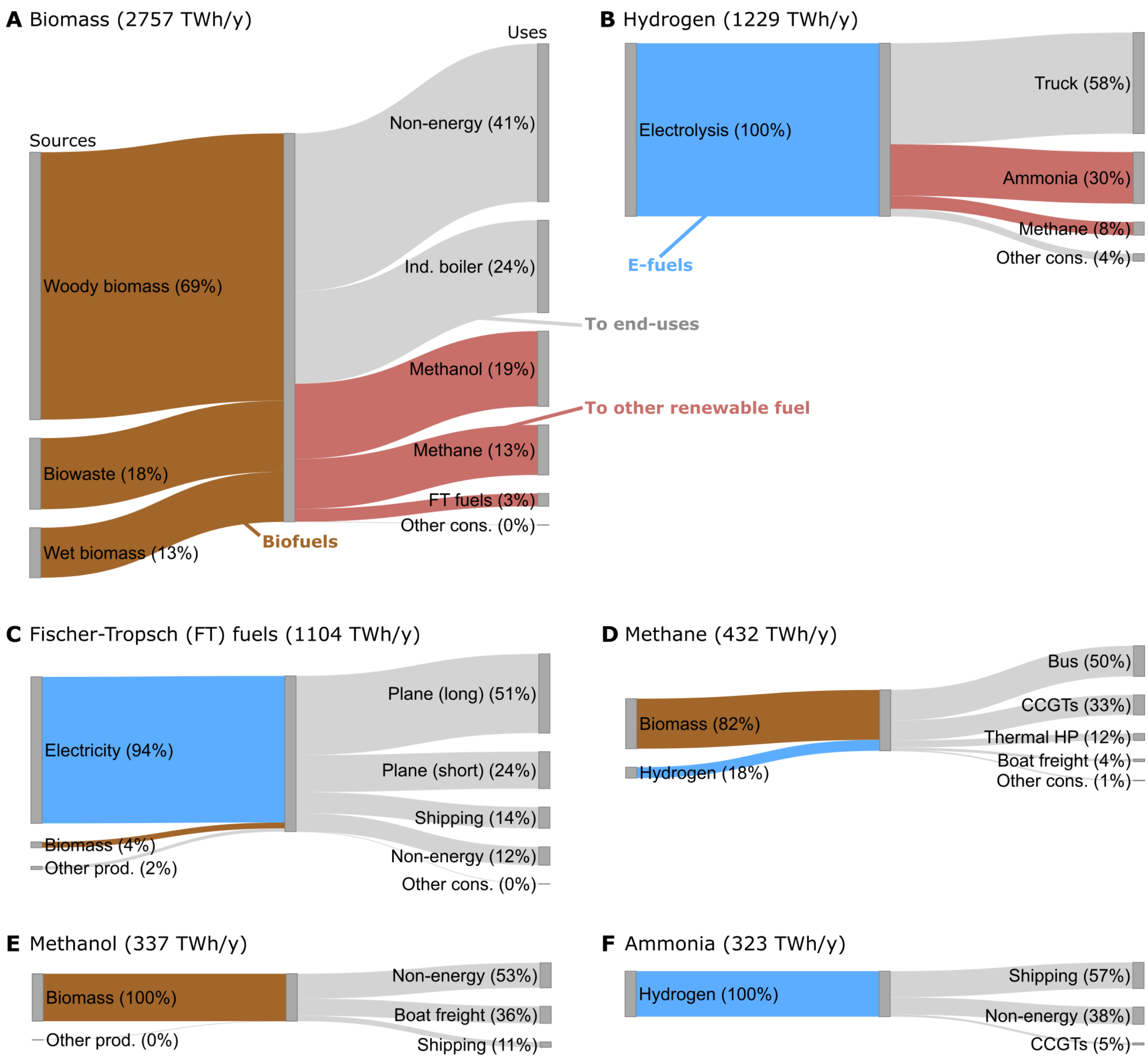

Figure 3.2: Renewable fuels are essential for defossilizing specific sectors such as aviation, shipping, freight, non-energy demand (NED), industrial heat, and busses. The figure presents the yearly aggregated balance of production and uses of the six renewable fuels considered, ordered by the quantity produced: **(A)** Biomass, **(B)** Hydrogen, **(C)** Fischer-Tropsch (FT) fuels, **(D)** Methane, **(E)** Methanol, and **(F)** Ammonia. Abbreviations: combined cycle gas turbines (CCGTs), consumption (cons.), Fischer-Tropsch (FT), industrial (Ind.), non-energy demand (NED), production (prod.).

energy: (i) Haber-Bosch process to produce ammonia; (ii) hydrogen methanation. Finally, other minor consumptions use 4% of the hydrogen produced.

Out of the four advanced renewable fuels in Figure 3.2(C-F), three are produced from biomass and e-hydrogen: methane, ammonia, and methanol. The fourth category, Fischer-Tropsch (FT) fuels, is mainly produced directly from electricity into integrated plants (94%).

The balance of the carbon flows is integrated into the model. Hence, the carbon needed to produce these molecules either comes from the biomass in the case of biofuels or is captured into post-combustion carbon capture units that are placed onto energy assets (e.g., industrial biomass furnaces). This is a conservative approach as some carbon sources outside the energy system are more interesting to capture CO_2 (e.g. cement plant). These process emissions are not included in our model but can be added as a source of carbon that can be captured. Furthermore, the model does not include any carbon sequestration. Hence, the carbon that enters the energy system can be captured and cycled in carbonaceous fuels, but it is always emitted at some point.

FT fuels are the advanced renewable fuels that are the most produced. This production is driven by the aviation demand for synthetic jet fuels (75%). The other FT fuels, co-products of the Fischer-Tropsch process, are used in cargo ships for international shipping and as a feedstock for the non-energy demand.

Methane ranks as the second most produced advanced fuel, with its primary application being the propulsion of busses for public mobility (50%). Additionally, a part of it (33%) is used in CCGTs for power production and flexibility. Other notable applications include decentralized thermal heat pumps and gas-powered boats for freight transport on rivers.

Ammonia and methanol, although produced in comparatively lower quantities than the previously mentioned fuels, hold pivotal roles in specific sectors. Methanol is a crucial feedstock for the non-energy demand and is the primary fuel for freight boats operating on rivers. Meanwhile, ammonia serves as the primary fuel for cargo ships and is also utilized in the non-energy demand for fertilizer production and in small-scale CCGTs for power flexibility.

3.1.3 Renewable fuels and energy storage

Renewable fuels are produced for specific applications where replacing fuels with another source of energy is difficult. They also play an essential role in tackling the temporal and spatial disparity of variable renewable energy sources. Figure 3.3(A) presents the storage capacity installed across Europe sorted by size. Storage of FT fuels, methane and ammonia collectively accounts for 45% of the storage capacity in Europe. Alongside renewable fuel storage, other significant storage capacities can be observed. Thermal storage in DHN enhances flexibility for low-temperature heat and power-to-heat applications. Hydro dams store a portion of the natural water inflow to delay the production of electricity and pumped hydro storage (PHS) stores electricity through water pumping and turbining.

Figures 3.3(B-C) provide further information on the operation of the storage technologies. Figure 3.3(B) presents the total energy stored over the year in each type of storage technology sorted by quantity. Figure 3.3(C) illustrates the normalized state of charge of the nine main storage technologies at each hour (y-axis) of each day (x-axis) of the year, aggregated at the European scale and sorted by installed capacity. This graph evaluates qualitatively the use of each type of storage. Colour transitions along the x-axis indicate energy storage on a weekly to seasonal scale, while transitions along the y-axis signify storage on an hourly to daily scale.

Distinct patterns emerge in storage utilization. Some types, like DHN thermal storage, FT fuels storage and methane storage, serve as seasonal storage, undergoing one main cycle annually. They discharge during the cold season until March and charge during the warm season until October.

Other storages, such as ammonia storage and hydro dams, undergo two superimposed cycles yearly. One cycle involves long-term storage, with the lowest level reached by the end of February. The other, smaller cycle charges until early July, then discharges reaching a local minimum around August or September. However, all these storages are never utilized on a daily scale.

In contrast, PHS operates on various time scales. From April to August, it functions mainly as daily storage, shifting excess solar production from day to night and early morning. During the rest of the year, it serves as longer-term storage, charging from September to November for discharge in December and January.

Additionally, other storage assets like low-temperature decentralized thermal storage, space cooling storage, and electric vehicle batteries primarily offer daily storage during the warm season.

This analysis of cycle lengths can be complemented with Figure 3.3(A-B). Despite small installed capacities, certain storage technologies, such as pumped hydro storage, electric vehicle batteries, and decentralized thermal storage, have a significant contribution to total energy stored over the year due to more frequent cycling. For instance, pumped hydro storage represents only 2% of the storage installed capacity but stores 34% of the total energy stored over the year. However, seasonal storage technologies, despite one or two annual cycles, contribute substantially to stored energy owing to their large installed

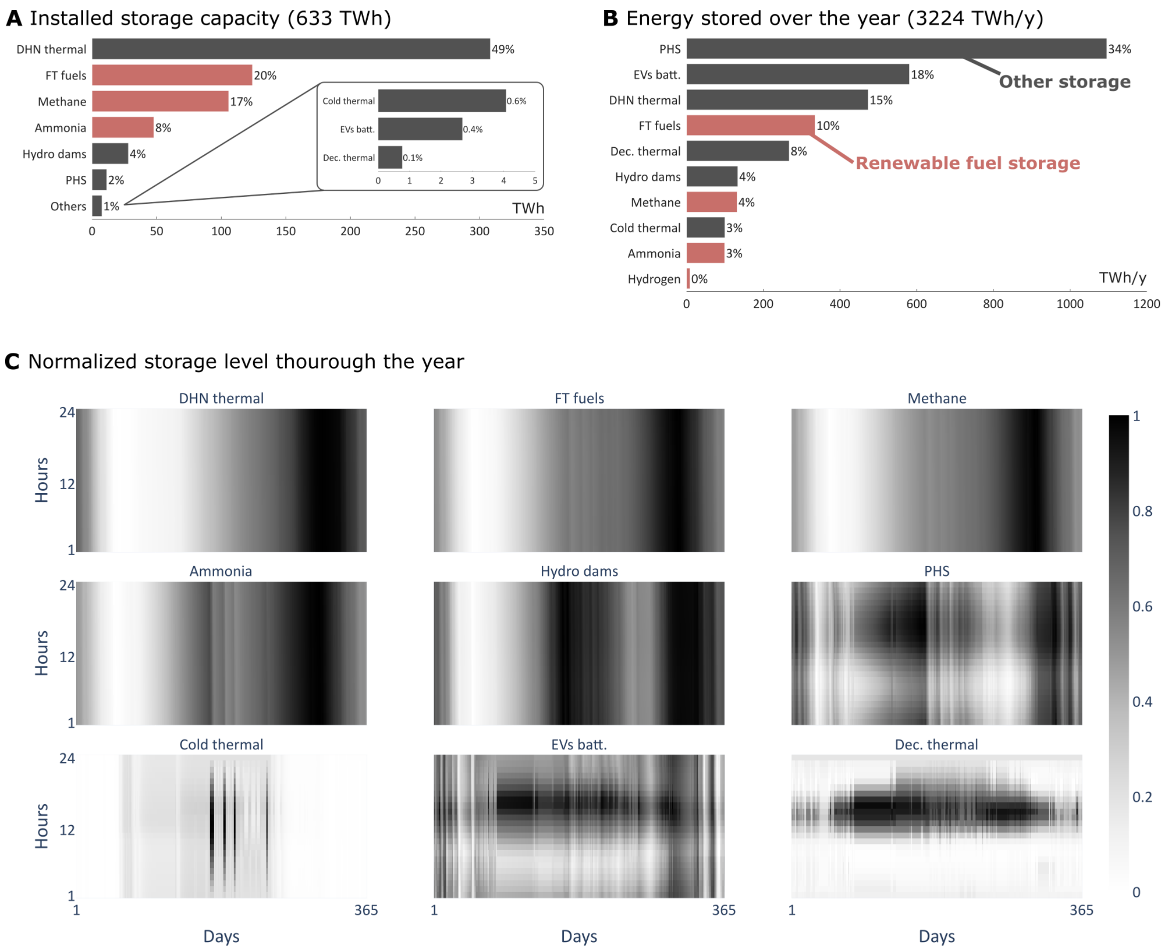

Figure 3.3: Renewable fuels play a key role in seasonal storage, in collaboration with district heating network (DHN) thermal storage and hydro storage (both dams and pumped hydro storage). **(A)** Installed storage capacity in Europe sorted by size. **(B)** Energy stored by each storage technology over the year, sorted by quantity. **(C)** Normalized hourly level of storage of the nine main storage technologies in Europe from fully discharged (0) to fully charged (1). The days start from January 1st to December 31st, meaning that the cold season lies at the extreme left and right of the graphs, and the warm season lies in the middle. Abbreviations: decentralized (Dec.), district heating network (DHN), electric vehicle batteries (EVs batt.), Fischer-Tropsch (FT), pumped hydro storage (PHS).

capacities. For instance, FT fuels storage is responsible for 10% of the energy stored and 20% of the storage capacity installed.

This analysis underlines the critical role of renewable fuels in seasonal storage. They are primarily stored in the form of complex liquid or gaseous fuels rather than hydrogen storage itself. Furthermore, only a small share (3%) of the 4760 TWh of renewable fuels produced are converted back into electricity (Figure 3.2). Hence, renewable fuels provide flexibility by being produced during periods with high renewable electricity production and being stored for later use.

3.1.4 Renewable fuels and energy exchanges

In addition to their contribution to the seasonal storage of energy, renewable fuels play a pivotal role in the exchanges of energy between countries. Figure 3.4(A) provides an overview of the yearly exchanges of all the energy carriers considered in the model, sorted by order of magnitude. Remarkably, electricity constitutes only 26% of the total energy exchanged in Europe. Hydrogen emerges as the primary resource for exchanges, accounting for 35%. Its transportation utilizes a grid created by retrofitting existing methane pipelines and constructing new ones.

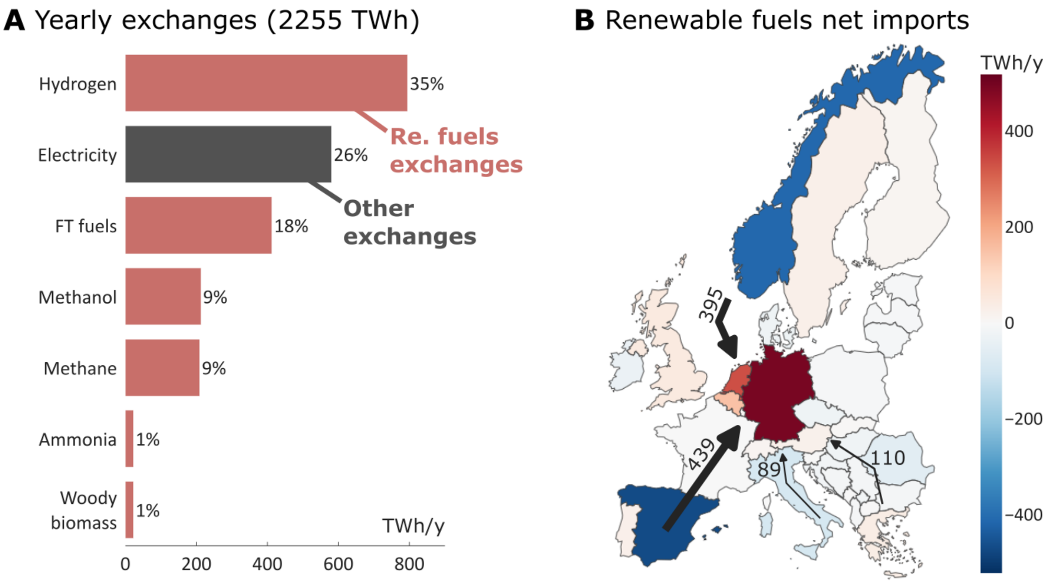

Figure 3.4: **(A)** Renewable fuels transport the bulk of energy exchanged **(B)** from countries with high renewable energy potentials to countries with high energy demand.

Three key means of exchange — hydrogen, electricity, and methane — rely on extensive networks connecting various countries. There exists a trade-off between retrofitting methane pipelines to accommodate hydrogen and keeping methane pipelines for the substantial exchanges of methane (209 TWh).

Liquid and solid fuels, on the other hand, are transported via freight. The possibility of building a network for those resources is not considered in the model. Notably, advanced molecules like FT fuels, methanol, and ammonia, are traded in lesser quantities compared to network-based exchanges but are well-suited for specific end-uses such as aviation, shipping, and non-energy.

Figure 3.4(B) outlines the aggregated net yearly imports of renewable fuels for each country, where negative values (blue) indicate net exporters and positive values (red) signify net importers. The three main importing countries are Germany (496 TWh), the Netherlands (337 TWh) and Belgium (154 TWh). These countries are characterized by a high population density, energy-intensive industries, and trading centres, leading to both high international shipping and freight. Additionally, their renewable energy potentials are relatively limited, necessitating the importation of renewable energy from abroad. However, these countries drastically improve their energy sovereignty. For instance, in this fossil-free European energy system, Germany imports 31% of its energy whereas it imports 70% nowadays. It achieves that reduction by installing 45% of its solar and wind potential. This is higher than the European average in our results (34%). Other European countries like the United Kingdom (49 TWh), Greece (39 TWh), Sweden (31 TWh), Portugal (28TWh), Austria (26 TWh), Switzerland (14 TWh), and Finland (12 TWh) also exhibit a net importing status.

These countries with a shortage of local renewable energy import it from other European countries rather than from the rest of the world. Indeed, there exist high untapped and cost-competitive renewable energy potentials in other European countries like Spain or Norway. Renewable fuels can be produced both in a country with high solar energy (i.e. Spain with 80% of its electricity) and in a country with high wind energy (i.e. Norway with 89% of its electricity). For example, Spain can supply hydrogen on the European hydrogen network, including the cost of electricity, electrolyzer, storage and network at an average cost of around 50-60 €/MWh. This cost falls under the 25th cheapest percentile of the review of Genge et al. [195] and illustrates the cost-competitiveness of certain European regions. The cost of renewable fuels in a future international market is highly uncertain. With other assumptions, Europe could import some renewable fuels. However, these results show that producing and trading renewable fuels in Europe is interesting and that some regions could become actors in an international market. This is even reinforced by the fact that they are close to a market with a high demand for these fuels, which leads to low transport costs.

Notably, four main corridors facilitate the transportation of these molecules to various countries: (i) from the south-west, the biggest corridor transports 439 TWh originating from Spain (ii) from the north-west, through the North Sea, the second corridor transports 395 TWh originating from countries such as Norway and Ireland; (iii) from the south-east, the third corridor transports 110 TWh sourced from countries such as Romania (58 TWh) and

Hungary (22 TWh); (iv) from the south, the fourth corridor transports 89 TWh from Italy.

3.2 Discussion and perspectives

This section compares the results presented before to the existing literature. Then it discusses the approach's limitations and underlines the perspective to overcome them. Finally, it draws the main conclusions of this study.

3.2.1 Comparison with the literature

In terms of energy supply, our study indicates a significant reliance on the large-scale deployment of wind turbines (3940 TWh) and PV systems (4583 TWh), consistent with recent studies encompassing final energy consumption across various sectors [52, 53]. While our results align with Neumann et al.'s [52] findings regarding the high production of wind and PV energy (>8700 TWh), discrepancies arise in the distribution among technologies. For instance, Neumann et al. install more onshore and offshore wind but less PV. However, they obtain a similar distribution among PV technology: a majority of utility-scale PV (84%) and a smaller share of rooftop PV (14%).

In contrast, Pickering et al. [53] project an even higher quantity of wind and solar energy production, exceeding 13000 TWh, with variations in PV and wind capacities across different scenarios. In some cases, they end up with up to 8000 TWh of gross available energy from PV and in other cases, more than 12500 TWh of onshore wind.

In general, the study of Pickering et al. has much higher gross available energy (15000-19000 TWh/y) than our results (12451 TWh/y). This discrepancy is attributed to differences in defining energy demand, with our study focusing on a whole-energy system approach while others define demand solely in terms of final energy consumed. This implies exogenous assumptions on end-use technologies, thus underestimating potential sector coupling and efficiency. This underestimation leads to a higher gross available energy supply.

Moreover, Pickering's model and Neumann's model [52, 53] neglect the costs associated with end-use technologies (e.g. heating systems, private cars, trucks, etc.), resulting in underestimations of transition costs of a factor 1.77 to 2.10 compared to our results. This underscores the importance of accounting for end-use technologies to provide comprehensive cost assessments and identify potential synergies between final energy supply and end-use sectors.

Numerous studies highlight the urgent need for a substantial increase in the deployment of wind and PV technologies [46, 52, 53, 197]. Victoria et al. [197], for instance, stress the importance of scaling up these technologies rapidly, advocating for the installation of up to 500 GW/y of new wind and solar capacity during the period 2025-2035.

However, compared to our findings, some scenarios underestimate the required installed quantities. These scenarios can be categorized into two groups: (i) those that only consider electricity demand [85, 260–265] or electricity and some other demand such as private mobility [55, 266] and space heating [51, 67, 267]; (ii) scenarios that do not consider fully renewable energy system for 2050 [34, 71, 72, 273].

The first category underestimates electricity production because it misses the sector-coupling effect, resulting in wind and solar installed capacities around three times smaller than our projections [55, 260]. In the case of Dubois et al. [85], the wind and PV capacities are six times smaller than our results. This emphasizes the necessity of modelling the whole-energy system to adequately address the challenges of the energy transition.

Conversely, scenarios in the second category continue to rely on fossil fuels, sometimes incorporating negative emission technologies. Consequently, the installed PV and wind technologies vary significantly based on assumptions regarding fossil energy use and carbon capture. For instance, in their energy transition scenarios with the JRC-EU-TIMES model, the JRC allows remaining emissions in Europe around 1500 $MtCO_2$/y (i.e. 37% of 1990 emissions) by assuming that half of it can be captured and stored [60]. By doing this, they keep fossil fuels for more than 20% of the final energy, and they end up with much lower ambitions in terms of deployment of wind and solar energy, with only 28% of the deployment obtained in our results. In a later study, the European Commission considers that the carbon in fuels for non-energy is stored in the products[273]. This assumption is questionable as the circularity of plastics is limited [274]. Preliminary results from the Procura project [275] estimate a typical duration of 0.35 to 2.36 years for carbon storage in plastics. The nine scenarios of the European Commission retain between 15 and 50% of fossil fuels in the energy mix and underestimate the required capacities of renewables by up to 2.36 compared to our results. This difference emphasises the importance of avoiding reliance on uncertain technologies such as carbon capture and storage [276], as it can lead to less ambitious and less robust planning outcomes.

Furthermore, our study and others highlight a significant increase in electricity production and high levels of electrification across end-use sectors[34, 46, 52, 273]. Neumann et al. [52] project a threefold increase in electricity production compared to current levels. They observe a rule of one-third of the electricity corresponding to current production levels, one-third for electrification of new sectors and one-third for producing e-fuels. Our findings closely align with this distribution, with 9232 TWh of electricity produced, representing a 2.62-fold increase over current production levels. This electricity is distributed as follows: 23% for specific electrical uses, 37% for newly electrified sectors, and 40% for e-fuels production. The electricity for specific electrical uses and for newly electrified end-uses represents 52% of the final energy consumed, falling within the range of 42-60% suggested by Schreyer et al. [46].

A significant portion (40%) of the increase in electricity generation is used for producing e-hydrogen and its derivatives. Accounting for the electrolyzers present in the FT fuels synthesis chain (51% of the hydrogen production), our model forecasts an e-hydrogen production of 2509 TWh/y with 407 GW of electrolyzer installed in Europe. This estimate falls within the mid-range of values reported in existing literature. For instance, Schreyer et al. [46] present a conservative prediction of 1000 TWh/y for the EU27, while Blanco et al. [71] propose a more optimistic projection of 5000 TWh/y. Other publications offer estimates ranging from 1700 TWh/y to 3100 TWh/y, some using optimization models similar to ours [34, 52, 71, 72, 197] and others based on expert knowledge such as the European Hydrogen Backbone [202].

Other cross-sectoral studies [46, 52] similarly conclude on few direct uses for hydrogen. Hydrogen is rather upgraded to more advanced and dense fuels for aviation, shipping, heavy-duty land transport, fertilizers, and production of HVC. This finding aligns with our results, wherein 31% of the hydrogen is directly used, and the rest is upgraded to FT fuels, ammonia and methane used in the above-mentioned sectors. However, those studies include the hydrogen consumption for direct iron reduction. This specific demand is not explicitly defined in our model but regrouped with other high-temperature industrial heat demands. Consequently, our model may overlook approximately 180 TWh of hydrogen demand [202].

A notable disparity among these scenarios lies in the modelling of biomass potentials and the conversion chain of biofuels. Some studies [46, 52] have very low estimates, 1.7 to 2.0 times smaller than the JRC estimates [159]. Others [53] lack detail regarding the role and utilization of these resources. Finally, others overestimate significantly the potential. For instance, the European Hydrogen Backbone [202] relies on a biomethane supply that is 3.3 times higher than the JRC estimates [159] which are already optimistic for the biomethane potential [74]. In our case, biomass is regarded as a scarce and strategic resource. It is essential in certain sectors, such as the non-energy demand and the high-temperature heat for the industry. But it is also upgraded to complex fuels such as methanol, methane, and FT fuels. This underlines the importance of these resources and the lack of consistent modelling across the literature.

In terms of backup power plants, this study aligns with other cross-sectoral study [52, 53] in indicating their small size (114 GW, in our results) compared to wind and PV capacities (5185 GW). Neumann et al. [52] also observe low levels of re-electrification of e-hydrogen and derivatives. In our findings, CCGTs generate 99.5 TWh of electricity with 24% from e-fuels and 76% from biofuels. Pickering et al. [53] even go further with their exploration of diverse options. They state that backup power plant capacity is not strictly necessary.

Other studies focusing solely on the electricity transmission grid [260] or including both electricity and hydrogen transmission grids [52] have emphasized the importance of energy exchanges in Europe to address the spatio-temporal disparity of renewable energy sources. In our analysis, this importance is further underscored as we consider additional means of exchanges (e.g. FT fuels, methane, methanol), representing 39% of energy exchanges overlooked in other studies.

As in our results, studies including the possibility of building a hydrogen network find it cost-effective to install [52, 197]. Neumann et al. [52] install a larger quantity of hydrogen pipelines (204 to 309 TWkm) than in our results (154 TWkm). This is due to two main reasons: (i) their finer spatial resolution (181 regions) leads to more accurate and longer distances; (ii) they neglect other means of exchange such as methane, methanol and FT fuels, which play a crucial role in our results, thereby underestimating the competition between different means of energy transportation.

This difference is even stronger for electricity transmission lines. Several studies focus on the electricity sector and only consider electricity as a means of exchange. They have a very high increase in transmission line capacities [67, 85, 260]. For example, Schlachtberger et al. [260], in their study on Europe at the country scale, project an expansion of the electricity network from 31.25 TWkm to 285.70 TWkm in their optimal case. However, considering the delays already observed in electricity transmission expansion, achieving such levels by 2050 is questionable [277–280]. Consequently, Schlachtberger et al. propose a compromise grid expansion of up to 125 TWkm. This aligns more closely with the 86 TWkm obtained in our results, which include the competition with other means of exchanges.

Other studies identify patterns of net importers and exporters similar to our results. For instance, Neumann et al. [52] identify Northern Germany and the Netherlands as importing regions and Spain as a strong net exporter. Caglayan et al. [55] identify the Nordic countries and Ireland as primary exporters of electricity and hydrogen. While these findings align with our observations to some extent, there are also notable differences. Some regions, such as the United Kingdom and Greece, have the status of net exporters in those studies, whereas they are net importers in our results.

The European Hydrogen Backbone [203] proposes five corridors to transport hydrogen in Europe. Three of them coincide with our results. These differences arise because we use a model to find the optimal system design and use of resources. In contrast, the European Hydrogen Backbone designed its scenario with assumptions based on the literature and expert knowledge. Furthermore, they consider hydrogen imports through pipelines from North Africa and through boats in the North Sea, whereas in our case, Europe does not import renewable fuels, finding it more cost-effective to produce them locally.

Predicting the exact topology of future energy networks and exchanges is inherently complex, with outcomes varying based on different assumptions. Furthermore, the location of production assets and the implied exchanges have many different and equivalent designs, as shown by other studies [53, 88]. According to the design, certain regions could be net importers or net exporters. For instance, in our results, the United Kingdom is a net importer, whereas it has the potential to be a net exporter and is one in other studies. Nonetheless, certain trends persist across studies. For instance, countries like Germany, the Netherlands, and Belgium depend highly on energy imports. Other countries like Spain and Norway have cheap and abundant renewable energy potential and can become exporters of renewable electricity and fuels. These trends underscore the importance of strategic planning and collaborative efforts in shaping Europe's future energy systems.

3.2.2 Limitations and perspectives

The European model used in this work generates results that are aligned with the related literature. Furthermore, its whole-energy system approach reveals novel insights about fossil-free energy systems. However, it has several limitations. This section details five key technical limitations and perspectives. More general limitations and perspectives are also presented in the conclusion of the thesis.

First of all, the model searches for a global optimum for Europe. This approach has the advantage of showing what a European energy system could look like with perfect cooperation among countries. However, it neglects the diverging interests of the different countries. An alternative approach would be to develop a multi-agent version of the model where countries can cooperate while preserving their own interest. We tested a first simple version of this approach in a master thesis [281]. Middelhauve et al. [217] developed a similar multi-level approach to model a district in Geneva, Switzerland. They decompose this district into 31 houses with each one its own optimization.

Secondly, our model application does not consider electricity, gas and hydrogen interconnections with countries around Europe. Several studies [121, 282–284] have underlined the potential of importing electricity or hydrogen through a network from neighbouring regions, such as Northern Africa. These imports are expected to have a lower cost than the cost for renewable fuel imports used in our model. Considering these imports may change the optimal networks' topology and the production of renewable energy and renewable fuels in European countries. Similarly, the connection of the offshore wind parks with the mainland is not modelled in this work. Instead, we assume that each country is able to bring back this electricity to the mainland with a small cost of integration into the grid. Another approach would be to create a fictive cell in the North Sea with all the North Sea offshore wind potential and no energy demand. This cell would then have the possibility to build offshore wind farms and connect them with subsea HVDC cables to any country around the North Sea. Thirdly, we model Europe with one node per country. For large countries like France or Germany, the model misses some challenges both in terms of local energy resources and in terms of transmission networks. Other European studies reach a more refined spatial representation of Europe. For instance, Pickering et al.[53] consider 98 regions, and Neumann et al.[52] consider 181 regions in their sector-coupled European energy system model. Improving our model in this way faces two challenges: (i) data availability; (ii) computational tractability. When data is unavailable at the regional scale, we could do as Pickering et al., who distribute them with population density or industry density according to the data type. Then, if we increase the number of nodes in our model, we increase its size, leading to larger computational time and memory usage. Further model reduction techniques should be applied to improve the model's computational tractability. Otherwise, we could get inspired by the work of Ram et al. [269]. They use a multi-level approach. In a first step, they model Europe into 5 macro-regions. Then, they model each macro-region divided into smaller regions with boundary conditions from the first step. They apply this method until they reach a refined enough spatial scale. This method could even be extended to have a bi-directional linking, giving back information from more refined spatial scales to the macro-model and iterating until we reach convergence. This approach could be used to study more precisely one specific country. In this thesis, we developed a model that allows us to define boundary conditions for any European country. Then, this country could be modelled more precisely in future works.

A fourth limitation concerns the technical resolution of the model. It covers many potential improvements, from global ones to more specific ones. One global limitation is that the model ensures the energy balance of each energy carrier at each hour but does not integrate any operation constraints. In particular, dispatch constraints such as ramp-up, start-up costs, and minimal time up are not implemented as they would increase the complexity of the model and thus reduce its computational tractability. Another approach we have explored on the Belgian version of the model is to couple it with an economic dispatch model, Dispa-SET [125]. The EnergyScope model provides a system design for Dispa-SET. Dispa-SET tests it and returns information on the need for more flexibility in the electricity grid. EnergyScope is run with this new constraint, and so on. We showed that within two or three iterations, the system design converges to a system with more backup power plants than first estimated by EnergyScope. This result is specific to the Belgian case study explored. Further investigation is needed to obtain a general prescription for the results of energy system optimisation models like ours. However, the need for backup power plants might be underestimated in our results. To continue this work, the European version of EnergyScope presented in this thesis could be coupled with the European version of Dispa-SET. Similarly, the model could be coupled with other models to verify other technical feasibility issues, such as power system adequacy and reliability, DHN installation and operation, or energy grids reinforcement needs. For instance, Schnidrig et al. [285] evaluated that for a net-zero Swiss energy system. In that case, a high reinforcement of low-voltage (+61%) and medium-voltage (+82%) electricity grids is needed. Other specific technical improvements could be made. For instance, the evaluation of wave energy potentials and time series of Satymov et al. [286] could be integrated into the model. Better heating and cooling time series generated by Staffel et al. [156] could replace the heating and cooling degree hours used as a proxy in our model. Time series could be added to some technologies, such as heat pumps, to represent the impact of outdoor temperature on their operation [287, 288]. The modelling of mobility (e.g. share of public mobility, V2G) could be challenged and improved.

A fifth limitation concerns the evaluation of energy demand. To improve our whole-energy system approach, all demands should be quantified as close as possible to the energy service. In particular, the industrial demand is an essential challenge for the energy transition and could be better quantified. The current version quantifies it with general categories:

electricity, high-temperature heat, process cooling, hot water, space heating and space cooling. We propose to use the AIDRES database [289, 290] to quantify the demands in terms of kilotonnes of the main energy-intensive industries, such as steel and glass. Then, we could integrate into the model the different conversion paths to produce them with their energy consumption and emissions. This would provide a more precise quantification and a better understanding of the industry's needs. A more precise industry modelling could also allow us to integrate the industrial challenge of building and installing all the technologies needed for a fossil-free energy system. The impact of producing these technologies in Europe or importing them from outside should also be studied, both from an energy standpoint and a geopolitical standpoint. Indeed, a European fossil-free energy system risks to go from our current fossil resources dependency to an energy technology dependency. Another improvement would be to formalize and complete the modelling of the demand-side management. Indeed, as the model defines the energy demand as end-use demand, it intrinsically includes the demand-side management that happens between the final energy consumption and the energy service consumption. For instance, a decentralised heat pump can consume electricity during high solar or wind production peaks. The heat produced can be stored in decentralised heat storage for later use when the end-use needs it. Similar patterns can be seen for other end-use demands. However, the demand-side management of the energy service consumption is not integrated into the model and could change the design. For instance, some industrial processes could reduce their production temporarily because of a lack of energy and compensate for this reduced process production by producing more during another period when there is excess energy. This possibility is highly dependent on the energy service. Similarly, some demand elasticity could be modelled, inducing a variation of the demand according to the cost of the final energy.

3.2.3 Conclusions

Through modelling with EnergyScope Multi-Cells, this chapter demonstrates the feasibility of achieving a fossil-free, nuclear-free and energy-independent Europe. The European energy system relies on cooperation between countries and a high deployment of PV panels (3548 GW) and wind turbines (1637 GW). Significant energy efficiency gains are achieved through electrification of end-use demands. Electricity supplies 52% of the final energy consumed. However, a large number of applications still need to use fuel. In this system, fuels are derived from renewable sources, including electricity and biomass, and represent 43% of the final energy consumed. The remaining 5% comes from waste incineration in the industry.

These renewable fuels supply final uses under different forms: (i) biomass (1755 TWh/y); (ii) FT fuels (1100 TWh/y); (iii) hydrogen (771 TWh/y); (iv) methane (432 TWh/y); (v) methanol (337 TWh/y); (vi) ammonia (323 TWh/y). Meeting these demands necessitates the installation of extensive conversion plants, such as deploying 407 GW of electrolyzers to produce 2509 TWh/y of e-hydrogen across Europe. Renewable fuels are essential to defossilize some applications. Biomass, biomethanol, e-ammonia and FT fuels phase out fossil fuels in the non-energy demand. Biomass, along with waste and electricity, supplies the process heat for the industry. Heavy transportation, including aviation, international shipping, inland freight and busses, relies on various e-fuels and biofuels.

Additionally, renewable fuels provide essential services to the energy system to address the spatio-temporal disparity of renewable energy sources : (i) energy storage; (ii) energy exchanges. Firstly, renewable fuels are the second largest form of energy storage after DHN thermal storage. They serve as seasonal storage, shifting the excess energy from summer to winter. Secondly, renewable fuels constitute the main means of energy exchange in Europe (74%). Hydrogen is the primary energy carrier for energy exchanges (35%) through a network made of retrofitted pipelines from methane networks and new ones. This highlights the importance of diversifying energy carriers for exchanges rather than relying exclusively on electricity, leading to a more balanced transmission network expansion. Similarly, considering only electricity and hydrogen overlooks 39% of exchanges through other energy carriers such as FT fuels (18%), methanol (9%), and methane (9%), resulting in oversized electricity and hydrogen networks. The spatial distribution of energy exchanges underscores the importance of cooperation in Europe, as some countries emerge as net importers of renewable fuels (e.g. Germany, the Netherlands and Belgium) and others as net exporters (e.g. Spain, Norway and Italy).

Finally, this study emphasizes the importance of having a holistic approach that encompasses all the energy-consuming sectors. Defining energy demands as closely as possible to the energy service enables leveraging all possible synergies within the system. However, it only explores one cost-optimal system design based on specific assumptions. The two next chapters overcome this limitation. Chapter 4 develops a hybrid method combining scenario analysis and near-optimal space exploration. With this method, we generate eleven alternative designs to the one presented here. Chapter 5 analyzes these designs and underlines trade-offs and must-haves to reach a fossil-free European energy system.

4 Hybrid method to explore a diversity of options

Decision is a risk rooted in the courage of being free.
Paul Tillich

Chapter overview

- Hybrid method to explore a diversity of options.
- Description of two alternative scenarios: Sufficiency and Nuclear.
- Description of three exploration directions: Onshore renewables, biomass and cross-border electricity grid.

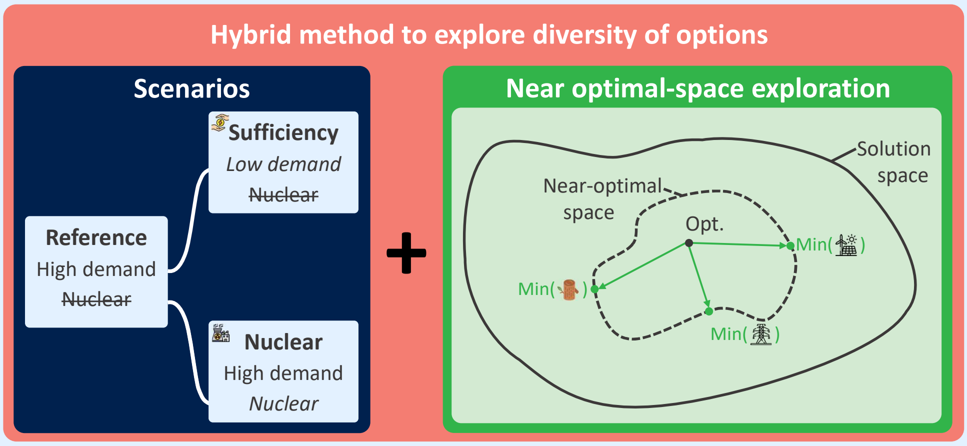

Figure 4.1: Summary of the hybrid method: combining scenario analysis and near-optimal space exploration.

The previous chapter presented a fossil-free European energy system for 2050. This system is designed by optimizing the annual cost of the energy system with the energy system optimization model EnergyScope Multi-Cells. However, one system design is insufficient to present the possible options for a future fossil-free energy system. To overcome that limitation, this chapter develops a hybrid method combining scenario analysis and near-optimal space exploration.

> The chapter is structured as follows. Section 4.1 presents the general concept and equations of the hybrid method. Then, Section 4.2 describes and motivates the two alternative scenarios: Sufficiency and Nuclear. Finally, Section 4.3 presents the three exploration directions, minimizing: (i) the onshore renewable technologies; (ii) the use of biomass; (iii) the expansion of the cross-border electricity network. This section motivates the choice of each direction and describes the additional equation to implement the near-optimal space exploration.

4.1 A hybrid method: combining scenario analysis and near-optimal space exploration

The hybrid method combines intuitions from the scenario analysis field and from the near-optimal space exploration field, see Figure 4.2. Scenario analysis considers the uncertainty of the environment in which the design is optimised. If this environment changes, so does the optimal design and the solution space. Near-optimal space exploration underlines the fact that in energy system design problems the optimum is flat. This implies that many solutions are very similar to the optimum in terms of cost but have very different designs that may be of interest for other socio-politico-environmental dimensions that are not modelled in the energy system optimisation model. By combining both, we provide more insights into the possible design trade-offs and must-haves according to the environment.

We consider two alternative scenarios in addition to the Reference scenario analyzed in Chapter 3. The two scenarios include partially the uncertainty of the environment in which the energy system unfolds by changing one key assumption. The first alternative scenario, Sufficiency, assumes that sufficiency measures are applied in Europe and lead to a low demand in 2050, in opposition to the high demand in the Reference scenario. The second alternative scenario, Nuclear, assumes that nuclear power plants are massively deployed in Europe while keeping the high demand of the Reference scenario.
In most studies [53, 58, 84, 87–95], the near-optimal space approach for energy system design is inspired from the Modelling to Generate Alternatives field. This approach aims to

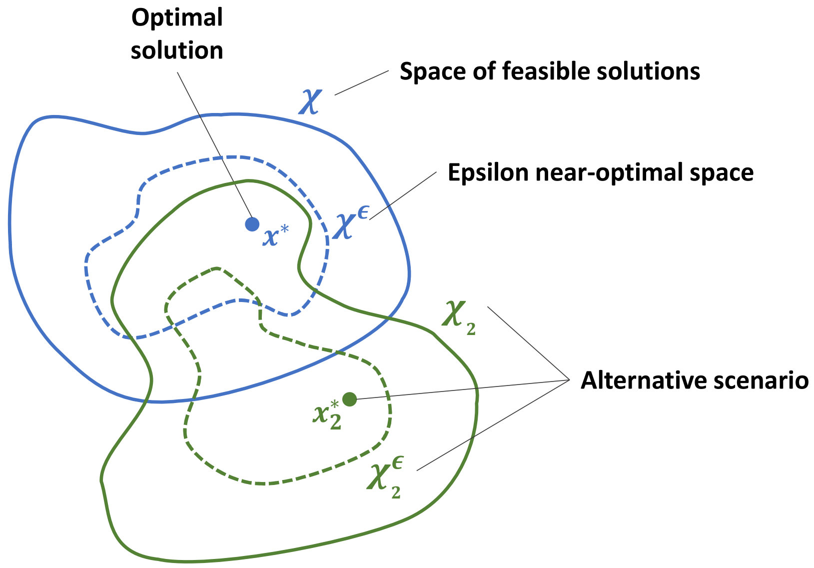

Figure 4.2: The near-optimal space exploration intends to propose alternatives to the optimal solution (x^*) inside of the epsilon near-optimal space (χ^ϵ). This space is the space of all feasible solutions (χ) with a relative cost increase below epsilon compared to the optimal solution. Considering alternative scenarios changes the solution space, thus the optimal solution and the epsilon near-optimal space.

uniformly explore the near-optimal space and represent all alternative solutions within this space. However, it requires hundreds of model evaluations, which causes problems both for computational tractability and to analyze in detail the obtained designs. Therefore, we opt for the approach of Dubois et al. [85]. They explore a specific direction to determine the minimal value certain variables can reach within the near-optimal space. This provides the intersection between the direction of interest and the near-optimal space boundary. This means that rather than representing the entire near-optimal space through hundreds of model evaluations, it identifies the bounds of this space for certain variables of interest with only a few model evaluations. However, the directions must be chosen wisely to lead to valuable results and analyses.

In practice, the exploration direction is defined by changing the objective function from the total annualized cost to another quantity of interest. This quantity depends on the direction and is described for each direction in Section 4.3. In this work, we choose three directions: (i) minimizing onshore renewables (i.e. utility PV, onshore wind and CSP); (ii) minimizing the use of biomass; (iii) minimizing the expansion of the cross-border electricity network.

To ensure near-optimality, an additional constraint bounds the increase in total cost at a maximum percentage (ϵ) of the total cost at the optimum ($c_{tot,opt}$) :

$$\sum_{r \in REG} \mathbf{C_{tot}}\ (\mathbf{r}) \leq c_{tot,opt}\ (1+\epsilon). \tag{4.1}$$

In this work, we limit the cost increase to 5% for the near-optimal designs.

4.2 Description of the scenarios

Each scenario differs from the Reference scenario by one key characteristic and follows a trending storyline (Figure 4.1). The next Subsections present how they are modelled. First, the Sufficiency scenario is detailed. Then the Nuclear scenario is presented.

4.2.1 Sufficiency

The Sufficiency scenario differs from the Reference one by assuming the implementation of sufficiency measures at the European scale. These measures and the low demand they induce are derived from the work of the CLEVER project [291, 292]. CLEVER stands for a Collaborative Low Energy Vision for the European Region. It is a four-year project led by Association négaWatt, with over 20 years of experience in energy transition scenarios based on sufficiency. This project regroups 25 organisations from academia and civil society from more than 20 European countries. Together, they developed a bottom-up scenario based on the Sufficiency-Efficiency-Renewables framework [293].

The CLEVER project proposes the following definition of sufficiency:

Sufficiency means redesigning collective and individual infrastructures and practices to minimise demand (energy, materials, land, water and other natural resources) while delivering human well-being for all within planetary boundaries.

This definition underlines two key aspects. Firstly, sufficiency goes well further than behaviour scenarios or the impact of individual acts. It is about societal organisations fostering the well-being of all with lower material and energy uses. Secondly, the sufficiency approach is based on equity. They inspire themselves from the doughnut economy [294] and try to define energy services that ensure staying within planetary boundaries while fulfilling everyone's needs for services to live a decent life. This notion of balance is in line with the basic definition of sufficiency from the Cambridge dictionary: *an amount of something that is enough, or the quality of being good enough* [295].

In the CLEVER project, partners from each country have built their own national trajectories. These national trajectories were harmonised through an iterative process and discussions to reach a European scenario with low-demand projections for each European country. One concept they developed during this harmonisation phase is the convergence corridors [296–299]. They are inspired by the doughnut economy approach. The idea is that everyone should have access to a minimum energy service and not go above a maximum energy service; otherwise, they keep other people from achieving decent energy services within planetary boundaries. The corridors are built based on discussion among project's partners and comparison with the literature on low-demand scenarios [300–302] and on decent living standards [303–307]. Typical examples of convergence corridors are residential space heating and passenger mobility; see Figure 4.3. In both cases, the demand per capita is very unequal across Europe in 2015 and converges towards a corridor in 2050. Not all countries can reach the corridors for practical reasons, but they try to get as close as possible. For instance, in Belgium, the floor area per capita was very high in 2015 (50.5 $m^2/pers$) and drove high space heating demand. This floor area per capita cannot be reduced enough up to 2050 to reach the convergence corridor because these houses have already been built.

The strength of the CLEVER scenario is its bottom-up approach to propose energy demand projections based on sufficiency. However, this scenario designs the energy system to meet these demands through annual energy balances and a rule of thumb for storage and flexibility. Based on a benchmark, they assume that flexible assets produce 18% of the final electricity consumption. They size the storage, batteries only, to store over the year 3% of the final electricity consumption. Therefore, we use CLEVER's energy demands to define our Sufficiency scenario and adapt the demand to end-use demands input for the EnergyScope Multi-Cells model. With this model, we propose designs for a European energy system that supplies a low-energy demand. As the CLEVER scenario details its hypotheses for end-use technologies in each country, we can directly convert their final energy consumption per sector into end-use demands for EnergyScope Multi-Cells. The only exception is the industry sector, where the data is insufficient to compute end-use demands. We process the energy and non-energy demands separately. For the industry energy demand, we apply the same method for high-demand computation. We split the final energy consumption into end-use types thanks to the data of Heat Roadmap Europe (HRE4). For the industry non-energy demands, we use historical non-energy demand computed previously as a baseline. Then, we project this demand to 2050 by applying

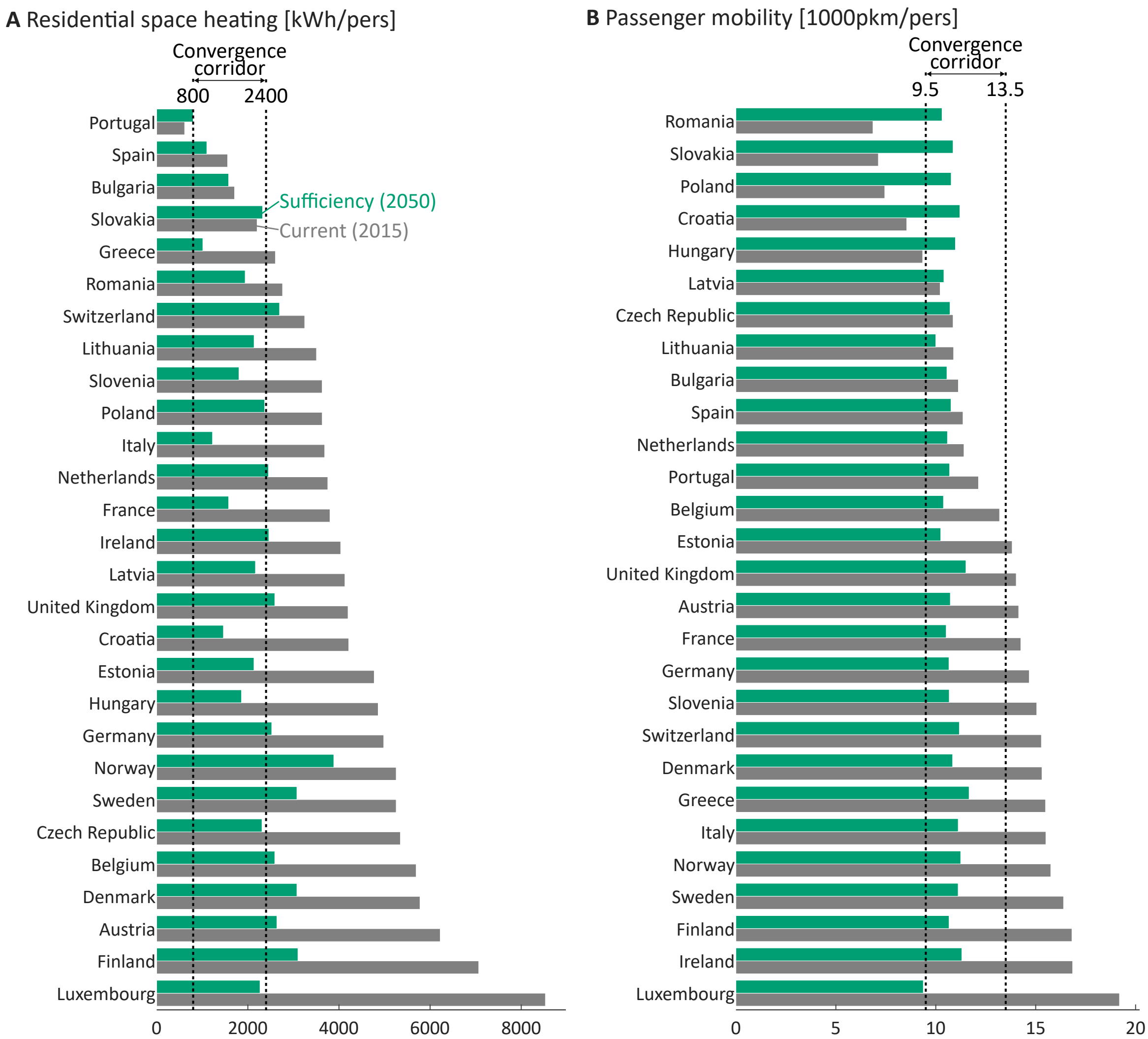

Figure 4.3: The demands per capita of space heating and passenger mobility were very unequal in Europe in 2015. In the Sufficiency scenario, these demands converge towards a corridor that ensures a decent living for all within planetary boundaries.

CLEVER's assumption on reductions in this sector.

The resulting demands are less intense than the high demands of the EU Reference Scenario, see Figure 4.4. However, the reduction varies according to the end-use type. The most impacted end-use types are space cooling and shipping, where low demand represents only 35 and 38% of the high demand. Then, six other end-use types have a low demand between 52 and 68% of the high demand: long-haul aviation, space heating, hot water, freight, passenger mobility and non-energy. Finally, three end-use types are less impacted, with low demands between 78 and 88% of the high demand: process cooling, high-temperature heat and electricity.

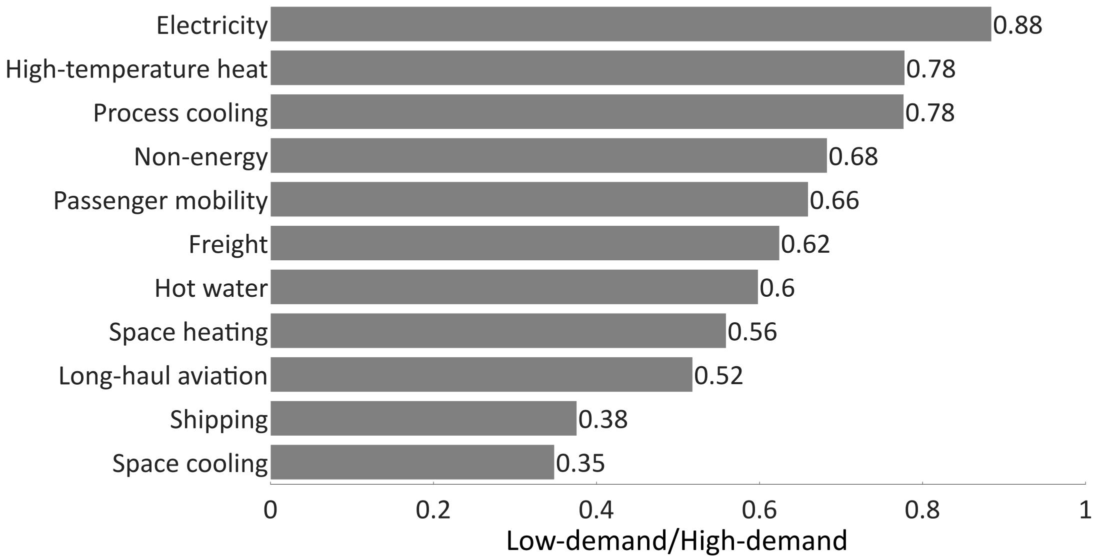

Figure 4.4: The Sufficiency measures of the CLEVER scenario have different impacts on different end-use types. The end-use types with the highest impact are space cooling and shipping and the ones with the lowest impact are electricity, high-temperature heat and process cooling.

Although the demands in the Sufficiency scenario are reduced to meet convergence corridors, the particularity of the different countries still appears, see Figure 4.5. However, the demands per capita are much more equal across Europe, see Figure 4.6. This is especially true for demands like passenger mobility, electricity, hot water or space heating. Other demands keep strong spatial disparity. For instance, the space cooling is mostly located in the south. Energy-intensive industries in Finland, Norway and Sweden increase the demand per capita for electricity, hot water, space heating and high-temperature heat. Non-energy and shipping demands per capita stay very high in countries such as Belgium or the Netherlands.

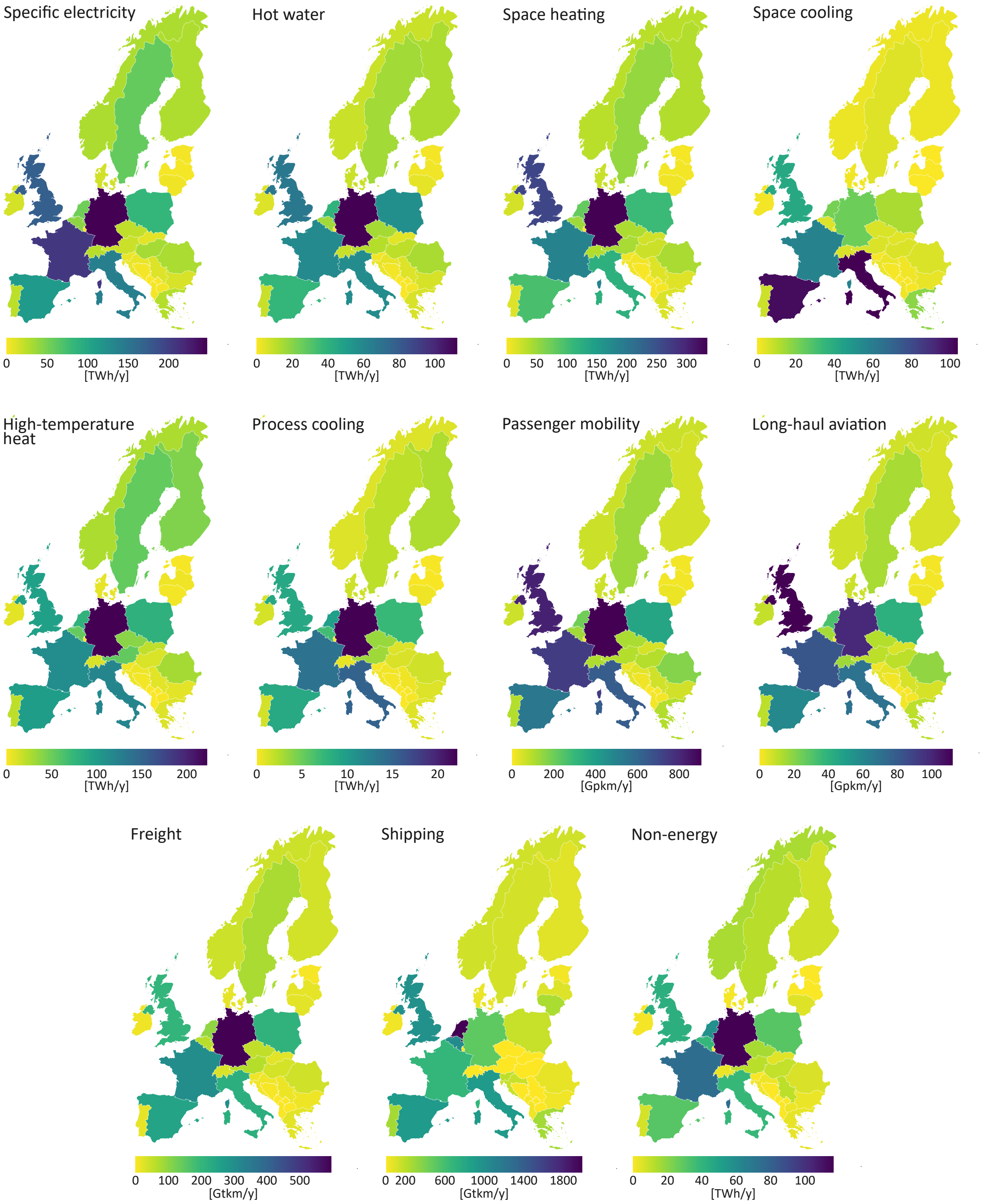

Figure 4.5: Map of the end-use demands in Europe in 2050 in the Sufficiency scenario.

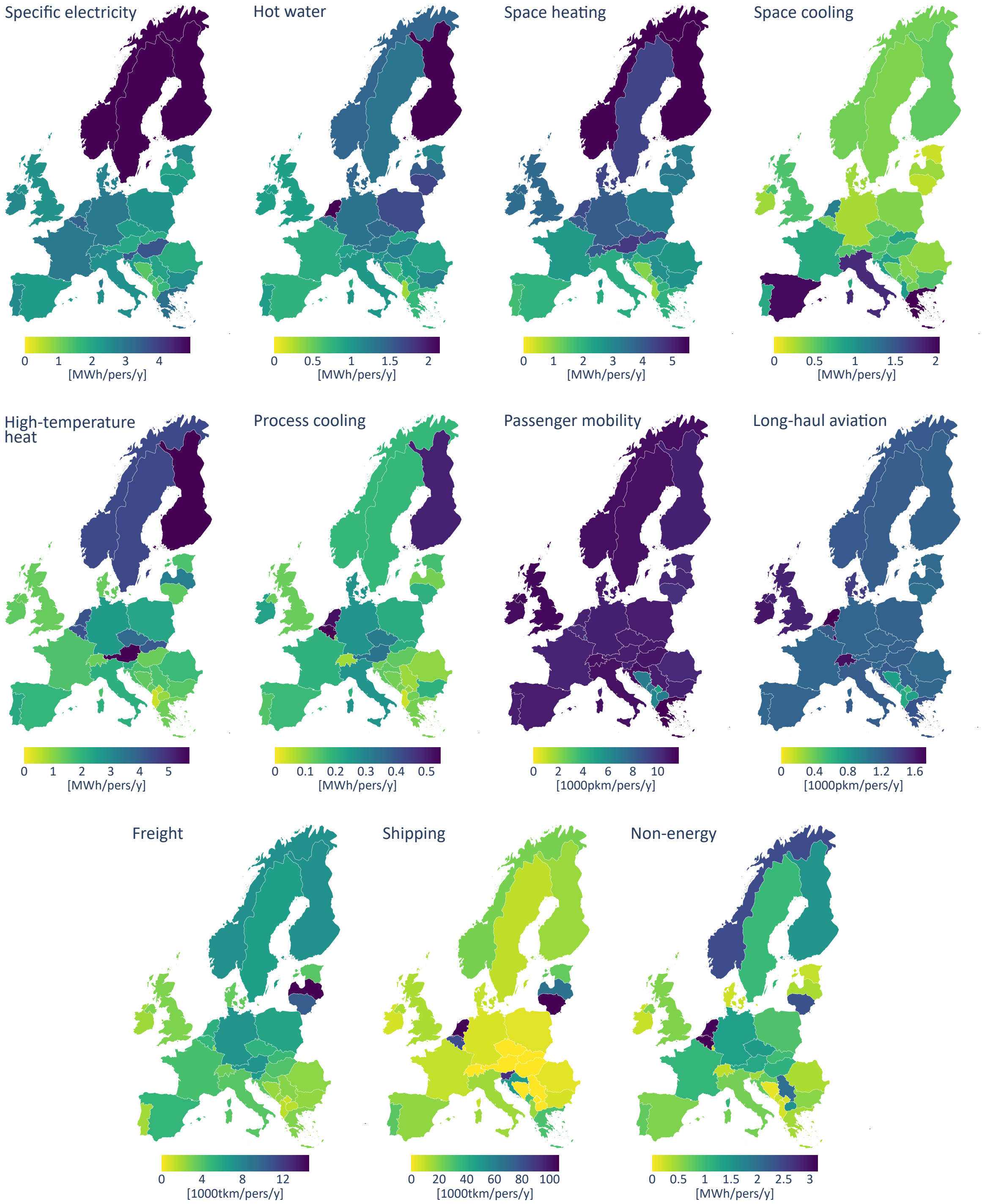

Figure 4.6: Map of the end-use demands per capita in Europe in 2050 in the Sufficiency scenario.

4.2.2 Nuclear scenario

Nuclear energy is a low-carbon energy that has the advantage of providing dispatchable production. This is why a coalition of 14 European countries led by France, the Nuclear Alliance, signed a statement in favour of nuclear energy [308]. In this statement, they position nuclear power in Europe's energy strategy. Their plan proposes to install 150 GW of nuclear power plants in Europe by 2050. This is ambitious as Europe has currently 105 GW of nuclear power plants [309]. Most of these power plants are old and will be shut down before 2050.

The statement of the Nuclear Alliance is the base for our nuclear scenario. However, it does not provide information on how these 150 GW are dispatched among countries. To dispatch them, we consider all countries who signed this statement and distribute the 150 GW according to their current and under construction capacity [309, 310], see Figure 4.7.

Similarly to the Sufficiency scenario, we assume that installing nuclear energy is a political decision stated exogenously. Therefore, we force the model to install these capacities by fixing the lower and upper bounds of the nuclear power plants to this capacity. Furthermore, the new nuclear power plants installed are genIII small modular reactors. As the cost of these reactors is highly uncertain [311, 312], we use the characteristics of the classical genII reactors from the previous version of the EnergyScope model, except that we allow them to have a flexible operation.

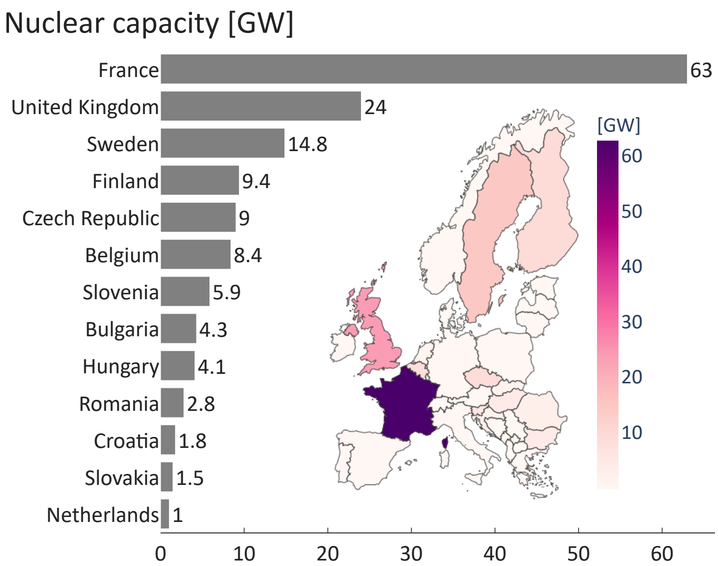

Figure 4.7: Distribution of the 150 GW of nuclear capacity among countries of the Nuclear Alliance.

4.3 Description of exploration directions

Each exploration direction is motivated by three different taxonomic levels. First, it plays an important role in the Reference scenario analyzed in the previous chapter. Second, it has other environmental impacts linked with planetary boundaries. Third, it has socio-political consequences.

The next sections present the motivations for each direction and formulate the objective function related to it. The directions are presented in the following order: (i) the direction minimizing the onshore renewables; (ii) the direction minimizing the use of biomass is described; (iii) the direction minimizing the cross-border electricity network.

4.3.1 Minimizing onshore renewables

The onshore renewables regroup essential technologies in our results: utility PV, CSP (parabolic trough (PT) and solar tower (ST)) and onshore wind. These technologies supply 69% of the gross available energy in our results. They represent the primary source of energy and supply both end-use demands through direct electrification and through the production of e-fuels.

However, these utility-scale onshore renewables have other socio-politico-environmental impacts. Regarding environmental impacts, onshore wind turbines can have a negative effect on biodiversity. For instance, studies underline impacts on bats and migratory birds [313–315]. Utility-scale solar energy, both PV and CSP have an impact on land use [316]. On the socio-political level, despite high acceptance of the energy transition at the overall level, local opposition has hindered renewable electricity projects [278, 280, 317]. This opposition is related, for instance, to loss in property values, negative impact on the landscape or sound annoyance [279]. In addition to this low social acceptance, solar technologies suffer from competing uses for land with agriculture, for instance. Furthermore, from our previous results, to reach a fossil-free energy system, Europe must deploy vast capacities of onshore wind and utility PV. This deployment is above the statistical projections [318] and it is not sure whether we can reach this objective. For all these reasons, the socio-technical potential of onshore renewable might be overestimated. This raises the question of whether it is possible to design a European fossil-free energy system with a smaller contribution from these onshore renewables.

Several of the motivations are related to the fact that onshore renewables have an impact on their surrounding area. Thus, we choose to minimize the land use instead of the installed capacity. The new land area allocated to onshore renewables ($\mathbf{New\_area_{onshore,re}}$) is computed based on the new capacity installed for each onshore renewable technology in each region, see Eq.(4.2). The new capacity is the difference between the installed capacity ($\mathbf{F}$) and the capacity in 2021 (or lower bound, f_{min}). The new capacity is then converted into land area thanks to the power density of each technology ($power\_density_i$). These power densities are already defined for all solar technologies in the description of the European model, see Table 1.13. The power density of onshore wind is added for this direction with a value of 8.8 W/m^2 [319]. This power density is low due to the spacing between turbines. Hence, there is a lot of available space between the turbines for other uses. However, the main negative impacts of wind turbines are linked with their influence over a larger area (noise, view, biodiversity and habitat). Thus, we choose to keep this low power density to represent its "area of influence".

$$\begin{aligned}\mathbf{New\_area_{onshore,re}} = \sum_{r \in REG} \Bigg(& \frac{(\mathbf{F}(r, PV_{utility}) - f_{min}(r, PV_{utility}))}{power\_density_{pv}} \\ & + \frac{(\mathbf{F}(r, WIND_{onshore}) - f_{min}(r, WIND_{onshore}))}{power\_density_{won}} \\ & + \frac{(\mathbf{F}(r, PT_{collector}) - f_{min}(r, PT_{collector}))}{power\_density_{pt}} + \frac{(\mathbf{F}(r, ST_{collector}) - f_{min}(r, PT_{collector}))}{power\_density_{st}} \Bigg).\end{aligned} \tag{4.2}$$

The new objective function is to minimise this new area allocated to onshore renewables:

$$\min \ \mathbf{New\_area_{onshore,re}}. \tag{4.3}$$

4.3.2 Minimizing biomass use

Biomass is a key energy resource in our fossil-free energy system. It is the second source of gross available energy with 22%. It is essential for flexibility and to supply several hard-to-abate sectors both through direct use of biomass (e.g. industrial boiler, non-energy demand) and through upgrading into advanced biofuels (e.g. methanol, methane, FT fuels).

However, biomass has either socio-politico-environmental impacts. On the environmental aspects, the use of biomass for energy can have several impacts on other planetary boundaries such as biosphere integrity, land system change, fresh water and biogeochemical nitrogen flows [320, 321]. These impacts depend on the type of bioenergy and how it is produced. They are not modelled in our work. However, we explore the possibility of decreasing all types of biomass for energy use. The use of biomass has other socio-political implications. For instance, competing use between energy valorisation and repurposing, recycling or composting. For some types of biomass, such as second-generation energy crops, there is even a competing use for land. The biomass potentials from ENSPRESO rely on current intensive agricultural policies, which have notable biodiversity and health impacts, likely necessitating future adjustments and potentially altering biomass potentials for energy use [74]. Therefore, we choose to explore the lowest use of biomass to reach a fossil-free European energy system with a cost increase of 5% compared to the optimum.

To implement that in the model, the new objective function is to minimize the use of local biomass, see Eq.(4.4). The use of biomass is computed as the sum over each region ($r \in REG$) and each hour of the year ($t(h, td) \in T$) of the local use ($\mathbf{R_{t,local}}$)) of each biomass resources ($i \in BIOM$):

$$\min \sum_{n \in REG, i \in BIOM, t(h,td) \in T} \left(\mathbf{R_{t,local}}\ (\mathbf{r, i, h, td})\right). \tag{4.4}$$

4.3.3 Minimizing electricity transmission grid

The electricity grid transports 26% of the energy exchanges in our fossil-free Europe. As in other studies, these exchanges are essential to integrate high shares of renewable energy sources [51, 52, 67, 260]. Furthermore, for some countries, such as Belgium, these electricity imports represent more than 37% of the electricity consumption in the country and become critical for the energy supply.

However, electricity transmission grids are large infrastructures implying high costs, material use [322] and local impacts, for instance, on the landscape. They suffer from a low social acceptance which causes delays in power grid extension projects [278, 280, 323]. Therefore, we choose to explore the lowest expansion of the cross-border electricity transmission grid with a cost increase of 5% compared to the optimum.

The negative impacts of electricity transmission grid expansion mainly occur at the local level (e.g. social acceptance and landscape degradation). Therefore, we choose to minimize the largest new cross-border transfer capacity, Eq.(4.6). Compared to minimizing the total expansion of the cross-border electricity grid, this objective function avoids reducing the expansion in some countries to keep high expansion in other countries. It allows to have a more equal repartition of the burden and to reduce the local impact of the transmission grid expansion in all countries.

A new equation computes the largest new transfer capacity, Eq. (4.5). For each pair of regions (r_1, r_2), the new transfer capacity is the difference between the optimized transfer capacity (**Tc**) and the current transfer capacity (tc_{min}). This is then summed over each electrical network type (i.e. inland overhead lines and sub-sea cables) to get the total transfer capacity across each border. The largest new transfer capacity is greater or equal to any new transfer capacity between two countries:

$$\mathbf{New\_tc_{elec,max}} \geq \sum_{n \in NT(Elec)} \big(\mathbf{Tc}(r_1, r_2, Elec, n) - tc_{min}(r_1, r_2, Elec, n)\big) \qquad \forall r_1, r_2 \in REG. \quad (4.5)$$

The new objective function is to minimize the biggest expansion of transfer capacity:

$$\min \ \mathbf{New\_tc_{elec,max}}. \qquad (4.6)$$

4.4 Summary of the hybrid method

This chapter describes a hybrid method for exploring a diversity of options for a fossil-free European energy system. This hybrid method combines scenario analysis and near-optimal exploration fields.

In addition to the Reference scenario, this chapter presents two alternative scenarios: (i) the Sufficiency scenario builds on the bottom-up CLEVER scenario to propose a low demand for Europe in 2050 induced by sufficiency measures; (ii) the Nuclear scenario installs nuclear power plants in the 14 European countries of the Nuclear Alliance to reach a total capacity of 150 GW in 2050.

For each scenario, four system designs are explored: the cost-optimal system and three near-optimal systems. The near-optimal designs are obtained by allowing a cost increase of 5% compared to the optimal case and minimizing a direction of interest. We choose the three exploration directions because of their importance in the results of the previous chapter and their socio-politico-environmental impacts that are not quantified in this work. The three directions are: (i) minimizing the area allocated to onshore renewable technologies (i.e. utility PV, onshore wind, and CSP); (ii) minimizing the use of biomass;

(iii) minimizing the expansion of the cross-border electricity transmission network.

Many other studies exploring near-optimal solutions for energy system designs pursue the objective of exploring the entire near-optimal space. On the contrary, our approach aims at reaching the boundary of this near-optimal space in specific directions. For each direction, as we minimize it, the obtained design is the intersection between this direction and the near-optimal space boundary. In this way, we surround the near-optimal space.

5 Diversity of options for a fossil-free European energy system

Caminante, no hay camino, se hace camino al andar.
Antonio Machado

Chapter overview

- What is the impact of Sufficiency or Nuclear at the European scale?
- Can a fossil-free European energy system reduce its dependence on onshore renewables, biomass and electricity cross-border grid?
- What are the trade-offs in the system design?
- What are the must-haves in a fossil-free European energy system?

Chapter 3 presented a cost-optimal design for a fossil-free and nuclear-free European whole-energy system in 2050. However, as there are many uncertainties in the context in which such a system unfolds, and the cost is not the sole indicator, we proposed in Chapter 4 a hybrid method to explore diverse designs for a fossil-free energy system. This method combines two fields that provide alternative solutions: scenario analysis and near-optimal space exploration. Together, we explore 12 different designs, Table 5.1: three scenarios (columns) with for each one an optimal design and three near-optimal directions explored (rows).

The scenario analysis approach is based on storylines and applies changes in the assumptions and environment in which the design is optimised. The scenario analyzed in Chapter 3 is called the Reference scenario. The two alternative scenarios differ from the Reference scenario by one key storyline: (i) the Sufficiency scenario includes a low energy demand due to sufficiency measures at the European scale; (ii) the Nuclear scenario installs 150 GW of new nuclear power plants distributed among several European countries. The entire details of the scenario definition can be found in Section 4.2.

The near-optimal space approach relies on two characteristics of energy system optimization models: they have high uncertainties on cost, and they have a flat optimum. Therefore, many solutions cost-efficient solutions exist. Alternative designs can be found by optimizing another set of variables while constraining the cost increase compared to the optimal case. In our approach, the cost increase is constrained to 5% and the set of variables is chosen in a specific direction according to socio-politico-environment concerns. The three directions explored are: (i) Min(Onshore renewables): minimizing the land area allocated to onshore renewable technologies, that is, utility PV, wind onshore and CSP; (ii) Min(Biomass use): minimizing the use of all types of biomass; (iii) Min(Electricity grid): minimizing the expansion of the cross-border electricity transmission network. This near-optimal exploration method ensures to reach non-implied necessary conditions [85]. The obtained design is at the intersection of the exploration direction with the near-optimal space boundary. This means that the quantity obtained in the explored direction is necessary to reach a fossil-free energy system with a cost lower or equal to 105% the optimal cost. The detailed motivation and implementation of those exploration directions are described in Section 4.3.

Table 5.1: The hybrid exploration method provides 12 different designs: three scenarios with each an optimal design and three near-optimal designs.

	Reference	**Sufficiency**	**Nuclear**
Optimal	(Ref., Opt.)	(Suff., Opt.)	(Nuc., Opt.)
Min(Onshore renewables)	(Ref., Onsh.)	(Suff., Onsh.)	(Nuc., Onsh.)
Min(Biomass use)	(Ref., Biom.)	(Suff., Biom.)	(Nuc., Biom.)
Min(Elecricity grid)	(Ref., Elec.)	(Suff., Elec.)	(Nuc., Elec.)

> This chapter presents the results of the hybrid exploration method. It provides insights into the diversity of options to reach a fossil-free European energy system. First, Section 5.1 compares the optimal results of the two alternative scenarios (Sufficiency and Nuclear) with the Reference scenario's results. Then, Section 5.2 presents, for each of the three scenarios, how the near-optimal design affects the decision variables compared to the optimal design. This Section underlines the main trade-offs observed and the impact of the different scenarios. Section 5.3 introduces eight key design

aspects that are present, whatever the scenario and exploration direction –the must-haves. Finally, Section 5.4 summarizes the key trade-offs in the system design.

5.1 Scenario analysis

This Section describes the differences between each alternative scenario and the Reference scenario analyzed in Chapter 3. It underlines the gains and losses to go towards sufficiency or to invest in nuclear. First, Subsection 5.1.1 presents the Sufficiency scenario. Then, Subsection 5.1.2 presents the Nuclear scenario.

5.1.1 Impact of sufficiency

The Sufficiency scenario costs 29% less than the Reference one, see Figure 5.1(A).

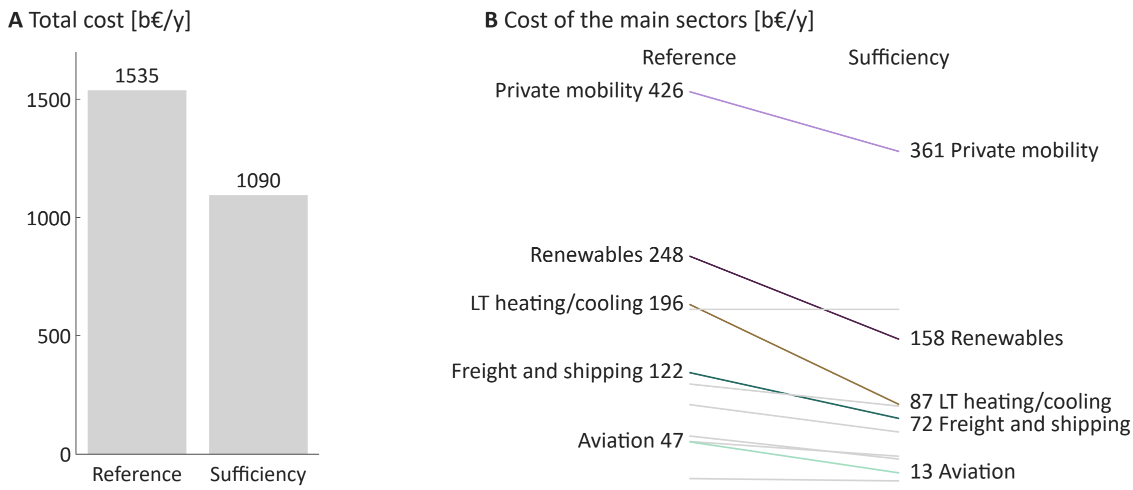

Figure 5.1: **(A)** The total annualized cost of the system decreases by 29% with sufficiency. **(B)** A general decrease in the cost occurs in all sectors, with five sectors especially impacted: private mobility, renewables, low-temperature (LT) heating/cooling, freight and shipping, and aviation.

The sufficiency measures implemented across all sectors generate a general cost decrease. However, certain sectors are especially impacted, see Figure 5.1(B): mobility in diverse forms, renewable energy infrastructure and low-temperature heating and cooling. In both scenarios, private mobility emerges as the primary cost of the transition (>28 %). However, thanks to lower passenger mobility in the Sufficiency scenario, private mobility is 65 b€/y cheaper. Subsequently, the cost related to renewable energies, such as PV and wind turbines, decreases by 90 b€/y. Notably, the supply of low-temperature (LT) heat and cooling for space heating, hot water and space cooling experiences the most substantial relative decrease (44%), resulting in a savings of 109 b€/y. Finally, freight, shipping, and aviation sectors cost together 84 b€/y less.

This strong decrease in cost is due to significant changes in the energy system. The gross available energy decreases by 36% (-4446 TWh/y), and the final energy consumed by 34% (-3770 TWh/y). Going for sufficiency allows phasing out fossil fuels with much lower installation of PV and wind turbines, see Figure 5.2(A). The total energy provided by those two energy sources decreases from 8544 TWh/y to 4426 TWh/y. However, the curtailment of these variable energy sources (4.7%) remains similar to the one of the Reference scenario (4.3%). In the Sufficiency scenario, the woody biomass use decreases from 1898 TWh/y to 1637 TWh/y. The other energy sources remain constant: (i) wet biomass, biowaste and waste because they are cost-competitive resources and have already reached their upper bound; (ii) hydro and geothermal because they are more costly than other energy sources.

Regarding the final energy carriers, electricity remains the main carrier (51%), see Figure 5.2(B). With or without sufficiency, electrification is an efficient way to supply end-uses like private mobility and low-temperature heat. However, with much lower demands, the final electricity consumption decreases from 5682 to 3661 TWh/y. The final use of woody biomass decreases by 345 TWh/y. This is 83 TWh/y more than the decrease in gross available energy from woody biomass. This portion of the woody biomass is redirected to produce more advanced renewable fuels.

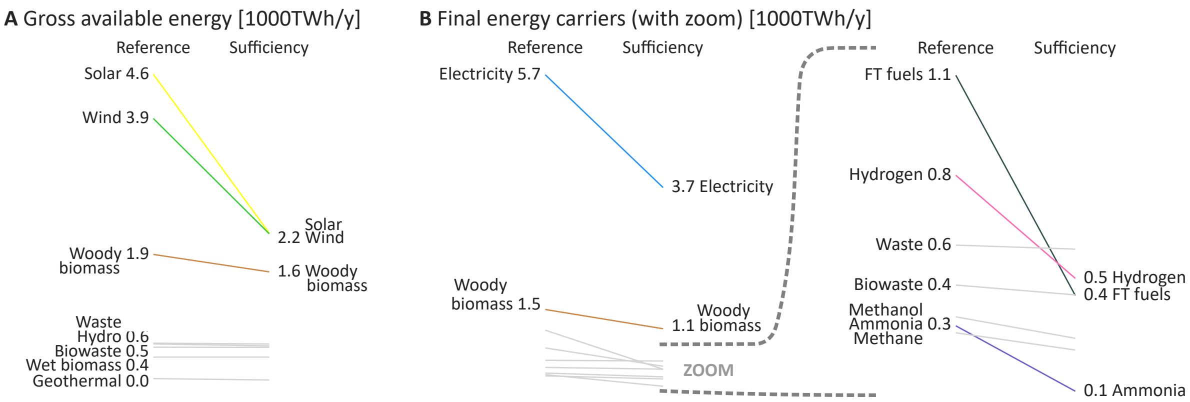

Figure 5.2: **(A)** The energy supply from solar and wind decreases drastically with sufficiency. **(B)** This decrease is the consequence of much lower final consumption of electricity and e-fuels such as Fischer Tropsch (FT) fuels, hydrogen and ammonia.

Looking at the zoom on other final energy carriers, ammonia, FT fuels, and hydrogen are the most impacted, with a decrease of 67, 63, and 42%, respectively. Ammonia becomes the smallest final energy carrier with only 100 TWh/y. FT fuels and hydrogen switch places with one another and become less important than waste incinerated in the industry. In the Reference scenario, those three energy carriers are produced as e-fuels. This lower e-fuels production reinforces the decreasing need for renewable energy and implies a much lower quantity of electrolysers to be installed: from 407 to 149 GW.

Compared to the Reference scenario, the Sufficiency scenario uses 34% less renewable fuels. This lower use comes from a decrease in e-fuel production (63%) rather than in biofuel production (10%), see Figure 5.3(A).

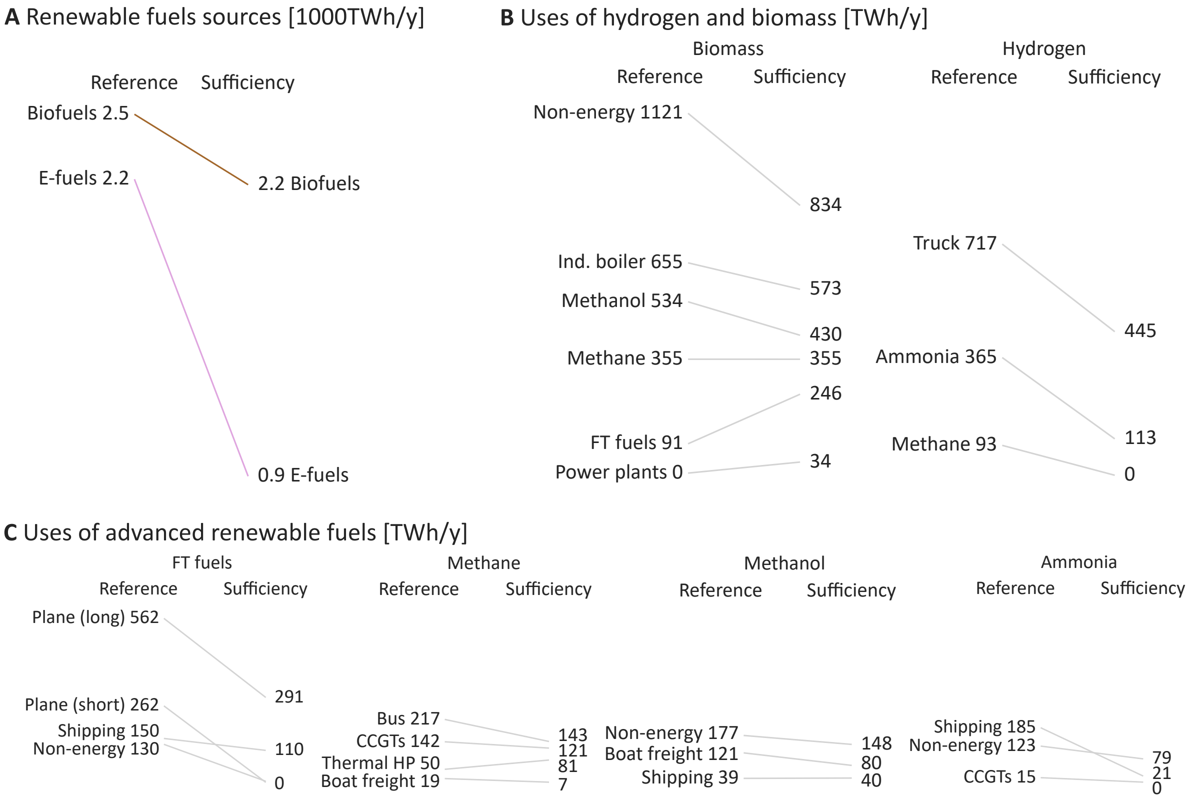

Figure 5.3: **(A)** With sufficiency measures, the e-fuel production decreases by 1371 TWh/y whereas biofuel production decreases by 325 TWh/y. **(B-C)** This decrease is led by a strong reduction in sectors such as non-energy, freight, aviation and shipping. Abbreviations: combined cycle gas turbine (CCGT), Fischer-Tropsch (FT), heat pumps (HP), industrial (ind.), long-haul aviation (Plane (long)), short-haul aviation (Plane (short)).

The lower consumption and production of e-fuels has several impacts. It reduces the installation of electrolyzers and the consumption of electricity for e-fuel production. This lower electricity production decreases the installed capacity of PV and wind turbines. Combined with the reduced electrification of end-uses, it leads to a total electricity production of 5086 TWh/y. This is 1.81 times lower than in the Reference scenario and only 1.45 times the current electricity production.

As seen before, the most impacted fuels are FT fuels, hydrogen and ammonia. Figure 5.3(B) illustrates which uses of these fuels and the other renewable fuels change the most. The consumption of FT fuels for aviation and non-energy is drastically reduced. The consumption of synthetic kerosene in long-haul planes decreases by 48%, whereas the consumption of synthetic kerosene in short-haul aviation and synthetic oil in non-energy falls to zero. Indeed, the Sufficiency scenario assumes that all short-haul aviation is replaced with other means of mobility such as trains, cars and busses. On the contrary, the non-energy demand is not reduced to zero but is now supplied only by biomass, methanol and ammonia. The hydrogen consumption decreases both in trucks and to produce of e-ammonia and e-methane. The e-methane production falls to zero whereas the e-ammonia production decreases by 69%. The largest change in ammonia consumption lies in the use for shipping, with a reduction of 89%. Furthermore, no more ammonia CCGTs are installed and the use of ammonia for fertilizers decreases.

In addition to these consequent changes in consumption of FT fuels, hydrogen and ammonia, the uses of biomass change, see Figure 5.3(B). The consumption decreases for non-energy (-293 TWh/y), in industrial boilers (-82 TWh/y) and for the production of methanol (-104 TWh). It permits to use less biomass in total and to diversify the use of the remaining biomass feedstock: (i) more biomass is used to produce FT fuels (+154 TWh/y) reducing the need for e-FT fuels; (ii) some biomass power plants (+34 TWh/y) are installed for power flexibility and replace a part of the methane-fueled CCGTs (-21 TWh/y) and all ammonia-fueled CCGTs. Finally, methane and methanol use decreases with sufficiency, but the final uses remain the same as in the Reference scenario.

In the Sufficiency scenario, the storage capacity decreases by 41%. Figure 5.4(A) presents the three seasonal storage technologies that decrease the most: DHN thermal storage; FT fuels storage; and ammonia storage. DHN thermal storage remains the largest storage capacity but decreases by 48%. FT fuels storage is the second largest storage in the Reference scenario with 20% but only represents 13% in the Sufficiency scenario. Ammonia storage decreases by 48% and becomes as small as hydro dam storage. For both FT fuels and ammonia storage, the main cause for smaller storage size is the smaller amount produced and the smaller final use for those fuels.

The energy stored throughout the year decreases even further than the storage capacity installed, 51% against 41%. The five main providers of energy storage in the reference scenario experience a strong decrease: (i) PHS; (ii) EVs batteries,; (iii) DHN thermal storage;

(iv) FT fuels storage; (v) Decentralised thermal storage. The PHS decreases the most (-60%). However, it remains the first provider of energy storage with 444 TWh/y. Electric vehicle batteries experience a smaller decrease (-28%) and end up with a quantity of energy stored nearly as large as the one of PHS. The DHN thermal storage decreases even more its stored energy (-56%) than its storage capacity (-48%). FT fuels storage decreases by 62% and stores as few as 126 TWh/y. Decentralised thermal stores only 68 TWh/y and stores less energy than hydro dam and methane storage.

In addition to this smaller need for energy storage, the Sufficiency scenario displays much smaller installed capacities of thermal power plants, 50 GW against 115 GW in the Reference scenario. However, these power plants have an average capacity factor of 20% which is higher than the 9.9% of the Reference scenario. In the end, they reach similar production. This makes the business case for those power plants much more favourable.

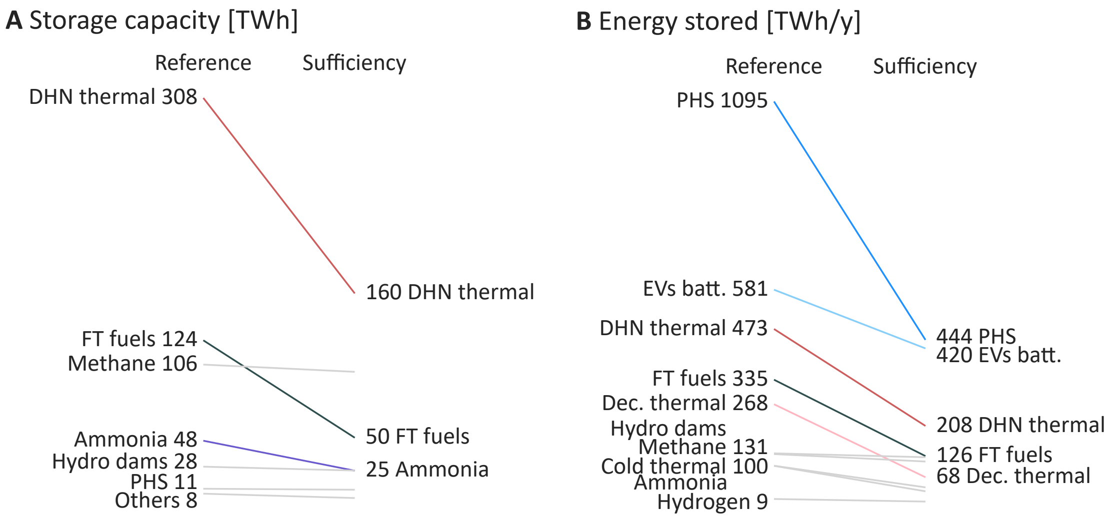

Figure 5.4: **(A)** Three large seasonal storage technologies decrease the most in the Sufficiency scenario: DHN thermal, FT fuels and ammonia storage. **B** The energy stored by the five main storage types in the Reference scenario decreases significantly in the Sufficiency scenario.

Going toward sufficiency measures reduces the energy exchanges by 40%. Three resources are most impacted, see Figure 5.5(A): hydrogen, electricity and FT fuels. Hydrogen exchanges decrease by 48% and become smaller than electricity exchanges. At the same time, electricity exchanges are reduced by 28%. FT fuels exchanges decrease by 55% but remain the third means of exchanges. Other energy carriers such as methane, methanol, ammonia and woody biomass have much smaller decreases (<50 TWh/y).

The decrease in energy exchanged is reflected in a decrease in transmission networks,

Figure 5.5(B). In particular, 96 GW less retrofitted hydrogen pipelines are built, and a larger methane network is kept and used to exchange 159 TWh/y. The expansion of the electricity network only reaches 15.7 GW in the Sufficiency scenario, whereas it is 56.4 GW in the Reference scenario.

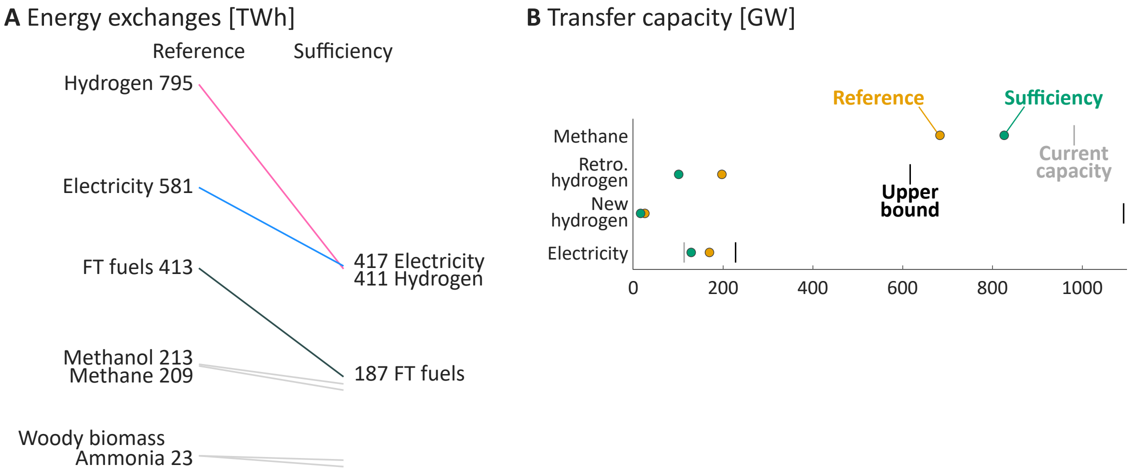

Figure 5.5: **(A)** In the Sufficiency scenario, the three largest exchanges decrease consequently: hydrogen, electricity and Fischer-Tropsch (FT) fuels. **(B)** This decrease in energy exchanges implies much lower new transmission infrastructures: (i) less retrofitted (retro.) hydrogen pipelines and thus more remaining methane pipelines; (ii) lower expansion of the electricity grid.

To conclude, the Sufficiency scenario facilitates the energy transition. Indeed, it requires much less energy to be produced. This induces lower installed capacities of PV and wind turbines, reducing the investment in these technologies.

Furthermore, our Sufficiency scenario does not impact all sectors in the same way. Particularly, the hard-to-abate sectors such as aviation, shipping, inland freight, and non-energy reduce drastically, leading to an important decrease in e-fuels production (-63%). This strong reduction in demand for e-fuels induces a cascading positive impact. It lowers the need for installing a high quantity of electrolyzers, it reduces the quantity of electricity produced, and it reduces the installation of PV and wind turbines. All those elements are consequent scaling-up challenges to reach a fossil-free energy system and are reduced and thus facilitated by sufficiency measures.

Sufficiency also impacts energy exchanges, leading to lower expansion of the electricity transmission grid and less retrofitting of the methane grid to a hydrogen grid. This reduction in new infrastructure facilitates the energy transition. Similarly, the investment in flexibility means, both storage capacity (-41%) and back-up power plants, (-57%) are reduced. Furthermore, this smaller capacity of power plants has a higher capacity factor, up to 20%, making a better business case than in the Reference scenario.

In general, the assets that are the most reduced due to sufficiency are the ones that require large investments. Furthermore, most suffer low social acceptance, such as onshore wind turbines, electricity, and hydrogen transmission networks.

5.1.2 Impact of nuclear

The Nuclear scenario has the same cost as the Reference scenario (<0.03% difference), see Figure 5.6(A). Investing in nuclear energy costs 45 billion euros annually, Figure 5.6(B). This new cost is compensated by a decreased investment in renewable energy sources (-31 b€/y) and in transmission networks (- 7b€/y).

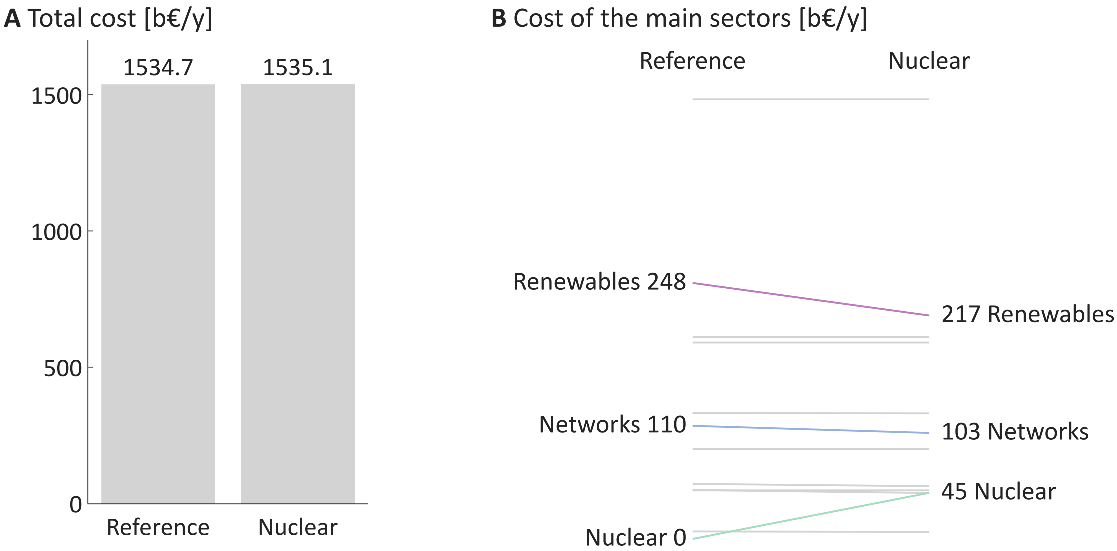

Figure 5.6: **(A)** The Nuclear scenario has no impact on the total annualized cost of the system. **(B)** The increase in cost due to nuclear energy is compensated by a decrease in renewables and transmission networks.

As the Nuclear scenario invests less into solar and wind, their energy supply decreases to 7376 TWh/y and is replaced by nuclear energy, which provides 2789 TWh/y, see Figure 5.7(A). Installing nuclear power also reduces the curtailment of renewables from 4.3% in the Reference scenario to 3.6% in the Nuclear scenario. In total, the gross available energy in Europe increases by 1597 TWh/y as the nuclear heat still needs to be converted into electricity leading to higher losses in the energy system.

Although the energy sources change, the inner structure of the energy system is not much impacted, and the final energy carriers used to supply the end-use demands stay constant, Figure 5.7(B). Both renewable and nuclear energy provide electricity. This electricity is either used for final electricity consumption or upgraded into e-fuels.

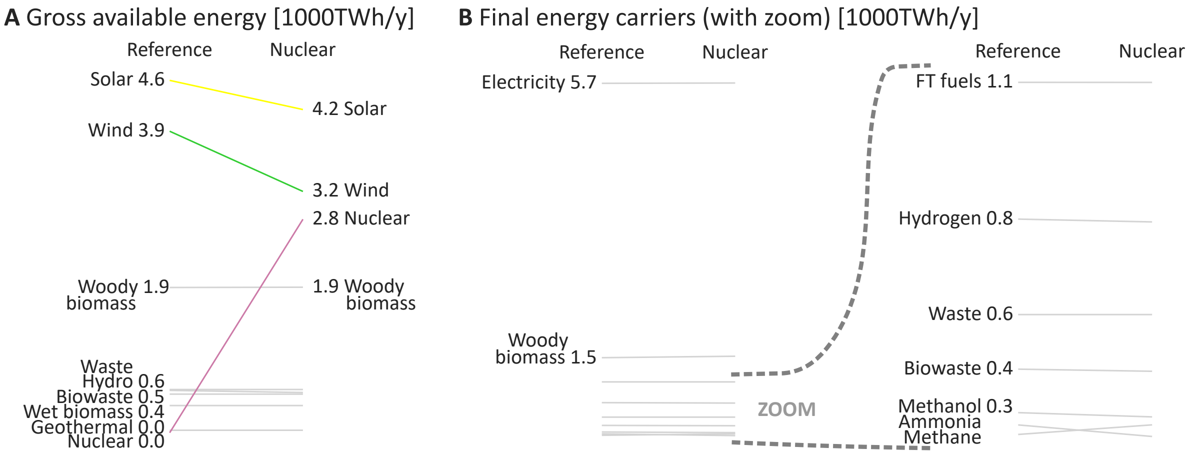

Figure 5.7: **(A)** Nuclear energy replaces solar and wind energy. However, wind and solar remain the primary energy sources. **(B)** Installing nuclear power does not impact the final energy carriers consumed.

Installing nuclear energy induces lower electricity exchanges (-66 TWh/y), see Figure 5.8. At the European scale, this only represents a decrease of 6% of electricity exchanges and electricity network expansion of only 41.3 GW instead of 56.4 GW in the Reference scenario. The other energy exchanges have even lower changes (< 12TWh/y). Although the changes at the European scale are low, installing nuclear power induces some local changes. Some countries that install nuclear power plants, such as France, reduce the amount of local renewable production (-36%) and increase their electricity exports. In the Nuclear scenario, France has net electricity exports of 79 TWh/y, compared to 38 TWh/y in the Reference scenario. It has become the biggest exporter of electricity in Europe. However, as a counterpart, France increases its net import of renewable fuels by 32 TWh/y. Other countries, such as Belgium, also install nuclear but keep their local renewable energy production nearly as high as in the Reference scenario (-9%). This allows Belgium to decrease its reliance on electricity imports from 66 TWh/y to 34 TWh/y. Furthermore, in the case of Belgium, installing nuclear energy decreases by 6.5% the net imports of renewable fuels. Another example is Germany, which does not install nuclear power plants and relies heavily on electricity imports in the Reference scenario. Its net electricity imports increase from 115 in the Reference scenario to 151 TWh/y in the Nuclear scenario.

Additionally, installing nuclear power plants reduces the storage capacity needed in Europe by 92 TWh and the energy stored by 300 TWh/y. In particular, the capacity of methane storage, DHN thermal storage, and FT fuels storage decreases by 30%, 16% and 8%, respectively. The energy stored by decentralised thermal storage and PHS decreases by 29% and 9%.

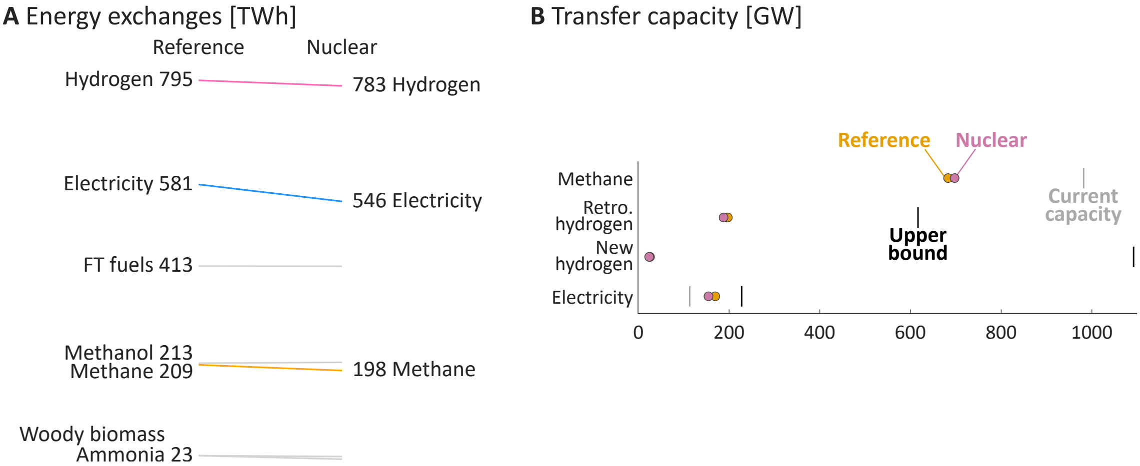

Figure 5.8: **(A)** Electricity exchanges decrease by 66 TWh/y in the Nuclear scenario. The exchanges of the other energy carriers are less impacted (< 12 TWh/y) **(B)** These small changes in energy exchanges induce only marginal changes in transmission networks capacity.

To conclude, the Nuclear scenario mainly replaces 1168 TWh/y of renewable energy supply with 2789 TWh/y of nuclear energy. However, solar and wind remain the primary energy sources with 7376 TWh/y produced. At the European scale, this change in supply does not imply significant changes in the energy system structure and final energy carriers consumed. The only impacts are on energy storage and electricity exchanges, as nuclear power plants provide flexibility in the countries where they are installed. Furthermore, locally, in the countries where nuclear energy is installed, it can lower the dependence on electricity imports at the cost of dependence on uranium imports from the rest of the world. However, electricity is not the main means of exchange in any scenario and for some countries installing more nuclear means importing more renewable fuels.

5.2 Near-optimal cases analysis

This section presents the changes in the fossil-free energy system when exploring the near-optimal space in three directions: (i) minimizing the land area allocated for onshore renewables, that is, utility PV, onshore wind and CSP; (ii) minimizing the use of all types of biomass; (iii) minimizing the largest extension of cross-border electricity transmission network. These three directions are explored for three different scenarios: (i) the Reference scenario, which is fossil-free and nuclear-free and supplies a high energy demand derived from current trends; (ii) the Sufficiency scenario, which is fossil-free and nuclear-free and supplies a low energy demand; (iii) the Nuclear scenario which is fossil-free but installs nuclear power plants and supplies a high energy demand. In total, 12 system configurations are analyzed. This analysis underlines the diverse options to reach a fossil-free energy system in Europe.

5.2.1 Minimizing onshore renewable technologies

In the near-optimal direction that minimizes the installation of onshore renewable energy technologies, in all scenarios, onshore wind decreases down to the current installed capacity, Figure 5.9. However, the Reference and the Nuclear scenario both keep consequent installed capacities of utility-scale PV: in the Reference scenario, 1908 GW produce 2681 TWh/y, and in the Nuclear scenario, 925 GW produce 1352 TWh/y. As seen in the analysis of the optimal results, installing nuclear reduces the use of local renewables. The Sufficiency scenario goes further and does not install any utility-scale PV. This means that under certain conditions, Europe can become fossil-free without installing any new utility-scale PV or onshore wind turbines. The CSP capacity is not presented as it is already installed to its current capacity (i.e. its lower bound) in the optimal design of all scenarios.

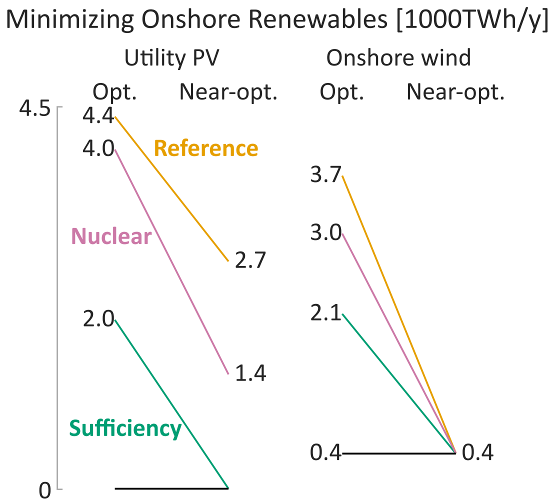

Figure 5.9: A fossil-free Europe with a low new installation of utility PV and no installation of new onshore wind turbine is feasible in all three scenarios.

The drastic reduction of energy produced with utility PV and onshore wind in this exploration direction is compensated by other energy sources, see Figure 5.10: (i) offshore wind and rooftop PV; (ii) renewable fuels imports; (iii) other renewable and woody biomass.

In all scenarios, offshore wind and rooftop PV are installed to their upper bound. When their less expensive counterparts (onshore wind and utility PV) can not be installed, these renewable energy sources become major energy suppliers: offshore wind supplies 11.5 to 18.2% of the gross available energy and rooftop PV supplies 11% to 16.6%. A similar trend is observed nowadays in several European countries: the low social acceptance for onshore wind turbines has drawn the wind industry to focus on offshore wind turbine installation[171].

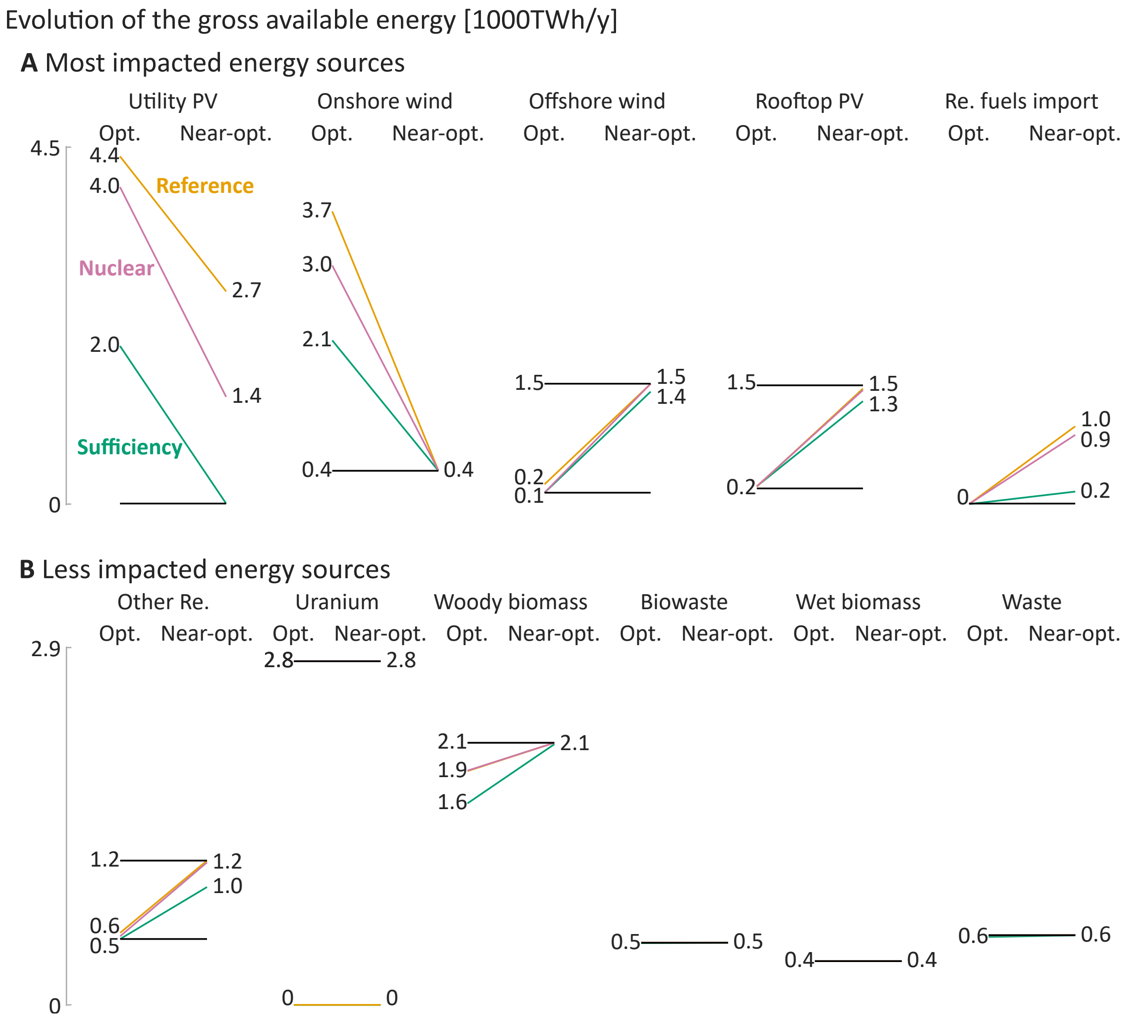

Figure 5.10: For all scenarios, the energy produced by utility PV and onshore wind decreases drastically from their value at the optimum to their near-optimal value. This decrease is compensated by increased production by offshore wind, rooftop PV and other renewable sources as well as imports of renewable ammonia and jet fuel. Abbreviations: optimal (opt.), photovoltaic panel (PV), renewable (re.).

Additionally, in the Reference and the Nuclear scenario, Europe imports consequent quantities of renewable fuels, 981 and 872 TWh/y, respectively. These imports occur in the form of liquid fuels: ammonia and FT fuels. These imports are less than 8.7 times smaller than the current imports of fossil fuels. Although these quantities are smaller than the increase in offshore wind and rooftop PV, they should not be underestimated. This energy is in the form of fuels and thus much more versatile. Furthermore, these fuels have been produced from renewable electricity somewhere else in the world, meaning that they require much larger amounts of renewable electricity. Without counting the energy necessary to transport them, the production of these fuels consumed 1706 TWh (Reference) and 1527 TWh (Nuclear) of renewable electricity somewhere else in the world.

In opposition to the Reference and Nuclear scenarios, the Sufficiency scenario can choose not to install any new utility PV and onshore wind while keeping low imports of renewable fuels (157 TWh).

In all scenarios, the other renewable energy sources, that is, hydro and geothermal, as well as woody biomass, reach their upper bound to compensate for the lower installation of PV and wind.

Though some other sources of renewable electricity are installed to compensate for the decrease of onshore renewables, the total electricity production decreases for all scenarios (-1655 TWh for Reference, -1902 TWh for Nuclear and -723 TWh for Sufficiency), see Figure 5.11. The lower electricity production induces lower e-fuels production: 1405 TWh less electricity dedicated to e-fuels production in the Reference and the Nuclear scenarios and 481 TWh in the Sufficiency one. Another impact of the lower electricity is a lower electrification of end-use sectors. In particular, low- and high-temperature heat productions are less electrified and rely more on biomass.

The lower production of e-fuels is compensated with imports of renewable fuels and larger and more diverse use of biomass. The imports of renewable ammonia and FT fuels replace e-fuels produced locally in the optimum case. More biomass is upgraded to FT fuels, and methanol and biomass final uses are more diversified. For instance, the HVC production from biomass declines in favour of heat production. The Sufficiency scenario installs 21 GW biomass power plants which produce 49 TWh/y.

In addition, renewable fuel imports from the rest of the world are essentially present in the countries that rely heavily on renewable fuel imports from other European countries in the optimal case. Therefore, they imply a reduction in energy exchanges in Europe. Furthermore, reducing local renewable energy production and increasing renewable fuel imports lead to a lower curtailment than in the optimal cases, ranging from 2.1% in the Reference scenario to 3.8% in the Sufficiency scenario.

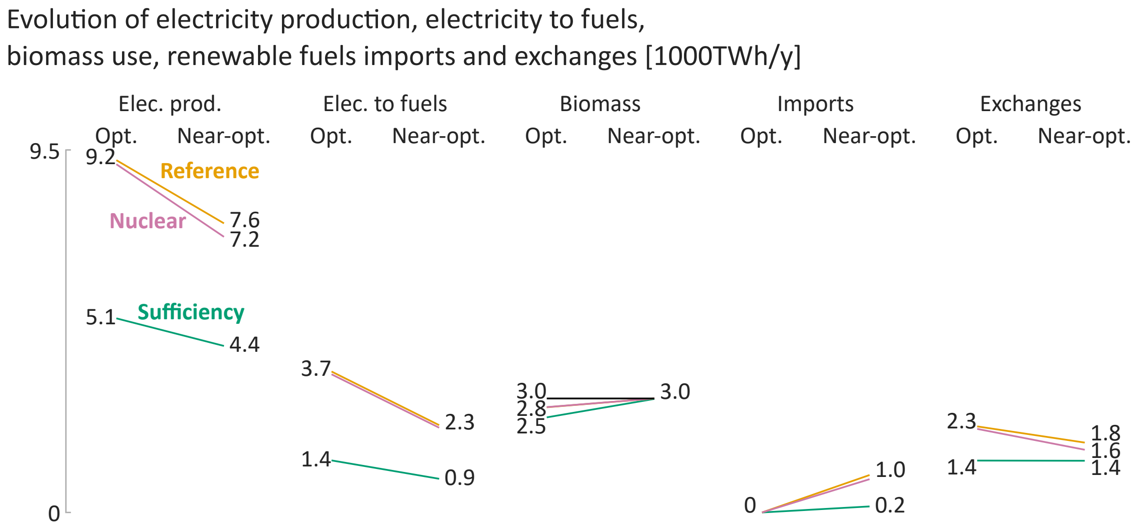

Figure 5.11: The electricity production and electricity to fuels decrease in favour of the imports of renewable fuels and biomass use. Increased imports imply lower exchanges inside Europe. Abbreviations: electricity (elec.), optimal (opt.), production (prod.).

To conclude, the expansion of onshore renewable can be reduced by 64% in the Reference scenario and to zero with sufficiency measures. To compensate for this energy source loss, Europe relies more on offshore wind, rooftop PV, imports of renewable fuels, other renewable energy sources (e.g. hydro and geothermal), and woody biomass. It also implies a lower electricity production. This lower electricity production results in lower e-fuels production (-1405 $TWh_{elec.}$ in Reference) and lower electrification (-371 $TWh_{elec.}$ in Reference) of some end-uses such as heat production.

5.2.2 Minimizing biomass use

In the near-optimal direction that minimizes the use of biomass, in all scenarios, woody biomass and biowaste use decreases to 0, see Figure 5.12. However, in all scenarios, some wet biomass is kept to produce strategic and cost-competitive biomethane, from 203 TWh in the Reference scenario to 90 TWh in the Sufficiency scenario.

To compensate for the lower energy from biomass, the system installs more utility PV and onshore wind, see Figure 5.13. The Reference scenario also produces 488 TWh of additional offshore wind. The curtailment of these energy sources remains similar to one of the optimal designs.

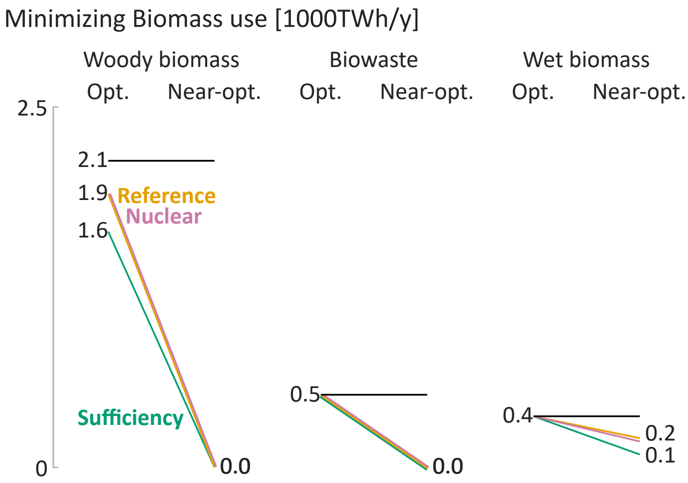

Figure 5.12: A fossil-free Europe with no use of woody biomass and biowaste and low use of wet biomass is feasible in all three scenarios.

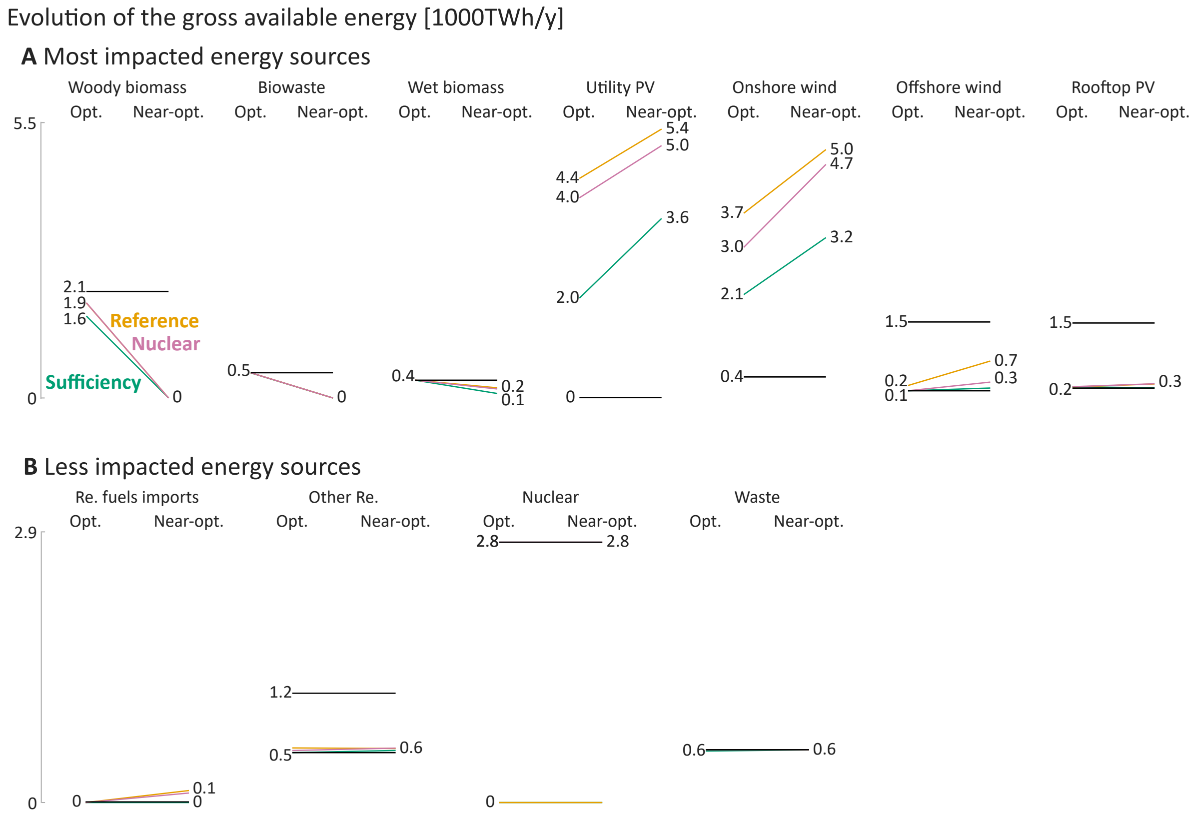

Figure 5.13: In the near-optimal cases minimizing the use of biomass, the woody biomass and biowaste are no longer used and wet biomass decreases. Increased production of utility PV and onshore wind compensate for this decrease in biomass. Abbreviations: optimal (opt.), photovoltaic panel (PV), renewable (re.).

Furthermore, the Reference and the Nuclear scenarios import 128 and 102 TWh of renewable ammonia, Figure 5.13(B). This import is much smaller than in the direction of minimizing the onshore renewable. The other sources of energy, i.e. rooftop PV, other renewables, nuclear and waste, are not impacted by the reduction of biomass use. However, already in the optimal cases, Europe is not sure to be able to reach the high installed capacities of PV and wind by 2050 as they require high investments and suffer delays due to social acceptance. In this near-optimal direction, the installed capacities of PV and wind are even higher. Thus, this doubt is exacerbated. If Europe cannot reach these high installed capacities, it may need to import more renewable fuels.

The Nuclear scenario has similar trends to the Reference one, with an even higher increase in the installation of onshore wind. However, the Sufficiency scenario stands out by not relying on renewable fuel imports and reaching much lower production from utility PV (3585 TWh) and onshore wind (3202 TWh). Even though they increase, these onshore renewables productions stay lower than their production in the optimal case of the Reference scenario.

With the decrease in biomass use, the electricity production, which was already 2.62 times larger than today in the optimal case for the Reference and the Nuclear scenarios, increases even more to 3.40 times the current production, see Figure 5.14.

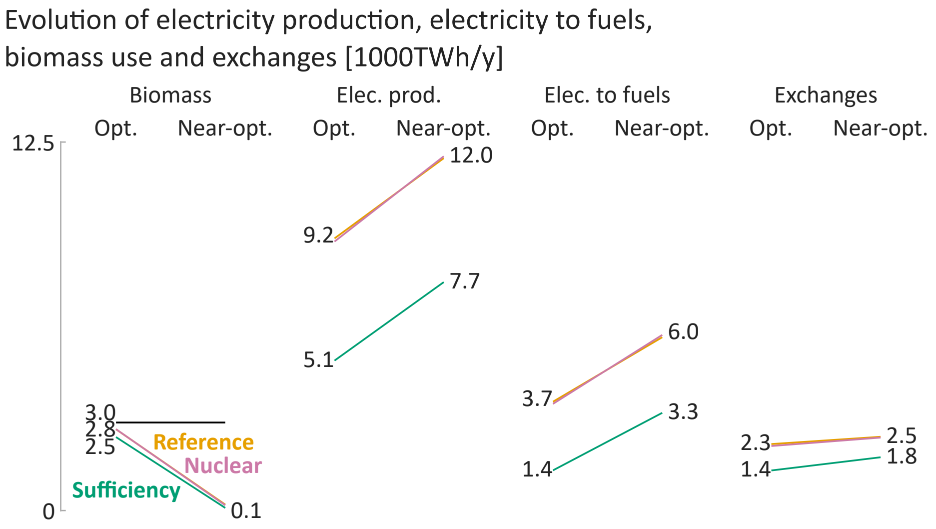

Figure 5.14: To reduce biomass use, the system increases electricity production. This increase in electricity is mainly used to produce e-fuels. Abbreviations: electricity (elec.), optimal (opt.), production (prod.).

In the Sufficiency scenario, electricity production increases to 7749 TWh but remains below the 9232 TWh of the optimal design for the Reference scenario. In all scenarios, the increase in electricity production is firstly used to produce fuels that represent up to 50%

of the electricity consumption. The e-fuel production consumes up to 5958 TWh in the Nuclear scenario and 3315 TWh in the Sufficiency scenario. Actually, in these near-optimal designs, e-fuels represent the main part of renewable fuels: 91.3% (Reference), 92.7(Nuclear) and 95.7% (Sufficiency). The remaining fuels are biomethane from wet biomass (5.3% in Reference, 4.7% in Nuclear and 4.3% in Sufficiency) and imported ammonia (3.4% in Reference and 2.6% in Nuclear).

Additionally, biomass is a versatile energy carrier. In the optimal designs, it is used in many end-use applications and brings flexibility both at the temporal scale and at the spatial scale. Reducing the biomass use implies installing more storage capacity (up to +142 TWh) and stroring energy (up to +852 TWh/y). In addition, some regions that are already dependent on energy exchanges in the optimal designs become even more dependent with the loss of local biomass feedstocks. For instance, in the optimal design for the Reference scenario, Belgium imports 153 TWh of renewable fuels whereas in the near-optimal design, it imports 195 TWh. These higher exchanges also imply building a larger hydrogen network.

In optimal cases, biomass produces advanced renewable fuels such as methane and methanol. It is also used in two hard-to-abate sectors: (i) producing HVC for the non-energy demand; (ii) producing high-temperature heat for the industry. Figure 5.15 presents how these uses of biomass are replaced.

In all the scenarios, biomass is replaced by e-methanol and e-FT fuels to produce HVC, Figure 5.15(A). In the optimal cases, woody biomass is the main feedstock for producing HVC with 834 to 1141 TWh of woody biomass. In the near-optimal cases, it falls to zero, and methanol becomes the main feedstock with 499 to 651 TWh of methanol. FT fuels are the second feedstock with 115 to 277 TWh. To allocate these FT fuels to the non-energy demand, the system increases the production of ammonia to supply international shipping demand, which no longer relies on FT fuels. The total amount of feedstock for HVC production decreases as methanol and FT fuels conversion to HVC are more efficient than from woody biomass. However, those e-fuels are produced from renewable electricity, inducing important losses and in the end, more primary energy is used for HVC production in the near-optimal cases. Additionally, methanol and FT fuels are liquid fuels. This allows countries with high HVC production, like Belgium, to import all the feedstocks for this production. Other countries, like Germany, rather import hydrogen through pipelines and produce methanol locally for their non-energy demand.

The production of high-temperature heat for the industry switches from biomass boilers to more electrical furnaces combined with methane boilers, Figure 5.15(B). In the optimal designs, combining woody biomass and biowaste, biomass supplies up to 662 TWh to produce high-temperature heat. This supply falls to zero in the near-optimal cases. To compensate for this, the Reference and the Nuclear scenarios increase the electricity consumption (+363 TWh) and install new boilers consuming 293 TWh of methane. The Sufficiency scenario uses the same techniques but with a new consumption of 384 TWh of electricity and 173 TWh of methane. In all scenarios, the waste incinerator provides a constant supply of high-temperature heat.

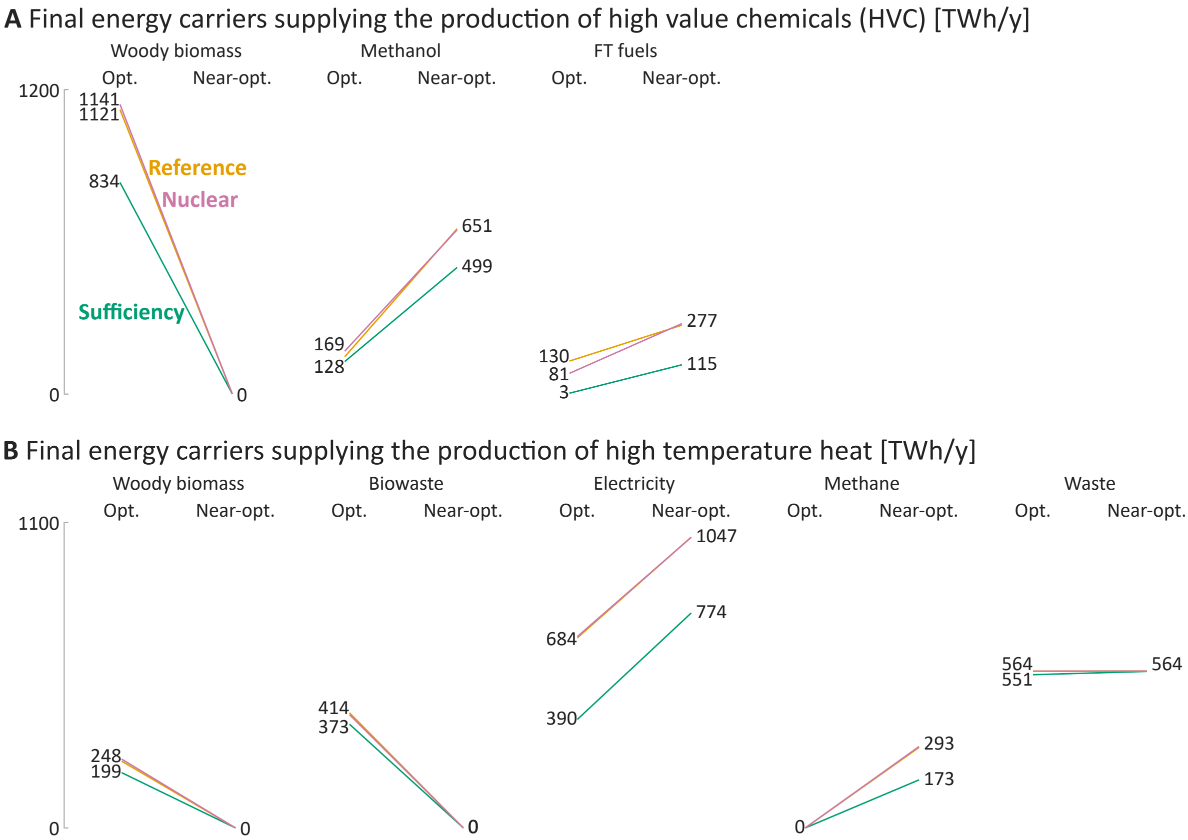

Figure 5.15: Sectors relying on biomass in the optimal case change their supply. The HVCs are produced from e-methanol and e-FT fuels instead of woody biomass. The high-temperature heat is further electrified and uses methane boilers.

In general, when decreasing the use of biomass, the Nuclear scenario follows the same trends as the Reference one and the Sufficiency scenario follows similar trends but to a lesser extent. For instance, in the near-optimal design of the Sufficiency scenario, the production of e-fuels consumes 3315 TWh/y. This consumption is still 305 TWh smaller than the optimal case of the other scenarios. Similarly, the production of e-methanol and e-FT fuels reaches 614 TWh in the Sufficiency scenarios, whereas it reaches 928 TWh in the other scenarios.

To conclude, Europe can become fossil-free while reducing its use of biomass if it installs large PV and wind facilities to produce high quantities of e-fuels. Those fuels replace biomass in two ways. Firstly, they replace biomass as final energy carrier for end-use sectors such as the non-energy demand and the high-temperature heat. Secondly, they replace biomass to produce advanced renewable fuels like methane and methanol. However, the feasibility of scaling up renewable infrastructure to these levels can be questioned. Even in optimal scenarios, the deployment of high quantities of PV, wind, and electrolysers surpasses statistical projections. Moreover, these infrastructures often encounter challenges related to low social acceptance. Therefore, there is uncertainty regarding Europe's ability to achieve the deployment levels envisioned in optimal designs and a fortiori in near-optimal designs minimizing biomass use. In this regard, the Sufficiency scenario has the advantage of always keeping the deployment of these renewable infrastructures low. However, the sufficiency measures of this scenario also face social acceptance challenges.

5.2.3 Minimizing electricity transmission grid

In the near-optimal direction minimizing the biggest expansion of cross-border electricity transmission lines, in all scenarios, the expansion is null and the size of the cross-border transmission network is the one of the actual transmission network, see Figure 5.16. As we reach the lower bound, minimizing the biggest cross-border expansion is equivalent to minimizing the expansion of the total network. Therefore, the figure presents only the total size of the transmission grid.

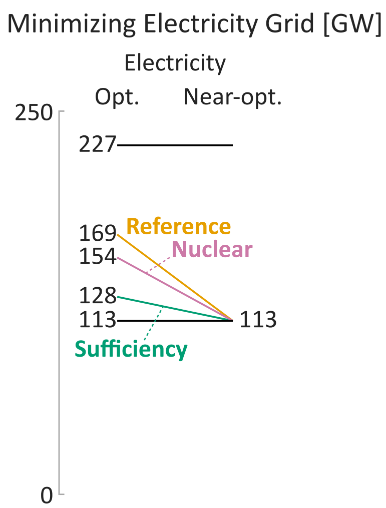

Figure 5.16: A fossil-free Europe with no expansion of the electricity cross-border transmission grid is feasible in all three scenarios.

In a fossil-free European energy system, the electricity grid can stay at its actual capacity if larger hydrogen and methane grids are deployed, see Figure 5.17. In particular, both in the Nuclear and the Sufficiency scenario, more hydrogen pipelines are installed both in terms of hydrogen pipelines retrofitted methane ones (+ 111 and 73 GW) and in terms of new hydrogen pipelines (+ 128 and 84 GW). Additionally, in other locations, the methane grid is reinforced with new pipelines (+ 68 and 81 GW). The Reference scenario only reinforces the hydrogen network, with more retrofitted pipelines (+ 117 GW) and more new pipelines (+ 101 GW).

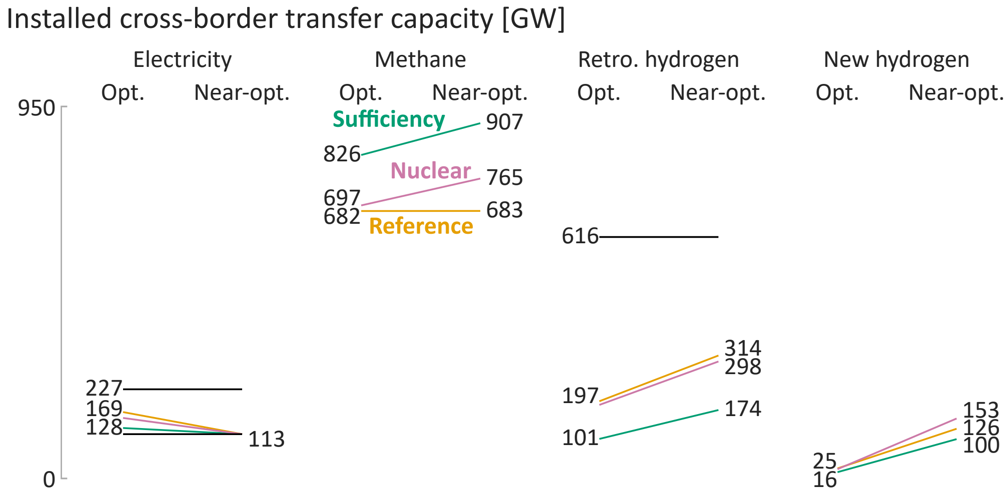

Figure 5.17: Reducing the European electricity network to the actual capacity increases the infrastructure for hydrogen and methane exchanges.

The decreased capacity of the electricity transmission network implies a lower quantity of electricity exchanges, Figure 5.18(A). However, this decrease is small compared to the total electricity exchanges (12 to 27%) and even more compared to total exchanges (3.8 to 7.1%). This small decrease does not imply fundamental changes in the European energy system. Local reallocation of some resources and higher exchanges of other energy carriers compensate for the reduction of electricity exchanges. In the Sufficiency scenario, which already has a small expansion of the electricity grid at the optimum, the impact is even smaller.

The lower electricity exchanges are compensated by an increase in other exchanges. In all scenarios, hydrogen exchanges increase: by 163 TWh in Reference, 174 Wh in Nuclear and 38 TWh in Sufficiency. In the Reference and the Nuclear scenarios, the FT fuels exchanges also increase significantly (+139 TWh).

Methanol is used more locally, and its exchanges decrease, Figure 5.18(B). In the optimal designs, some sectors and countries rely on imports for their methanol supply. In the near-optimal designs, these methanol uses are replaced by other fuels. For instance, some countries replace methanol-fueled freight boats with methane-fueled ones. Other countries increase their ammonia-fueled ships to reduce the methanol-fueled ships. Hence, increased methane, ammonia and woody biomass exchanges compensate for decreased methanol exchanges. Furthermore, the uses of biomass are diversified. Some countries, such as Germany, install biomass DHN boilers to replace a part of the heat pumps and biomass power plants. They both have an impact on power production and power flexibility.

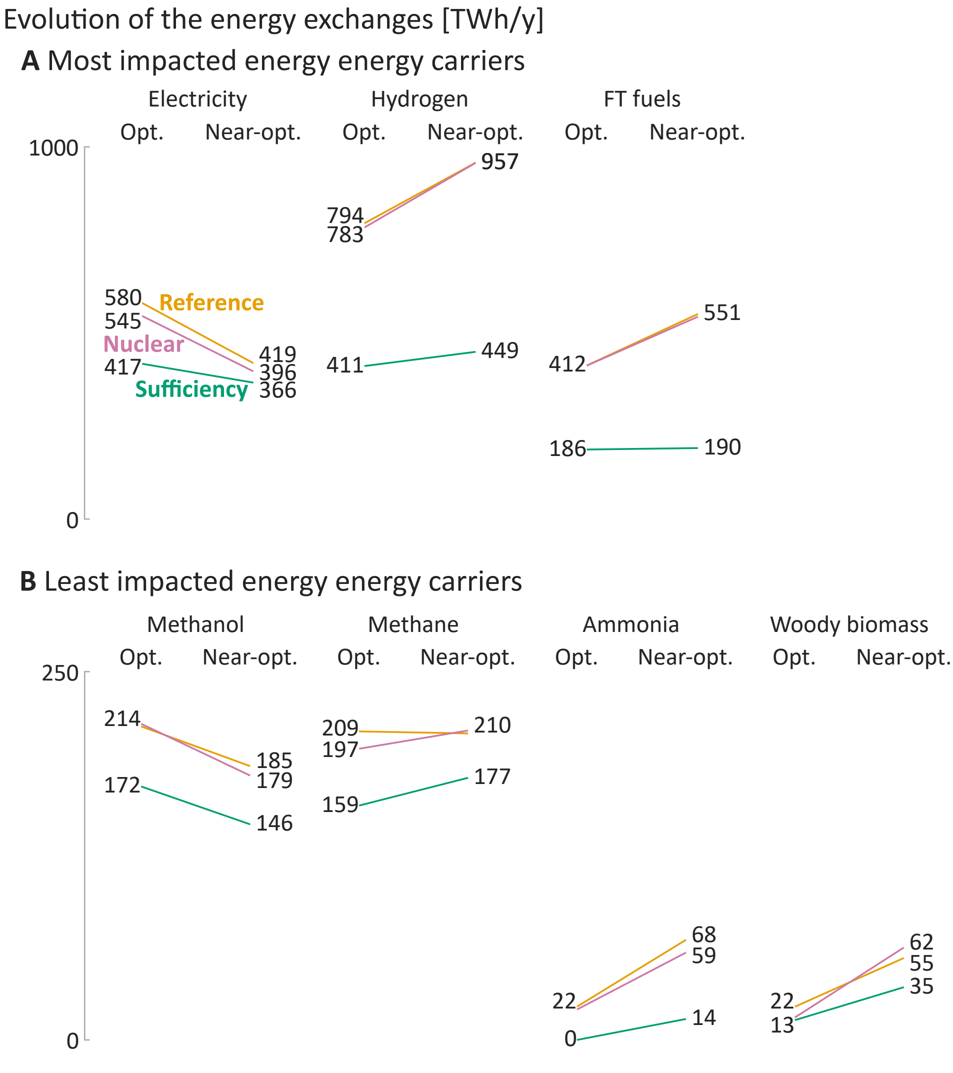

Figure 5.18: Reducing the European electricity network to the actual capacity leads to increased infrastructure for hydrogen and increased hydrogen and Fischer-Tropsch (FT) fuels exchanges.

In addition to these changes in energy exchanges, the countries with high dependence on electricity imports at the optimum, such as Belgium, North Macedonia, the Netherlands or Germany, need to deploy other strategies to compensate for the lower electricity imports. Their strategies consist of reallocating some resources and increasing, when possible, their local renewable production. For instance, Germany and Belgium install more utility PV and Germany and the Netherlands install more offshore wind. In addition, some countries install more thermal power plants. Germany installs biomass power plants and reduces its electricity consumption in other applications (HVC production and industrial boilers). Belgium imports more methane to run CCGTs.

Another example of resource reallocation is related to FT fuels production and exchanges. At the European level, the sources for FT fuels production are more diversified: 79% integrated production from electricity, 12% production from hydrogen after exchanges and 9% production from biomass. The total use of FT fuels stays the same. However, some FT fuels are reallocated from shipping to non-energy demand. The lower shipping supply from FT fuels is compensated by more ammonia supply. The different sources and uses of FT fuels represent the situation of different countries. Some countries, such as Germany, do not have enough renewable potentials but are well connected to the hydrogen network. They produce a part of their FT fuels with imported hydrogen from neighbouring countries. Other countries, such as Romania, have large biomass potentials and can afford to produce FT fuels from biomass for export. Another type of country, such as Spain, has a vast potential for PV and wind. They can overproduce renewable electricity to convert it into FT fuels both for their own use and for export. This example shows how, by reallocation of certain resources, the system deals with lower electricity exchanges.

Additionally, the reduced electricity transmission capacities lead to increased curtailment of renewables, with 4.9% in the Sufficiency scenario, 6.8% in the Reference scenario and 7.4% in the Nuclear scenario.

To conclude, Europe can become fossil-free without any expansion of its cross-border electricity transmission grid by increasing the exchanges of other resources, in particular hydrogen and FT fuels. This implies installing an even larger hydrogen transmission network, increasing the retrofitted and new pipelines. In addition, some local reallocation of resources is necessary, especially in countries with a high dependence on electricity imports, such as Belgium or Germany. But at the European level, the other changes in system design are minor.

5.3 Must have in all system designs

As presented above, diverse designs exist to reach a fossil-free European energy system. However, all the system designs have in common eight must-haves, see Table 5.2. Although the ranges are large for some variables, those variables always stay consequent. In all twelve cases explored, European wind turbines must produce from 3.95 to 12.25 times the current wind energy production, and in half of the cases, they must produce more than 7.05 times the current wind production. Even in the Sufficiency scenario when minimizing the onshore renewables, that is the case with the lowest increase of wind production, Europe still must produce 3.95 times more wind energy than today. To reach these objectives, Europe must install, on average, between 9 (45 MW) and 37 (185 MW) new wind turbines daily.

The increase in solar production is even larger than the one for wind. In half of the system designs obtained, solar production increased more than 18-fold. In the most solar-intense design, i.e., the Reference scenario minimizing biomass, solar production is multiplied by 25.73 compared to today. Even the least solar-based design, i.e., the Sufficiency scenario minimizing onshore renewables, relies on 5.94 times more solar energy than today. To reach these objectives, Europe must install, on average, between 275 000 (96 MW) and 1 134 000 (397 MW) new PV panels daily.

Table 5.2: In all designs, eight variables are essential. Although their value varies from design to design, they are always essential elements for the energy system and key challenges for reaching a fossil-free energy system. Abbreviations: Consumption (cons.), renewable fuels (Re. fuels), biomass use near-optimal direction (Biom.), onshore renewables near-optimal direction (Onsh.), electricity grid near-optimal direction (Elec.), nuclear scenario (Nuc.), reference scenario (Ref.), Sufficiency scenario (Suff.),

Variable	Normalized by	Range	Median	Extreme designs
Wind production	Current prod. (465 TWh/y)	3.95 - 12.25	7.05	(Suff., Onsh.) - (Ref., Biom.)
Solar production	Current prod. (219 TWh/y)	5.94 - 25.73	18.13	(Suff., Onsh.) - (Ref., Biom.)
Electricity production	Current prod. (3518 TWh/y)	1.24 - 3.42	2.4	(Suff., Onsh.) - (Nuc., Biom.)
Electricity to fuels	Total electricity production	0.2 - 0.5	0.4	(Suff., Onsh.) - (Nuc., Biom.)
Electricity final cons.	Total final energy cons.	0.49 - 0.62	0.51	(Suff. Onsh.) - (Suff., Biom.)
Re. fuels final cons.	Total final energy cons.	0.3 - 0.45	0.42	(Suff., Biom.) - (Nuc., Onsh.)
Re. fuels exchanges	Total exchanges	0.69 - 0.84	0.74	(Suff., Opt.) - (Nuc., Elec.)
Re. fuels storage capacity	Total storage capacity	0.39 - 0.54	0.47	(Nuc., Onsh.) - (Suff., Biom.)

Shifting from fossil fuels to renewables leads to increased electrification. Over all designs, the electricity production is multiplied by 1.24 to 3.42 compared to the current production.

A significant part of this additional electricity is allocated to the e-fuels production, that is more than 40% in half of the designs. The electrification of several end-uses, such as heating and private mobility, drives the rest of the increase in electricity production. Electricity reaches a share of 49 to 62% of the final consumption. This is a high increase compared to today's 21%.

However, regardless of the scenario and near-optimal direction, a significant part (30-45%) of the final energy consumption uses renewable fuels. Several end-use applications, such as aviation, shipping, public mobility, non-energy, and high-temperature heat, cannot be fully or at all electrified and require fuels. The cost-efficient system designs produce them in Europe rather than importing them from the rest of the world. Renewable fuel imports are only used as a last resort. Inside Europe, these fuels are produced from biomass and electricity. The relative share depends on the design. For instance, on the near-optimal direction of minimizing biomass, biofuels represent less than 5.3% of renewable fuels and go up to 53.5% of renewable fuels when minimizing onshore renewables.

Another essential result is the critical role of renewable fuels in tackling the spatio-temporal disparity of wind and solar energies. Indeed, they are essential in terms of energy exchanges and storage capacity. In terms of energy exchanges, in all designs, a hydrogen network is built both from retrofitting methane pipelines and from building new ones. However, a part of the methane network is always kept for methane exchanges. These two resources, with others traded through freight (e.g. FT fuels, methanol), transport the bulk energy in Europe (69-84%). They reach their largest share when electricity grid expansion is minimized. The counterpart of this importance of renewable fuels exchanges is that electricity exchanges are low and represent only 16 to 31% of all exchanges. Regarding storage, the largest storage capacity is always the DHN thermal storage but renewable fuels storage comes as the second largest storage with 39 to 54% of the total storage capacity. They operate as seasonal storage and reach their largest share when biomass use is minimized.

5.4 Discussion on trade-offs to reach a fossil-free energy system

This chapter analyzes the diverse options to reach a fossil-free European energy system. We apply a hybrid method combining scenario analysis and near-optimal space exploration to derive 12 different system designs. Three different scenarios are modelled: (i) the Reference scenario with a high demand and without nuclear energy; (ii) the Sufficiency scenario with a low demand and without nuclear energy; (iii) the Nuclear scenario with a high demand and nuclear energy. For each scenario, we explore one optimal design and three near-optimal designs : (i) minimizing onshore renewables, that is, utility PV and onshore wind; (ii) minimizing biomass use; (iii) minimizing cross-border electricity network expansion.

The analysis of the 12 designs reveals the wide range of possibilities for reaching a fossil-free European energy system. This result is in line with other publications showing that by increasing slightly (<5%) the cost of the system, we can completely change the energy supply and system design [53, 85, 88, 89]. However, this chapter goes further than other publications by analysing the compromises and must-haves of these different designs.

In terms of energy supply, four categories of sources compete and complement each other: (i) Biomass; (ii) Utility PV and onshore wind; (iii) Rooftop PV and offshore wind; (iv) Imports of renewable fuels. They are presented here in order of priority. Indeed, the system relies on a resource only when the previous ones are saturated. In some cases, it means that the full potential is reached across Europe, but most of the time, it means that all the most profitable locations for this resource are exploited.

Europe can rely less on any of the four supplies mentioned above if it increases the supply from other sources. We argue in favour of a trade-off between all the extreme designs presented in this chapter as the most reliable and robust option. Indeed, it implies a diversification of sources and avoids relying on extreme deployment of some technologies which Europe is not sure to reach. For instance, the design minimizing the use of biomass relies on very high deployment of utility PV and onshore wind. This is well above the statistical projection of their deployment [318]. Furthermore, installing those energy assets already suffers delays nowadays due to low social acceptance [278, 280, 323]. On the contrary, minimizing the deployment of onshore renewables leads to a dependence on high imports of renewable fuels. This reduces Europe's energy sovereignty and implies relying on a future international market that is uncertain to develop. Furthermore, it externalizes the socio-environmental impacts of renewable fuel production in other countries.

However, whatever the system design, Europe must install high quantities of wind turbines and PV to reach at least 4 and 6 times the current production. In some scenarios, wind production reaches 12 times its current production and solar production 26 times its current production. In parallel, electricity production increases drastically in all designs, from 1.2 to 3.4 times the current production. This electricity is used to produce substantial quantities of e-fuels (20 to 50% of electricity production) and to electrify end-uses such as heating and private mobility.

The final energy carriers consumed are way less impacted by the choices in supply than the intermediary conversion chain elements. Indeed, whatever the system, electricity is the first final energy carrier (49 to 62%). Renewable fuels are the second final energy carriers, covering 30 to 45 % of final energy consumption and waste incineration the third with 5 to 8%. However, the type of supply induces the energy conversion chain. For instance, a system relying heavily on utility PV and onshore wind produces vast amounts of e-fuels. These e-fuels supply up to 3527 TWh/y of final energy consumption for the Nuclear scenario in the direction of minimizing biomass use. On the contrary, in all scenarios, when minimizing onshore renewables, few renewable fuels are produced from electricity (down to 584 TWh/y). They are rather produced from biomass (up to 2301 TWh/y) or imported from the rest of the world (up to 981 TWh/y).

In any design, vast amounts of energy are exchanged to cope with the spatio-temporal disparity of renewable energy sources. There is a trade-off between increased electricity exchanges and increased renewable fuel exchanges. However, in any case, renewable fuels remain the main means of exchange (69 to 84 %). In particular, a European hydrogen network becomes the first means of energy exchange and transports up to 958 TWh/y when minimizing the electricity grid.

In terms of storage, in all designs, large DHN thermal storage and renewable fuel storage are the main installed capacity, 13 to 49% and 39 to 54%, respectively. Renewable fuel storage is essential for seasonal storage. The shorter-term storage is ensured by technologies like PHS, electric vehicle batteries and decentralised thermal storage.

Finally, the different scenarios lead to different solution spaces with specific trends to underline. The Sufficiency scenario facilitates the energy transition. In all cases, it reduces the amount of uncertain energy sources and energy conversion technologies. For instance, the import of renewable fuels is always smaller than 158 TWh/y in this scenario, whereas it reaches up to 981 TWh/y in the Reference scenario. There is lower deployment of utility PV and onshore wind than in other scenarios. Reducing their deployment facilitates the energy transition. Furthermore, the Sufficiency scenario always leads to lower production, exchanges and use of e-hydrogen and FT fuels. It always installs less than 367 GW of electrolysers, produces less than 2238 TWh/y of e-hydrogen and installs less than 274 GW of cross-border hydrogen pipelines. Finally, the Sufficiency scenario leads to an optimal cost that is 29% lower than the Reference scenario. However, the effect of the sufficiency measure on the economic system is not evaluated here. Furthermore, the Sufficiency scenario may face social acceptance challenges not considered in this work.

On the contrary, the Nuclear scenario does not induce fundamental changes at the European level. It reduces the wind and PV supply by 1168 TWh/y and replaces it with 2789 TWh/y of nuclear energy. This difference in supply with the Reference scenario is present in all exploration directions. In the design with the highest imports of renewable fuels, the Nuclear scenario has 11% less imports than the Reference one. However, those imports are still consequent (872 TWh/y). At the European scale, this scenario has the same responses as the Reference one to the stimulus of exploring a specific direction. However, in certain countries, such as Belgium, that are strongly dependent on electricity imports in the Reference scenario, it reduces this dependence.

Conclusions and perspectives

Overview

- Five main outcomes of this work.
- Five perspectives for future works.

This work contributes to the discussion on the energy transition to tackle climate change. It applies a whole-energy system optimisation model, EnergyScope Multi-Cells, to explore designs for a fossil-free European energy system in 2050. This work uses a hybrid method combining scenario analysis and near-optimal space exploration to analyse 12 system designs for phasing out fossil fuels. The two scenarios explore the impact of sufficiency measures and the impact of a nuclear deployment on the energy system design. This work explores the near-optimal space in three directions in each scenario to find equivalent systems in terms of cost (5% increase) but with significantly different designs. We choose the three directions according to socio-politico-environmental concerns: (i) minimising the land area allocated to onshore renewables technologies, that is, wind onshore, utility photovoltaic (PV) and concentrated solar power (CSP); (ii) minimising the use of biomass; (iii) minimising the expansion of the cross-border electricity transmission grid.

> Based on this approach, we present critical outcomes for the energy transition in Europe and the challenges of energy systems relying on renewable energy sources. Then, we underline the main limitations of this work and the perspectives for future works.

Main outcomes

This section summarises the five main outcomes of this thesis. The full technical descriptions of the main conclusions can be found at the end of each chapter.

(M-1) **A diversity of designs is feasible to reach a fossil-free system with some trade-offs and must-haves.** Through 12 different designs, this work showed that developing an energy system for Europe without fossil fuels is feasible. This idea aligns with other studies that underline the diversity of options for a fully renewable European energy system [53, 89, 90]. This diversity of designs comes with trade-offs. Not everything is possible, and any choice has its counterparts. This work explores two trade-offs: trade-offs in gross available energy supply and trade-offs in the type of energy exchange between countries. The key supply for a fossil-free European energy system can be divided into four complementary and competing categories: (i) biomass; (ii) onshore renewables (utility PV and onshore wind); (iii) rooftop PV and offshore wind; (iv) renewable fuels imports. These four categories are presented in order of preference by the energy system. All system designs combine these four categories for their energy supply. According to the objectives, some key energy supplies can be reduced, as shown in the near-optimal directions, by minimising the onshore renewable or biomass use. However, reducing these energy sources means relying on other supplies such as rooftop PV, offshore wind and imports of renewable fuels. Although the supply changes from one design to the other, the general structure of the final energy consumption remains unchanged, with electricity as the first energy carrier (49 to 62%) and renewable fuels as the second one (30 to 45%). However, the type of energy supply changes the conversion chain to produce electricity and renewable fuels. Another essential result is that in most system designs, Europe is energy self-sufficient. It has large, untapped, and cost-competitive renewable energy potentials. The spatial disparity between these potentials and the location of the energy demands fosters cooperation among European countries and substantial energy exchanges. For these energy exchanges, there is a trade-off between increased electricity exchanges and increased renewable fuel exchanges. However, in any case, renewable fuels remain the main means of exchange. Although some trade-offs exist, some must-haves are always present in the energy system. The next paragraphs detail these must-haves.

(M-2) **Defossilization of Europe requires high deployment of PV and wind turbines.** In any design, PV and wind are the main sources of energy. This has several impacts. First, we can ask ourselves if Europe can reach such a high deployment, consistent with other scenarios in the literature but well above statistical projection and with social acceptance challenges. This high renewables deployment comes with a high increase in electricity production, from 1.2 to 3.4 times the current production. The increase in electricity production is due to the high electrification of several end-uses and the high electricity consumption to produce e-fuels. The end-uses electrification increases energy efficiency and occurs in four sectors: (i) low-temperature heat for space heating and hot water; (ii) private and public mobility; (iii) up to 60% of the high-temperature heat for the industry; (iv) space and process cooling. The e-fuel production consumes up to 20 to 50 % of the electricity. This comes with a high deployment of electrolysers, up to 615 GW, where a real scale-up is needed compared to today's capacity. Furthermore, the high electricity production from renewables comes with a spatio-temporal disparity. This requires investing in large transmission networks of electricity, methane and hydrogen and in large seasonal storage capacities.

(**M-3**) **Renewable fuels are essential in fossil-free energy systems.** These renewable fuels are both produced from electricity and biomass. They are often only discussed in the literature as e-hydrogen and its derivative. In this work, we showed the essential role of biomass both for direct use and upgraded into more advanced fuels such as methane or methanol. Biomass is often overlooked in the literature but is a pillar of fossil-free energy systems and should be given more attention. Then, as not all end-uses can be electrified, in a fossil-free energy system, a consequent part of the final energy is consumed as renewable fuels (30 to 45%). These renewable fuels require a vast amount of energy to be produced (from 1450 to 6800 TWh of gross available energy). They are essential in specific applications: international shipping, aviation, non-energy demand, high-temperature heat for the industry, trucks and boats for freight, busses for public mobility, and thermal power plants for power flexibility. Additionally, renewable fuels are essential to tackle the spatio-temporal disparity of renewable energy sources. They provide large storage capacities for seasonal storage (39 to 54% of storage capacity) and are the primary means of exchanges (69 to 84%), well above electricity exchanges (16 to 31%).

(**M-4**) **Nuclear energy is not a game changer at European scale.** Compared to the scenario without nuclear, installing nuclear power replaces 14% of the energy supply from wind and PV. However, wind and PV remain the primary sources of gross available energy (53%). This change in energy sources does not change the system structure or the energy carriers used for final energy consumption. Nuclear electricity replaces renewable electricity. The only changes are a slight reduction in storage capacity

(-15%) and in electricity exchanges (-6%). Although nuclear energy is not a game changer at the European scale, it has an impact locally in countries installing it. For instance, countries such as Belgium, which imports 37% of its electricity (66 TWh/y) in the Reference scenario, reduce its electricity imports to 18% in the Nuclear scenario. However, nuclear fuel imports replace these electricity imports, as nuclear power plants produce 63 TWh_{elec}/y in Belgium. The import of uranium is subject to geopolitical issues[258] Furthermore, even with these uranium imports, Belgium still needs to import a significant amount of renewable fuels (140 TWh/y). Furthermore, the Nuclear scenario responds like the Reference one to the stimulus of exploring near-optimal directions.

(**M-5**) **Sufficiency reduces the investment in energy infrastructures.** With the sufficiency measures, the energy demand is reduced; thus, Europe taps less into its renewable resources. This provides larger margins to navigate and choose between diverse options. This scenario leads to a much lower energy system cost, 29% less than the Reference one. Although the energy system's general size decreases, sufficiency's impact is the strongest on e-fuels use and production (-63%). This lower e-fuels production also implies lower installed capacities of PV and wind (-48%) and lower transmission infrastructure both in electricity (-24%) and hydrogen (-53%). However, as fewer methane pipelines are retrofitted to hydrogen, the Sufficiency scenario has a larger remaining methane grid. By reducing the need for energy infrastructure, the Sufficiency scenario reduces their additional environmental and social impacts. Furthermore, due to their lower level, the deployment of these infrastructures is more accessible. However, these results have limitations as our work does not quantify the retroaction of the economic system or the social acceptance.

Limitations and perspectives

This section outlines five main perspectives related to the limitations of this work.

(**P-1**) **The development of a model is a continuous effort.** The energy system optimisation model presented can still be improved in several ways. For instance, the definition of energy demand should come as close as possible to the energy service to relate to the real need for energy and design the whole energy conversion chain. The representation is not at an equal level in all sectors. In particular, the industrial demand for processes is defined only in terms of electricity, high-temperature heat, process cooling, hot water, space heating, and space cooling. It misses many implications and challenges related to the defossilisation of the industry. The industry demand modelling could be improved by detailing the material production of the industries with high energy consumption, such as steel and glass, and then modelling the potential defossilized production chain. Girardin et al. [289] quantified those demands in Europe and modelled production chains with their energy inputs. Their work could be integrated into our model for a more refined industry representation. From there, different industrial pathways could be explored. Another improvement could be integrating more agent-based modelling and comparing it with the central planning approach to underline the advantages and challenges of working together at a European scale. A third essential improvement is coupling the model with other models to improve its representation. For instance, we coupled the Belgian version of the model with the Dispa-SET model [125]. This model better represents the dispatch constraint in the electricity network and gives EnergyScope feedback on whether it has enough flexibility on the grid. Within three to four iterations, the coupling converges and underlines that in the (uni-cell) Belgian case, EnergyScope underestimates the required backup power plants. Other improvements directly relate to the next perspectives (e.g. improving computational tractability, integrating life-cycle assessment indicators, integrating social aspects). Some other technical improvements of the model are not detailed here but are listed in Section 3.2.2.

(**P-2**) **Searching further into computational tractability improvements.** We need models with good computational tractability to explore diverse options for future energy systems. This work studied how the use typical days improves the computational tractability of ESOMs. It presented a method to evaluate the impact of this model reduction technique on the energy system design. However, typical days clustering is not the only performance enhancement technique for energy system optimisation models. Other techniques could be tested using the evaluation approach proposed here. In the end, several methods could be combined. In the first instance, we would advise adapting model decomposition techniques to ESOMs, as proposed in [217]. These ESOMs have very empty matrices and, therefore, can gain much from decomposition. From our experience, we think these performance enhancement techniques could at least improve the computational time by two and reduce memory usage.

(**P-3**) **From the carbon tunnel to doughnuts economy.** This work showed that from a techno-economic standpoint, many equivalent designs are feasible to reach a fossil-free energy system. However, it did not explore the other environmental and social challenges of the holistic transformation, that is, the transition. Therefore, we propose a perspective towards linking this model with an approach based on the doughnut economy [294], which underlines the planetary boundaries [324] ceiling and social floor necessary for a sustainable society. Climate change is only one of the symptoms of the socio-environmental breakdown we are living. The other planetary boundaries should be integrated into the model through life cycle assessment (LCA). The integration of LCA into this energy system model has already been explored in previous works [97, 325]. However, it lacked a full quantification of the impact of the energy system in all planetary boundaries and thresholds to estimate whether this is acceptable. To overcome these limitations, we can build on the work of Coppitters et al. [326], who assessed the planetary limits for hydrogen imports. The social impact of the energy transition is much more complex to quantify. However, a qualitative appreciation could lead to better-designed scenarios, exploration directions or a qualitative classification of energy system designs obtained from a social standpoint. Integrating this field with energy system modelling is much more challenging and needs a new approach, as presented in the next paragraph.

(**P-4**) **Towards a transdisciplinary planning of the energy transition.** As mentioned in the previous paragraph, the energy transition is a complex socio-environmental problem with many possible technical solutions. Therefore, we should evaluate those solutions from the perspective of other disciplines or even build those solutions in collaboration with other disciplines, which calls for interdisciplinarity. For instance, renewable energy potentials can be reviewed based on criteria such as social acceptance as is explored by [327]. The impact of high infrastructure investments on the macroeconomic world can be evaluated as in [328–330]. The economic profitability of these investments can also be studied as in [331]. This aspect is crucial for having actors who build these assets. Another aspect for building these infrastructure is related to social acceptance and community involvement [332, 333]. The energy demand can be evaluated by discussing decent living standards and equity as is done into [306]. All those examples bring more depth and viewpoint to the analysis but remain theoretical approaches done by researchers. However, in the end, the energy transition will have a very practical impact on everyday life and the organisation of society. Therefore, we argue in favour of going one step further towards transdisciplinary or research action where the research projects are built with other stakeholders such as companies and citizens. For instance, van Moeseke et al. [334, 335] have developed the concept of *SlowHeat*. They evaluated theoretically and experimentally, with people trying it at home, how much we can reduce heating while maintaining thermal comfort. Another avenue to explore is a multi-level approach integrating local projects and constraints into more macro-models. For instance, transdisciplinary research on energy communities at the neighbourhood level can feed larger models at the city, region, country or even continent level, such as the one developed in this thesis. This way, macro-models like ours can propose scenarios and options that better integrate and respect local problematics. Conversely, the macro-models can provide feedback to local projects on which role they can have at a larger level. Furthermore, by fostering discussion and participation, transdisciplinary research on the energy transition can improve energy literacy in the population. It can induce a better energy democracy and justice by fostering community-led energy projects rather than energy colonialism.

(**P-5**) **Representing a diversity of possible future energy systems with its implications for society.** The previous perspective implies efficiently communicating results to a broad audience, from researchers in other fields to local stakeholders. Therefore, there is a need to generate quick and meaningful scenarios and analyse their key socio-politico-environmental implications to foster discussion with other research fields, companies, public instances and citizens. This research challenge should not be underestimated. Future energy systems will be highly coupled and complex. In this thesis, we proposed ways to analyse and describe those systems, but there is room for improvement. Entire research could be conducted on this, and gather both engineers who design and run those models and experts from other fields.

Given the socio-environmental collapse of our modern societies, it is time for technical science to transcend itself. Its strength for centuries, its ability to classify problems to better understand and solve them, has now become its weakness. This science has brought us material comfort but has disconnected us from our roots. Today, it is reaching its limits in the face of the complex and interconnected challenges of our time, such as climate change, mass extinction, and the crisis of democracy. It is now high time for this science to question itself and open up to other approaches to gain an in-depth understanding of these complex challenges and propose paths towards sustainable and desirable futures. This work is a first step towards that openness in that it shows how a techno-economic model can propose various options for phasing out fossil fuels. First, these options can be presented to and challenged by other fields of study or stakeholders. Secondly, the scenarios and avenues explored can evolve from these discussions to propose desirable and sustainable futures.

On s'bat pour être à l'avant dans un avion qui va droit vers le crash.
Orelsan.
L'odeur de l'essence (2021)

J'insiste un instant sur ce point. Ne pas confondre le tenable ou le durable et le souhaitable est indispensable. Ça n'a rien à voir, c'est une faute catégorielle. (...) Qu'un État puisse perdurer ne signifie pas du tout qu'il soit éthiquement, esthétiquement ou épistémiquement louable. C'est une question qui n'a rien à voir. Pour le dire de façon très claire et insister, les mille milliards d'animaux que nous tuons chaque année dans des conditions souvent épouvantables et la plupart du temps en les ayant, ce qui est encore plus grave d'ailleurs, privés de vie avant la mort seraient-ils sans importance, sans valeur, sans conséquences, si la situation était pérenne ? Les 800 000 (...) êtres humains qui meurent chaque année en Europe de la pollution, seraient-ils sans importance s'ils étaient compensés par le même nombre de naissances ? C'est insensé. Donc faites attention qu'une situation soit durable ne signifie pas qu'une situation est souhaitable. La nôtre n'est ni durable ni souhaitable. Donc la question, ce n'est pas comment y arriver ?, la question c'est à quoi veut-on arriver ?

Aurélien Barrau.
A-t'on encore besoin d'ingénieurs ? (2022)

A Data and code availability

The EnergyScope Multi-Cells model and its applications are open-source and documented. The full documentation of the model and its application to Europe can be consulted online at https://energyscope-multi-cells.readthedocs.io/en/master/ (accessed on 12 May 2024).

The input data, the model, the output data and the analysis script for Chapter 2 are available on a Zenodo repository: https://zenodo.org/records/7527344 (accessed on 10 March 2023).

Similarly, the input data, the model, the output data and the analysis script for Chapters 3 and 5 are available on a Zenodo repository: https://doi.org/10.5281/zenodo.11144189 (accessed on 12 May 2024).

In both cases, the Zenodo repository is a copy of the model state at the moment of the study. We add to this copy outputs of the case of interest and the analysis scripts. The model is meant to continue to evolve. Its latest version is stored on a GitHub repository: https://github.com/energyscope/EnergyScope_multi_cells (accessed on 12 May 2024).

B List of European countries and country codes

Tables B.1 and B.2 present the 34 European countries considered in our study with their two-letter code from the ISO 3166 Alpha 2 norm [336]. These codes are used in the model.

Table B.1: List of European countries and two-letter country code from the ISO 3166 Alpha 2 norm (part1). Countries are sorted alphabetically by country code.

Country	**Code**
Albania	AL
Austria	AT
Bosnia and Herzegovina	BA
Belgium	BE
Bulgaria	BG
Switzerland	CH
Czech Republic	CZ
Germany	DE
Denmark	DK
Estonia	EE
Spain	ES
Finland	FI
France	FR
Greece	GR
United Kingdom	GB
Croatia	HR
Hungary	HU
Ireland	IE
Italy	IT
Lithuania	LT
Luxembourg	LU
Latvia	LV

Table B.2: List of European countries and two-letter country code from the ISO 3166 Alpha 2 norm (part 2). Countries are sorted alphabetically by country code.

Country	Code
Montenegro	ME
North Macedonia	MK
Netherlands	NL
Norway	NO
Poland	PL
Portugal	PT
Romania	RO
Serbia	RS
Sweden	SE
Slovenia	SI
Slovakia	SK
Kosovo	XK

C Sensitivity of the design error

This appendix discusses the sensitivity of the design error presented in Chapter 2. Section C.1 motivates the use of the design error instead of the apparent design error and illustrates the flat optimum consequence with a simple example. Section C.2 discusses the impact of choosing another threshold on element error inside of the design error equation.

C.1 Oscillation in Design Error and Smoothing

This section explains in more detail the oscillating behaviour of the design error. The 3R-AntlanticEU case is used as an example to present this phenomenon, but it could be underlined in any case study. Firstly, the difference between apparent design error (aDE) and design error is illustrated. Then, an example of changes due to the flat optimum is presented.

As explained in Section 2.1.2, the optimisation of the design and operation of large integrated energy systems has a flat optimum. Indeed, several equivalent solutions exist with different designs. This explains the interest in near-optimal solutions exploration in the field [53, 58, 85–89, 93]. Figure C.1 presents the difference between the apparent design error and the design error. There is an oscillating behaviour where sometimes a higher number of typical days (TDs) leads to a higher design error. The problem considered is a whole-energy system where the different energy sectors are highly coupled. It leads to complex energy systems where all decisions are linked. Hence, it is not possible to determine, in general, which part of the error comes from the lower temporal resolution and which part comes from the flat optimum. However, when an increase in the number of TDs implies an increase in design error, this is most likely due to a switch from an equivalent solution to another. Therefore, we can approximate the design error at a certain number of TDs by the minimum of the apparent design error for this number or lower numbers of TDs (Equation

2.7). This reveals a part of the oscillation due to the flat optimum, but there is no way to prove that it considers its whole effect.

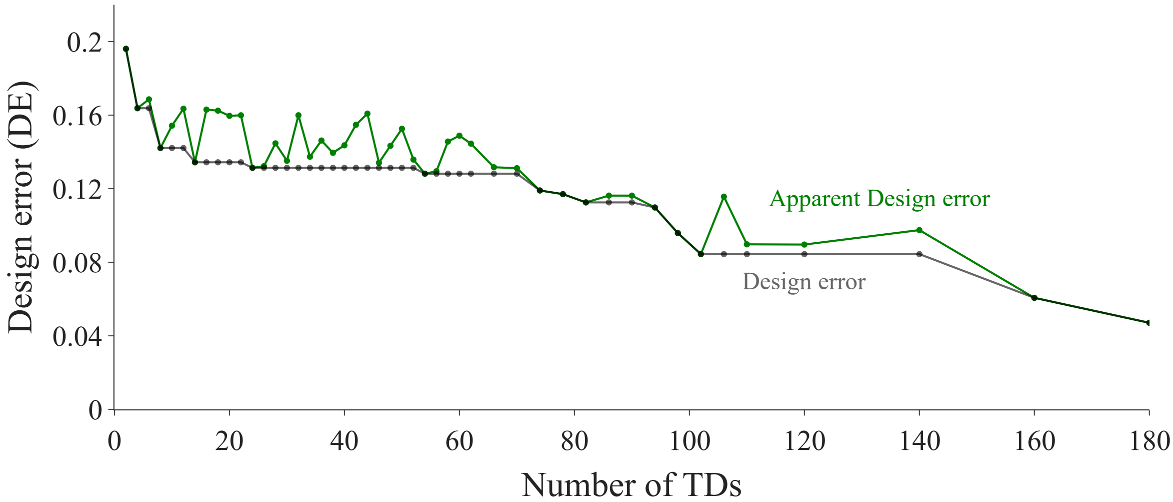

Figure C.1: Evolution of the apparent design error and the design error for the 3R-AtlanticEU case study. The apparent design error has an oscillating behaviour due to the flat optimum of the optimisation problem. Therefore, it is approximated by its lower bound.

Figure C.2 provides an example of oscillating behaviour due to the flat optimum. It presents the relative error in assets and resources used to provide the non-energy demand for high-value chemicals (HVC) for the British Islands in the 3R-AtlanticEU case study. There are two competing routes: (i) importing more renewable methanol and converting it to HVC (i.e., green and orange curves); (ii) importing more oil, converting it to HVC, and emitting less in other energy sectors (i.e., blue curve). The error on those two options oscillates in opposite directions from one number of TDs to the other. This even occurs at a high number of TDs, with very accurate temporal resolution. For instance, the relative error on those elements becomes very small at 102 and 120 TDs and increases both between and after those numbers. This shows that those two options are equivalent.

C.2 Impact of the Threshold on the Elements Error

Based on the approach explained in Section 2.1.2, Figure C.3 is built, taking different acceptable thresholds for the error on elements (2.5, 5 and 7.5%). This is performed on the 3R-AtlanticEU case study to illustrate the results, but it could be extended to any other case. Taking those acceptable thresholds increases or decreases, respectively, the design error by less than 3.5%. In addition, the general shape of the curve stays unchanged; that is, most of the gain in accuracy is reached around 14 TDs, and then the error is nearly constant.

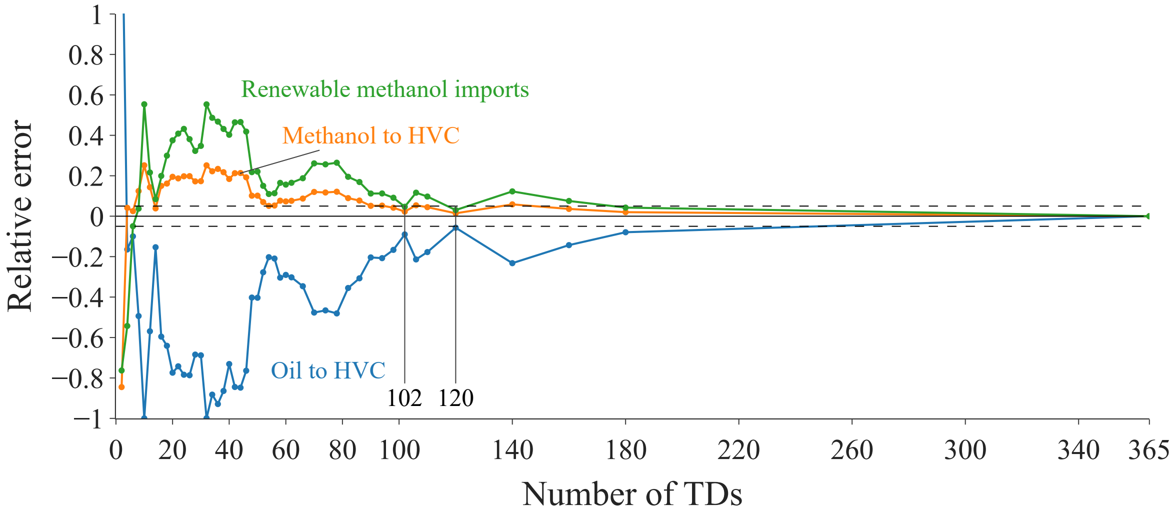

Figure C.2: Example of oscillating elements in the production of high-value chemicals (HVC) for the British Islands for the case 3R-AtlanticEU. At high numbers of TDs, the problem oscillates between two equivalent solutions: one with more production from renewable methanol and less from oil and another with the opposite.

As the goal of this metric is to find trade-offs between the accuracy of the model results and computational cost, any of those thresholds are equivalent.

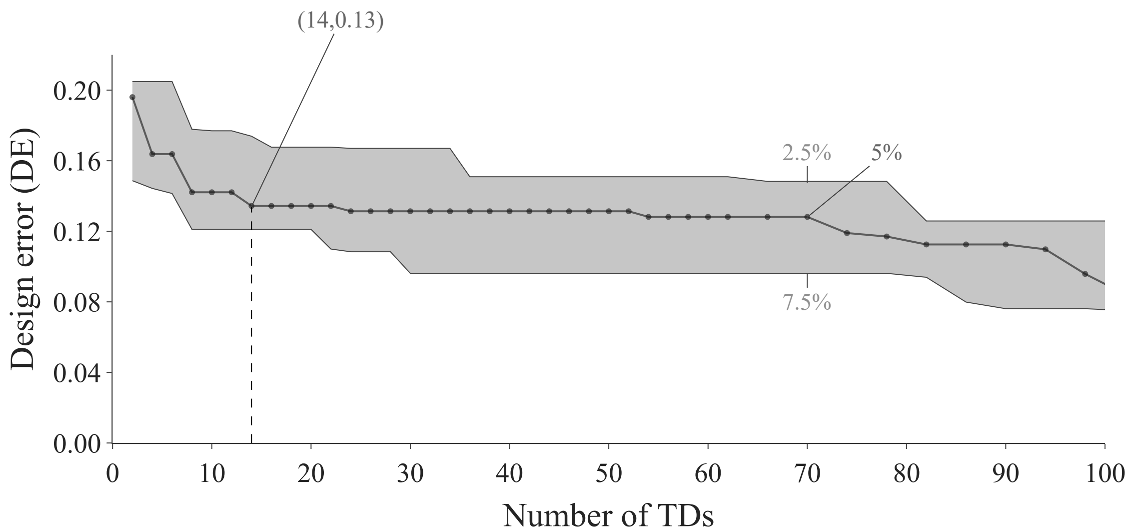

Figure C.3: Evolution of the design error (DE) with the number of typical days (TDs) for the 3R-AtlanticEU case study. The grey curve is made with the reference threshold of 5% for the error on each element. The grey area around it is obtained by exploring the sensitivity of this threshold down to 2.5% and up to 7.5%.

Bibliography

[1] European Commission. *Eurostat - Complete energy balances*. Jan. 28, 2024. URL: https://ec.europa.eu/eurostat/databrowser/view/nrg_bal_c/default/table?lang=en&category=nrg.nrg_quant.nrg_quanta.nrg_bal (visited on 03/18/2024).

[2] Swiss Federal Office of Energy. *Switzerland's energy balance*. July 7, 2023. URL: https://www.bfe.admin.ch/bfe/en/home/versorgung/statistik-und-geodaten/energiestatistiken/gesamtenergiestatistik.html.

[3] K. Harris. *Digest of UK Energy Statistics (DUKES) - Aggregate energy balances*. Department for Energy Security and Net Zero - UK National Statistics, Feb. 29, 2024. URL: https://www.gov.uk/government/statistics/energy-chapter-1-digest-of-united-kingdom-energy-statistics-dukes (visited on 04/03/2024).

[4] V. Masson-Delmotte et al., eds. *Climate Change 2021: The Physical Science Basis. Contribution of Working Group I to the Sixth Assessment Report of the Intergovernmental Panel on Climate Change*. Cambridge, United Kingdom and New York, NY, USA: Cambridge University Press, 2021. DOI: 10.1017/9781009157896.

[5] H.-O. Pörtner et al., eds. *Climate Change 2022: Impacts, Adaptation and Vulnerability. Contribution of Working Group II to the Sixth Assessment Report of the Intergovernmental Panel on Climate Change*. 2022.

[6] S. Pfenninger, A. Hawkes, and J. Keirstead. "Energy systems modeling for twenty-first century energy challenges". In: *Renewable and Sustainable Energy Reviews* 33 (2014), pp. 74–86. ISSN: 13640321. DOI: 10.1016/j.rser.2014.02.003. URL: http://dx.doi.org/10.1016/j.rser.2014.02.003.

[7] S. Moret et al. "Characterization of Input Uncertainties in Strategic Energy Planning Models". In: *Applied Energy* 202 (Sept. 2017), pp. 597–617. ISSN: 0306-2619. DOI: 10.1016/j.apenergy.2017.05.106.

[8] X. Rixhon et al. “The role of electrofuels under uncertainties for the belgian energy transition”. In: *Energies* 14 (13 2021), pp. 1–23. ISSN: 19961073. DOI: 10.3390/en14134027.

[9] K. B. Debnath and M. Mourshed. “Forecasting methods in energy planning models”. In: *Renewable and Sustainable Energy Reviews* 88 (March 2018 2018). Publisher: Elsevier Ltd, pp. 297–325. ISSN: 18790690. DOI: 10.1016/j.rser.2018.02.002. URL: https://doi.org/10.1016/j.rser.2018.02.002.

[10] M. G. Prina et al. “Comparison methods of energy system frameworks, models and scenario results”. In: *Renewable and Sustainable Energy Reviews* 167 (Oct. 2022), p. 112719. ISSN: 13640321. DOI: 10.1016/j.rser.2022.112719. URL: https://linkinghub.elsevier.com/retrieve/pii/S1364032122006086.

[11] D. Connolly et al. “A review of computer tools for analysing the integration of renewable energy into various energy systems”. In: *Applied Energy* 87.4 (2010). Publisher: Elsevier Ltd, pp. 1059–1082. ISSN: 03062619. DOI: 10.1016/j.apenergy.2009.09.026. URL: http://dx.doi.org/10.1016/j.apenergy.2009.09.026.

[12] P. R. Shukla et al., eds. *Climate Change 2022: Mitigation of Climate Change. Contribution of Working Group III to the Sixth Assessment Report of the Intergovernmental Panel on Climate Change.* 2022. ISBN: 978-92-9169-160-9. DOI: 10.1017/9781009157926.

[13] J. Rogelj et al. “Scenarios towards limiting global mean temperature increase below 1.5 °C”. In: *Nature Climate Change* 8.4 (Apr. 2018). Publisher: Nature Publishing Group, pp. 325–332. ISSN: 1758-6798. DOI: 10.1038/s41558-018-0091-3. URL: https://www.nature.com/articles/s41558-018-0091-3 (visited on 05/12/2024).

[14] G. Luderer et al. “Impact of declining renewable energy costs on electrification in low-emission scenarios”. In: *Nature Energy* 7.1 (Jan. 2022). Publisher: Nature Publishing Group, pp. 32–42. ISSN: 2058-7546. DOI: 10.1038/s41560-021-00937-z. URL: https://www.nature.com/articles/s41560-021-00937-z (visited on 05/12/2024).

[15] J. DeAngelo et al. “Energy systems in scenarios at net-zero CO2 emissions”. In: *Nature Communications* 12.1 (Oct. 20, 2021). Publisher: Nature Publishing Group, p. 6096. ISSN: 2041-1723. DOI: 10.1038/s41467-021-26356-y. URL: https://www.nature.com/articles/s41467-021-26356-y (visited on 05/12/2024).

[16] G. Luderer et al. *Description of the REMIND Model (Version 1.6)*. Rochester, NY, Nov. 30, 2015. DOI: 10.2139/ssrn.2697070. URL: https://papers.ssrn.com/abstract=2697070 (visited on 05/12/2024).

[17] S. Fujimori, T. Masui, and Y. Mtsuoka. *AIM/CGE [Basic] Manual*. Tsukuba, Japan: Center for Social and Environmental Systems Research, NIES, 2012, p. 87.

[18] B. Valentina, C. Carlo, and G. Marzio. "WITCH. A world induced technical change hybrid model". In: *Energy Journal* 27 (2006).

[19] K. Calvin et al. *GCAM Wiki documentation*. Richland, WA, USA: Pacific Northwest National Laboratory, 2011.

[20] S. Messner and M. Strubegger. *User's Guide for MESSAGE III*. Laxenburg, Austria: International Institute for Applied Systems Analysis (IIASA), 1995.

[21] E. Stehfest et al. *Integrated assessment of global environmental change with IMAGE 3.0: Model description and policy applications*. Netherlands Environmental Assessment Agency (PBL), 2014.

[22] Integrated Assessment Modeling Consortium (IAMC). *What are IAMs?* 2020. URL: https://www.iamconsortium.org/what-are-iams/ (visited on 05/12/2024).

[23] J. Weyant. "Some Contributions of Integrated Assessment Models of Global Climate Change". In: *Review of Environmental Economics and Policy* 11.1 (Jan. 2017). Publisher: The University of Chicago Press, pp. 115–137. ISSN: 1750-6816. DOI: 10.1093/reep/rew018. URL: https://www.journals.uchicago.edu/doi/full/10.1093/reep/rew018 (visited on 05/12/2024).

[24] K. Fisher-Vanden and J. Weyant. *The Evolution of Integrated Assessment: Developing the Next Generation of Use-Inspired Integrated Assessment Tools*. Rochester, NY, Oct. 1, 2020. DOI: 10.1146/annurev-resource-110119-030314. URL: https://papers.ssrn.com/abstract=3716727 (visited on 05/12/2024).

[25] G. Luderer et al. "Assessment of wind and solar power in global low-carbon energy scenarios: An introduction". In: *Energy Economics* 64 (May 1, 2017), pp. 542–551. ISSN: 0140-9883. DOI: 10.1016/j.eneco.2017.03.027. URL: https://www.sciencedirect.com/science/article/pii/S0140988317301044 (visited on 05/12/2024).

[26] R. C. Pietzcker et al. "System integration of wind and solar power in integrated assessment models: A cross-model evaluation of new approaches". In: *Energy Economics* 64 (May 1, 2017), pp. 583–599. ISSN: 0140-9883. DOI: 10.1016/j.eneco.2016.11.018. URL: https://www.sciencedirect.com/science/article/pii/S0140988316303395 (visited on 05/12/2024).

[27] M Brinkerink et al. "Assessing global climate change mitigation scenarios from a power system perspective using a novel multi-model framework". In: *Environmental Modelling & Software (Submitted)* (2021), pp. 6–8. URL: http://pure.iiasa.ac.at/17116.

[28] M. Victoria et al. “Solar photovoltaics is ready to power a sustainable future”. In: *Joule* 5.5 (May 19, 2021), pp. 1041–1056. ISSN: 2542-4351. DOI: 10.1016/j.joule.2021.03.005. URL: https://www.sciencedirect.com/science/article/pii/S2542435121001008 (visited on 03/18/2024).

[29] M. Jaxa-Rozen and E. Trutnevyte. “Sources of uncertainty in long-term global scenarios of solar photovoltaic technology”. In: *Nature Climate Change* 11.3 (Mar. 2021). Publisher: Nature Publishing Group, pp. 266–273. ISSN: 1758-6798. DOI: 10.1038/s41558-021-00998-8. URL: https://www.nature.com/articles/s41558-021-00998-8 (visited on 05/12/2024).

[30] F. Creutzig et al. “The underestimated potential of solar energy to mitigate climate change”. In: *Nature Energy* 2.9 (Aug. 25, 2017). Publisher: Nature Publishing Group, pp. 1–9. ISSN: 2058-7546. DOI: 10.1038/nenergy.2017.140. URL: https://www.nature.com/articles/nenergy2017140 (visited on 05/12/2024).

[31] S. Collins et al. “Integrating short term variations of the power system into integrated energy system models : A methodological review”. In: *Renewable and Sustainable Energy Reviews* 76 (July 2016 2017). Publisher: Elsevier Ltd, pp. 839–856. ISSN: 1364-0321. DOI: 10.1016/j.rser.2017.03.090. URL: http://dx.doi.org/10.1016/j.rser.2017.03.090.

[32] J. Rogelj et al. “Mitigation Pathways Compatible with 1.5°C in the Context of Sustainable Development”. In: *Global warming of 1.5 °C*. Intergovernmental Panel on Climate Change, 2018, pp. 93–174. URL: https://www.ipcc.ch/site/assets/uploads/sites/2/2018/07/SR15_Chapter2_High_Res.pdf (visited on 05/12/2024).

[33] N. Grant et al. “Cost reductions in renewables can substantially erode the value of carbon capture and storage in mitigation pathways”. In: *One Earth* 4.11 (Nov. 19, 2021). Publisher: Elsevier, pp. 1588–1601. ISSN: 2590-3330, 2590-3322. DOI: 10.1016/j.oneear.2021.10.024. URL: https://www.cell.com/one-earth/abstract/S2590-3322(21)00610-2 (visited on 05/12/2024).

[34] I. Tsiropoulos et al. *Towards net-zero emissions in the EU energy system by 2050*. ISBN: 9789276130963 9789276130970 ISSN: 1831-9424, 1018-5593. JRC European Commission, Apr. 20, 2020. DOI: 10.2760/081488. URL: https://publications.jrc.ec.europa.eu/repository/handle/JRC118592 (visited on 04/05/2024).

[35] D. P. van Vuuren et al. “Alternative pathways to the 1.5 °C target reduce the need for negative emission technologies”. In: *Nature Climate Change* 8.5 (May 2018). Publisher: Nature Publishing Group, pp. 391–397. ISSN: 1758-6798. DOI: 10.1038/

s41558-018-0119-8. URL: https://www.nature.com/articles/s41558-018-0119-8 (visited on 05/12/2024).

[36] A. Gambhir et al. “A Review of Criticisms of Integrated Assessment Models and Proposed Approaches to Address These, through the Lens of BECCS”. In: *Energies* 12.9 (Jan. 2019). Number: 9 Publisher: Multidisciplinary Digital Publishing Institute, p. 1747. ISSN: 1996-1073. DOI: 10.3390/en12091747. URL: https://www.mdpi.com/1996-1073/12/9/1747 (visited on 05/12/2024).

[37] N. E. Koltsaklis and A. S. Dagoumas. “State-of-the-art generation expansion planning : A review”. In: 230 (August 2018), pp. 563–589. DOI: 10.1016/j.apenergy.2018.08.087.

[38] M. Fodstad et al. “Next frontiers in energy system modelling: A review on challenges and the state of the art”. In: *Renewable and Sustainable Energy Reviews* 160 (May 1, 2022). Publisher: Elsevier Ltd. ISSN: 18790690. DOI: 10.1016/j.rser.2022.112246.

[39] M. G. Prina et al. “Classification and challenges of bottom-up energy system models - A review”. In: *Renewable and Sustainable Energy Reviews* 129 (129 Sept. 2020), p. 109917. ISSN: 18790690. DOI: 10.1016/j.rser.2020.109917.

[40] P. Colbertaldo, F. Parolin, and S. Campanari. “A comprehensive multi-node multi-vector multi-sector modelling framework to investigate integrated energy systems and assess decarbonisation needs”. In: *Energy Conversion and Management* 291 (Sept. 1, 2023), p. 117168. ISSN: 0196-8904. DOI: 10.1016/j.enconman.2023.117168. URL: https://www.sciencedirect.com/science/article/pii/S0196890423005149 (visited on 03/18/2024).

[41] G. Limpens et al. “EnergyScope TD : A novel open-source model for regional energy systems”. In: *Applied Energy* 255 (July 2019), p. 113729. ISSN: 0306-2619. DOI: 10.1016/j.apenergy.2019.113729. URL: https://doi.org/10.1016/j.apenergy.2019.113729.

[42] M. Borasio and S. Moret. “Deep decarbonisation of regional energy systems: A novel modelling approach and its application to the Italian energy transition”. In: *Renewable and Sustainable Energy Reviews* 153 (December 2020 2022), p. 111730. ISSN: 18790690. DOI: 10.1016/j.rser.2021.111730. URL: https://doi.org/10.1016/j.rser.2021.111730.

[43] A. H. Azadnia et al. “Green hydrogen supply chain risk analysis: A european hard-to-abate sectors perspective”. In: *Renewable and Sustainable Energy Reviews* 182 (Aug. 1, 2023), p. 113371. ISSN: 1364-0321. DOI: 10.1016/j.rser.2023.113371. URL:

https://www.sciencedirect.com/science/article/pii/S1364032123002289 (visited on 05/12/2024).

[44] O. Roelofsen et al. *Plugging in: What electrification can do for industry*. McKinsey & Company, May 2020.

[45] M. Wei, C. A. McMillan, and S. de la Rue du Can. “Electrification of Industry: Potential, Challenges and Outlook”. In: *Current Sustainable/Renewable Energy Reports* 6.4 (Dec. 1, 2019), pp. 140–148. ISSN: 2196-3010. DOI: 10.1007/s40518-019-00136-1. URL: https://doi.org/10.1007/s40518-019-00136-1 (visited on 02/22/2024).

[46] F. Schreyer et al. “Distinct roles of direct and indirect electrification in pathways to a renewables-dominated European energy system”. In: *One Earth* 7.2 (Feb. 2024), pp. 226–241. ISSN: 25903322. DOI: 10.1016/j.oneear.2024.01.015. URL: https://linkinghub.elsevier.com/retrieve/pii/S259033222400037X (visited on 03/12/2024).

[47] I. Staffell et al. “The role of hydrogen and fuel cells in the global energy system”. In: *Energy & Environmental Science* 12.2 (Feb. 13, 2019). Publisher: The Royal Society of Chemistry, pp. 463–491. ISSN: 1754-5706. DOI: 10.1039/C8EE01157E. URL: https://pubs.rsc.org/en/content/articlelanding/2019/ee/c8ee01157e (visited on 05/11/2024).

[48] International Energy Agency. *The Future of Hydrogen*. IEA, 2019.

[49] J. Ramsebner, A. Ajanovic, and M. Wietschel. “The sector coupling concept : A critical review”. In: (January 2021), pp. 1–27. DOI: 10.1002/wene.396.

[50] M. Chang et al. “Trends in tools and approaches for modelling the energy transition”. In: *Applied Energy* 290 (2021). ISSN: 03062619. DOI: 10.1016/j.apenergy.2021.116731.

[51] T. Brown, M. Schäfer, and M. Greiner. “Sectoral interactions as carbon dioxide emissions approach zero in a highly-renewable european energy system”. In: *Energies* 12.6 (2019), pp. 1–16. ISSN: 19961073. DOI: 10.3390/en12061032.

[52] F. Neumann et al. “The potential role of a hydrogen network in Europe”. In: *Joule* 7.8 (Aug. 2023), pp. 1793–1817. ISSN: 25424351. DOI: 10.1016/j.joule.2023.06.016. URL: https://linkinghub.elsevier.com/retrieve/pii/S2542435123002660 (visited on 03/18/2024).

[53] B. Pickering, F. Lombardi, and S. Pfenninger. “Diversity of options to eliminate fossil fuels and reach carbon neutrality across the entire European energy system”. In: *Joule* 6 (6 June 2022), pp. 1253–1276. ISSN: 2542-4351. DOI: 10.1016/J.JOULE.2022.05.009.

[54] D. Bogdanov et al. "Full energy sector transition towards 100% renewable energy supply: Integrating power, heat, transport and industry sectors including desalination". In: *Applied Energy* 283 (Feb. 1, 2021). Publisher: Elsevier, p. 116273. ISSN: 0306-2619. DOI: 10.1016/J.APENERGY.2020.116273. (Visited on 01/30/2023).

[55] D. G. Caglayan et al. "Robust design of a future 100% renewable european energy supply system with hydrogen infrastructure". In: *International Journal of Hydrogen Energy* 46.57 (Aug. 18, 2021). Publisher: Elsevier Ltd, pp. 29376–29390. ISSN: 03603199. DOI: 10.1016/j.ijhydene.2020.12.197.

[56] G. Limpens, H. Jeanmart, and F. Maréchal. "Belgian Energy Transition: What Are the Options?" In: *Energies* 13 (1 2020), p. 261. ISSN: 1996-1073. DOI: 10.3390/en13010261.

[57] S. Moret, M. Bierlaire, and F. Maréchal. "Strategic Energy Planning under Uncertainty: A Mixed-Integer Linear Programming Modeling Framework for Large-Scale Energy Systems". In: *Computer Aided Chemical Engineering*. Vol. 38. Elsevier, 2016, pp. 1899–1904. DOI: 10.1016/B978-0-444-63428-3.50321-0.

[58] J. F. DeCarolis. "Using modeling to generate alternatives (MGA) to expand our thinking on energy futures". In: *Energy Economics* 33 (2 2011), pp. 145–152. ISSN: 01409883. DOI: 10.1016/j.eneco.2010.05.002. URL: http://dx.doi.org/10.1016/j.eneco.2010.05.002.

[59] L. G. Fishbone and H. Abilock. "Markal, a Linear-Programming Model for Energy Systems Analysis: Technical Description of the Bnl Version". en. In: *International Journal of Energy Research* 5.4 (Jan. 1981), pp. 353–375. ISSN: 1099-114X. DOI: 10.1002/er.4440050406. (Visited on 11/28/2014).

[60] S. Simoes et al. *The JRC-EU-TIMES model. Assessing the long-term role of the SET Plan Energy technologies*. Tech. rep. EUR 26292 EN. 2013, p. 382. DOI: 10.2790/97596.

[61] K. Hunter, S. Sreepathi, and J. F. DeCarolis. "Modeling for insight using Tools for Energy Model Optimization and Analysis (Temoa)". In: *Energy Economics* 40 (2013), pp. 339–349. ISSN: 01409883. DOI: 10.1016/j.eneco.2013.07.014.

[62] H. Eshraghi, A. R. De Queiroz, and J. F. DeCarolis. "US Energy-Related Greenhouse Gas Emissions in the Absence of Federal Climate Policy". In: *Environmental Science & Technology* 52.17 (Sept. 4, 2018), pp. 9595–9604. ISSN: 0013-936X, 1520-5851. DOI: 10.1021/acs.est.8b01586. URL: https://pubs.acs.org/doi/10.1021/acs.est.8b01586 (visited on 06/20/2024).

[63] S. Pfenninger et al. "The importance of open data and software: Is energy research lagging behind?" In: *Energy Policy* 101 (October 2016 2017), pp. 211–215. ISSN: 03014215. DOI: 10.1016/j.enpol.2016.11.046.

[64] G. Lopez et al. "Assessing European supply chain configurations for sustainable e-polyethylene production from sustainable CO2 and renewable electricity". In: *Energy Conversion and Management* 306 (Apr. 15, 2024), p. 118295. ISSN: 0196-8904. DOI: 10.1016/j.enconman.2024.118295. URL: https://www.sciencedirect.com/science/article/pii/S019689042400236X (visited on 03/20/2024).

[65] P. Perey and M. Mulder. "International competitiveness of low-carbon hydrogen supply to the Northwest European market". In: *International Journal of Hydrogen Energy* (Oct. 2022). ISSN: 03603199. DOI: 10.1016/j.ijhydene.2022.10.011. URL: https://linkinghub.elsevier.com/retrieve/pii/S0360319922046341.

[66] F. Contino et al. "Whole-energy system models: The advisors for the energy transition". In: *Progress in Energy and Combustion Science* 81 (2020), p. 100872. URL: https://doi.org/10.1016/j.pecs.2020.100872.

[67] T. Brown et al. "Synergies of sector coupling and transmission reinforcement in a cost-optimised, highly renewable European energy system". In: *Energy* 160 (2018), pp. 720–739.

[68] E. Cabrera and J. M. M. de Sousa. "Use of Sustainable Fuels in Aviation—A Review". In: *Energies* 15.7 (Jan. 2022). Number: 7 Publisher: Multidisciplinary Digital Publishing Institute, p. 2440. ISSN: 1996-1073. DOI: 10.3390/en15072440. URL: https://www.mdpi.com/1996-1073/15/7/2440 (visited on 05/08/2024).

[69] J. Soone. *Sustainable maritime fuels - Fit for 55 package: The FuelEU Maritime proposal.* Brussels: European Parliamentary Research Service, Nov. 2023.

[70] G. Pawelec and C.-F. Berthon. *System-Based Solutions for H2-Fuelled Water Transport in North-West Europe: Comparative report on alternative fuels for ship propulsion.* H2SHIPS - Interreg North-West Europe, July 2020. URL: https://vb.nweurope.eu/media/14694/210225_h2ships_t232_compassesmtaltfuels-02.pdf (visited on 05/08/2024).

[71] H. Blanco et al. "Potential of Power-to-Methane in the EU energy transition to a low carbon system using cost optimization". In: *Applied Energy* 232 (August 2018). Publisher: Elsevier, pp. 323–340. ISSN: 0306-2619. DOI: 10.1016/j.apenergy.2018.08.027. URL: https://doi.org/10.1016/j.apenergy.2018.08.027.

[72] G. S. Seck et al. “Hydrogen and the decarbonization of the energy system in europe in 2050: A detailed model-based analysis”. In: *Renewable and Sustainable Energy Reviews* 167 (Oct. 1, 2022), p. 112779. ISSN: 1364-0321. DOI: 10.1016/j.rser.2022.112779. URL: https://www.sciencedirect.com/science/article/pii/S1364032122006633 (visited on 04/05/2024).

[73] M. Colla, J. Blondeau, and H. Jeanmart. “Optimal use of lignocellulosic biomass for the energy transition , including the non-energy demand : the case of the Belgian energy system”. In: *Frontiers in Energy Research* 10 (March 2022), pp. 1–12. DOI: 10.3389/fenrg.2022.802327.

[74] M. Colla et al. *Navigating Bioenergy Horizons: A Critical Examination of Europe’s Potential, with Belgium as a Case Study*. Apr. 1, 2024. DOI: 10.21203/rs.3.rs-4168347/v1. URL: https://www.researchsquare.com/article/rs-4168347/v1 (visited on 04/08/2024).

[75] World Bioenergy Association. *GLOBAL BIOENERGY STATISTICS 2020*. 2020.

[76] X. Rixhon et al. “Taxonomy of the Fuels in a Whole-Energy System”. In: 9 (June 2021), pp. 1–6. DOI: 10.3389/fenrg.2021.660073.

[77] S. Pfenninger et al. “Opening the black box of energy modelling: Strategies and lessons learned”. In: *Energy Strategy Reviews* 19 (2018), pp. 63–71.

[78] L. Kotzur et al. “A modeler’s guide to handle complexity in energy systems optimization”. In: *Advances in Applied Energy* 4 (August 2021), p. 100063. ISSN: 26667924. DOI: 10.1016/j.adapen.2021.100063. URL: https://doi.org/10.1016/j.adapen.2021.100063.

[79] K. K. Cao et al. “Classification and evaluation of concepts for improving the performance of applied energy system optimization models”. In: *Energies* 12 (24 2019). ISSN: 19961073. DOI: 10.3390/en12244656.

[80] M. Hoffmann et al. “A review on time series aggregation methods for energy system models”. In: *Energies* 13 (3 2020). ISSN: 19961073. DOI: 10.3390/en13030641.

[81] D. Coppitters, W. De Paepe, and F. Contino. “Surrogate-assisted robust design optimization and global sensitivity analysis of a directly coupled photovoltaic-electrolyzer system under techno-economic uncertainty”. In: *Applied Energy* 248 (2019), pp. 310–320.

[82] K. Riahi et al. “The Shared Socioeconomic Pathways and their energy, land use, and greenhouse gas emissions implications: An overview”. In: *Global Environmental Change* 42 (Jan. 1, 2017), pp. 153–168. ISSN: 0959-3780. DOI: 10.1016/j.gloenvcha.2016.05.009. URL: https://www.sciencedirect.com/science/article/pii/S0959378016300681 (visited on 05/12/2024).

[83] J. Finke, C. Weber, and V. Bertsch. *Linking Modelling to Generate Alternatives, Multi-Objective Optimisation and Market Equilibria – On the Economic Interpretation of Near-Cost-Optimal Solutions in Energy System Models.* Rochester, NY, Apr. 30, 2024. DOI: 10.2139/ssrn.4812751. URL: https://papers.ssrn.com/abstract=4812751 (visited on 06/25/2024).

[84] P. B. Berntsen and E. Trutnevyte. “Ensuring diversity of national energy scenarios: Bottom-up energy system model with Modeling to Generate Alternatives”. In: *Energy* 126 (2017). Publisher: Elsevier Ltd, pp. 886–898. ISSN: 03605442. DOI: 10.1016/j.energy.2017.03.043.

[85] A. Dubois and D. Ernst. “Computing necessary conditions for near-optimality in capacity expansion planning problems”. In: *Electric Power Systems Research* 211 (Oct. 1, 2022). Publisher: Elsevier, p. 108343. ISSN: 0378-7796. DOI: 10.1016/J.EPSR.2022.108343. arXiv: 2109.14272. (Visited on 01/09/2023).

[86] A. Dubois et al. “Multi-objective near-optimal necessary conditions for multi-sectoral planning”. In: *Applied Energy* 350 (Nov. 15, 2023), p. 121789. ISSN: 0306-2619. DOI: 10.1016/j.apenergy.2023.121789. URL: https://www.sciencedirect.com/science/article/pii/S0306261923011534 (visited on 08/28/2023).

[87] A. Grochowicz et al. “Intersecting near-optimal spaces: European power systems with more resilience to weather variability”. In: *Energy Economics* (2023), p. 106496. URL: http://arxiv.org/abs/2206.12242.

[88] F. Lombardi et al. “Policy Decision Support for Renewables Deployment through Spatially Explicit Practically Optimal Alternatives”. In: *Joule* 4 (10 2020), pp. 2185–2207. ISSN: 25424351. DOI: 10.1016/j.joule.2020.08.002. URL: https://doi.org/10.1016/j.joule.2020.08.002.

[89] F. Neumann and T. Brown. “The near-optimal feasible space of a renewable power system model”. In: *Electric Power Systems Research* 190 (Jan. 2021). ISSN: 03787796. DOI: 10.1016/j.epsr.2020.106690.

[90] F. Neumann and T. Brown. “Broad ranges of investment configurations for renewable power systems, robust to cost uncertainty and near-optimality”. In: *iScience* 26.5 (May 19, 2023), p. 106702. ISSN: 2589-0042. DOI: 10.1016/j.isci.2023.106702. URL: https://www.sciencedirect.com/science/article/pii/S2589004223007794 (visited on 05/10/2024).

[91] T. T. Pedersen et al. “Modeling all alternative solutions for highly renewable energy systems”. In: *Energy* 234 (Nov. 1, 2021), p. 121294. ISSN: 0360-5442. DOI: 10.1016/j.energy.2021.121294. URL: https://www.sciencedirect.com/science/article/pii/S0360544221015425 (visited on 05/10/2024).

[92] T. T. Pedersen et al. “Using Modeling All Alternatives to explore 55% decarbonization scenarios of the European electricity sector”. In: *ISCIENCE* (2023), p. 106677. DOI: 10.1016/j.isci.2023.106677. URL: https://doi.org/10.1016/j.isci.2023.106677. (visited on 04/24/2023).

[93] J. Price and I. Keppo. “Modelling to generate alternatives: A technique to explore uncertainty in energy-environment-economy models”. In: *Applied Energy* 195 (2017), pp. 356–369. ISSN: 03062619. DOI: 10.1016/j.apenergy.2017.03.065. URL: http://dx.doi.org/10.1016/j.apenergy.2017.03.065.

[94] H. Schwaeppe et al. “Finding better alternatives: Shadow prices of near-optimal solutions in energy system optimization modeling”. In: *Energy* 292 (Apr. 1, 2024), p. 130558. ISSN: 0360-5442. DOI: 10.1016/j.energy.2024.130558. URL: https://www.sciencedirect.com/science/article/pii/S036054422400330X (visited on 02/07/2024).

[95] P. Voll et al. “The optimum is not enough: A near-optimal solution paradigm for energy systems synthesis”. In: *Energy* 82 (Mar. 15, 2015). Publisher: Elsevier Ltd, pp. 446–456. ISSN: 03605442. DOI: 10.1016/j.energy.2015.01.055.

[96] M. G. Prina et al. “Classification and challenges of bottom-up energy system models-A review”. In: *Renewable and Sustainable Energy Reviews* 129 (2020), p. 109917.

[97] B. Muyldermans et al. “Multi-criteria optimisation of an energy system and application to the Belgian case”. MA thesis. Louvain-la-Neuve, Belgium: Université Catholique de Louvain, 2021. URL: http://hdl.handle.net/2078.1/thesis:33139.

[98] G. Limpens et al. “The impact of uncertainties on the Belgian energy system : application of the Polynomial Chaos Expansion to the EnergyScope TD model .” In: *ECOS2020 - The 33nd International Conference on efficiency, cost, optimization, simulation and environmental impact of energy systems, Osaka, Japan June 29-July 3*. 2020.

[99] G. Limpens. “Generating energy transition pathways : application to Belgium”. PhD thesis. Louvain-la-Neuve, Belgium: Université Catholique de Louvain, 2021.

[100] G. Limpens et al. “The role of storage in the Swiss energy transition”. In: *ECOS2019 - The 32nd International Conference on efficiency, cost, optimization, simulation and environmental impact of energy systems, Wroclac, Poland, June 23-28*. 2019.

[101] X. Rixhon et al. “Integration of non-energy among the end-use demands of bottom-up whole-energy system models”. In: *Frontiers in Energy Research* 10 (Sept. 2022). ISSN: 2296-598X. DOI: 10.3389/fenrg.2022.904777. URL: https://www.frontiersin.org/articles/10.3389/fenrg.2022.904777/full.

[102] P. Thiran et al. “Flexibility options in a multi-regional whole-energy system : the role of energy carriers in the Italian energy transition”. In: *ECOS2021 - The 34th International Conference on Efficiency, Cost, Optimization, Simulation and Environmental Impact of Energy Systems, Taormina, Italy, June 28–2 July*. 2021.

[103] A. Hernandez et al. “EnergyScope Multi-Cell : A novel open-source model for multi-regional energy systems and application to a 3-cell , low-carbon energy”. MA thesis. Louvain-la-Neuve, Belgium: Université Catholique de Louvain, 2020. URL: http://hdl.handle.net/2078.1/thesis:25229.

[104] N. Cornet et al. “Energy Exchanges between Countries for a Future Low-Carbon Western Europe By merging cells in EnergyScope MC to handle wider regions”. MA thesis. Louvain-la-Neuve, Belgium: Université Catholique de Louvain, 2021.

[105] P. Thiran, H. Jeanmart, and F. Contino. “Validation of a Method to Select a Priori the Number of Typical Days for Energy System Optimisation Models”. In: *Energies 2023, Vol. 16, Page 2772* 16.6 (Mar. 16, 2023). Publisher: Multidisciplinary Digital Publishing Institute, p. 2772. ISSN: 1996-1073. DOI: 10.3390/EN16062772. URL: https://www.mdpi.com/1996-1073/16/6/2772/htm (visited on 04/07/2023).

[106] S. Moret et al. “Characterization of input uncertainties in strategic energy planning models”. In: *Applied Energy* 202 (September 2017), pp. 597–617. ISSN: 03062619. DOI: 10.1016/j.apenergy.2017.05.106.

[107] J. Jacquemin, S. Quoilin, and P. Thiran. “Decarbonizing western Europe: an optimal integration of renewable fuels and hydrogen in transitioning to net zero emissions”. PhD thesis. Université de Liège, 2023. URL: http://hdl.handle.net/2268.2/18053.

[108] J. Jacquemin, P. Thiran, and S. Quoilin. “Decarbonizing Western Europe: Extension of the Model ’EnergyScope MultiCell’ for the Analysis of Renewable Fuel Potential”. In: 4th LA Conference on Sustainable Development of Energy, Water and Environment Systems (SDEWES). 2024.

[109] J. Dommisse and J.-L. Tychon. “Modelling of Low Carbon Energy Systems for 26 European Countries with EnergyScopeTD : Can European Energy Systems Reach Carbon Neutrality Independently?” MA thesis. UCLouvain, 2020. URL: http://hdl.handle.net/2078.1/thesis:25202.

[110] P. Ruiz et al. “ENSPRESO - an open, EU-28 wide, transparent and coherent database of wind, solar and biomass energy potentials”. In: *Energy Strategy Reviews* 26 (June 2019 2019). Publisher: Elsevier, p. 100379. ISSN: 2211467X. DOI: 10.1016/j.esr.2019.100379. URL: https://doi.org/10.1016/j.esr.2019.100379.

[111] European Commission, Joint Research Centre (JRC) (2019). *JRC Hydro-power database.* European Commission, Joint Research Centre (JRC) [Dataset]. Apr. 10, 2019. URL: http://data.europa.eu/89h/52b00441-d3e0-44e0-8281-fda86a63546d (visited on 01/31/2024).

[112] e-Highway 2050. *Database per country*. 2016. URL: https://docs.entsoe.eu/baltic-conf/bites/www.e-highway2050.eu/fileadmin/documents/Results/e-Highway_database_per_country-08022016.xlsx (visited on 05/09/2024).

[113] M. Gimeno-Gutiérrez and R. Lacal-Arántegui. “Assessment of the European potential for pumped hydropower energy storage based on two existing reservoirs”. In: *Renewable Energy* 75 (Mar. 1, 2015), pp. 856–868. ISSN: 0960-1481. DOI: 10.1016/j.renene.2014.10.068. URL: https://www.sciencedirect.com/science/article/pii/S096014811400706X (visited on 10/16/2023).

[114] Danish Energy Agency. *Technology Data for Energy Plants for Electricity and District heating generation - Feb. 2019*. Tech. rep. February. 2019.

[115] P. Thiran et al. *EnergyScopeMC repository*. 2024. URL: https://github.com/energyscope/EnergyScope_multi_cells (visited on 04/08/2024).

[116] P. Thiran et al. *EnergyScopeMC documentation 1.3*. 2024. URL: https://energyscope-multi-cells.readthedocs.io/en/master/ (visited on 04/08/2024).

[117] P. Thiran, H. Jeanmart, and F. Contino. *Application of EnergyScope Multi-Cells to a fossil-free European energy system (Zenodo repository)*. 2024. URL: https://doi.org/10.5281/zenodo.11144189.

[118] R. Fourer, D. M. Gay, and B. W. Kernighan. "AMPL: A Mathematical Programming Language". In: *Management Science* 36.5 (1990), pp. 519–554.

[119] F. Meinke-Hubeny, L. P. N. De Oliveira, and J. Duerinck. *Energy Transition in Belgium – Choices and Costs*. Tech. rep. 2017, p. 35.

[120] P. Capros et al. "EU Reference Scenario 2016-Energy, transport and GHG emissions Trends to 2050." In: *European Commission Directorate-General for Energy, Directorate-General for ...* (2016).

[121] R. van Rossum et al. *European Hydrogen Bakcbone: A European hydrogen infrastructure vision covering 28 countries*. European Hydrogen Backbone, Apr. 2022.

[122] European Commission - Eurostat. *Statistical pocketbook 2017*. Tech. rep. 4. 2017, pp. 474–478. DOI: 10.2832/147440.

[123] G. Limpens et al. "EnergyScope TD: A novel open-source model for regional energy systems". In: *Applied Energy* 255.March (2019), p. 113729. ISSN: 03062619.

[124] E. Dupont, R. Koppelaar, and H. Jeanmart. "Global available solar energy under physical and energy return on investment constraints". In: *Applied Energy* 257 (January 2020), p. 113968. ISSN: 03062619. DOI: 10.1016/j.apenergy.2019.113968.

[125] M. Pavicevic et al. "Bi-directional soft-linking between a whole energy system model and a power systems model". In: *2022 IEEE PES/IAS PowerAfrica*. IEEE, Aug. 22, 2022, pp. 1–5. ISBN: 978-1-66546-639-4. DOI: 10.1109/PowerAfrica53997.2022.9905392. URL: https://ieeexplore.ieee.org/document/9905392/.

[126] S. Quoilin, I. Hidalgo Gonzalez, and A. Zucker. *JRC TECHNICAL REPORTS Modelling Future EU Power Systems Under High Shares of Renewables*. Tech. rep. European Union, 2017. DOI: 10.2760/25400.

[127] Danish Energy Agency. *Technology catalogues*. Aug. 25, 2016. URL: https://ens.dk/en/our-services/technology-catalogues (visited on 05/08/2024).

[128] Danish Energy Agency. *Technology data for Energy storage*. Tech. rep. November 2018. 2018. arXiv: ISBNwww:978-87-7844-931-3.

[129] Danish Energy Agency. *Technology Data for Renewable Fuels - 0001*. Tech. rep. February. 2019, pp. 1–235. URL: www.ens.dk.

[130] P Capros et al. *EU Reference scenario 2020 : Energy, transport and GHG emissions - Trends to 2050*. European Commission Directorate-General for Energy, Directorate-General for Climate Action, Directorate-General for Mobility and Transport, 2021. DOI: doi/10.2833/35750.

[131] F. Clora and W. Yu. “GHG emissions, trade balance, and carbon leakage: Insights from modeling thirty-one European decarbonization pathways towards 2050”. In: *Energy Economics* 113 (Sept. 1, 2022), p. 106240. ISSN: 0140-9883. DOI: 10.1016/j.eneco.2022.106240. URL: https://www.sciencedirect.com/science/article/pii/S014098832200384X (visited on 05/08/2024).

[132] Potsdam Institute for Climate Impact Research. *EUCalc*. 2022. URL: http://tool.european-calculator.eu/intro (visited on 04/15/2021).

[133] T. Fleiter et al. *Profile of heating and cooling demand in 2015*. Heat Roadmap Europe, 2017. URL: https://heatroadmap.eu/wp-content/uploads/2018/11/HRE4_D3.1.pdf (visited on 05/08/2024).

[134] *Heat Roadmap Europe*. 2019. URL: https://heatroadmap.eu/ (visited on 11/09/2020).

[135] European Commission. *Eurostat - Statistics on the production of manufactured goods*. 2023. URL: https://ec.europa.eu/eurostat/web/prodcom/database (visited on 05/08/2024).

[136] UNFCCC. *National Inventory Submissions*. 2023. URL: https://unfccc.int/ghg-inventories-annex-i-parties/2023 (visited on 05/08/2024).

[137] World Bank. *World Integrated Trade Solution*. 2023. URL: https://wits.worldbank.org/trade/comtrade/en/country/ALL/year/2019/tradeflow/Imports/partner/WLD/product/291211 (visited on 05/08/2024).

[138] European Commission. *Eurostat - Air transport measurment - passengers*. Jan. 28, 2024. URL: https://ec.europa.eu/eurostat/databrowser/explore/all/transp?lang=en&subtheme=avia.avia_pa&display=list&sort=category (visited on 03/18/2024).

[139] EUROCONTROL. *Aviation Outlook 2050*. Apr. 2022.

[140] International Energy Agency. *The Future of Petrochemicals*. OECD/IEA, 2018.

[141] M. Barrientos and C. Soria. *IndexMundi - Country Facts*. 2023. URL: https://www.indexmundi.com/ (visited on 05/08/2024).

[142] R. Neiva et al. *Research for TRAN Committee – Investment scenario and roadmap for achieving aviation Green Deal objectives by 2050*. Brussels: European Parliament, Policy Department for Structural and Cohesion Policies, Sept. 2022.

[143] European Commission. *Eurostat - Maritime freight and vessels statistics*. 2022. URL: https://ec.europa.eu/eurostat/statistics-explained/index.php?title=Maritime_freight_and_vessels_statistics (visited on 05/08/2024).

[144] C. R. Hansen. *Preparing Container Vessels for Conversion to Green Fuels: A technical, environmental, and techno-economic analysis of the impacts of preparation and conversion*. Mærsk Mc-Kinney Møller Center for Zero Carbon Shipping, 2022.

[145] European Maritime Safety Agency. *Update on potential of biofuels in shipping*. Lisbon: ESMA, 2022.

[146] Statbank Norway. *11403: Domestic goods transport, by mode of transport 2010 - 2022*. 2023. URL: https://www.ssb.no/en/statbank/table/11403/ (visited on 05/08/2024).

[147] Statbank Norway. *Air transport*. 2024. URL: https://www.ssb.no/en/transport-og-reiseliv/luftfart/statistikk/lufttransport (visited on 05/08/2024).

[148] ODYSSEE-MURE. *Norway energy efficiency & Trends policies | Norway profile*. 2018. URL: https://www.odyssee-mure.eu/publications/efficiency-trends-policies-profiles/norway.html (visited on 05/08/2024).

[149] International Energy Agency. *Norway 2022: Energy Policy Review*. IEA, 2022. URL: https://iea.blob.core.windows.net/assets/de28c6a6-8240-41d9-9082-a5dd65d9f3eb/NORWAY2022.pdf (visited on 05/08/2024).

[150] European Commission. *Eurostat - Population projections*. 2024. URL: https://ec.europa.eu/eurostat/databrowser/view/TPS00002__custom_6059246/default/table (visited on 05/08/2024).

[151] United Nations. *UN Population Division Data Portal*. 2024. URL: https://population.un.org/dataportal/data/indicators/49/locations/8,70,300,191,412,100,499,642,807,688/start/2015/end/2050/table/pivotbylocation?df=84ab8336-7e4f-4846-8b42-edab14ca13c9 (visited on 05/08/2024).

[152] ENTSO-E. *ENTSO-E Transparency Platform*. URL: https://transparency.entsoe.eu/dashboard/show (visited on 05/09/2024).

[153] M. M. Rienecker et al. "MERRA: NASA's Modern-Era Retrospective Analysis for Research and Applications". In: *Journal of Climate* 24.14 (July 15, 2011). Publisher: American Meteorological Society Section: Journal of Climate, pp. 3624–3648. ISSN: 0894-8755, 1520-0442. DOI: 10.1175/JCLI-D-11-00015.1. URL: https://journals.ametsoc.org/view/journals/clim/24/14/jcli-d-11-00015.1.xml (visited on 05/09/2024).

[154] A. Santos et al. *Summary of Travel Trends: 2009 National Household Travel Survey*. FHWA-PL-11-022. June 1, 2011. URL: https://rosap.ntl.bts.gov/view/dot/50506 (visited on 05/07/2024).

[155] OPSD. *Open Power System Data – A platform for open data of the European power system.* 2020. URL: https://open-power-system-data.org/ (visited on 05/09/2024).

[156] I. Staffell, S. Pfenninger, and N. Johnson. "A global model of hourly space heating and cooling demand at multiple spatial scales". In: *Nature Energy* (Sept. 14, 2023). Publisher: Nature Publishing Group, pp. 1–17. ISSN: 2058-7546. DOI: 10.1038/s41560-023-01341-5. URL: https://www.nature.com/articles/s41560-023-01341-5 (visited on 10/05/2023).

[157] E. Dupont, R. Koppelaar, and H. Jeanmart. "Global available wind energy with physical and energy return on investment constraints". In: *Applied Energy* 209 (Jan. 2018), pp. 322–338. ISSN: 03062619. DOI: 10.1016/j.apenergy.2017.09.085.

[158] E. Dupont and H. Jeanmart. "Global potential of wind and solar energy with physical and energy return on investment (EROI) constraints; application at the European level (EU 28 countries)". In: *ECOS 2019 - Proceedings of the 32nd International Conference on Efficiency, Cost, Optimization, Simulation and Environmental Impact of Energy Systems* (2019). ISBN: 9788361506515, pp. 489–503.

[159] R. C. P et al. *The JRC-EU-TIMES model. Bioenergy potentials for EU and neighbouring countries.* Scientific analysis or review LD-NA-27575-EN-C (print),LD-NA-27575-EN-N (online). Luxembourg (Luxembourg), 2015. DOI: 10.2790/01017(print),10.2790/39014(online).

[160] C. R. Chamorro et al. "Enhanced geothermal systems in Europe: An estimation and comparison of the technical and sustainable potentials". In: *Energy* 65 (Feb. 1, 2014), pp. 250–263. ISSN: 0360-5442. DOI: 10.1016/j.energy.2013.11.078. URL: https://www.sciencedirect.com/science/article/pii/S0360544213010487 (visited on 04/30/2024).

[161] T. J. Hammons. "Tidal Power in the UK and Worldwide to Reduce Greenhouse Gas Emissions". In: *International Journal of Engineering Business Management* 3 (Jan. 1, 2011), p. 13. ISSN: 1847-9790, 1847-9790. DOI: 10.5772/50933. URL: http://journals.sagepub.com/doi/10.5772/50933 (visited on 04/30/2024).

[162] T. Tröndle, S. Pfenninger, and J. Lilliestam. "Home-made or imported: On the possibility for renewable electricity autarky on all scales in Europe". In: *Energy Strategy Reviews* 26 (2019), pp. 1–28. ISSN: 2211467X. DOI: 10.1016/j.esr.2019.100388.

[163] D. S. Ryberg, M. Robinius, and D. Stolten. "Evaluating land eligibility constraints of renewable energy sources in Europe". In: *Energies* 11.5 (2018). ISSN: 19961073. DOI: 10.3390/en11051246.

[164] D. S. Ryberg et al. “The future of European onshore wind energy potential: Detailed distribution and simulation of advanced turbine designs”. In: *Energy* 182 (Sept. 1, 2019), pp. 1222–1238. ISSN: 0360-5442. DOI: 10.1016/j.energy.2019.06.052. URL: https://www.sciencedirect.com/science/article/pii/S0360544219311818 (visited on 05/09/2024).

[165] D. S. Ryberg et al. “Uniformly constrained land eligibility for onshore European wind power”. In: *Renewable Energy* 146 (Feb. 1, 2020), pp. 921–931. ISSN: 0960-1481. DOI: 10.1016/j.renene.2019.06.127. URL: https://www.sciencedirect.com/science/article/pii/S0960148119309619 (visited on 05/09/2024).

[166] D. G. Caglayan et al. “The techno-economic potential of offshore wind energy with optimized future turbine designs in Europe”. In: *Applied Energy* 255 (August 2019). Publisher: Elsevier, p. 113794. ISSN: 03062619. DOI: 10.1016/j.apenergy.2019.113794. URL: https://doi.org/10.1016/j.apenergy.2019.113794.

[167] J. Bosch, I. Staffell, and A. D. Hawkes. “Temporally explicit and spatially resolved global offshore wind energy potentials”. In: *Energy* 163 (Nov. 15, 2018), pp. 766–781. ISSN: 0360-5442. DOI: 10.1016/j.energy.2018.08.153. URL: https://www.sciencedirect.com/science/article/pii/S036054421831689X (visited on 08/08/2023).

[168] R. McKenna et al. “High-resolution large-scale onshore wind energy assessments: A review of potential definitions, methodologies and future research needs”. In: *Renewable Energy* 182 (Jan. 1, 2022). Publisher: Pergamon, pp. 659–684. ISSN: 0960-1481. DOI: 10.1016/J.RENENE.2021.10.027. (Visited on 10/12/2022).

[169] European Commission. *Eurostat - Electricity production capacities for renewable and waste*. Jan. 28, 2024. URL: https://ec.europa.eu/eurostat/databrowser/view/nrg_inf_epcrw__custom_9459927/default/table (visited on 03/18/2024).

[170] Joint Research Centre (JRC) European Commission. *JRC Hydro-power database*. Publisher: European Commission, Joint Research Centre (JRC). Apr. 10, 2019. URL: http://data.europa.eu/89h/52b00441-d3e0-44e0-8281-fda86a63546d (visited on 01/31/2024).

[171] G. Costanzo and G. Brindley. *Wind energy in Europe - 2023 Statistics and the outlook for 2024-2030*. WindEurope, 2023.

[172] T. Van der Straeten et al. *Ostend declaretation of energy ministers on the North Seas as Europe’s green power plant*. Ostend, May 18, 2022. URL: https://kefm.dk/Media/638179241345565422/Declaration%20ENERGY_FINAL_21042023.pdf (visited on 05/09/2024).

[173] M. Gronau, A. Dusch, and K. Strunz. *Modular Development Plan of the Pan-European Transmission System 2050*. e-Highway 2050, 2015. URL: https://docs.entsoe.eu/baltic-conf/bites/www.e-highway2050.eu/fileadmin/documents/Results/D4.3-Data_sets_of_scenarios_and_intermediate_grid_architectures_for_2040-20151202.pdf (visited on 05/09/2024).

[174] M. Gimeno-Gutiérrez and R. Lacal-Arántegui. "Assessment of the European potential for pumped hydropower energy storage". In: January 2013 (2013). ISSN: 18790682. DOI: 10.2790/86815.

[175] B. Elbersen et al. *Atlas of EU biomass potentials: spatially detailed and quantified overview of EU biomass potential taking into account the main criteria determining biomass availability from different sources*. IEE 08653 S12.529 241. IIASA, 2012.

[176] IEA-SHC. *Recommendation: Converting solar thermal collector area into installed capacity*. 2004. URL: https://www.iea-shc.org/data/sites/1/documents/statistics/technical_note-new_solar_thermal_statistics_Conversion.pdf (visited on 05/09/2024).

[177] L. Rybach and M. Mongillo. "Geothermal sustainability-a review with identified research needs". In: *GRC Transactions* 30 (2006), pp. 1083–1090.

[178] L. Rybach. "Geothermal Sustainability". In: (2007).

[179] E. Dupont. *World EROI*. original-date: 2022-03-11T13:55:16Z. July 5, 2022. URL: https://github.com/EliseDup/WorldEROI (visited on 05/09/2024).

[180] E. Dupont. "Potential of wind and solar resources and macroeconomic implications of the energy transition". PhD thesis. UCLouvain, June 2021. URL: https://dial.uclouvain.be/pr/boreal/object/boreal%3A248075/datastream/PDF_01/view (visited on 05/09/2024).

[181] S. Pfenninger and I. Staffell. *Renewables.ninja*. 2016. URL: https://www.renewables.ninja/ (visited on 05/09/2024).

[182] S. Pfenninger and I. Staffell. "Long-term patterns of European PV output using 30 years of validated hourly reanalysis and satellite data". In: *Energy* 114 (2016). Publisher: Elsevier Ltd, pp. 1251–1265. ISSN: 03605442. DOI: 10.1016/j.energy.2016.08.060. URL: http://dx.doi.org/10.1016/j.energy.2016.08.060.

[183] I. Staffell and S. Pfenninger. "Using bias-corrected reanalysis to simulate current and future wind power output". In: *Energy* 114 (2016). Publisher: Elsevier Ltd, pp. 1224–1239. ISSN: 03605442. DOI: 10.1016/j.energy.2016.08.068. URL: http://dx.doi.org/10.1016/j.energy.2016.08.068.

[184] R. Müller et al. “Digging the METEOSAT Treasure—3 Decades of Solar Surface Radiation”. In: *Remote Sensing* 7.6 (June 2015). Number: 6 Publisher: Multidisciplinary Digital Publishing Institute, pp. 8067–8101. ISSN: 2072-4292. DOI: 10.3390/rs70608067. URL: https://www.mdpi.com/2072-4292/7/6/8067 (visited on 05/09/2024).

[185] F. Onea, E. Rusu, and L. Rusu. “Assessment of the Offshore Wind Energy Potential in the Romanian Exclusive Economic Zone”. In: *Journal of Marine Science and Engineering* 9.5 (May 2021). Number: 5 Publisher: Multidisciplinary Digital Publishing Institute, p. 531. ISSN: 2077-1312. DOI: 10.3390/jmse9050531. URL: https://www.mdpi.com/2077-1312/9/5/531 (visited on 04/30/2024).

[186] OEMOF. *OEMOF Thermal*. 2014. URL: https://oemof-thermal.readthedocs.io/en/latest/# (visited on 05/09/2024).

[187] N. Janotte et al. “Dynamic Performance Evaluation of the HelioTrough® Collector Demonstration Loop–Towards a New Benchmark in Parabolic Trough Qualification”. In: *Energy Procedia*. Proceedings of the SolarPACES 2013 International Conference 49 (Jan. 1, 2014), pp. 109–117. ISSN: 1876-6102. DOI: 10.1016/j.egypro.2014.03.012. URL: https://www.sciencedirect.com/science/article/pii/S1876610214004664 (visited on 05/09/2024).

[188] W. F. Holmgren, C. W. Hansen, and M. A. Mikofski. “pvlib python: a python package for modeling solar energy systems”. In: *Journal of Open Source Software* 3.29 (Sept. 7, 2018), p. 884. ISSN: 2475-9066. DOI: 10.21105/joss.00884. URL: https://joss.theoj.org/papers/10.21105/joss.00884 (visited on 05/09/2024).

[189] European Commission and Joint Research Centre (JRC). *SARAH-2 Solar Radiation Data - European Commission*. 2021. URL: https://joint-research-centre.ec.europa.eu/photovoltaic-geographical-information-system-pvgis/pvgis-data-download/sarah-2-solar-radiation-data_en (visited on 05/09/2024).

[190] European Commission and Joint Research Centre (JRC). *Photovoltaic Geographical Information System (PVGIS) - European Commission*. Feb. 14, 2024. URL: https://joint-research-centre.ec.europa.eu/photovoltaic-geographical-information-system-pvgis_en (visited on 05/09/2024).

[191] European Commission and Joint Research Centre (JRC). *JRC-EFAS-Hydropower*. Publisher: European Commission, Joint Research Centre (JRC). Oct. 13, 2020. URL: http://data.europa.eu/89h/297b6de3-8c78-4da1-97d4-4c766dc4260d (visited on 05/09/2024).

[192] M. De Felice. “Hydropower information for power system modelling: the JRC-EFAS-Hydropower dataset”. In: *Earth ArXiv* (Oct. 22, 2020). Publisher: EarthArXiv. DOI: https://doi.org/10.31223/X58591. URL: https://eartharxiv.org/repository/view/1735/ (visited on 05/09/2024).

[193] M. De Felice. *ENTSO-E Hydropower modelling data (PECD) in CSV format*. Version 4. Aug. 14, 2020. DOI: 10.5281/zenodo.3985078. URL: https://zenodo.org/records/3985078 (visited on 05/09/2024).

[194] ENTSOE. *ERAA 2021 - Annex 3: Methodology*. 2021. URL: https://eepublicdownloads.azureedge.net/clean-documents/sdc-documents/ERAA/ERAA_2021_Annex_3_Methodology.pdf (visited on 05/09/2024).

[195] L. Genge, F. Scheller, and F. Müsgens. “Supply costs of green chemical energy carriers at the European border: A meta-analysis”. In: *International Journal of Hydrogen Energy* (July 1, 2023). ISSN: 0360-3199. DOI: 10.1016/j.ijhydene.2023.06.180. URL: https://www.sciencedirect.com/science/article/pii/S0360319923030847 (visited on 08/02/2023).

[196] Hydrogen Import Coalition. *Shipping sun and wind to Belgium is key in climate neutral economy Hydrogen Import Coalition - Period 2017-2027*. Tech. rep. April. 2020, p. 13.

[197] M. Victoria, E. Zeyen, and T. Brown. “Speed of technological transformations required in Europe to achieve different climate goals”. In: *Joule* 6.5 (May 18, 2022). Publisher: Cell Press, pp. 1066–1086. DOI: 10.1016/j.joule.2022.04.016. eprint: 2109.09563v2. (Visited on 01/26/2023).

[198] P. Colbertaldo et al. “Clean mobility infrastructure and sector integration in long-term energy scenarios: The case of Italy”. In: *Renewable and Sustainable Energy Reviews* 133 (June 2020). Publisher: Elsevier Ltd, p. 110086. ISSN: 18790690. DOI: 10.1016/j.rser.2020.110086. URL: https://doi.org/10.1016/j.rser.2020.110086.

[199] F. Frischmuth et al. *Quantifying seasonal hydrogen storage demands under cost and market uptake uncertainties in energy system transformation pathways*. Apr. 19, 2024. arXiv: 2404.12974[econ,q-fin]. URL: http://arxiv.org/abs/2404.12974 (visited on 04/26/2024).

[200] I. Kountouris et al. *A unified European hydrogen infrastructure planning to support the rapid scale-up of hydrogen production*. preprint. In Review, Aug. 1, 2023. DOI: 10.21203/rs.3.rs-3185467/v1. URL: https://www.researchsquare.com/article/rs-3185467/v1 (visited on 08/08/2023).

[201] A. Wang et al. *European Hydrogen Backbone*. Issue: July. European Hydrogen Backbone, 2020, p. 24. URL: https://transparency.entsog.eu/.

[202] A. Wang et al. *European Hydrogen Backbone: Analasing future demand, supply, and transport of hydrogen*. European Hydrogen Backbone, June 2021.

[203] European Hydrogen Backbon. “Five hydrogen supply corridors for Europe in 2030”. May 2022.

[204] J. Jens et al. *Extending the European Hydrogen Backbone*. Issue: April. 2021.

[205] Fuel Cells and Hydrogen 2 Joint Undertaking. *Hydrogen roadmap Europe – A sustainable pathway for the European energy transition*. Publications Office, 2016. URL: https://data.europa.eu/doi/10.2843/341510.

[206] B. Vivanco-Martín and A. Iranzo. “Analysis of the European Strategy for Hydrogen: A Comprehensive Review”. In: *Energies* 16.9 (Jan. 2023). Number: 9 Publisher: Multidisciplinary Digital Publishing Institute, p. 3866. ISSN: 1996-1073. DOI: 10.3390/en16093866. URL: https://www.mdpi.com/1996-1073/16/9/3866 (visited on 05/10/2024).

[207] ENTSO-E. *European Resource Adequacy Assessment*. 2022.

[208] ENTSO-E. *TYNDP 2022 Scenario Report*. Apr. 2022.

[209] D. Oeding and B. R. Oswald. *Elektrische Kraftwerke und Netze*. Berlin, Heidelberg: Springer, 2011. ISBN: 978-3-642-19245-6 978-3-642-19246-3. DOI: 10.1007/978-3-642-19246-3. URL: https://link.springer.com/10.1007/978-3-642-19246-3 (visited on 05/10/2024).

[210] ENTSOG. *System development map 2021-2022*. 2022.

[211] OECD and IEA. *The Power of Transformation: Wind, Sun and the Economics of Flexible Power Systems*. OECD/IEA, 2014. URL: https://www.oecd-ilibrary.org/content/publication/9789264208032-en?site=fr (visited on 04/30/2020).

[212] E. Liu, C. Li, and Y. Yang. “Optimal Energy Consumption Analysis of Natural Gas Pipeline”. In: *The Scientific World Journal* 2014 (May 13, 2014). Publisher: Hindawi, e506138. ISSN: 2356-6140. DOI: 10.1155/2014/506138. URL: https://www.hindawi.com/journals/tswj/2014/506138/ (visited on 07/26/2023).

[213] The Engineering Toolbox. *Fuels - Higher and Lower Calorific Values*. 2003. URL: https://www.engineeringtoolbox.com/fuels-higher-calorific-values-d_169.html (visited on 05/10/2024).

[214] A. Flores-Quiroz et al. “A column generation approach for solving generation expansion planning problems with high renewable energy penetration”. In: *Electric Power Systems Research* 136 (2016), pp. 232–241. ISSN: 03787796. DOI: 10.1016/j.epsr.2016.02.011. URL: http://dx.doi.org/10.1016/j.epsr.2016.02.011.

[215] J. H. Roh, M. Shahidehpour, and Y. Fu. “Market-based coordination of transmission and generation capacity planning”. In: *IEEE Transactions on Power Systems* 22 (4 2007), pp. 1406–1419. ISSN: 08858950. DOI: 10.1109/TPWRS.2007.907894.

[216] S. Binato, M. V. F. Pereira, and S. Granville. “A new Benders decomposition approach to solve power transmission network design problems”. In: *IEEE Transactions on Power Systems* 16 (2 2001), pp. 235–240. ISSN: 08858950. DOI: 10.1109/59.918292.

[217] L. Middelhauve, C. Terrier, and F. Maréchal. “Decomposition Strategy for Districts as Renewable Energy Hubs”. In: *IEEE Open Access Journal of Power and Energy* 9 (2022). Conference Name: IEEE Open Access Journal of Power and Energy, pp. 287–297. ISSN: 2687-7910. DOI: 10.1109/OAJPE.2022.3194212. URL: https://ieeexplore.ieee.org/abstract/document/9841579 (visited on 05/10/2024).

[218] C. Haikarainen, F. Pettersson, and H. Saxén. “A decomposition procedure for solving two-dimensional distributed energy system design problems”. In: *Applied Thermal Engineering* 100 (2016), pp. 30–38. ISSN: 13594311. DOI: 10.1016/j.applthermaleng.2016.02.012. URL: http://dx.doi.org/10.1016/j.applthermaleng.2016.02.012.

[219] R Romero and A Monticelli. “A hierarchical decomposition approach for transmission network expansion planning”. In: *IEEE Transactions on Power Systems* 9 (1 1994), pp. 373–380.

[220] K. Poncelet et al. “Impact of the level of temporal and operational detail in energy-system planning models”. In: *Applied Energy* 162 (2016), pp. 631–643. ISSN: 03062619. DOI: 10.1016/j.apenergy.2015.10.100. URL: http://dx.doi.org/10.1016/j.apenergy.2015.10.100.

[221] B. A. Frew and M. Z. Jacobson. “Temporal and spatial tradeoffs in power system modeling with assumptions about storage: An application of the POWER model”. In: *Energy* 117 (Dec. 2016), pp. 198–213. ISSN: 03605442. DOI: 10.1016/j.energy.2016.10.074.

[222] M. Hoffmann et al. “Typical periods or typical time steps ? A multi-model analysis to determine the optimal temporal aggregation for energy system models”. In: *Applied Energy* 304 (2021).

[223] M. Hoffmann, L. Kotzur, and D. Stolten. "The Pareto-Optimal Temporal Aggregation of Energy System Models". In: *Applied Energy* 315 (2022), p. 119029. URL: http://arxiv.org/abs/2111.12072.

[224] H. Teichgraeber and A. R. Brandt. "Time-series aggregation for the optimization of energy systems: Goals, challenges, approaches, and opportunities". In: *Renewable and Sustainable Energy Reviews* 157 (January 2022), p. 111984. ISSN: 13640321. DOI: 10.1016/j.rser.2021.111984. URL: https://doi.org/10.1016/j.rser.2021.111984.

[225] T. Anderski et al. *European cluster model of the Pan-European transmission grid.* Tech. rep. eHIGHWAY2050, 2014.

[226] J. Horsch and T. Brown. "The role of spatial scale in joint optimisations of generation and transmission for European highly renewable scenarios". In: *International Conference on the European Energy Market, EEM* (2017), pp. 1–8. ISSN: 21654093. DOI: 10.1109/EEM.2017.7982024.

[227] K. Schaber, F. Steinke, and T. Hamacher. "Transmission grid extensions for the integration of variable renewable energies in Europe: Who benefits where?" In: *Energy Policy* 43 (2012), pp. 123–135. ISSN: 03014215. DOI: 10.1016/j.enpol.2011.12.040. URL: http://dx.doi.org/10.1016/j.enpol.2011.12.040.

[228] V. Aryanpur et al. "A review of spatial resolution and regionalisation in national-scale energy systems optimisation models". In: *Energy Strategy Reviews* 37 (Sept. 2021). ISSN: 2211467X. DOI: 10.1016/j.esr.2021.100702.

[229] R. Martínez-Gordón et al. "A review of the role of spatial resolution in energy systems modelling: Lessons learned and applicability to the North Sea region". In: *Renewable and Sustainable Energy Reviews* 141 (May 2021). ISSN: 18790690. DOI: 10.1016/j.rser.2021.110857.

[230] T. Tröndle et al. "Trade-Offs between Geographic Scale, Cost, and Infrastructure Requirements for Fully Renewable Electricity in Europe". In: *Joule* 4 (9 2020), pp. 1929–1948. ISSN: 25424351. DOI: 10.1016/j.joule.2020.07.018.

[231] F. D. Munoz, E. E. Sauma, and B. F. Hobbs. "Approximations in power transmission planning: Implications for the cost and performance of renewable portfolio standards". In: *Journal of Regulatory Economics* 43 (3 2013), pp. 305–338. ISSN: 0922680X. DOI: 10.1007/s11149-013-9209-8.

[232] N. Langrené, W. V. Ackooij, and F. Bréant. "Dynamic constraints for aggregated units: Formulation and application". In: *IEEE Transactions on Power Systems* 26 (3 2011), pp. 1349–1356. ISSN: 08858950. DOI: 10.1109/TPWRS.2010.2089539.

[233] C. Nolden et al. “Network constraints in techno-economic energy system models: Towards more accurate modeling of power flows in long-term energy system models”. In: *Energy Systems* 4 (3 2013), pp. 267–287. ISSN: 18683967. DOI: 10.1007/s12667-013-0078-0.

[234] S. Pfenninger. “Dealing with multiple decades of hourly wind and PV time series in energy models: A comparison of methods to reduce time resolution and the planning implications of inter-annual variability”. In: *Applied Energy* 197 (July 2017), pp. 1–13. ISSN: 03062619. DOI: 10.1016/j.apenergy.2017.03.051.

[235] K. Poncelet et al. “Selecting representative days for capturing the implications of integrating intermittent renewables in generation expansion planning problems”. In: *IEEE Transactions on Power Systems* (August 2017), pp. 1–23.

[236] S. Ludig et al. “Fluctuating renewables in a long-term climate change mitigation strategy”. In: *Energy* 36 (11 2011), pp. 6674–6685. ISSN: 03605442. DOI: 10.1016/j.energy.2011.08.021. URL: http://dx.doi.org/10.1016/j.energy.2011.08.021.

[237] G. Haydt et al. “The relevance of the energy resource dynamics in the mid/long-term energy planning models”. In: *Renewable Energy* 36 (11 2011), pp. 3068–3074. ISSN: 09601481. DOI: 10.1016/j.renene.2011.03.028. URL: http://dx.doi.org/10.1016/j.renene.2011.03.028.

[238] H. Teichgraeber and A. R. Brandt. “Systematic Comparison of Aggregation Methods for Input Data Time Series Aggregation of Energy Systems Optimization Problems”. In: *Computer Aided Chemical Engineering* 44 (2018), pp. 955–960. ISSN: 15707946. DOI: 10.1016/B978-0-444-64241-7.50154-3. URL: https://doi.org/10.1016/B978-0-444-64241-7.50154-3.

[239] H. Teichgraeber and A. R. Brandt. “Clustering methods to find representative periods for the optimization of energy systems: An initial framework and comparison”. In: *Applied Energy* 239 (August 2018 2019), pp. 1283–1293. ISSN: 03062619. DOI: 10.1016/j.apenergy.2019.02.012. URL: https://doi.org/10.1016/j.apenergy.2019.02.012.

[240] T. Schütz et al. “Comparison of clustering algorithms for the selection of typical demand days for energy system synthesis”. In: *Renewable Energy* 129 (Dec. 2018), pp. 570–582. ISSN: 18790682. DOI: 10.1016/j.renene.2018.06.028.

[241] N. Baumgärtner et al. “RiSES4 Rigorous Synthesis of Energy Supply Systems with Seasonal Storage by relaxation and time-series aggregation to typical periods”. In: *ECOS2019 - The 32nd International Conference on efficiency, cost, optimization,*

simulation and environmental impact of energy systems, Wroclac, Poland, June 23-28. 2019. ISBN: 9788361506515.

[242] S. Gonzato, K. Bruninx, and E. Delarue. “Long term storage in generation expansion planning models with a reduced temporal scope”. In: *Applied Energy* 298 (2021). ISSN: 03062619. DOI: 10.1016/j.apenergy.2021.117168.

[243] P. Gabrielli et al. “Optimal design of multi-energy systems with seasonal storage”. In: *Applied Energy* 219 (June 2018), pp. 408–424. ISSN: 03062619. DOI: 10.1016/j.apenergy.2017.07.142.

[244] F. Domínguez-Muñoz et al. “Selection of typical demand days for CHP optimization”. In: *Energy and Buildings* 43 (11 2011), pp. 3036–3043. ISSN: 03787788. DOI: 10.1016/j.enbuild.2011.07.024.

[245] L. Kotzur et al. “Time series aggregation for energy system design: Modeling seasonal storage”. In: *Applied Energy* 213 (January 2018), pp. 123–135. ISSN: 03062619. DOI: 10.1016/j.apenergy.2018.01.023. URL: https://doi.org/10.1016/j.apenergy.2018.01.023.

[246] P. Nahmmacher et al. “Carpe diem : A novel approach to select representative days for long- term power system modeling”. In: *Energy* 112 (2016), pp. 430–442. ISSN: 0360-5442. DOI: 10.1016/j.energy.2016.06.081. URL: http://dx.doi.org/10.1016/j.energy.2016.06.081.

[247] W. W. Tso et al. “A hierarchical clustering decomposition algorithm for optimizing renewable power systems with storage”. In: *Applied Energy* 270 (July 2020). ISSN: 03062619. DOI: 10.1016/j.apenergy.2020.115190.

[248] S. Pineda and J. M. Morales. “Chronological Time-Period Clustering for Optimal Capacity Expansion Planning With Storage”. In: *IEEE Transactions on Power Systems* (2018). DOI: 10.1109/TPWRS.2018.2842093.

[249] H. Teichgraeber et al. “Extreme events in time series aggregation: A case study for optimal residential energy supply systems”. In: *Applied Energy* 275 (October 2020), p. 115223.

[250] H. Teichgraeber, L. E. Küpper, and A. R. Brandt. “Designing reliable future energy systems by iteratively including extreme periods in time-series aggregation”. In: *Applied Energy* 304 (May 2021), p. 117696. ISSN: 03062619. DOI: 10.1016/j.apenergy.2021.117696. URL: https://doi.org/10.1016/j.apenergy.2021.117696.

[251] S. Collins et al. "Impacts of Inter-annual Wind and Solar Variations on the European Power System". In: *Joule* 2 (10 2018), pp. 2076–2090. ISSN: 25424351. DOI: 10.1016/j.joule.2018.06.020.

[252] L. Kotzur et al. "Impact of different time series aggregation methods on optimal energy system design". In: *Renewable Energy* 117 (2018), pp. 474–487. ISSN: 0960-1481. DOI: 10.1016/j.renene.2017.10.017. URL: https://doi.org/10.1016/j.renene.2017.10.017.

[253] L. Middelhauve et al. "Data reduction for mixed integer linear programming in complex energy systems". In: *ECOS2021 - The 34th International Conference on Efficiency, Cost, Optimization, Simulation and Environmental Impact of Energy Systems, Taormina, Italy, June 28–2 July*. 2021.

[254] D. A. Tejada-Arango et al. "Enhanced representative days and system states modeling for energy storage investment analysis". In: *IEEE Transactions on Power Systems* 33 (6 2018), pp. 6534–6544. ISSN: 08858950. DOI: 10.1109/TPWRS.2018.2819578.

[255] RTE. *Futurs énergétiques 2050*. Tech. rep. RTE, 2022.

[256] E. Commission et al. *EU reference scenario 2016 : energy, transport and GHG emissions : trends to 2050*. Publications Office, 2016. DOI: doi/10.2833/001137.

[257] Regulation (EU). "2021/1119 of the European Parliament and of the Council of 30 June 2021 establishing the framework for achieving climate neutrality and amending Regulations (EC) No 401/2009 and (EU) 2018/1999 ('European Climate Law'). Off". In: *J. Eur. Union* 50 (2021), p. 243.

[258] M. Schneider and A. Froggatt. *The World Nuclear Industry Status Report 2023*. Paris, 2023. DOI: 10.1142/9789811213953_0021. URL: https://www.worldscientific.com/doi/abs/10.1142/9789811213953_0021 (visited on 03/28/2024).

[259] L. Haywood, M. Leroutier, and R. Pietzcker. "Why investing in new nuclear plants is bad for the climate". In: *Joule* 7.8 (Aug. 16, 2023), pp. 1675–1678. ISSN: 2542-4351. DOI: 10.1016/j.joule.2023.07.006. URL: https://www.sciencedirect.com/science/article/pii/S2542435123002817 (visited on 04/09/2024).

[260] D. P. Schlachtberger et al. "The benefits of cooperation in a highly renewable European electricity network". In: *Energy* 134 (2017). Publisher: Elsevier Ltd, pp. 469–481. ISSN: 03605442. DOI: 10.1016/j.energy.2017.06.004. arXiv: 1704.05492. URL: http://dx.doi.org/10.1016/j.energy.2017.06.004.

[261] M. Child, D. Bogdanov, and C. Breyer. "The role of storage technologies for the transition to a 100% renewable energy system in Europe". In: *Energy Procedia* 155 (2018). Publisher: Elsevier B.V. ISBN: 3584082978, pp. 44–60. ISSN: 18766102. DOI: 10.1016/j.egypro.2018.11.067. URL: https://doi.org/10.1016/j.egypro.2018.11.067.

[262] M. Child et al. "Flexible electricity generation, grid exchange and storage for the transition to a 100% renewable energy system in Europe". In: *Renewable Energy* 139 (2019). Publisher: Elsevier Ltd, pp. 80–101. ISSN: 18790682. DOI: 10.1016/j.renene.2019.02.077. URL: https://doi.org/10.1016/j.renene.2019.02.077.

[263] J. Horsch and T. Brown. "The role of spatial scale in joint optimisations of generation and transmission for European highly renewable scenarios". In: *International Conference on the European Energy Market, EEM* (2017). ISBN: 9781509054992, pp. 1–8. ISSN: 21654093. DOI: 10.1109/EEM.2017.7982024. arXiv: 1705.07617.

[264] F. Cebulla, T. Naegler, and M. Pohl. "Electrical energy storage in highly renewable European energy systems: Capacity requirements, spatial distribution, and storage dispatch". In: *Journal of Energy Storage* 14 (2017). Publisher: Elsevier Ltd, pp. 211–223. ISSN: 2352152X. DOI: 10.1016/j.est.2017.10.004. URL: http://dx.doi.org/10.1016/j.est.2017.10.004.

[265] M. G. Rasmussen, G. B. Andresen, and M. Greiner. "Storage and balancing synergies in a fully or highly renewable pan-European power system". In: *Energy Policy*. Renewable Energy in China 51 (Dec. 1, 2012), pp. 642–651. ISSN: 0301-4215. DOI: 10.1016/j.enpol.2012.09.009. URL: https://www.sciencedirect.com/science/article/pii/S0301421512007677 (visited on 04/06/2024).

[266] D. G. Caglayan et al. *The Impact of Temporal Complexity Reduction on a 100% Renewable European Energy System with Hydrogen Infrastructure*. Oct. 13, 2019. DOI: 10.20944/preprints201910.0150.v1. URL: https://www.preprints.org/manuscript/201910.0150/v1 (visited on 04/06/2024).

[267] M. Victoria et al. "The role of storage technologies throughout the decarbonisation of the sector-coupled European energy system". In: *Energy Conversion and Management* 201 (Dec. 2019), p. 111977. ISSN: 01968904. DOI: 10.1016/j.enconman.2019.111977. arXiv: 1906.06936. URL: https://doi.org/10.1016/j.enconman.2019.111977.

[268] D. Bogdanov et al. "Low-cost renewable electricity as the key driver of the global energy transition towards sustainability". In: *Energy* 227 (July 15, 2021), p. 120467. ISSN: 0360-5442. DOI: 10.1016/j.energy.2021.120467. URL: https://www.sciencedirect.com/science/article/pii/S0360544221007167 (visited on 04/04/2024).

[269] M. Ram et al. *Accelerating the european renewable energy transition.* LUT University, 2022. URL: https://www.greens-efa.eu/en/article/document/accelerating-the-european-renewable-energy-transition (visited on 11/14/2022).

[270] M. Yue et al. "Hydrogen energy systems: A critical review of technologies, applications, trends and challenges". In: *Renewable and Sustainable Energy Reviews* 146 (Aug. 1, 2021), p. 111180. ISSN: 1364-0321. DOI: 10.1016/j.rser.2021.111180. URL: https://www.sciencedirect.com/science/article/pii/S1364032121004688 (visited on 04/09/2024).

[271] H. Ishaq, I. Dincer, and C. Crawford. "A review on hydrogen production and utilization: Challenges and opportunities". In: *International Journal of Hydrogen Energy*. SI: Progress in Hydrogen Production, Storage and Distribution (Ahmadi) 47.62 (July 22, 2022), pp. 26238–26264. ISSN: 0360-3199. DOI: 10.1016/j.ijhydene.2021.11.149. URL: https://www.sciencedirect.com/science/article/pii/S0360319921045377 (visited on 04/09/2024).

[272] IRENA. *The Geopolitics of Energy Transformation: The Hydrogen Factor.* Publication Title: IRENA ISBN: 9789292603700 ISSN: 01445987. IRENA, 2022.

[273] European Commission. *In-depth analysis in support on the COM(2018) 773: A Clean Planet for all - A European strategic long-term vision for a prosperous, modern, competitive and climate neutral economy | Knowledge for policy.* Brussels, Nov. 28, 2018. URL: https://knowledge4policy.ec.europa.eu/publication/depth-analysis-support-com2018-773-clean-planet-all-european-strategic-long-term-vision_en (visited on 04/08/2024).

[274] M. T. Brouwer et al. "Technical Limits in Circularity for Plastic Packages". In: *Sustainability* 12.23 (Nov. 30, 2020), p. 10021. ISSN: 2071-1050. DOI: 10.3390/su122310021. URL: https://www.mdpi.com/2071-1050/12/23/10021 (visited on 05/12/2024).

[275] Procura Belgium. *Procura.* URL: https://procurabelgium.be/en (visited on 05/12/2024).

[276] K. Anderson and G. Peters. "The trouble with negative emissions". In: *Science* 354.6309 (Oct. 14, 2016). Publisher: American Association for the Advancement of Science, pp. 182–183. DOI: 10.1126/science.aah4567. URL: https://www.science.org/doi/10.1126/science.aah4567 (visited on 04/09/2024).

[277] S. Batel, P. Devine-Wright, and T. Tangeland. "Social acceptance of low carbon energy and associated infrastructures: A critical discussion". In: *Energy Policy* 58 (July 1, 2013), pp. 1–5. ISSN: 0301-4215. DOI: 10.1016/j.enpol.2013.03.018. URL:

https://www.sciencedirect.com/science/article/pii/S0301421513001729 (visited on 04/08/2024).

[278] V. Bertsch et al. “Public acceptance and preferences related to renewable energy and grid expansion policy: Empirical insights for Germany”. In: *Energy* 114 (Nov. 1, 2016), pp. 465–477. ISSN: 0360-5442. DOI: 10.1016/j.energy.2016.08.022. URL: https://www.sciencedirect.com/science/article/pii/S0360544216311252 (visited on 04/08/2024).

[279] H. S. Boudet. “Public perceptions of and responses to new energy technologies”. In: *Nature Energy* 4.6 (June 2019). Publisher: Nature Publishing Group, pp. 446–455. ISSN: 2058-7546. DOI: 10.1038/s41560-019-0399-x. URL: https://www.nature.com/articles/s41560-019-0399-x (visited on 04/08/2024).

[280] J. J. Cohen, J. Reichl, and M. Schmidthaler. “Re-focussing research efforts on the public acceptance of energy infrastructure: A critical review”. In: *Energy* 76 (Nov. 1, 2014), pp. 4–9. ISSN: 0360-5442. DOI: 10.1016/j.energy.2013.12.056. URL: https://www.sciencedirect.com/science/article/pii/S0360544213011262 (visited on 04/08/2024).

[281] N. Goux. *Multi-regional energy systems: a multi-agent modelling approach*. PhD thesis. 2022.

[282] I. Boie et al. “Opportunities and challenges of high renewable energy deployment and electricity exchange for North Africa and Europe - Scenarios for power sector and transmission infrastructure in 2030 and 2050”. In: *Renewable Energy* 87 (Mar. 1, 2016). Publisher: Elsevier Ltd, pp. 130–144. ISSN: 18790682. DOI: 10.1016/j.renene.2015.10.008. (Visited on 10/12/2022).

[283] M. Cavana and P. Leone. “Solar hydrogen from North Africa to Europe through greenstream: A simulation-based analysis of blending scenarios and production plant sizing”. In: *International Journal of Hydrogen Energy* 46.43 (June 23, 2021), pp. 22618–22637. ISSN: 0360-3199. DOI: 10.1016/j.ijhydene.2021.04.065. URL: https://www.sciencedirect.com/science/article/pii/S0360319921013951 (visited on 05/10/2024).

[284] T. Galimova et al. “Feasibility of green ammonia trading via pipelines and shipping: Cases of Europe, North Africa, and South America”. In: *Journal of Cleaner Production* 427 (Nov. 15, 2023), p. 139212. ISSN: 0959-6526. DOI: 10.1016/j.jclepro.2023.139212. URL: https://www.sciencedirect.com/science/article/pii/S095965262303370X (visited on 05/10/2024).

[285] J. Schnidrig et al. "On the role of energy infrastructure in the energy transition. Case study of an energy independent and CO2 neutral energy system for Switzerland". In: *Frontiers in Energy Research* 11 (2023). ISSN: 2296-598X. URL: https://www.frontiersin.org/articles/10.3389/fenrg.2023.1164813 (visited on 06/08/2023).

[286] R. Satymov et al. "Techno-economic assessment of global and regional wave energy resource potentials and profiles in hourly resolution". In: *Applied Energy* 364 (June 15, 2024), p. 123119. ISSN: 0306-2619. DOI: 10.1016/j.apenergy.2024.123119. URL: https://www.sciencedirect.com/science/article/pii/S0306261924005026 (visited on 04/06/2024).

[287] O. Ruhnau, L. Hirth, and A. Praktiknjo. "Time series of heat demand and heat pump efficiency for energy system modeling". In: *Scientific Data* 6.1 (Oct. 1, 2019). Publisher: Nature Publishing Group, p. 189. ISSN: 2052-4463. DOI: 10.1038/s41597-019-0199-y. URL: https://www.nature.com/articles/s41597-019-0199-y (visited on 05/10/2024).

[288] O. Ruhnau and J. Muessel. *When2Heat Heating Profiles*. Version 2023-07-27. July 27, 2023. DOI: 10.25832/WHEN2HEAT/2023-07-27. URL: https://data.open-power-system-data.org/when2heat/2023-07-27 (visited on 05/10/2024).

[289] L. Girardin et al. "AIDRES: A database for the decarbonisation of the heavy industry in Europe". In: THE 36TH INTERNATIONAL CONFERENCE ON EFFICIENCY, COST, OPTIMIZATION, SIMULATION AND ENVIRONMENTAL IMPACT OF ENERGY SYSTEMS. Las Palmas de Gran Canaria, Spain, June 2023.

[290] European Commission et al. *AIDRES, "Advancing industrial decarbonization by assessing the future use of renewable energies in industrial processes": assessment and geo mapping of renewable energy demand for technological paths towards carbon neutrality of EU energy intensive industries : methodology and results in support to the EU industrial plants database*. Publications Office of the European Union, 2023. ISBN: 978-92-68-07186-1. URL: https://data.europa.eu/doi/10.2833/696697 (visited on 05/10/2024).

[291] S. Bourgeois et al. *Climate neutrality, Energy security and Sustainability: A pathway to bridge the gap through Sufficiency, Efficiency and Renewables*. Association négaWatt, June 2023.

[292] CLEVER and Association négaWatt. *CLEVER - A Collaborative Low Energy vision for the European Region*. 2023. URL: https://clever-energy-scenario.eu/ (visited on 04/27/2024).

[293] négaWatt. *Energy sufficiency: Towards a more sustainable and fair society*. 2018. URL: www.energysufficiency.org.

[294] K. Raworth. *Doughnut Economics: Seven Ways to Think Like a 21st-Century Economist*. Google-Books-ID: 7A4lDgAAQBAJ. Chelsea Green Publishing, 2017. 322 pp. ISBN: 978-1-60358-674-0.

[295] Cambridge Dictionnary. *Sufficiency*. May 8, 2024. URL: https://dictionary.cambridge.org/dictionary/english/sufficiency (visited on 05/11/2024).

[296] N. Taillard et al. *Establishment of energy consumption convergence corridors to 2050: Residential sector*. 2022.

[297] A. Toledano et al. *Establishment of energy consumption convergence corridors to 2050: Industrial sector*. 2022.

[298] A. Toledano et al. *Establishment of energy consumption convergence corridors to 2050: Mobility sector*. CLEVER, Mar. 2023. URL: https://clever-energy-scenario.eu/wp-content/uploads/2023/03/2403-Convergence-corridors-Mobility.pdf (visited on 04/27/2024).

[299] C. Couturier et al. *Agriculture, forestry, other land-use changes and bioenergy (AFOLUB): Main assumptions and preliminary trajectory of the CLEVER scenario*. CLEVER, Solagro, Mar. 2022. URL: https://clever-energy-scenario.eu/wp-content/uploads/2023/03/2303-CLEVER-AFOLUB-note.pdf (visited on 04/27/2024).

[300] A. Grubler et al. "A low energy demand scenario for meeting the 1.5 °C target and sustainable development goals without negative emission technologies". In: *Nature Energy* 3.6 (June 4, 2018), pp. 515–527. ISSN: 2058-7546. DOI: 10.1038/s41560-018-0172-6. URL: https://www.nature.com/articles/s41560-018-0172-6 (visited on 06/06/2023).

[301] J. Barrett et al. *The role of energy demand reduction in achieving net-zero in the UK*. ISBN: 978-1-913299-11-8. Oxford, UK: Centre for Research into Energy Demand Solutions, 2021.

[302] J. Günther et al. *Resource-Efficient Pathways towards Greenhouse-GasNeutrality – RESCUE: Summary Report*. Nov. 2019.

[303] L. I. Brand-Correa and J. K. Steinberger. "A Framework for Decoupling Human Need Satisfaction From Energy Use". In: *Ecological Economics* 141 (Nov. 1, 2017). Publisher: Elsevier B.V., pp. 43–52. ISSN: 09218009. DOI: 10.1016/j.ecolecon.2017.05.019. (Visited on 11/02/2020).

[304] J. Millward-Hopkins et al. “Providing decent living with minimum energy: A global scenario”. In: *Global Environmental Change* 65 (September 2020). Publisher: Elsevier Ltd, p. 102168. ISSN: 09593780. DOI: 10.1016/j.gloenvcha.2020.102168. URL: https://doi.org/10.1016/j.gloenvcha.2020.102168.

[305] R. Costanza et al. “Quality of life: an approach integrating opportunities, human needs, and subjective well-being”. In: *Ecol. Econ.* 61.2 (Mar. 1, 2007), pp. 267–276. ISSN: 09218009. DOI: 10.1016/j.ecolecon.2006.02.023. (Visited on 10/12/2022).

[306] N. D. Rao and J. Min. “Decent Living Standards: Material Prerequisites for Human Wellbeing”. In: *Social Indicators Research* 138.1 (July 1, 2018). Publisher: Springer Netherlands, pp. 225–244. ISSN: 15730921. DOI: 10.1007/S11205-017-1650-0/TABLES/1. URL: https://link.springer.com/article/10.1007/s11205-017-1650-0 (visited on 10/12/2022).

[307] I. Gough. “Recomposing consumption: defining necessities for sustainable and equitable well-being”. In: *Philosophical Transactions of the Royal Society A: Mathematical, Physical and Engineering Sciences* 375.2095 (June 13, 2017). Publisher: The Royal Society Publishing. ISSN: 1364503X. DOI: 10.1098/RSTA.2016.0379. URL: https://royalsocietypublishing.org/doi/10.1098/rsta.2016.0379 (visited on 10/12/2022).

[308] Nuclear Alliance. *Nuclear Alliance meeting - Joint Statement*. Paris, May 16, 2023. URL: https://www.ecologie.gouv.fr/sites/default/files/16_05_23_REUNION_DES_PAYS_MEMBRES_DE_L%E2%80%99ALLIANCE_DU_NUCLEAIRE_A_PARIS.pdf (visited on 05/11/2024).

[309] European Commission. *Eurostat - Electricity production capacities by main fuel groups and operator*. 2024. URL: https://ec.europa.eu/eurostat/databrowser/view/nrg_inf_epc__custom_8858058/default/table?lang=en (visited on 05/11/2024).

[310] World Nuclear Association. *Reactor Database Global Dashboard*. 2024. URL: https://world-nuclear.org/nuclear-reactor-database/summary (visited on 05/11/2024).

[311] J. Riesz et al. “Quantifying key uncertainties in the costs of nuclear power”. In: *International Journal of Energy Research* 41.3 (Mar. 10, 2017). Publisher: John Wiley & Sons, Ltd, pp. 389–409. ISSN: 0363-907X. DOI: 10.1002/er.3618. URL: https://onlinelibrary.wiley.com/doi/abs/10.1002/er.3618 (visited on 05/11/2024).

[312] G. Maronati and B. Petrovic. “Estimating cost uncertainties in nuclear power plant construction through Monte Carlo sampled correlated random variables”. In: *Progress in Nuclear Energy* 111 (Mar. 1, 2019), pp. 211–222. ISSN: 0149-1970. DOI: 10.1016/j.

pnucene.2018.11.011. URL: https://www.sciencedirect.com/science/article/pii/S0149197018302944 (visited on 05/11/2024).

[313] S. P. Gaultier, G. Marx, and D. Roux. *Éoliennes et biodiversité : Synthèse des connaissances sur les impacts et moyens de les atténuer*. Office national de la chasse et de la faune sauvage/LPO, 2019, p. 120. URL: https://eolien-biodiversite.com/IMG/pdf/lpo_oncfs_2019.pdf.

[314] A. Z. Dhunny et al. "Sustainable renewable energy planning and wind farming optimization from a biodiversity perspective". In: *Energy* 185 (Oct. 15, 2019), pp. 1282–1297. ISSN: 0360-5442. DOI: 10.1016/j.energy.2019.07.147. URL: https://www.sciencedirect.com/science/article/pii/S0360544219314896 (visited on 05/11/2024).

[315] L. Millon et al. "Wind turbines impact bat activity, leading to high losses of habitat use in a biodiversity hotspot". In: *Ecological Engineering* 112 (Mar. 1, 2018), pp. 51–54. ISSN: 0925-8574. DOI: 10.1016/j.ecoleng.2017.12.024. URL: https://www.sciencedirect.com/science/article/pii/S0925857417306572 (visited on 05/11/2024).

[316] J. Fernández-González et al. "The Relevance of Life Cycle Assessment Tools in the Development of Emerging Decarbonization Technologies". In: *JACS Au* 3.10 (Oct. 23, 2023). Publisher: American Chemical Society, pp. 2631–2639. DOI: 10.1021/jacsau.3c00276. URL: https://doi.org/10.1021/jacsau.3c00276 (visited on 05/11/2024).

[317] D. Bell et al. "Re-visiting the 'Social Gap': Public Opinion and Relations of Power in the Local Politics of Wind Energy". In: *Environmental Politics* 22.1 (2013). Publisher: Routledge, pp. 115–135. ISSN: 0964-4016. DOI: 10.1080/09644016.2013.755793. URL: https://www.research.ed.ac.uk/en/publications/re-visiting-the-social-gap-public-opinion-and-relations-of-power- (visited on 04/21/2024).

[318] N. Zielonka and E. Trutnevyte. "Probabilities of reaching required diffusion of granular energy technologies in European countries". In: *Research Square* (Mar. 11, 2024). DOI: 10.21203/rs.3.rs-4039857/v1. URL: https://www.researchsquare.com (visited on 03/18/2024).

[319] T. Tröndle. "Supply-side options to reduce land requirements of fully renewable electricity in Europe". In: *PLOS ONE* 15.8 (Aug. 6, 2020). Publisher: Public Library of Science, e0236958. ISSN: 1932-6203. DOI: 10.1371/journal.pone.0236958. URL: https://journals.plos.org/plosone/article?id=10.1371/journal.pone.0236958 (visited on 03/18/2024).

[320] A. Valente et al. “The role of hydrogen in heavy transport to operate within planetary boundaries”. In: *Sustainable Energy & Fuels* 5.18 (2021). Publisher: Royal Society of Chemistry, pp. 4637–4649. DOI: 10.1039/D1SE00790D. URL: https://pubs.rsc.org/en/content/articlelanding/2021/se/d1se00790d (visited on 05/11/2024).

[321] L. K. Stranddorf et al. “Evaluation of life cycle impacts of European electricity generation in relation to the Planetary Boundaries”. In: *Sustainable Production and Consumption* 39 (July 1, 2023), pp. 414–424. ISSN: 2352-5509. DOI: 10.1016/j.spc.2023.05.026. URL: https://www.sciencedirect.com/science/article/pii/S2352550923001215 (visited on 05/11/2024).

[322] International Energy Agency. *The Role of Critical Minerals in Clean Energy Transitions.* 2021.

[323] V. Bertsch, M. Hyland, and M. Mahony. “What drives people’s opinions of electricity infrastructure? Empirical evidence from Ireland”. In: *Energy Policy* 106 (July 1, 2017), pp. 472–497. ISSN: 0301-4215. DOI: 10.1016/j.enpol.2017.04.008. URL: https://www.sciencedirect.com/science/article/pii/S0301421517302331 (visited on 04/21/2024).

[324] D. W. O’Neill et al. “A good life for all within planetary boundaries”. In: *Nature Sustainability* 1.2 (Feb. 2018). Publisher: Nature Publishing Group, pp. 88–95. ISSN: 2398-9629. DOI: 10.1038/s41893-018-0021-4. URL: https://www.nature.com/articles/s41893-018-0021-4 (visited on 05/11/2024).

[325] J. Dumas et al. “The energy return on investment of whole energy systems: application to Belgium”. In: *Biophysical Economics and Sustainability* 7.4 (May 13, 2022). Publisher: Springer Science and Business Media LLC. DOI: 10.1007/s41247-022-00106-0. arXiv: 2205.06727v4.

[326] D. Coppitters et al. *Towards importing renewable hydrogen within planetary boundaries.* ISSN: 2693-5015. Mar. 18, 2024. DOI: 10.21203/rs.3.rs-3920745/v1. URL: https://www.researchsquare.com/article/rs-3920745/v1 (visited on 05/12/2024).

[327] L. S. Plaga et al. “How public acceptance affects power system development—A cross-country analysis for wind power”. In: *Applied Energy* 359 (Apr. 1, 2024), p. 122745. ISSN: 0306-2619. DOI: 10.1016/j.apenergy.2024.122745. URL: https://www.sciencedirect.com/science/article/pii/S0306261924001284 (visited on 02/07/2024).

[328] E. Dupont, M. Germain, and H. Jeanmart. "Feasibility and Economic Impacts of the Energy Transition". In: *Sustainability* 13.10 (Jan. 2021). Number: 10 Publisher: Multidisciplinary Digital Publishing Institute, p. 5345. ISSN: 2071-1050. DOI: 10.3390/su13105345. URL: https://www.mdpi.com/2071-1050/13/10/5345 (visited on 05/09/2024).

[329] E. Dupont, M. Germain, and H. Jeanmart. "Estimate of the Societal Energy Return on Investment (EROI)". In: *Biophysical Economics and Sustainability* 6.1 (2021). Publisher: Springer International Publishing ISBN: 0123456789, pp. 1–14. ISSN: 2730-7204. DOI: 10.1007/s41247-021-00084-9. URL: https://doi.org/10.1007/s41247-021-00084-9.

[330] P. Jacques et al. "Assessing the economic consequences of an energy transition through a biophysical stock-flow consistent model". In: *Ecological Economics* 209 (July 1, 2023), p. 107832. ISSN: 0921-8009. DOI: 10.1016/j.ecolecon.2023.107832. URL: https://www.sciencedirect.com/science/article/pii/S0921800923000952 (visited on 05/12/2024).

[331] J. Finke, V. Bertsch, and V. Di Cosmo. "Exploring the feasibility of Europe's renewable expansion plans based on their profitability in the market". In: *Energy Policy* 177 (June 2023), p. 113566. ISSN: 03014215. DOI: 10.1016/j.enpol.2023.113566. URL: https://linkinghub.elsevier.com/retrieve/pii/S0301421523001519 (visited on 05/24/2023).

[332] T. Bauwens and P. Devine-Wright. "Positive energies? An empirical study of community energy participation and attitudes to renewable energy". In: *Energy Policy* 118 (July 1, 2018), pp. 612–625. ISSN: 0301-4215. DOI: 10.1016/j.enpol.2018.03.062. URL: https://www.sciencedirect.com/science/article/pii/S0301421518301976 (visited on 04/21/2024).

[333] K. Schumacher et al. "Public acceptance of renewable energies and energy autonomy: A comparative study in the French, German and Swiss Upper Rhine region". In: *Energy Policy* 126 (Mar. 1, 2019), pp. 315–332. ISSN: 0301-4215. DOI: 10.1016/j.enpol.2018.11.032. URL: https://www.sciencedirect.com/science/article/pii/S0301421518307614 (visited on 04/21/2024).

[334] G. Van Moeseke et al. *Slowheat.* URL: https://www.slowheat.org (visited on 05/12/2024).

[335] G. Van Moeseke. “SLOWHEAT@LOCI-LAB”. In: (2023). Number: UCL - Université Catholique de Louvain. URL: https://dial.uclouvain.be/pr/boreal/fr/object/boreal%3A275611 (visited on 05/12/2024).

[336] ISO. *ISO 3166 Country codes - Online Browsing Platform (OBP)*. 2024. URL: https://www.iso.org/obp/ui/#search (visited on 05/12/2024).